Technische Universität München

TUM School of Natural Sciences

Mononuclear-Homoleptic Transition Metal Compounds of GaTMP

Richard Johannes Josef Weininger

Vollständiger Abdruck der von der TUM School of Natural Sciences der Technischen Universität München zur Erlangung des akademisches Grades eines

Doktors der Naturwissenschaften (Dr. rer. nat.)

genehmigten Dissertation.

Vorsitz:	Prof. Dr. Jennifer Strunk
Prüfende der Dissertation:	1. Prof. Dr. Roland A. Fischer
	2. Prof. Dr. Fritz E. Kühn

Die Dissertation wurde am 28.07.2025 bei der Technischen Universität München eingereicht und durch die TUM School of Natural Sciences am 21.08.2025 angenommen.

Die vorliegende Arbeit wurde am Lehrstuhl für Anorganische und Metallorganische Chemie der Technischen Universität München im Zeitraum von März 2021 bis Juni 2025 erstellt.

Diese Arbeit ist gewidmet:

Meinen Freunden und Wegbegleitern aus allen Lebenslagen, die immer treu an meiner Seite standen, und davon besonders denen, die nicht mehr hier sein können, um mit mir diesen Abschnitt zu Ende zu bringen.

Leo-Heinrich Koch 1959 – 2021

Josef Bichler 1996 – 2023

DANKSAGUNG

Über die Jahre konnte ich mich auf die Unterstützung durch viele Menschen um mich herum verlassen. Nicht erschöpfend möchte ich an dieser Stelle die nachfolgenden hervorheben.

Prof. Dr. rer. nat. Dr. phil. h. c. Roland A. Fischer

Von Bachelorarbeit, Forschungspraktikum, Masterarbeit, bis Promotion, immer hatten sie spannende und fordernde Aufgaben für mich, an denen ich Neues lernen und wachsen konnte. Sie haben in mir ein Potential gesehen und mir über die Jahre den Raum gegeben, es selbst zu finden. Die Möglichkeiten, die ich dank ihrem Vertrauen am Lehrstuhl hatte, waren alles was ich mir jemals hätte wünschen können, und ich hoffe, dass mein Erbe den nachfolgenden Generationen gute Dienste leisten wird. Zum richtigen Zeitpunkt wussten sie immer die richtigen Worte zu finden und ich hatte immer das Gefühl, dass sie in mir den Menschen sehen der ich bin. Auch wenn die Zeiten schwer wurden, nicht einen einzigen Tag gab es an dem ich morgens nicht motiviert ins Labor gekommen bin und dafür bin ich unglaublich dankbar.

Dr. Christian Gemel: Als Kopf der OM-Gruppe warst du für mich da, wenn ich dich brauchte. Deine unermüdliche Arbeit an der MassenApp, die unsere ganze Herangehensweise verändert hat, sowie deine Arbeit rund um geometrische Rechnungen haben mich immer und immer wieder beeindruckt und mir gezeigt, dass sich unsere Forschung noch so viel weiter in Kontext setzen lässt. Nicht erst seit meiner Doktorandenzeit, sondern seit dem ersten Tag, hast du mich unter deine Fittiche genommen. Danke, dass ich diesen langen Weg immer an der Seite der OM gehen durfte.

Die OM-Subgroup: Über die Jahre sind natürlich viele gekommen und gegangen und ihr seid nicht vergessen aber hier sollen insbesondere diejenigen ihren Namen wieder finden, ohne die diese Dissertation nicht entstanden wäre. **Raphael Bühler**, **Johannes Stephan** und **Ivan Antsiburov**. Sei es thematisch, praktisch, theoretisch, oder technisch, ihr wart da als ich gar nicht wusste, dass ich euch am meisten brauche, und ihr habt mich nie hängen gelassen. Danke, dass die OM-Familie für mich da war.

Dr. Dana Weiß, **Martin Schellerer**, **Dr. Markus Drees**, **Rodica Dumitrescu** und all die anderen, die das Tagesgeschäft am Laufen halten. Vor allem bei euch kann ich gar nicht mehr zählen, wie oft ich unangekündigt mit irgendeinem Anliegen in euren Büros stand und immer bin ich mit einer Lösung wieder gegangen und meistens auch noch einem Lächeln. Danke für den unglaublichen Job, den ihr leistet.

Tobias Kubo, stellvertretend hier für alle Techniker und ansonsten unsichtbaren Mitarbeiter, die die Chemie am Laufen halten. Was man von euch lernen kann, ist in keinem Lehrbuch dieser Welt zu finden und ich war dankbar für jede Idee, jeden Tipp und jede Hilfestellung, die ich im Laufe der Jahre bekommen habe.

Dr. med. Martina Herrmann, meine Mentorin, die mich außerhalb der Wissenschaft begleitet hat, von der ich unglaublich viel lernen durfte und die mir immer das ungeschönte, ehrliche Feedback gegeben hat, dass ich brauchte, um zu wachsen.

Abseits der Akademischen Seite hatte ich das Glück von wundervollen Menschen umgeben zu sein, die mir zur Seite standen, mich unterstützt haben und mich daran erinnert haben, dass es da draußen noch eine ganze Welt gibt, die nicht in meinen Daten und Kolben zu finden ist.

Meine Eltern, es wäre ohne euch einfach nicht gegangen. Ihr habt mir hintenrum den Rücken freigehalten, Türen geöffnet und Möglichkeiten geschaffen.

Antonia Boczan, die Frau an meiner Seite, die in meinen Daten zwar immer nur Bäume gesehen hat, die mich aber trotzdem verstanden und unterstützt hat, ohne zu zögern.

Timo Van Iterson, als Katalysator für mein Doppelleben in der Veranstaltungstechnik, stellvertretend für alle die, mit denen ich oft das Unmögliche möglich gemacht habe. Der Vorhang hebt sich immer pünktlich, egal was passiert.

Elisabeth Iovkova, **Michael Becker**, **Jana Czerny**, **Dieter Röde**, **Maximilian Fuchs**, **Steffi Menacher**, ihr haltet hier die Stellung für noch so viele andere. Danke, dass ihr an meiner Seite steht. Ich freue mich auf die kommenden Kapitel mit euch allen gemeinsam.

"*Der Natur gegenüberzustehen und seinen Scharfsinn an Ihren Rätseln zu erproben, gibt dem Leben einen ungeahnten Inhalt.*"

Alfred Lothar Wegener 1880 – 1930

Meteorologe, Polar- und Geowissenschaftler

Abstract

[Ru(GaTMP)$_5$] and [Mo(GaTMP)$_6$] were synthesized as the first mononuclear, homoleptic compounds of GaTMP, by manner of ligand exchange from neutral olefinic precursor compounds. Their canonical characterization was contextualized alongside a review of the field of mononuclear, homoleptic compounds [M(E^{I}R)$_n$] with additional focus on mathematic descriptors of molecular geometry. Steric properties were investigated by buried volume calculations, expanding on the tools available for systematic analysis. Chemical properties of GaTMP compounds were elaborated on by an exhaustive review of related compounds, to identify promising avenues for continued research. A qualitative deduction of relative electronic properties from structural parameters was engaged in by application common principles in ligand bonding to structure the class of compounds across three decades. Furthermore this dissertation contains a dataset of buried volume calculations for the entire class of compounds [M(E^{I}R)$_n$] at the time of writing, insofar as the compounds are reported properly in databases and journals accessible to the common scientific community.

Zusammenfassung

[Ru(GaTMP)$_5$] und [Mo(GaTMP)$_6$] wurden als erste Vertreter der mononuclear, homoleptischen Verbindungen des GaTMP durch ligandenaustausch Reaktionen aus neutralen, olefinischen Vorläufern erhalten. Ihre kanonische Charakterisierung wurde durch eine Diskussion durch das Feld der mononuclear homoleptischen Verbindungen [M(E^{I}R)$_n$] in Kontext gesetzt, wobei zusätzlicher Fokus auf Anwendung mathematischer Methoden zur Beschreibung der Molekülgeometrie lag. Sterische Eigenschaften wurden anhand von Buried Volume Rechnungen erläutert, um diese als Werkzeug der Systematisierung zu etablieren. Chemische Eigenschaften der GaTMP Verbindungen wurden durch eine umfangreiche Diskussion der Verwandten Verbindungen erläutert, um vielversprechende Ansätze für weiterführende Forschung zu identifizieren. Relative, qualitative elektronische Eigenschaften wurden durch Anwendung gängiger Prinzipien der Ligandenbindung aus strukturellen Parametern abgeleitet, um Verbindungen der vergangenen drei Jahrzehnte gemeinsam zu strukturieren. Darüber hinaus enthält diese Dissertation einen Datensatz an Buried Volume Rechnungen für die gesamte Klasse der Verbindungen [M(E^{I}R)$_n$] zum Zeitpunkt der Niederschrift, insofern diese Verbindungen entsprechend wissenschaftlicher Praxis publiziert und in Datenbanken und Journalen der gewöhnlichen wissenschaftlichen Gemeinschaft zugänglich sind.

I. Table of Contents

Table of Contents

II. List of Abbreviations

%V_{Bur}	Percent buried volume
AO	Atomic Orbital
ATR	Attenuated Total Reflection
$BAr^F{}_4$	Tetrakis[3,5-bis(trifluoromethyl)phenyl]borate
C_4H_7	2-methylallyl
COD	1,5-Cyclooctadiene
COT	1,3,5-Cyclooctatriene
Cp	Cyclopentadienyl
Cp*	1,2,3,4,5-pentamethylcyclopentadienyl
Cp*$_{Cent}$	Mathematical centroid of the C_5-ring of Cp*
Cy	cyclohexyl
DDP	2-((2,6-diisopropylphenyl)amino-4-((2,6-diisopropylphenyl)imino)-2-pentene)
DMSO	Dimethylsulfoxide
dppe	1,2-Bis(diphenylphosphino)ethane
DVDS	1,3-divinyl-1,1,3,3-tetramethyldisiloxane
E	Group 13 Element (Al, Ga, In)
Et	ethyl
FT-IR	Fourier Transform Infrared
HOMO	Highest Occupied Molecular Orbital
hyp	Hypersilyl tris(trimethylsilyl)silyl
^{i}Pr	isopropyl
L	Neutral Ligand
LCAO	Linear Combination of Atomic Orbitals
LIFDI	Liquid Injection Field Desorption Ionization
LUMO	Lowest Unoccupied Molecular Orbital
M	Metal Atom

MO	Molecular Orbital
MS	Mass Spectrometry
NMR	Nuclear Magnetic Resonance
Nor	Norbornadiene / Bicyclo[2.2.1]hepta-2,5-diene
OTf	trifluoromethanesulfonate
p-cymene	1-Methyl-4-(propan-2-yl)benzene
ppm	Parts Per Million
RT	Room Temperature
SC-XRD	Single Crystal X-Ray Diffraction
^{t}Bu	Tert-butyl
THF	Tetrahydrofuran
TM	Transition Metal
TMEDA	N,N,N′,N′-Tetramethylethane-1,2-diamine
tmm	$(C(CH_3)_3)^-$
TMP	2,2,6,6-tetramethylpiperidine
TMS	trimethylsilyl
X	Ionic Ligand
θ	Tolman Cone Angle

1. Introduction

1.1 Basics on Metal–Ligand Bonding

A metal complex or metal coordination compound, note that these names are used interchangeably and inconsistently in literature, in its most simple form is made up from a single central metal atom or cation (M) to which a defined number (a + b) of anionic (X) and/or neutral (L) ligands is bound. The resulting compound differs in its properties and reactivities from its components and can be overall neutral, cationic, or anionic in nature. Denoting the coordination unit in writing is done with square brackets.[1]

$[MX_aL_b]^{c-}$	$[MX_aL_b]^{(0)}$	$[MX_aL_b]^{c+}$
$[AgCl_2]^-$	$[Ni(CO)_4]$	$[Ag(NH_3)_2]^+$
$[CrO_4]^{2-}$	$[Fe(Cp)_2]$	$[Cu(NH_3)_4]^{2+}$
$[VOCl_4]^{2-}$	$[Pt(NH_3)Cl_2]$	$[CoCl_2(NH_3)_4]^+$

The metal-ligand-bond can be formed by the overlapping of a free electron pair from the ligand, a Lewis-base, the donor, with an unoccupied orbital at the metal center, a Lewis acid, the acceptor, forming a coordinative bond. But the bond can also be of a more classic polar, covalent character. Compounds where the central atom is coordinated by a homogenous shell of a single distinct ligand, such as $[Ni(CO)_4]$ are called “homoleptic”, whereas compounds with a ligand shell of two or more distinct ligands are called “heteroleptic”.[1]

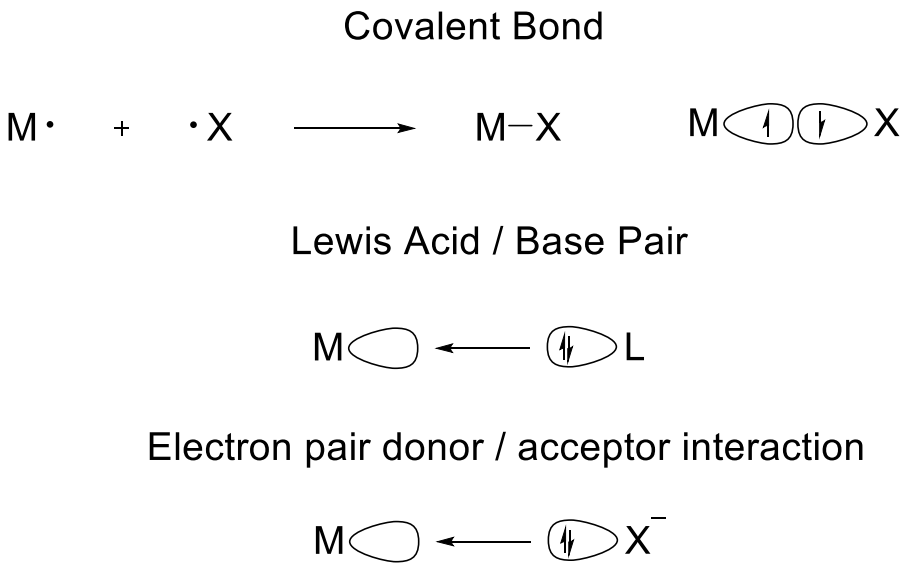

Figure 1: Examples of mechanisms by which bonds of coordination compounds can form. Top: A polar covalent bond formed from a single electron contributed by each atom. Middle: A coordinative bond formed by interaction of

Lewis acidic metal center and a neutral Lewis base. Bottom: A coordinative bond formed by interaction of an electron deficient metal center and a negatively charged electron pair donor. Figure created according to cited literature.[1]

In cases where a donor-acceptor interaction needs to be distinguished from a bond with a higher covalent character, the donor-acceptor interaction is denoted as L → M in contrast to the classic L – M notation. These however are relatively rare occurrences and thus the L – M notation is usually depicted regardless of the exact character of the bond in question. These two modes of binding can play a role in the formation of a single compound as is apparent in the following example.[1]

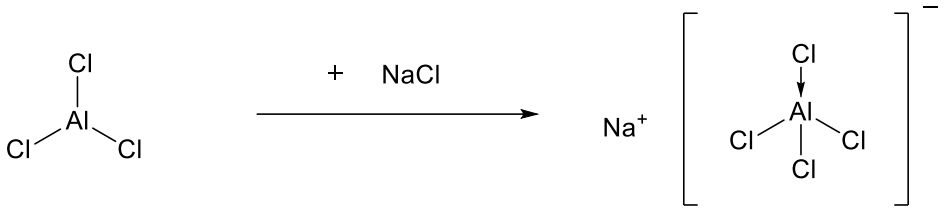

Figure 2: Reaction scheme of the gas phase reaction between $AlCl_3$ and NaCl to form the sodium tetrachloridoaluminat(III) complex. Note the arrow indicating the formation of a coordination bond between the newly introduced chloride and the aluminum center. Figure created according to cited literature.[1]

Comparing first bond dissociation energies for Al – Cl and Al ← Cl, it is found that it is reduced noticably from 502 $\mathrm{kJ/mol}$ for the first and 372 $\mathrm{kJ/mol}$ for the latter. However, all four of the compounds bonds are of equal length and indistinguishable.[1] This also means that once formed, a coordinative bond is indistinguishable from a covalent bond, since the past origin of the electrons involved, does not influence the bond. This extends also nonmetallic coordination compounds such as $[NH_4]^+$ or $[BF_4]^-$.[2]

1.2 Interactions between *π*-orbitals and their consequences

In addition to the aforementioned *σ*-donor/acceptor interactions, the *π*-orbitals of central atoms and ligands can supplement the bond by *π*-donor- and *π*-acceptor-bonds. This is viewed from the perspective of the central atom, thus a *π*-donor bond is present when electrons from a ligands highest occupied *π*-orbitals are donated into unoccupied *π*-orbitals of the central atom. This is most prominent in the case of metals in high oxidation states. Such compounds comprising only *σ*-donor and/or additional *π*-donor-bonds are considered “classic” or “*Werner*-type-complexes”, wherein the *π*-donor-bonds allow for additional electron density to be transferred to the highly oxidized, thus very electron deficient central atom. A *π*-acceptor-bond is present when electrons from the central atoms highest occupied *π*-orbitals are donated into unoccupied *π*-orbitals on the ligand. In contrast to the *Werner*-type-complexes, this is mostly present in when the central atom is in a low, neutral, or even negative oxidation state. In these cases, a hypothetical reliance only on the *σ*-donor bonds would cause destabilization through an excess accumulation of electron density close to the central atom, thus by donating electron density from the central atoms occupied *π*-orbitals back to unoccupied *π*-orbitals of the ligand, this is mitigated, hence why this is referred

to in literature as "*π*-backdonation" or "*π*-back-bonding". A classic example here is found in [Ni(CO)$_4$], where a purely *σ*-bond based interpretation would lead to a formal -IV oxidation state of the central atom, but by balancing the charge through mesomerism a more stable formula representing the effect *π*-back-bonding is found.[1-2]

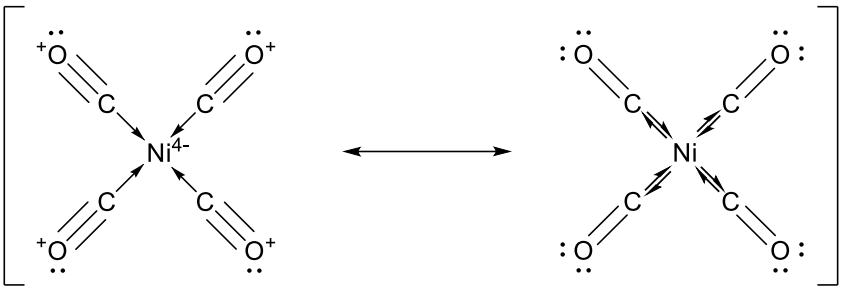

Figure 3: Schematic of mesomerism in [Ni(CO)$_4$] leading to π-back-bonding. The structure on the left shows a purely *σ*-donor based molecule where the addition of 4 electrons to the Ni^0 center leads to a formal -IV oxidation state. On the right, electron density from the central atoms *π*-orbitals is donated back into corresponding empty orbitals on the ligand, turning the C-O triple bond into a double bond, by moving the respective electron pair to the oxygen atoms, giving them two free electron pairs each. Figure created according to cited literature.[2]

Whilst a more detailed reflection on M-CO bonds and their associated compounds is offered hereafter, an important consequence of *π*-back-bonding is hinted at in the figure above. *π*-back-bonding changes the electronic structure of the ligand, in this case the C-O bond, and the M-C bond. Meaning that a M-CO bond that exhibits strong *π*-back-bonding has a strengthened/shortened M-C bond and a weakened/elongated C-O bond compared to compounds with weaker or no *π*-back-bonding. These differences can be observed prominently through vibrational spectroscopy, where the comparatively easy to observe $\tilde{\nu}_{CO}$ stretching vibration is reduced to lower wavenumbers, as *π*-back-bonding increases across a row of homologue compounds, thus giving a tool for quantification of this characteristic.[3]

1.3 Carbonyls as exemplary Compounds

To understand the importance of metal-carbonyl complexes in metal-organic chemistry, a deeper understanding of the ligand itself must be provided first.

A linear combination of the AO's of carbon and oxygen, according to MO theory gives first insights into the properties of carbon monoxide as a ligand.

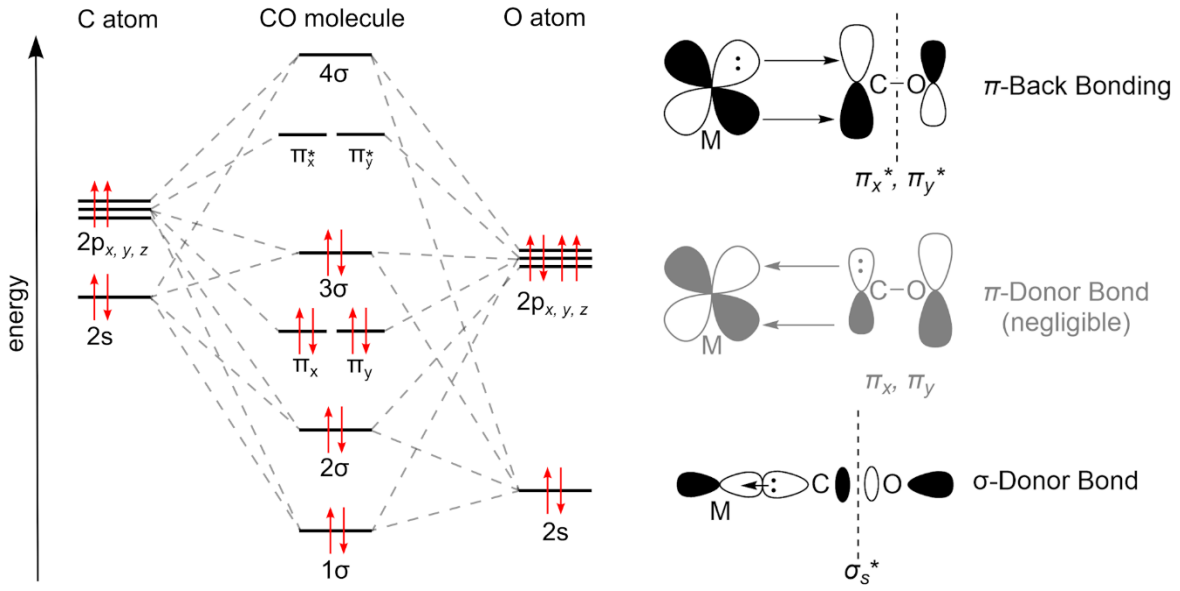

Figure 4: Left: Molecular orbital scheme of CO after Wiberg N., Inorganic chemistry, 2001, Academic Press, ISBN 0123526515 p. 1538. Labeling of sigma MOs after CATHERINE E. HOUSECROFT AND ALAN G. SHARPE, Inorganic Chemistry (By Muskid - Own work, CC BY-SA 3.0, https://commons.wikimedia.org/w/index.php?curid=34048482, 18.06.2025 – 10:30). Right: bonding mechanisms of CO to a metal center M (dotted lines indicate nodal planes). Figure created according to cited literature.[2]

Combination of the two 2*s* orbitals forms the molecules σ_s and the σ_s* orbital. A second set of σ orbitals, σ_p and σ_p* is formed from the two atoms respective 2p_z orbitals along the C-O bond axis. Perpendicular to the bond axis, the remaining p_x and p_y orbitals form the degenerate π_x and π_y orbitals along their antibonding π_x* and π_y* counterparts. This combination of orbitals is also known as sp^1 hybridization in the "Valence Bond*"* model. Filling in the electrons first fills σ_s and then σ_p with two paired electrons each, before π_x and π_y are fully populated as degenerate orbitals. σ_s* is populated with the remaining two electrons, making it the HOMO of the CO molecule. The LUMO is formed from the degenerate π_x* and π_y*.[2]

Classic calculation of the bond order of CO from this by counting the number of filled bonding MO's, subtracting the number of filled antibonding MO's gives 3, which on a qualitative level explains the stability of the C-O bond despite having a fully populated "antibonding" HOMO as well as the observation of C-O bond shortening when no π-back-bonding is present due to reduction of electron density in the σ_s* orbital when a coordinative bond between this HOMO and a electron deficient metal center is formed.[2]

This however must be regarded as incorrect, as calculations by *Goldman* and *Krogh-Jespersen* have shown that electron donation from σ_s* does not meaningfully increase $\tilde{\nu}_{CO}$, much rather electrostatic interactions, caused by the high positive charge density of a very electron deficient, thus non π-back-bonding, coordinated metal cation, cause electron density, which in CO, due to electronegativity is primarily located at the oxygen, to be drawn toward carbon, thereby reducing bond polarity, increasing the covalent character of the bond, therefore increasing $\tilde{\nu}_{CO}$. σ_s* is therefore recommended

to be viewed as essentially nonbonding and instead electrostatic interactions should be more focused on when analyzing structural and vibrational data for carbonyl compounds.[1-2, 4]

Whilst compared to the aforementioned *σ*-donor properties of CO, its *π*-donor properties are generally considered negligible and do not meaningfully contribute to the formation of coordination bonds as π_x and π_y are located closer to the oxygen. Its *π*-acceptor capabilities through the degenerate LUMO's π_x^* and π_y^*, located closer to the carbon atom, are in return very prominent. When electron density from an electron rich metal center populates these antibonding π_x^* and π_y^* orbitals, a weakening/elongation of the C-O bond length is observed, which in turn leads to a decrease in $\tilde{\nu}_{CO}$.[1]

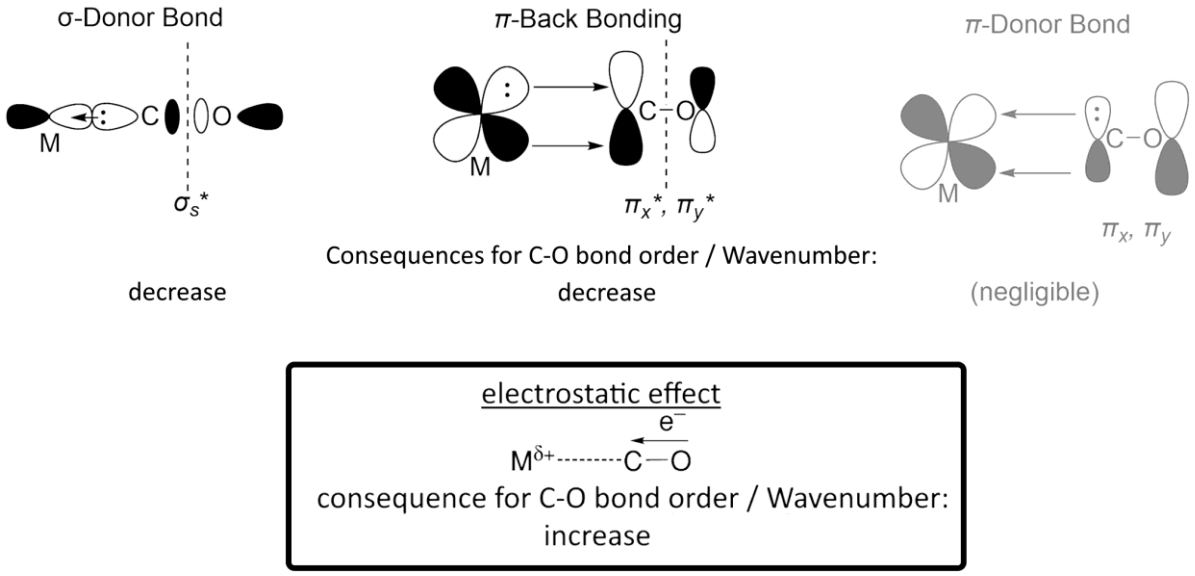

Figure 5: Breakdown of the contributions towards a metal-CO bond and their effects on $\tilde{\nu}_{CO}$. Figure created according to cited literature.[1]

In addition to binding to a single central atom, CO can bind to two or three centers at once in a bridging manner as denoted by [(μ^2-CO)M_2] respective [(μ^3-CO)M_3] for the most common alternative binding modes.[2, 5]

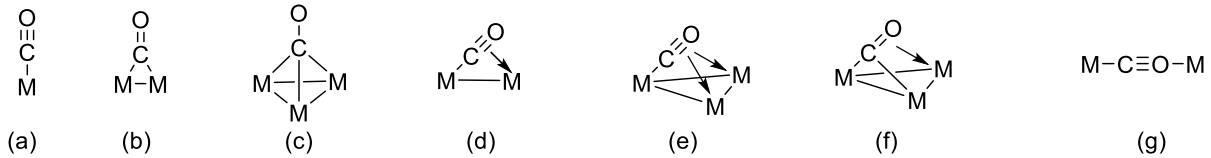

Figure 6: Depictions of the different binding modes encountered for binding CO to one or multiple metal atoms. a) [(μ^1-CO)M], b) [(μ^2-CO)M_2], c) [(μ^3-CO)M_3], d) [(μ^1-M)(CO)(η^1-M)], e) [(μ^1-M)(CO)(η^1-M)$_2$], f) [(μ^1-M)$_2$(CO)(η^1-M)], g) [(μ^1-M)(CO)(μ^1-M)]. Figure created according to cited literature.[2]

When bound in such a manner, a reduction in $\tilde{\nu}_{CO}$ is observable, making it possible to detect the different binding modes via vibrational spectroscopy.[1]

CO-Bonding	$\tilde{\nu}_{CO}/cm^{-1}$
free CO	2143
terminal CO	1850–2120
μ_2-CO 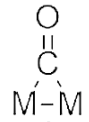	1750–1850
μ_3-CO 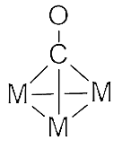	1620–1730

Figure 7: Characteristic vibrations for terminal and common bridging binding modes for compounds M-CO as well as free CO. Figure created according to cited literature.[1]

Another use of vibrational spectroscopy in this regard is the observation of the $\tilde{\nu}_{CO}$ of the axial carbonyl ligand in compounds of the type $[(L)(CO)_5M]$ to determine *π*-acceptor properties of L. In general, a strong *π*-acceptor L will cause $\tilde{\nu}_{CO}$ of the axial carbonyl ligand be similar to its value for $[(CO)_6M]$, a weaker *π*-acceptor, will attract less electron density from the central atom, allowing primarily the opposing carbonyl to attract more of the same, thus populating its antibonding *π** orbitals more, causing a weaking of the C-O bond, leading to a reduction of $\tilde{\nu}_{CO}$.[1] Whilst holding mostly true, this method should not be used singularly to determine a relative *π*-acceptor strength. As *Frenking* and *Fröhlich* have discussed $\tilde{\nu}_{CO}$ is also significantly influenced by *σ*-bonding and charge interactions.[6]

Their prevalence throughout the transition metals of the periodic table, multitude of mononuclear and polynuclear compounds known to literature, reactivity and widespread study, makes the transition metal carbonyls almost ideal reference compounds for metal organic research.

1.4 A brief excursion into magnetism and NMR

Many metal organic compounds present as paramagnetic which can lead to complications when attempting NMR characterization. Intense signal broadening and strong shifts necessitate special adaptation of measurement conditions to gain interpretable data but can be done very successfully.[7] Examples for this are found easily in the $[M(Cp)_2]$ family of sandwich compounds. $[FeCp_2]$ or ferrocene, first described by *E. O. Fischer*, is a diamagnetic d^6 18 e^- complex with ^{1}H- and ^{13}C-NMR shifts within common ranges.[8] $[VCp_2]$, a paramagnetic 15 e^- complex, exhibits a paramagnetic (isotropic) shift of -314 ppm for its protons, with a line width at half height of 2344 Hz. $[NiCp_2]$ on the other hand is a 20 e^- complex with two unpaired electrons with a paramagnetic shift of +257 ppm and a line width at half height of 471 Hz.[9]

Many nuclei are available for NMR spectroscopy that should not be disregarded, as these heteroatom NMR spectra can give valuable insight into new compounds, among other things, the oxidation state of a central atom. ^{195}Pt and ^{51}V are very well documented, but by far not the only practical nuclei.[10]

1.5 Ligands E^{I}R of group 13 elements

Central to our research are low-valent group 13 organyls (E^{I}R) which are employed as ligands to transition metals. Here the element E^{I} (= Al, Ga, In) has the formal oxidation state +1. The fragment E^{I}R as a ligand possesses an occupied *σ*-orbital at the electropositive metal, hence the ability to form a strong *σ*-donor bond by donating this electron density into empty *σ*-Aos on a TM. Furthermore, the *p*-orbitals of E^{I} are unoccupied, giving the fragment E^{I}R in principle the ability to accept *π*-electron density from a TM through *π*-back-bonding, though this property is less pronounced, due to the low electronegativity of E^{I}.[11] E^{I}R as a ligand can thus be viewed as isolobal to CO or PR_3.[12] The extend of *π*-back-bonding capabilities in E^{I}R are mainly determined by the organic group R. If R has one or more occupied *p*-/*π*-orbitals the TM→E^{I}R *π*-back-donation is competing with E^{I}←R *π*-donation. In practice this means that a ligand E^{I}R, where R is only a weak *π*-donor, is a good *π*-acceptor and vice versa.[11]

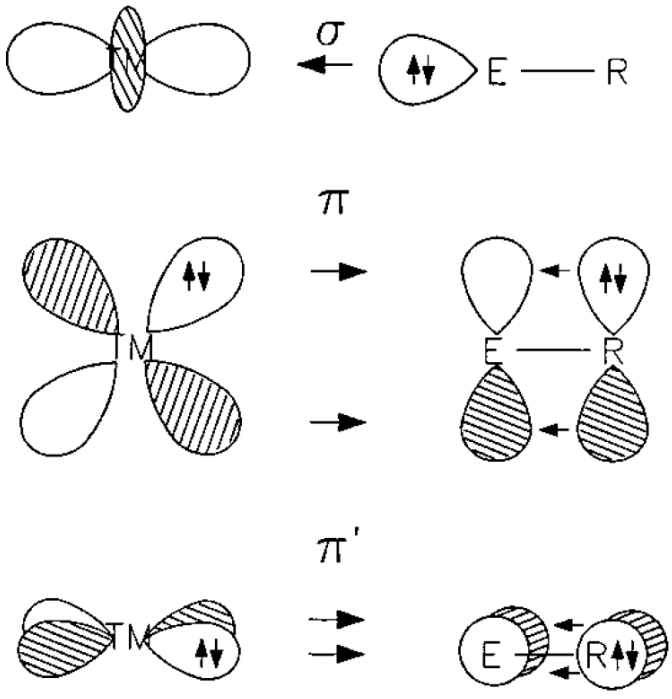

Figure 8: Schematic representation the bonding between a transition metal TM and E^{I}R, when R has occupied p(π)-orbitals. Reprinted (adapted) with permission from Organometallics 2000, 19, 4, 571–582. Copyright 2000 American Chemical Society.[11]

Uddin, Boehme and *Frenking* summarized the trends observed in their calculations for E^{I}R as follows. A substituent R that is only a weak *π*-donor, results in a particularly strong TM-E^{I}R bond. Bond dissociation energies follow the order (B >) Al > Ga ≈ In

(> Tl). The main contributor to the TM-E^{I}R bond are Coulomb interactions between the negatively charged TM atoms and the positively charged atoms E, covalent interactions are only of secondary importance and the TM-E^{I}R bond order is < 1. When R is a strong *π*-donor, the TM←E^{I}R *σ*-donation is larger than TM→E^{I}R *π*-back-bonding. The TM→E^{I}R *π*-back-donation becomes larger and can exceed TM←E^{I}R *σ*-donation when R is a sufficiently weak *π*-donor. Along group 13, the TM→E^{I}R *π*-back-donation mostly follows the row (B >) Al > Ga > In (> Tl). In contrast however TM←E^{I}R *σ*-donation is irregular, Al^{I}R is always the strongest *σ*-donor and Tl^{I}R the weakest whilst B^{I}R, Ga^{I}R and In^{I}R have similar *σ*-donor strength.[11]

1.6 Relevant Groups R

Whilst many compounds E^{I}R like $Al_4(hyp)_4$ have been reported, only a select few have been successfully employed to form mononuclear, homoleptic TM compounds.[13]

E^{I}(C(TMS)$_3$)

In the late 1990s *Uhl*, *Pohlmann* and *Wartchow* were the first to use a ligand of the type E^{I}(C(TMS)$_3$) to synthesize a mononuclear, homoleptic coordination compound of the type [M(E^{I}R)$_n$] with [Ni(In(C(TMS)$_3$)$_4$] .[14] A year later quantumchemical calculations confirmed previous assumptions that E^{I}(C(TMS)$_3$) ligands were indeed strong *π*-acceptors and their back-bonding capabilities within magnitude of carbonyls, due to the lack of *π*-donor properties of R.[15] Though the initial ligands in this class, no more mononuclear, homoleptic compounds of E^{I}(C(TMS)$_3$) have been reported since the early 2000s

E^{I}-NHC analogous ligands

Of this ligands class, two distinct lines have emerged, though only the Ga derivates have produced homoleptic, mononuclear compounds. *Green*, *Jones,* and *Stasch* have reported on transition metal compounds of Ga[N(C$_6$H$_3$^{i}Pr$_2$)]$_2$CN(Cy)$_2$ in the 2000s.[16] Our own group around *R. A. Fischer* has investigated *P. P. Power's* bis-imidinate ligand Ga(DDP) during the same time.[17] This work is in the 2020s expanded on by *Morris*, *Rajeshkumar*, *Maron*, and *Okuda*.[18]

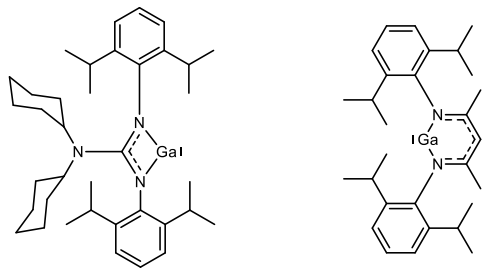

Figure 9: Structures of Ga[N(C$_6$H$_3$^{i}Pr$_2$)]$_2$CN(Cy)$_2$ (left) and Ga(DDP) (right).

Being isolobal to NHC's, these ligands are strong *σ*-donating ligands, having HOMOs of *sp* character on their Ga atoms, with unoccupied *p* orbitals giving them strong *π*-back-bonding capabilities. This, paired with their steric bulk makes them very suitable for stabilizing very low coordinated TM centers. It must be noted though that in the case of Ga(DDP), an additional ligand or solvent molecule is often bound to the Ga atoms in the form of $[M(Ga(L)(DDP))_n]$, a fact which the current research of *Okuda et. al.* is focusing on.[16-18]

*E^{I}Cp**

The synthesis of E^{I}Cp's have been reported as far back as the 1950s, with *E. O. Fischer et. al.* contributing InCp.[19] The more sterically demanding E^{I}Cp* were initially described between 1986 and 1993 by *O. T. Beachley et. al.* (InCp*) and *H. Schnöckel et. al.* (AlCp* & GaCp*).[20] Synthetic advancements of the recent decades have made these compounds more accessible as their initial syntheses relied on salt metathesis reactions of metastable E^I halogenides.[21] Shortly after their initial description, E^{I}Cp*s properties as ligands were realized. Initial studies by aforementioned groups quickly confirmed bonding behaviors akin to those found in carbonyls, such as μ^2-briding bonds.[21a, 22] The first homoleptic, mononuclear coordination compound of E^{I}Cp*, $[Ni(GaCp^*)_4]$ was reported in 1999 by *P. Jutzi et. al.*.[23] Continued interest, especially at our own group, since then has fostered an expansive list of reported TM-ECp* compounds of widely varying composition. Of those, the large clusters by *Ganesamoorthy*[24], *Weßing*[25], *Schütz*[26], *Muhr*[27] and *Antsiburov*[28] are amongst the most notable just out of this sub-class of compounds. In contrast to previous mentioned groups R, Cp* has filled, and delocalized *π*-orbitals, bound to E^I, thus the *π*-back-bonding properties of E^{I}Cp* are comparatively diminutive.[11]

E^{I}Cp* exhibits a high degree of variability in its bonding properties, which allows it to conform to a wide range of steric and electronic circumstances. Most commonly the C_5 ring of E^{I}Cp* is bound to E^I via all three of its delocalized *π*-electron pairs in an η^5-binding mode. η^3-, η^2- and η^1-binding can occur as a result of steric hinderance or increased electronic density competing at E^I competing with *π*-electron density from Cp*.[29] Alternatively, *σ*-binding via one of the carbon atoms in the C_5 ring, interrupting the aromaticity has been reported as a consequence of additional electron density introduced to the E^I atom by binding electron rich groups to E^I.[12]

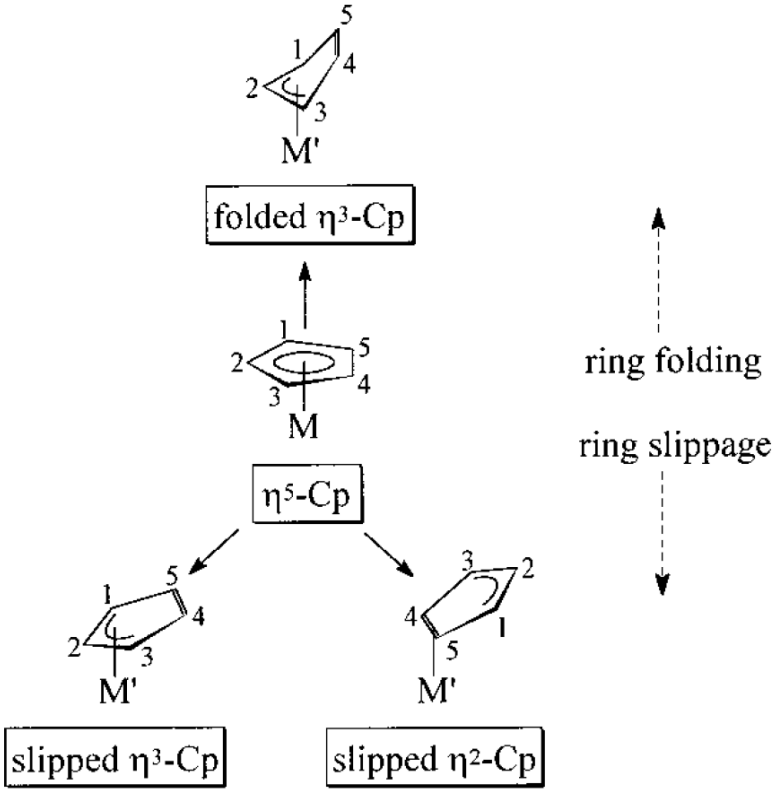

Figure 10: Depictions of the different η^n binding modes of Cp to a coordination center M. Reprinted (adapted) with permission from Organometallics 2000, 19, 26, 5549–5558. Copyright 2000 American Chemical Society.[29a]

The reduced *π*-electron density at E^I in lower hapticity-binding mode of E^{I}Cp* can be assumed to result in a qualitative increase in *π*-back-bonding properties at E^I, however an investigation into the effect of haptotropic shifts on the *π*-back-bonding properties of E^{I}Cp* specifically is absent from literature at the time of writing, so only inferences from related literature can be made with the quantitative extent still being an open question.[29a, 30]

Calculating a centroid in the C_5 ring of E$^I\eta^5$-Cp* allows to measure an angle M-E^I-Cp*. Contrary to intuition this angle consistently and significantly deviates from 180° in the crystal structure. These range from 6.5° deviation to 24.5°.[17b, 23, 31]

Another notable detail about E^{I}Cp* is that this ligand can undergo a Cp*-transfer, by which the Cp* group is transferred from E^I to a transition metal. This can be exploited synthetically, but in practice is often an unwanted side reaction.[32]

1.7 Quantification of Ligand Bulk and Geometry

Besides electronic and chemical properties, the geometric properties of a ligand have to be quantified to introduce a systematic description and understanding.

Tollman Cone Angle

In 1970 *C. A. Tolman* introduced the concept of cone angles to reason a systematic row of reactivity for phosphorous ligand exchange equilibria observed on zero valent nickel. A physical model of a ligand PR_3 was built from a CPK atomic model set to a scale of 1.25 cm/Å with the spheres representing the atoms in the model scaled to equal their respective *Van der Waals* radius. A ligand model was placed freely rotating atop a pin, equaling the length of a typical P-Ni bond (2.28 Å). The ligand model was rotated, and the maximum angle required for a straightedge to clear the model was measured off the axis of rotation. The sum of these angles on both sides of the ligand was defined as its cone angle θ. In models where R allowed for degrees of rotational freedom, an effort was made to minimize θ whilst maintaining threefold symmetry.[33]

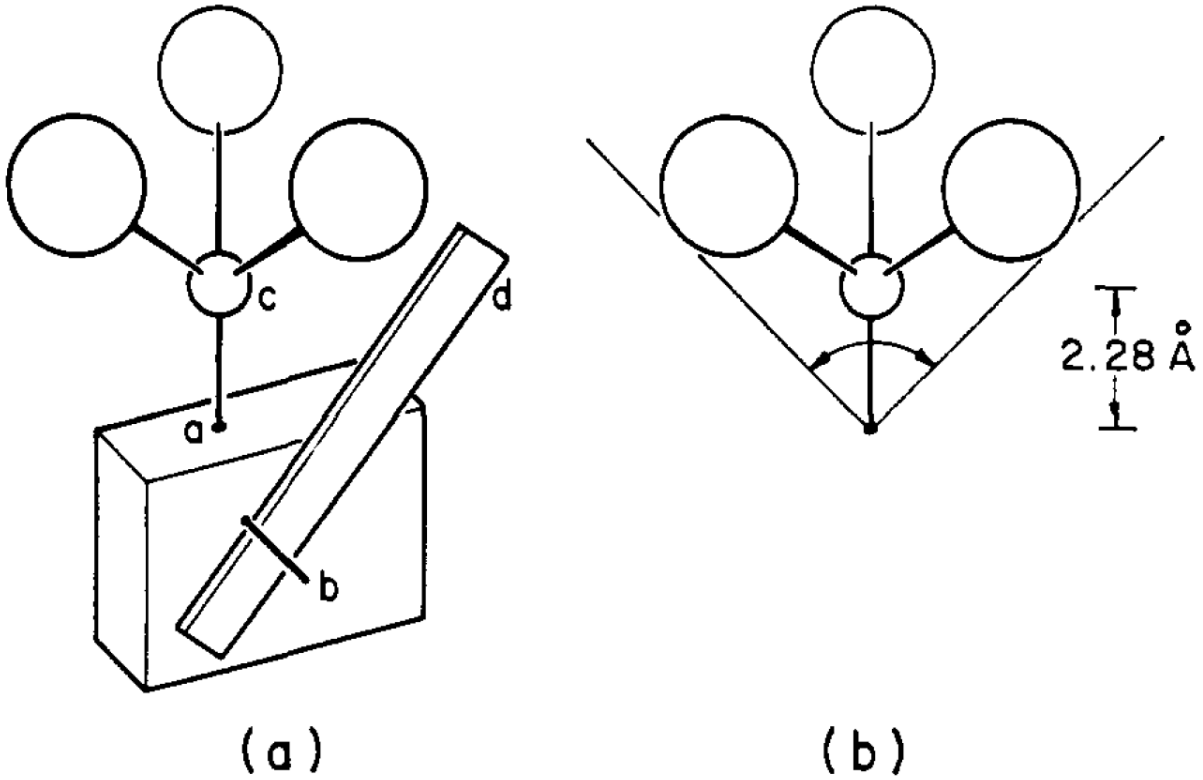

Figure 11: (a) schematic depiction of *Tolmans* ligand angle measurement device. The phosphorous atom c is supported by the freely rotating pin a with a length equating to 2.28 Å. The straightedge d measures the angle along the fulcrum b, which is the bottom of a. (b) the ligand cone. Reprinted (adapted) with permission from J. Am. Chem. Soc. 1970, 92, 10, 2956–2965. Copyright 1970 American Chemical Society.[33]

Tolman et. al. then later amended the original model to address inconsistencies that originated from initial simplifications. Minimizations of θ in the original work, caused to assume highly strained conformations of flexible PR_3 such as $P(O\text{-}^{i}Pr)_3$, PEt_3, or $P(O\text{-}o\text{-tolyl})_3$. Minimized angles θ based on mostly strain free ligand conformations now formed the basis of the measurements. A method to measure effective cone angles of asymmetrical ligands $PR^1R^2R^3$ was also introduced. In this every substituent R^i has its half angle $\theta_i/2$ determined individually to be combined into the effective cone angle defined as:[34]

$$\theta = \frac{2}{3}\sum_{i=1}^{3}\theta_i/2$$

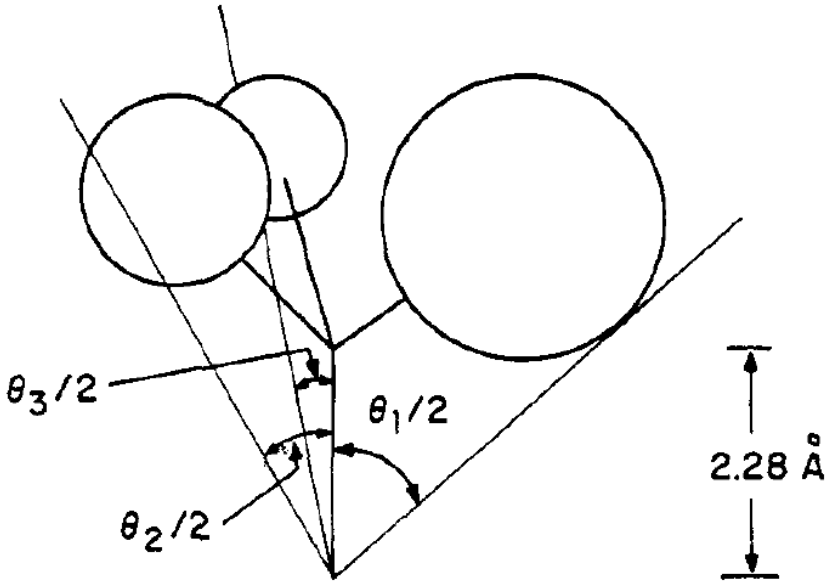

Figure 12: Measuring individual half angles for asymmetric ligands $PR^1R^2R^3$ according to *Tolman*. Reprinted (adapted) with permission from J. Am. Chem. Soc. 1974, 96, 1, 53–60. Copyright 1974 American Chemical Society.[34]

Its limitations however spawned a series of successors that tried to overcome those. Its reliance on physical models fails to accurately depict bond angles deviating from ideal tetrahedral geometry. Also, the balance between minimizing the cone angle of a ligand and the strain introduced is often more complex than just a minimization of strain to the maximum extent possible. Furthermore, though symmetrical in nature, a PR_3 ligand is not of cylindrical symmetry, so in practice phosphorous ligands can mesh their substituents, achieving higher coordination numbers than would be indicated just by their cone angle.[35]

The cone angle introduced by *Tolman* proved an easy to understand and apply tool to objectively quantify the steric bulk of phosphine ligands, some of its limitations were overcome in the years after its introduction and it remains a viable tool.[28] The principles introduced can be applied as starting point for the description of new ligands. *P. Jutzi et. al.* have applied these in 1998 to describe the geometric bulk of GaCp*.[21a]

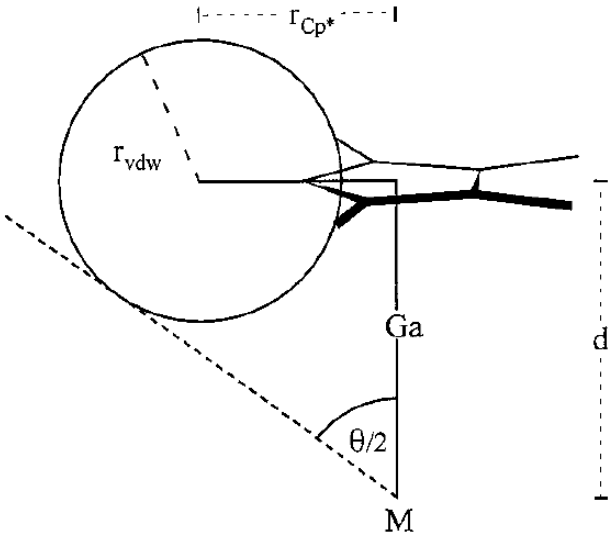

Figure 13: Determination of the cone angle of GaCp* according to *Jutzi* following the principles of *Tolman*. Reprinted (adapted) with permission from Organometallics 1998, 17, 7, 1305–1314. Copyright 1998 American Chemical Society.[21a]

Solid Cone Angle

Improving on the limitations of *Tolman's* cone angle is the concept of the solid cone angle, which borrows from the geometric concept of the solid angle as a unit of measurement. This considers the dependency of the ligand's angular encumbrance ½*θ* to the rotation of the ligand itself around the M-P bond axis *Φ*. Integration of the values 0 < *Φ* < 360° gives the generalized non-circular solid cone angle *Ω* in the unit [*sr*] (*steradian* or *square radian*).[36]

$$\Omega = \int_{\Phi=0}^{2\pi} (1 - \cos ½\theta)\mathrm{d}\Phi$$

Converting this into the angle *Θ* of an aperture of a circular cone having an equivalent solid cone angle *Ω* gives a more familiar set of values to work with.[36]

$$\Theta = 2\cos^{-1}\left(1 - \frac{\Omega}{2\pi}\right)$$

To this end, physical scale models of ligands were superseded by input data generated from quantum chemical calculations and/or crystal structures. Values obtained from this method are expectedly systematically lower than those reported from *Tolman's* method. Qualitatively this method can be visualized as the area of a "shadow" projected from the metal center of a coordination compound cast upon the inside of a unit sphere.[37] Moreover, the solid cone angle concept is expandable to include bidentate ligands.[38]

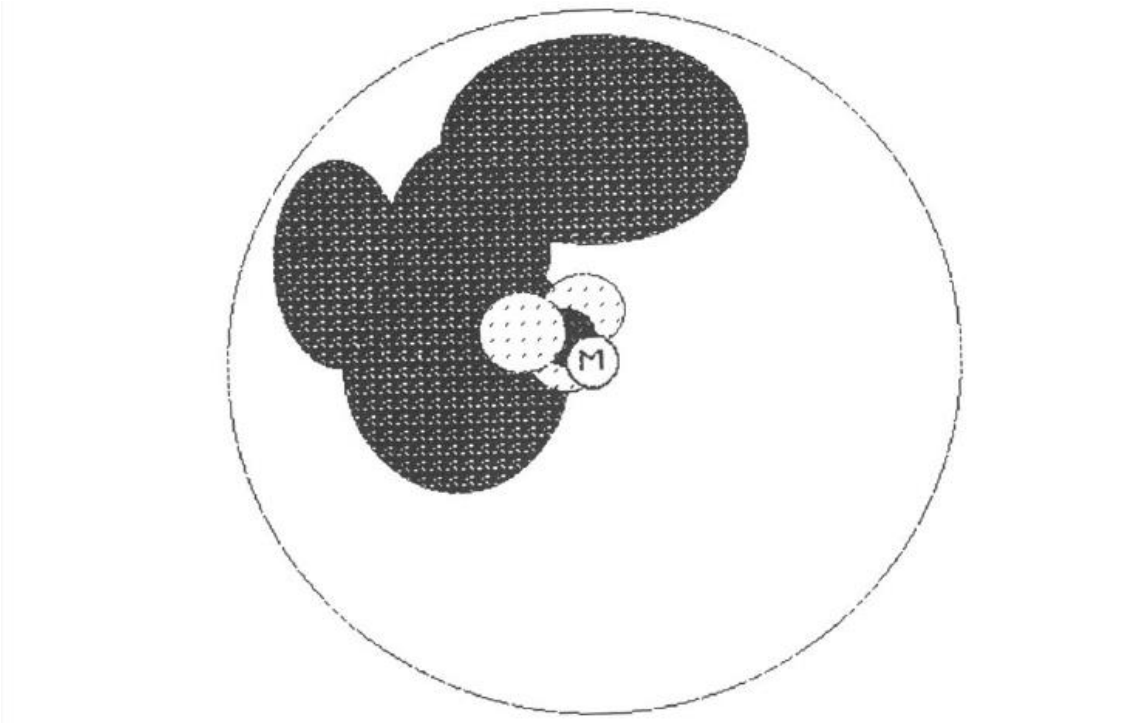

Figure 14: Illustration of the solid angle generated by a ligand bound to a metal M. Imagined as a light source, light cast from M is blocked by the ligand attached to M. A "shadow" (black) is projected upon the inside of a unit sphere, represented by the outer circle. Reprinted (adapted) with permission from T. L. Brown, K. J. Lee, Coordination Chemistry Reviews 1993, 128, 89-116 under license 6046480938290. Copyright 1993 Published by Elsevier B.V.[37]

Buried Volume and steric maps

The concept of buried volume (%V_{Bur}) is based on the amount of volume of a sphere centered around a central metal atom buried by overlap the atoms of a ligand. The volume of this spere represents the space around the central atom that must be shared by coordinated ligands, ergo the bulkier a ligand is, the more volume is buried beneath it, the higher %V_{Bur} is gonna be.[39]

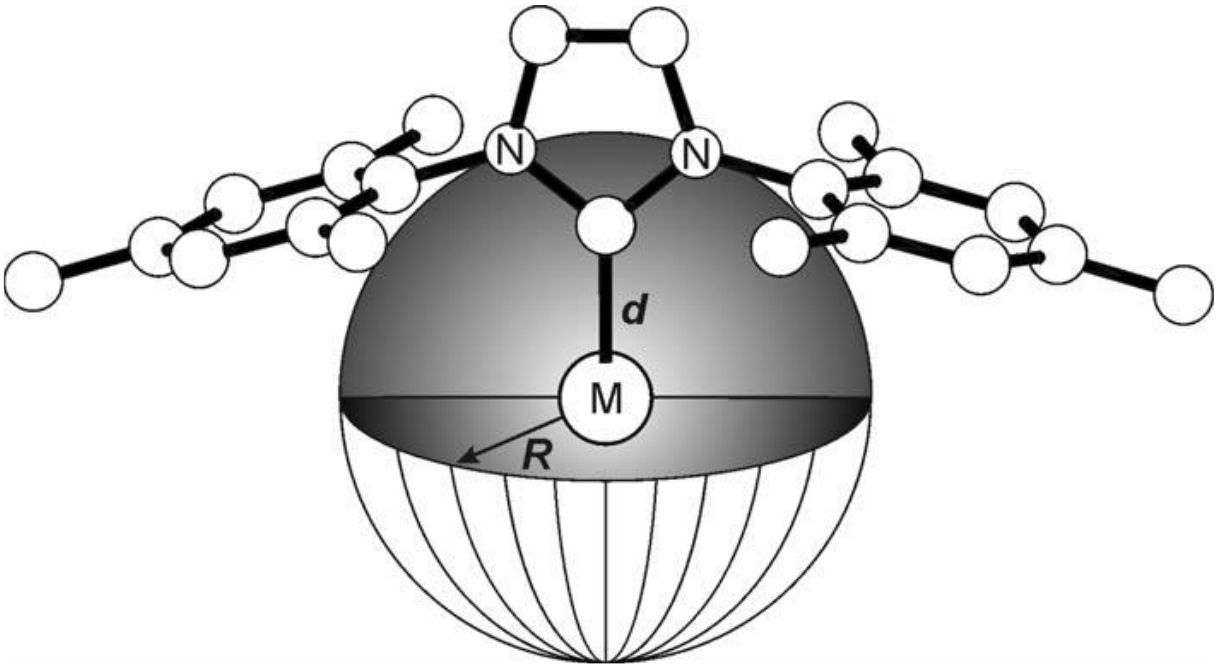

Figure 15: Graphical representation of the sphere with radius *R*, used to calculate %V_{Bur} values on the example of an NHC-type ligand bound to a metal center M at a distance *d*. Reprinted (adapted) with permission from Poater, A., Cosenza, B., Correa, A., Giudice, S., Ragone, F., Scarano, V. and Cavallo, L. (2009), SambVca: A Web Application for the Calculation of the Buried Volume of N-Heterocyclic Carbene Ligands. Eur. J. Inorg. Chem., 2009: 1759-1766. https://doi.org/10.1002/ejic.200801160 under license 604649007758. Copyright 2009 Wiley-VCH Verlag GmbH & Co. KGaA, Weinheim.[40]

To this end, the position of a metal center M is defined, either from crystal structure or by mathematical modeling. A sphere with radius *R* is built around M. This sphere is approximated by sectioning into a regular 3D cubic mesh of spacing *s*, which defines cubic voxels v_{xyz} with a volume of s^3. The distance from the center of each individual voxel to all atoms in the ligand is tested to check if any atoms are within van der Waals distance from the tested voxel. If this test is negative, i.e. no atom is within van der Waals distance from the voxel in question the volume s^3 of the voxel is counted towards the free Volume V_{free}. On the other hand, if the test is positive with an atom being within van der Waals distance of the center of the examined voxel, the volume s^3 of the voxel is counted towards the buried volume V_{bur}.[40]

$$V_{Sphere} = \sum v_{xyz} = V_{free} + V_{Bur} = \sum v_{xyz}(free) + \sum v_{xyz}(buried)$$

A more intuitive resulting value is obtained by transforming into %V_{bur} as follows:[40]

$$\%V_{bur} = 100 \cdot \frac{V_{Bur}}{V_{Sphere}}$$

The sphere radius *R* used in the calculations has commonly been chosen in the past to be 3.5 Å to best represent the relevant coordination sphere by correlation of V_{bur} to DFT bonding energies of NHC type ligands. In the same manner the atomic radii were chosen as Bondi radii scaled by a factor of 1.17.[40]

As convenient as the characterization of a ligand's steric properties in terms of a single one-dimensional number is, it oversimplifies and looses critical information, such as

symmetry or specific shape. A representation of these properties however can be obtained by a modification of the procedure outlined above. After all the voxels in the sphere are marked as either belonging to V_{Bur} or V_{free} for x and y coordinates, the sphere is examined from the top (i.e. positive z) to determine z of the first buried voxel. These points are defining a surface $S(x,y) = z_{bur}$, representing the surface of the ligand. The steric maps obtained with these methods are a two-dimensional isocontour representation of the interaction surface.[41]

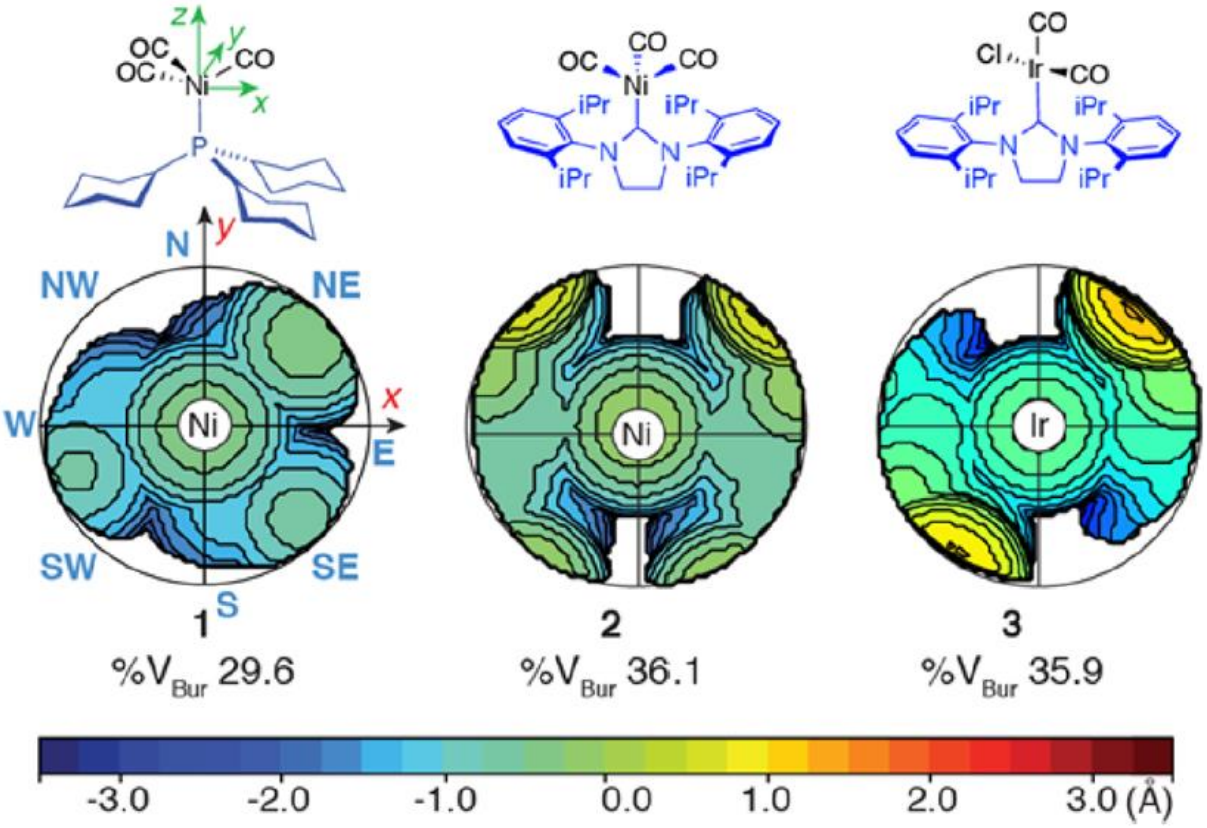

Figure 16: Steric maps of transition metal complexes. First row shows structural formula, second row shows the calculated steric maps. Central metal atom and CO ligands (marked black) were excluded from the calculations in order to obtain a steric map of the ligand (marked blue) the position of the central metal atom (white center circle) was edited in afterwards for orientation purposes. Colored strip on the bottom serves as a scale. Reprinted (adapted) under an ACS AuthorChoice License, which permits copying and redistribution of the article or any adaptations for non-commercial purposes from Organometallics 2016, 35, 13, 2286–2293. Copyright 2016 American Chemical Society.[41b]

1.8 Mathematical description of Compound Geometry

Depending on the number of ligands attached to a metal center (coordination number; CN), the ligands distribute in certain geometric body. These depend on a variety of factors, such as ligand bulk and shape, denticity as well as the electronic properties of both, the central atom and the ligand.[1] The bodies and deviation from the ideal bodies can give insight into the splitting of the *d*-orbitals of the central metal atom and thus into the effects stabilizing or destabilizing the compound. A method to mathematically quantify how close a given body is to a reference is Continuous Shape Measure. The method of continuous shape measure uses the N vertices of an experimentally

determined coordination polyhedron normalized and centered in the origin of a three-dimensional cartesian coordinate system as their position vectors Q_i (i = 1, 2, 3, …, N). These are compared to the position vectors P_i (i = 1, 2, 3, …, N) of the N vertices of an ideal reference polyhedron which is equally centered and normalized. This is expressed as:[42]

$$S_Q(P) = \frac{1}{N} min \sum_{i=1}^{N} \left|\overrightarrow{Q_i} - \overrightarrow{P_i}\right|^2 \times 100$$

A value of $S_Q(P) = 0$ thus represents the exact ideal shape, with increasing values indicating increasing distortions. This value was calculated from most ideal superimposition, determined by minimizing the distance between the superimposed polyhedral vertices by a numerical rotation algorithm. $S_Q(P)$ thus is the global minimum of these permutations. In general, $S_Q(P) = 0$ indicates no distortion from the reference, $S_Q(P) < 1.00$ indicates minor distortions and $1.00 < S_Q(P) < 3.00$ indicates major distortions from the reference shape.[42]

Another parameter to describe the geometry of a compound is the τ_5 value. This value is specifically calculated to describe five-coordinate compounds, which can form a trigonal bipyramidal or a square pyramidal geometry.[43]

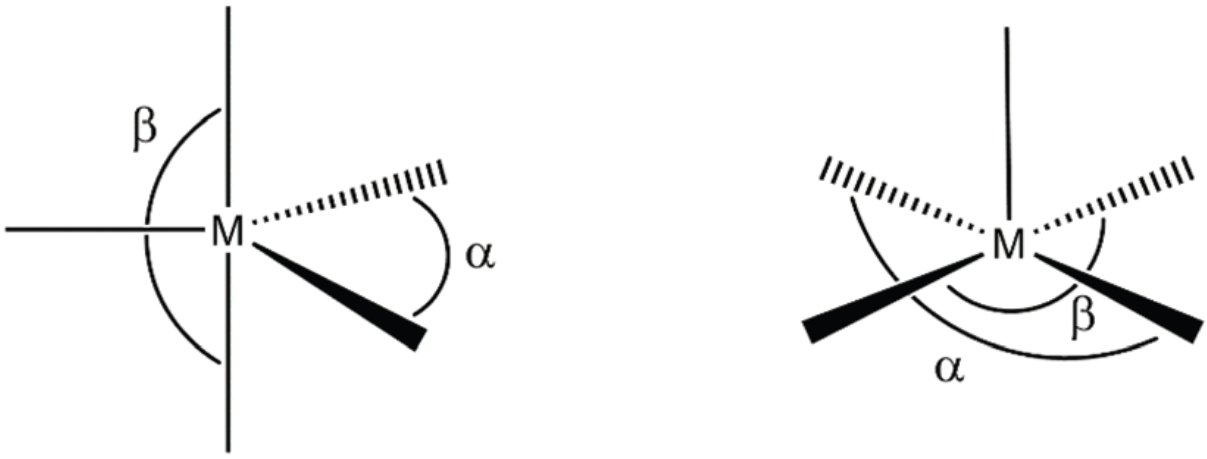

Figure 17: Idealized geometries of a trigonal bipyramid (left; $\alpha = 120°$, $\beta = 180°$, D_{3h}) and a square pyramid (right; $\alpha = \beta = 180°$, C_{4v}) around a metal center M. Reprinted (adapted) with permission from A. G. Blackman, E. B. Schenk, R. E. Jelley, E. H. Krenske, L. R. Gahan, Dalton Transactions 2020, 49, 14798-14806 under license 1619769-1. Copyright 2020 The Royal Society of Chemistry.[43]

Considering the ideal values for the angles α and β, a relationship can be formulated as $(\alpha - \beta) = 60$ for a trigonal bipyramid and $(\alpha - \beta) = 0$ for a square pyramid. The τ_5 is defined from this as:[43]

$$\tau_5 = \frac{(\alpha - \beta)}{60}$$

The τ_5 received from this calculation is mostly between 0 and 1 but can exceed 1. A value of $\tau_5 = 0$ is obtained for both, an ideal square pyramid as well as a basally distorted square pyramid, where M is elevated above the square plane, which is the

exceedingly more common of the two structures. A value of $\tau_5 = 1$ is obtained for an ideal trigonal bipyramid, whilst a value of $\tau_5 > 1$ indicates an equatorially distorted trigonal bipyramid. Therefore, structures where $0 < \tau_5 < 0.500$ are described as "distorted square pyramidal" and as "distorted trigonal bipyramidal" for $0.500 < \tau_5 < 1.000$. A value of exactly 0.500 for τ_5 can only be achieved in very unfavorable or transitionial geometries and crystallographic examples are absent from literature.[43]

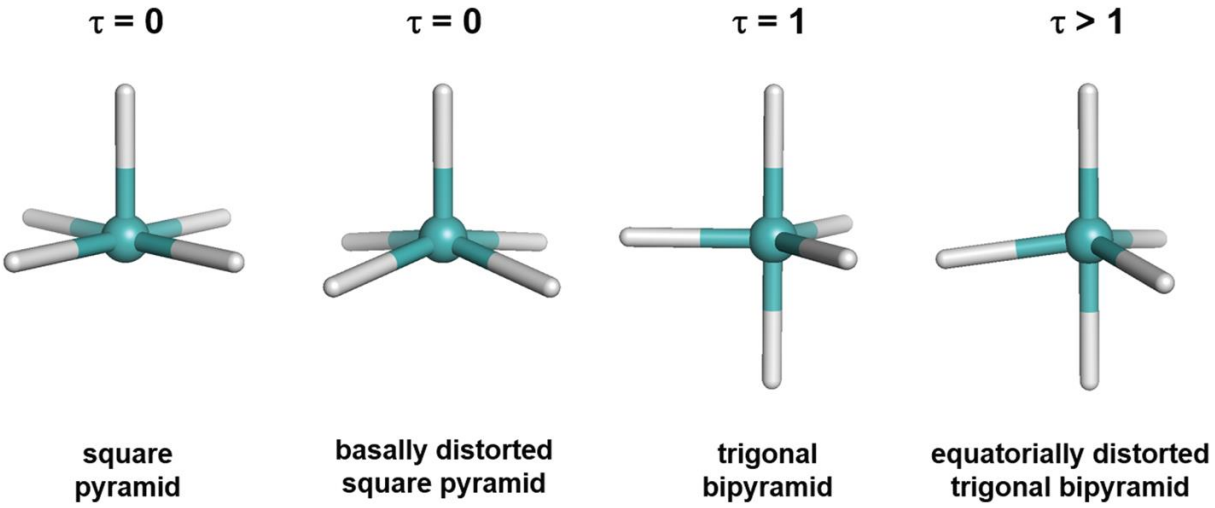

Figure 18: Five-coordinate structures with their associated τ_5 values. Reprinted (adapted) with permission from A. G. Blackman, E. B. Schenk, R. E. Jelley, E. H. Krenske, L. R. Gahan, Dalton Transactions 2020, 49, 14798-14806 under license 1619769-1. Copyright 2020 The Royal Society of Chemistry.[43]

1.9 A new Starting Point: GaTMP

Intruduced by *G. Linti et. al.* in 2007, GaTMP is the Ga(I) compound of 2,2,6,6-Tetramethylpiperidide, originally synthesized from “GaI” and LiTMP. Like many other compounds $E^{I}R$ it exhibits a tetrameric structure in the solid state.[44]

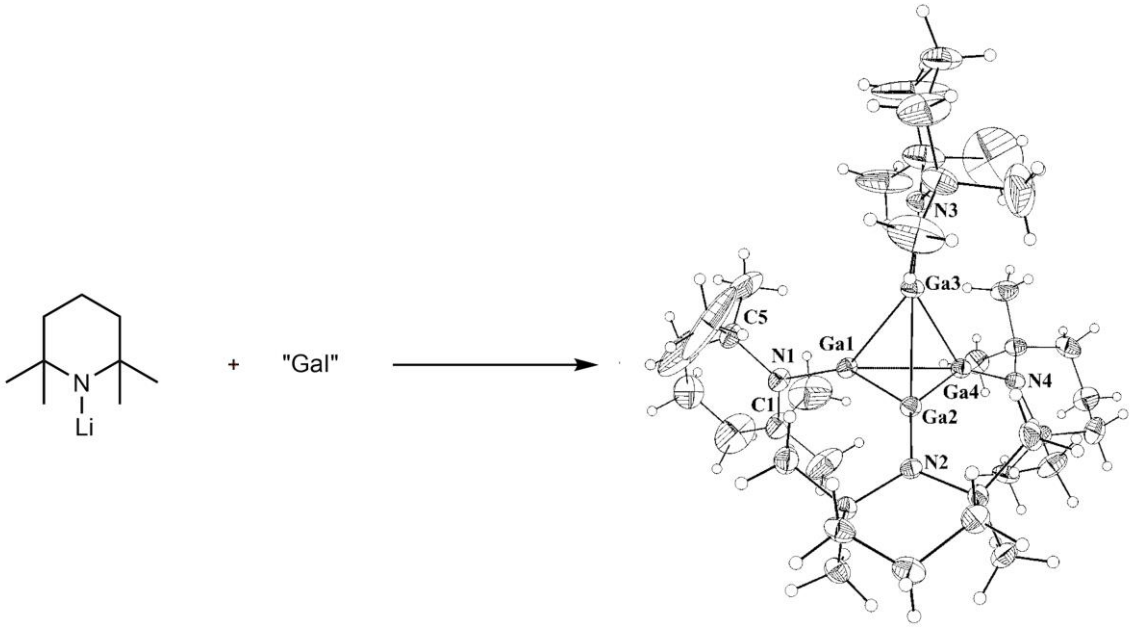

Figure 19: Simplified reaction scheme depicting the synthesis of GaTMP from LiTMP and “GaI”. GaTMP is depicted as the tetrameric form found in the crystal structure.(adapted graphic)[44] Note the deliberate use of quotation marks to denote “GaI” henceforth due to this reagent not being a single identifiable species but rather a mixture of different composition Ga-I clusters overall behaving as a monovalent Ga(I) halide. Reprinted (adapted) with permission from Seifert, A. and Linti, G. (2007), Synthesis and Structure of Tetrameric Gallium(I) Amides. Eur. J. Inorg. Chem., 2007: 5080-5086. https://doi.org/10.1002/ejic.200700537 under license 6046500000776. Copyright 2007 Wiley-VCH Verlag GmbH & Co. KGaA, Weinheim.[21b, 45]

In the solid state, the six membered piperidine ring of GaTMP presents in the “lawnchair” configuration with half of the four methyl groups directed equatorially and the other half directed axially. Note that those groups only present as one single, characteristic singlet signal at $\delta(C_6D_6)$ = 1.65 ppm in ^{1}H-NMR.[44] A decoalescence into two signals has not been observed yet even during low temperature measurements.

The central feature of GaTMP, the triangular coordination of an N atom by two C and one Ga atom, is nearly planar. The average Ga-N distances found in pure GaTMP are 1.885 Å.[44]

Quantum chemical calculations on the compound indicate that in the monomer of GaTMP, the HOMO-1 orbital is made up of the Ga 4s orbital, with the HOMO exhibiting properties of a *π*-bond between Ga and N, polarized towards N. LUMO and LUMO+1 on the other hand, exhibit mainly Ga 4p character. In the tetrameric form, the calculations indicate a loss of π-bond participation.[44]

As of now, there have only been two reports of transition metal compounds of GaTMP.

GaTMP was reacted with [(CO)$_5$Cr(cyclooctene)] to form [(CO)$_5$Cr(GaTMP)] and [(CO)$_3$Cr(GaTMP)$_3$Cr(CO)$_3$]. Similarly, [(CO)$_3$Co(GaTMP)$_2$Co(CO)$_3$] was obtained from [Co$_2$(CO)$_8$], and [Ni$_2$(GaTMP)$_7$] from [Ni(COD)$_2$].[46]

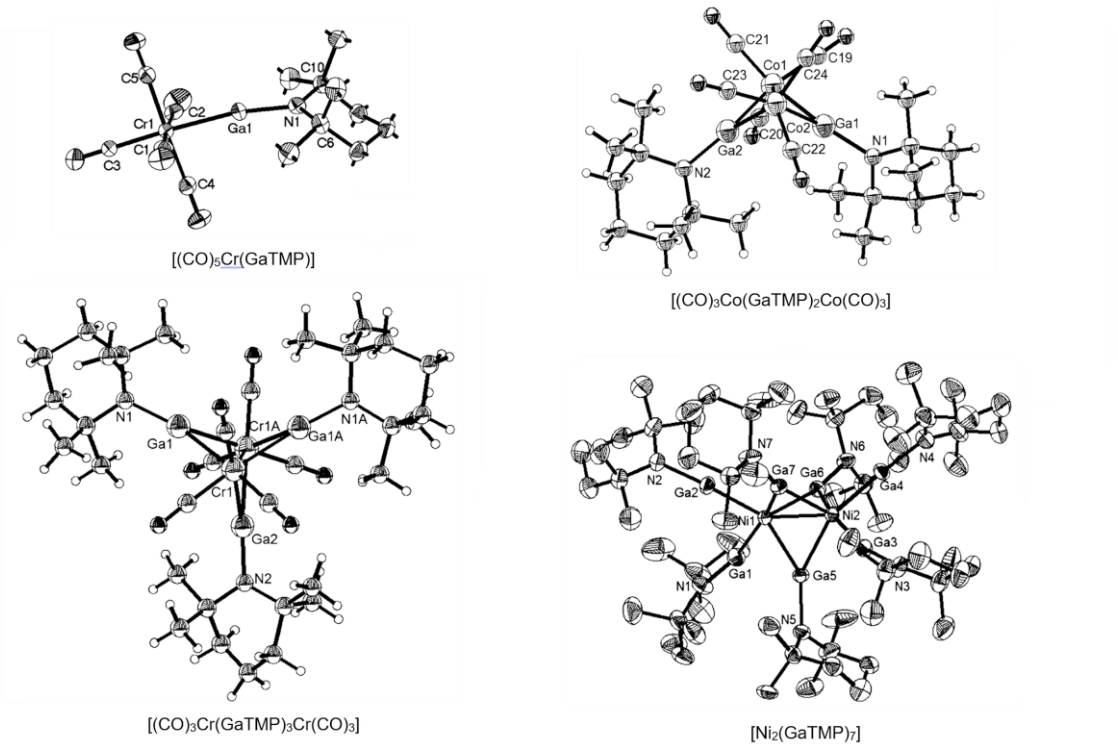

Figure 20: Transition metal compounds of GaTMP reported by *G. Linti et. al.* in 2008. Crystallographically determined molecular structures of [(CO)$_5$Cr(GaTMP)] (top left), [(CO)$_3$Cr(GaTMP)$_3$Cr(CO)$_3$] (bottom left), [(CO)$_3$Co(GaTMP)$_2$Co(CO)$_3$] (top right), and [Ni$_2$(GaTMP)$_7$] (bottom right). Thermal ellipsoids drawn at the 30% probability level. Reprinted (adapted) with permission from A. Seifert, G. Linti, Inorganic Chemistry 2008, 47, 11398-11404. Copyright 2008 American Chemical Society.[46]

This was only recently followed up by *M. Muhr* in 2023, synthesizing [Ni$_3$(GaTMP)$_7$] via a procedure adapted from the above mentioned synthesis of [Ni$_2$(GaTMP)$_7$] and investigating its properties as a semihydrogenation catalyst.[27b]

Both works clearly indicate that GaTMP reacts very similarly to the already widely explored GaCp*, though also has notable differences. This is especially apparent when considering another publication by *M. Muhr* describing the clusters formed by the reaction of [Ni(COD)$_2$] with GaCp*, wherein the products are defined by the Cp* transfer reaction from Ga to Ni.[27a] As this or a similar process apparently is not present in the reaction with GaTMP an entirely different product could be obtained.

Thus, further research into the chemistry of GaTMP-transition metal compounds is warranted. This is a) to determine any other significant differences in reactivity which might lead to reactivities with metals previously unsuitable, and b) to explore whether the products of those reactions show differences in their behavior when compared to their GaCp* analogues. Knowledge obtained from the previous exploration of GaCp* should be put to use in order to efficiently explore already mapped paths for their feasibility. Whilst the previous works have already produced cluster compounds, a step back should be taken to first establish a series of mononuclear, homoleptic

compounds, in order to gain insight into general procedures, reactivities and establish a common unified dataset, from which future works can deduce trends, reference and build up on. This is the aim of this thesis.

2. Results and Discussion

2.1 Characterization of new Compounds

*[Ru(GaTMP)$_5$](**1**)*[47]

Compound **1** was obtained as a brown, crystalline solid, suitable for SC-XRD, by reacting [Ru(η^4-COD)(η^6-COT)] with 1.25 eq. (GaTMP)$_4$ in toluene at 100 °C for 19 h. After recrystallization from *n*-hexane, **1** was isolated in a yield of 20% (based on Ru).

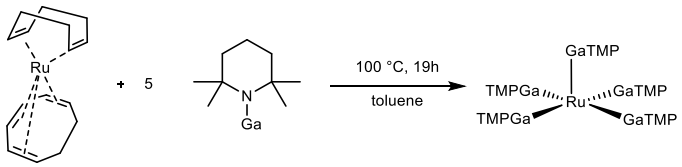

Figure 21: Reaction scheme for the synthesis of [Ru(GaTMP)$_5$] by ligand substitution of the olefinic precursor complex. Reprinted (adapted) with permission from R. Bühler, R. J. J. Weininger, J. Stephan, M. Muhr, B. M. T. Bock, C. Gemel, R. A. Fischer, Dalton Transactions 2024, under CC BY 3.0 license. Copyright 2024 The Royal Society of Chemistry.

The C, H and N values of **1** obtained by elemental analysis are within the expected range. The ^{1}H-NMR and ^{13}C-NMR in C_6D_6 (25 °C; see Fig. S 1) indicate the presence of five equivalent TMP groups with only minor shifts of all signals with respect to free (GaTMP)$_4$.[44] Trace impurities are almost absent. The presence of only one set of signals for all five GaTMP units indicates a fast fluxional process, which is very common for five-coordinate metal complexes.[48] The IR spectrum (see Fig. S 3) does not show absorption bands in the region associated with Ru-H vibrations (*ca.* 1900 cm^{-1}-1700 cm^{-1}) and all features can be assigned to the TMP groups.[49]

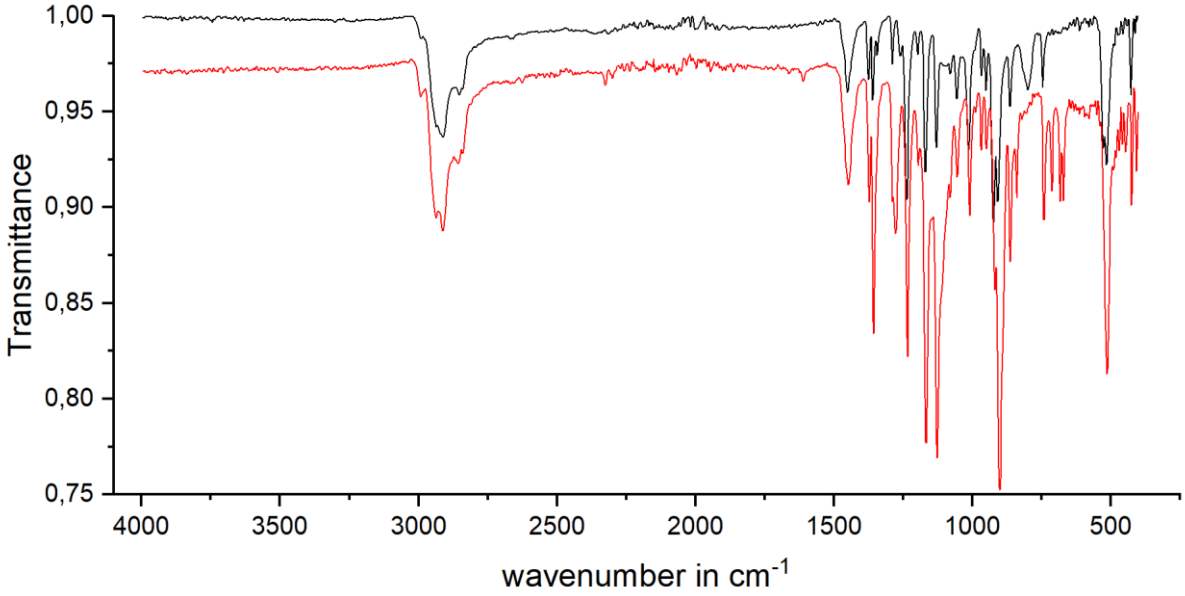

Figure 22: FT-ATR-IR spectra of (**1**) (black) and GaTMP (red). Reprinted (adapted) with permission from R. Bühler, R. J. J. Weininger, J. Stephan, M. Muhr, B. M. T. Bock, C. Gemel, R. A. Fischer, Dalton Transactions 2024, under CC BY 3.0 license. Copyright 2024 The Royal Society of Chemistry.

High resolution LIFDI-MS (see Fig. S 4) gives a molecular ion $[M]^+$ signal of 100% relative intensity at 1151.25 *m/z* (calcd. *m/z* 1151.25) and a fragment $[M\text{-}TMP]^+$ signal at 1011.11 *m/z* of 1.6% rel. intensity (calcd. *m/z* 1011.11).

Compound **1** crystallizes in the monoclinic space group *C2/c*. The molecular unit of **1** exhibits a square pyramidal coordinated Ru center that is slightly distorted along the z-axis, elevating the Ru above the Ga_4 plane by 0.545 Å, with Ga_{ax1}-Ru-Ga angles in the range of 103.0-104.6°. The Ru–Ga bond lengths show only a slight variance between 2.274 Å (Ru1-Ga3), 2.291 Å (Ru1-Ga1) and 2.281 Å (Ru1-Ga2) but are significantly shortened by 0.10 Å-0.15 Å compared to known Ru-GaCp* complexes.[49-50]

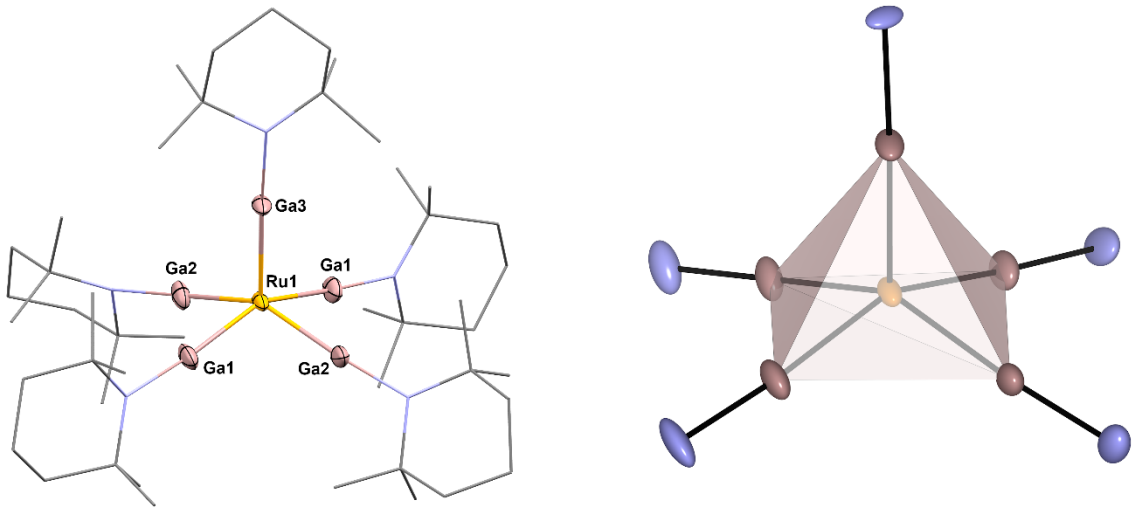

Figure 23: Left: molecular structure of $[Ru(GaTMP)_5]$ (**1**) in the solid state determined by single crystal X-ray diffraction. Ru: yellow, Ga: pink, N: blue and C: grey. Hydrogen atoms and disordered molecule fragments are omitted. C and N are displayed as wireframe. Right: square pyramidal coordination polyhedron calculated from crystal structure data. Thermal ellipsoids are shown at the 50% probability level. Selected bond lengths [Å] and

angles [°]: Ru1–Ga3: 2.274(10) Ru1–Ga2$^{\#1}$/Ga2: 2.281(7), Ru1–Ga1$^{\#1}$/Ga1: 2.291(6), Ga3–Ru1–Ga2$^{\#1}$/Ga2: 104.6(2), Ga3–Ru1–Ga1$^{\#1}$/Ga1: 103.0(2), Ga2–Ru1–Ga1: 84.2(3), Ga2–Ru1–Ga1$^{\#1}$: 89.3(2). Note: Ga1/Ga1$^{\#1}$ and Ga2/Ga2$^{\#1}$ are symmetry related. Reprinted (adapted) with permission from R. Bühler, R. J. J. Weininger, J. Stephan, M. Muhr, B. M. T. Bock, C. Gemel, R. A. Fischer, Dalton Transactions 2024, under CC BY 3.0 license. Copyright 2024 The Royal Society of Chemistry.

The geometry of the [RuGa$_5$] core was analyzed by means of continuous shape measure, finding $S_Q(P) = 0.99$, when comparing to a basally distorted square pyramidal structure where the central atom was placed in the centroid of the pyramid. Calculations for the ideal square pyramid gave a value of $S_Q(P) = 4.63$ and for ideal trigonal bipyramid a value of $S_Q(P) = 7.63$. The τ_5 value was found to be 0.0565, which is very close to the value associated with a basally distorted square pyramid of 0.

[Mo(GaTMP)$_6$](**2**)[47]

Compound **2** was obtained in an analogous synthesis to **1** by reaction of [Mo(η^4-C$_4$H$_6$)$_3$] with 1.5 eq. of (GaTMP)$_4$ in toluene at 110 °C for 22 h. **2** was isolated as a beige, crystalline solid suitable for SC-XRD in a total yield of 42% after workup (based on Mo).

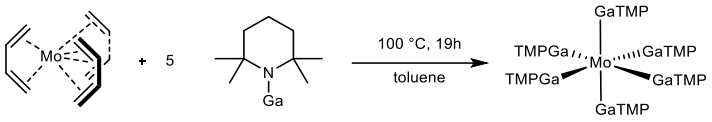

Figure 24: Reaction scheme for the synthesis of [Mo(GaTMP)$_6$] by ligand substitution of the olefinic precursor complex. Reprinted (adapted) with permission from R. Bühler, R. J. J. Weininger, J. Stephan, M. Muhr, B. M. T. Bock, C. Gemel, R. A. Fischer, Dalton Transactions 2024, under CC BY 3.0 license. Copyright 2024 The Royal Society of Chemistry.

The C, H and N values of **2** obtained by elemental analysis are within the expected range. ^{1}H-NMR and ^{13}C-NMR spectra in toluene-d_8 exhibit each set of TMP signals, which are only shifted slightly with respect to the signals of **1** or free (GaTMP)$_4$.[44] IR spectroscopy provides data very similar to **1** and shows no absorption in the range of typical Mo-H vibrations between 1900 cm^{-1} and 1650 cm^{-1} that would indicate the presence of hydrides (see Fig. S 8).[51]

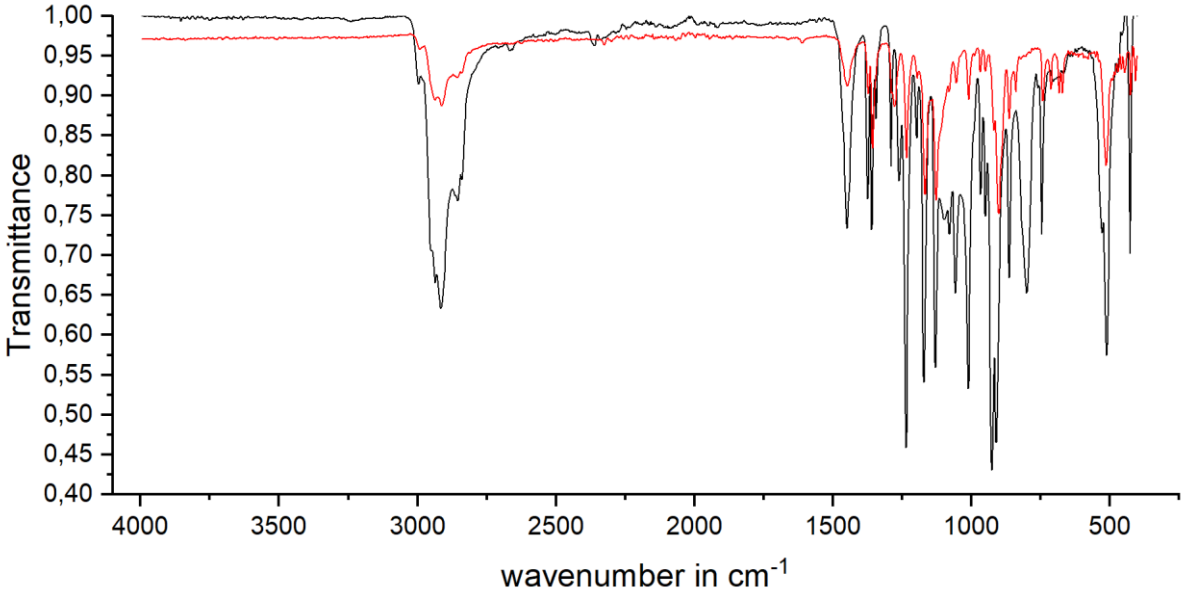

Figure 25: FT-ATR-IR spectra of (**2**) (black) and GaTMP (red). Reprinted (adapted) with permission from R. Bühler, R. J. J. Weininger, J. Stephan, M. Muhr, B. M. T. Bock, C. Gemel, R. A. Fischer, Dalton Transactions 2024, under CC BY 3.0 license. Copyright 2024 The Royal Society of Chemistry.

High resolution LIFDI-MS (see Fig. S 9) gives a molecular ion $[M]^+$ signal of 100% relative intensity at 1356.32 *m/z* (calcd. *m/z* 1356.32). Compound **2** crystallizes in the monoclinic space group $P2_1/c$, with two crystallographically distinct units per unit cell, both exhibiting six Ga(TMP) ligands coordinating in an octahedral fashion around the Mo centers. In relation to each other, the two independent octahedral units are rotated along all three axis. The average Mo-Ga bond lengths of the independent units are 2.385 Å and 2.386 Å with minimal deviation. Ga-Mo-Ga angles in both units point to a slight distortion from the ideal octahedral geometry and range between 81.9° and 94.2°. The analogous $[Mo(GaCp^*)_6]$ shows less angular distortion with Ga-Mo-Ga angles between 85.1° and 94.2° with slightly elongated Mo-Ga bonds (average: 2.462 Å, shortest bond: 2.358 Å).[29b]

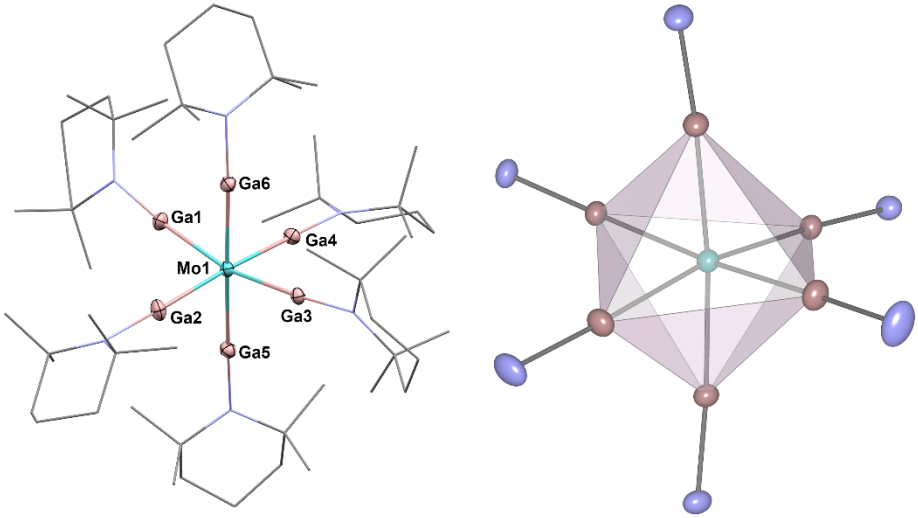

Figure 26: Left: molecular structure of $[Mo(GaTMP)_6]$ (**2**) in the solid state determined by single crystal X-ray diffraction. Mo: turquoise, Ga: pink, N: blue and C: grey. Hydrogen atoms and disordered molecule fragments are omitted. C and N are displayed as wireframe. Right: octahedral coordination polyhedron calculated from crystal structure data. The two crystallographically distinct units present in the SC-XRD data are very similar and most likely an effect of packing; the unit with higher deviations in bond lengths is depicted. Thermal ellipsoids are shown at the 50% probability level. Selected bond lengths [Å] and angles [°]: Mo1–Ga6: 2.374(2), Mo1–Ga3: 2.396(3), Ga6–Mo1–Ga1: 81.9(9), and Ga5–Mo1–Ga3: 97.7(9). (largest/smallest). Reprinted (adapted) with permission from R. Bühler, R. J. J. Weininger, J. Stephan, M. Muhr, B. M. T. Bock, C. Gemel, R. A. Fischer, Dalton Transactions 2024, under CC BY 3.0 license. Copyright 2024 The Royal Society of Chemistry.

Continuous shape measure calculations comparing the $[MoGa_6]$ core to the ideal octahedron gave a value of $S_Q(P) = 0.20$, which is almost identical to the value of $[Mo(GaCp^*)_6]$.[29b]

2.2 Current state of homoleptic mononuclear Compounds $[M(E^IR)_n]$[47]

Before the publication of compounds **1** and **2** there have been almost 25 years of research into $[M(E^IR)_n]$ compounds. And whilst the following list is exhaustive, the reader must be aware that it is limited to compounds with published crystallographic characterization. Many of the compounds are reported in conjunction with related heteroleptic or cluster compounds. A short chronology of the development in the field is presented thus.

In an endeavor to explore the then arising topic of isolobality between CO and E^IR ligands to gain access to a new class of mononuclear intermetallic complexes, *W. Uhl et. al.* in 1998 published the first compound $[M(E^IR)_n]$ with $[Ni(InC(TMS)_3)_4]$.[14] The homologous $[Ni(GaC(TMS)_3)_4]$ followed shortly after further proving the concept beyond Indium.[15] $[Pt(InC(TMS)_3)_4]$ provided the first example of a homoleptic 3rd row $[M(E^IR)_n]$ compound.[52] During this time *P. Jutzi et. al.* presented $[Ni(GaCp^*)_4]$, thus providing a vital broadening of the field.[23] With $[Pd(GaCp^*)_4]$, $[Pd(InC(TMS)_3)_4]$ and $[Pt(GaCp^*)_4]$ the homologous Ni-Pd-Pt rows of $InC(TMS)_3$ and $GaCp^*$ were completed by *R. A. Fischer et. al.* in 2003.[31b] The homologous homoleptic, mononuclear

compounds of AlCp*, [Ni(AlCp*)$_4$] and [Pd(AlCp*)$_4$] established AlCp* within the row of E^{I}R ligands employed with synthetic success.[31c, 53] The more electron rich transition metals yielded the respective cationic, homoleptic compounds [Zn(GaCp)$_4$][BAr$^F{}_4$]$_2$, [Cu(GaCp*)$_4$][BAr$^F{}_4$] and [Ag(GaCp*)$_4$][BPh4].[17b, 31a] [Fe(AlCp*)$_5$] and [Ru(AlCp*)$_5$] are the first examples of homoleptic C-H activated isomers of [M(E^{I}R)$_n$] complexes outside the d^{10} group with more than four group 13 metals coordinated.[50a] Though not strictly homoleptic [(GaCp*)$_4$Rh(MeGa(η^1-Cp*)] and [(GaCp*)$_4$Rh((OTf)Ga(η^1-Cp*)] continue a trend of higher coordination numbers.[29b, 54] The haptotropically shifted, halogen bridged [(GaCp*)$_3$Ru(GaCl(η^1-Cp*))(Ga$_2$(μ-Cl)(η^1-Cp*))$_2$] provided the first hexa group 13 coordinated compound within the family.[50c] The highest unhalogenated coordination number within the group stands at six provided by the only haptoropically shifted [Mo(GaCp*)$_6$].[29b, 55]

Another group of mononuclear homoleptic intermetallic [M(E^{I}R)$_n$] compounds is based on Ga(DDP). The first one [Au(Ga·(THF)(DDP))$_2$][BArF] was also presented by *R. A. Fischer et. al.* in 2006.[17a] This was followed up by [Zn(Ga(Me)(DDP))$_2$].[17b] With [Hg(Ga(SC$_6$F$_5$)(DDP))$_2$] the first homoleptic [M(E^{I}R)$_n$] compound of Mercury was obtained.[56] [Cu(Ga(DDP))$_2$][OTf] then was the first and as of now only homoleptic complex of the series where the Ga(DDP) was only bound to the central atom M.[17c] Interest in this class of compounds has not abated, just in 2022, *J. Okuda et. al.* published their work around [Zn(GaH(DDP))$_2$].[18] This group of compounds generally does not exceed a coordination number of two around the central metal atom. However, *C. Jones et. al.* reported a coordination number of three with their NHC analogous Ga[N(Ar)]$_2$CNCy$_2$ in the homoleptic [Pt(Ga[N(Ar)]$_2$CNCy$_2$)$_3$].[16]

Table 1: List of homoleptic and closely related [M(E^{I}R)$_n$] compounds reported previous to the publication of [Ru(GaTMP)$_5$] and [Mo(GaTMP)$_6$], sorted by coordination number of central atom M and element E. Reprinted (adapted) with permission from R. Bühler, R. J. J. Weininger, J. Stephan, M. Muhr, B. M. T. Bock, C. Gemel, R. A. Fischer, Dalton Transactions 2024, under CC BY 3.0 license. Copyright 2024 The Royal Society of Chemistry.

Compounds with central atom coordination number = 2	
[Au(Ga·(THF)(DDP))$_2$][BAr$^F{}_4$]	A.Kempter, C.Gemel, N.J.Hardman, R.A.Fischer, *Inorganic Chemistry*, 2006, **45**, 3133
[Hg(Ga(SC$_6$F$_5$)(DDP))$_2$]	G.Prabusankar, C.Gemel, M.Winter, R.W.Seidel, R.A.Fischer, *Chemistry-A European Journal*, 2010, **16**, 6041
[Zn(GaH(DDP))$_2$]	Louis J. Morris, Thayalan Rajeshkumar, Laurent Maron, Jun Okuda, *Chemistry-A European Journal*, 2022, **28**, e202201480, DOI: 10.1002/chem.202201480

$[Cu(Ga(DDP))_2][OTf]$	G.Prabusankar, S.Gonzalez-Gallardo, A.Doddi, C.Gemel, M.Winter, R.A.Fischer, *European Journal of Inorganic Chemistry*, 2010, 4415
$[Zn(Ga(Me)(DDP))_2]$	A.Kempter, C.Gemel, T.Cadenbach, R.A.Fischer, *Inorganic Chemistry*, 2007, **46**, 9481,
Compounds with central atom coordination number = 3	
$[Pt(Ga[N(Ar)]_2CNCy_2)_3]$	S.P.Green, C.Jones, A.Stasch, *Inorganic Chemistry*, 2007, **46**, 11
Compounds with central atom coordination number = 4	
$[Pt(GaCp^*)_4]$	C.Gemel, T.Steinke, D.Weiss, M.Cokoja, M.Winter, R.A.Fischer, *Organometallics*, 2003, **22**, 2705
$[Pd(GaCp^*)_4]$	C.Gemel, T.Steinke, D.Weiss, M.Cokoja, M.Winter, R.A.Fischer, *Organometallics*, 2003, **22**, 2705
$[Ni(GaCp^*)_4]$	P.Jutzi, B.Neumann, L.O.Schebaum, A.Stammler, H.-G.Stammler, *Organometallics*, 1999, **18**, 4462,
$[Ag(GaCp^*)_4][BPh_4]$	T.Bollermann, A.Puls, C.Gemel, T.Cadenbach, R.A.Fischer, *Dalton Transactions*, 2009, 1372
$[Zn(GaCp^*)_4][BAr^F{}_4]_2$	A.Kempter, C.Gemel, T.Cadenbach, R.A.Fischer, *Inorganic Chemistry*, 2007, **46**, 9481,
$[Cu(GaCp^*)_4][BAr^F]$	T.Bollermann, A.Puls, C.Gemel, T.Cadenbach, R.A.Fischer, *Dalton Transactions*, 2009, 1372
$[Ni(GaC(TMS)_3)_4]$	W.Uhl, M.Benter, S.Melle, W.Saak, G.Frenking, J.Uddin, *Organometallics*, 1999, **18**, 3778
$[Pd(AlCp^*)_4]$	B.Buchin, T.Steinke, C.Gemel, T.Cadenbach, R.A.Fischer, *Zeitschrift fur Anorganische und Allgemeine Chemie*, 2005, **631**, 2756,

$[Ni(AlCp^*)_4]$	B.Buchin, T.Steinke, C.Gemel, T.Cadenbach, R.A.Fischer, *Zeitschrift fur Anorganische und Allgemeine Chemie*, 2005, **631**, 2756,
$[Ni(InC(TMS)_3)_4]$	W.Uhl, M.Pohlmann, R.Wartchow, *Angewandte Chemie, International Edition*, 1998, **37**, 961, W.Uhl, M.Benter, S.Melle, W.Saak, G.Frenking, J.Uddin, *Organometallics*, 1999, **18**, 3778
$[Pt(InC(TMS)_3)_4]$	W.Uhl, S.Melle, *Zeitschrift fur Anorganische und Allgemeine Chemie*, 2000, **626**, 2043
$[Pd(InC(TMS)_3)_4]$	C.Gemel, T.Steinke, D.Weiss, M.Cokoja, M.Winter, R.A.Fischer, *Organometallics*, 2003, **22**, 2705
Compounds with central atom coordination number = 5	
$[(GaCp^*)_4Rh(Ga(O_3SCF_3)Cp^*)]$	T.Bollermann, T.Cadenbach, C.Gemel, K.Freitag, M.Molon, V.Gwildies, R.A.Fischer, *Inorganic Chemistry*, 2011, **50**, 5808
$[(GaCp^*)_4Rh(MeGa(\eta^1\text{-}Cp^*)]$	T.Cadenbach, C.Gemel, D.Zacher, R.A.Fischer, *Angewandte Chemie, International Edition*, 2008, **47**, 3438
$[Fe(AlCp^*)_5]$ (C-H activated)	T.Steinke, M.Cokoja, C.Gemel, A.Kempter, A.Krapp, G.Frenking, U.Zennek, R.A.Fischer, *Angewandte Chemie, International Edition*, 2005, **44**, 2943
$[Ru(AlCp^*)_5]$ (C-H activated)	T.Steinke, M.Cokoja, C.Gemel, A.Kempter, A.Krapp, G.Frenking, U.Zennek, R.A.Fischer, *Angewandte Chemie, International Edition*, 2005, **44**, 2943
Compounds with central atom coordination number = 6	
$[(GaCp^*)_3Ru(GaCl(\eta^1\text{-}Cp^*))(Ga_2(\mu\text{-}Cl)(\eta^1\text{-}Cp^*))_2]$	B.Buchin, C.Gemel, A.Kempter, T.Cadenbach, R.A.Fischer, *Inorganica Chimica Acta*, 2006, **359**, 4833

$[Mo(GaCp^*)_6]$ (Haptotropic Shifted)	T.Cadenbach, T.Bollermann, C.Gemel, I.Fernandez, M.von Hopffgarten, G.Frenking, R.A.Fischer, *Angewandte Chemie, International Edition*, 2008, **47**, 9150, T.Bollermann, T.Cadenbach, C.Gemel, K.Freitag, M.Molon, V.Gwildies, R.A.Fischer, *Inorganic Chemistry*, 2011, **50**, 5808

Marking the element of the central atom on an excerpt of the periodic table now gives a concise overview of the focus of published research as of writing.

Table 2: Excerpt of the periodic table of elements, limited to the d-block elements by group number from period four to six. Colorings indicate the elements of which homoleptic, mononuclear compounds have been reported previously or in this thesis. Dark green reflects that of this respective element at least one, mononuclear, homoleptic compound $[M(E^IR)_n]$ with a coordination number of or exceeding four is known. Light green indicates, that whilst at least one mononuclear, homoleptic compound $[M(E^IR)_n]$ is known, this has either a coordination number below four or exhibits intramolecular connections between the individual ligands. Light Orange indicates that the reported compounds of this element, whilst mononuclear, and exceeding a coordination number of four, contain one additional heterogeneous group bound to one ligand E^IR but not the central metal atom, thus making the compound heteroleptic. The superscript number attached to the element symbols indicate the number of reported compounds in the list above, where a +1 is noted one compound was added by this thesis.

III	IV	V	VI	VII	VIII	IX	X	XI	XII
Sc	Ti	V	Cr	Mn	Fe^1	Co	Ni^4	Cu^2	Zn^3
Y	Zr	Nb	Mo^{1+1}	Tc	Ru^{2+1}	Rh^2	Pd^3	Ag^1	Cd
Lu	Hf	Ta	W	Re	Os	Ir	Pt^3	Au^1	Hg^1

It is immediately apparent that most of the reported compounds are from the later, electron rich, transition metals (groups 8 – 12), mostly group 10, with a notable bias towards the lighter elements of the fourth and fifth period.

An exhaustive explanation of this current state can surely be compiled, though with current research into the compounds $[M(GaTMP)_n]$ progressing at a rapid pace at the same time as this very thesis is written down, such a snapshot would lose most of its value to the reader within the span of a year. Qualitatively, though it can be said that the research initially started at the compounds of Nickel in the late 1990's, then progressed down group 10 in the early 2000's, branching out towards neighboring groups towards the middle 2000's, with the presented extent being achieved during the late 2000's and early 2010's. Focus shifted then onto polynuclear cluster compounds for the following decade before the current (2023/2024) resurgence of interest in homoleptic, mononuclear compounds of $[M(E^IR)_n]$ due to the introduction of GaTMP into this specific field showing promise to give access to as of now inaccessible elements for central atoms.

When it comes to the matter of ligands, there are also notable absences. The obvious ones being InCp* and AlC(TMS)$_3$. Whilst the former just has no mononuclear homoleptic transition metal compounds reported, but has polynuclear ones reported, of the latter one, no transition metal compounds at all have been crystallographically reported as of now.[12, 57] There are of course a whole plethora of potential ligands E^{I}R, like Al(hyp), Ga(hyp), AlSi(^{t}Bu)$_3$, GaSi(^{t}Bu)$_3$.[13, 58] These ligands might very well be worth exploring in reactions with low-valent *d*-block metals, as we are only now starting to investigate deeper into the role of *π*-back bonding. Initial investigations by means of computational chemistry into the role of the Ga-N bond for compounds [M(GaTMP)$_n$] have been published, but the topic has just been opened, and whilst Ga(hyp) has been shown to form heteroleptic clusters with iron carbonyls, computational investigations did not consider the Ga-Si bond.[59]

2.3 An overview of Synthetic Procedures and Synthons

When collecting the successful synthetic access routes to compounds [M(E^{I}R)$_n$] over the last 25 years, there are clear trends visible, that one should keep in mind and try to apply with priority when pursuing this field.

Starting with the ligands E^{I}R, wherein the focus will be on the classes of E^{I}C(TMS)$_3$, E^{I}Cp* and GaTMP as their compounds have the highest coordination numbers. One key property of these compounds, aside from their sensitivity to oxygen and moisture, is that they are not present as monomeric compounds, but rather aggregates in the solid state.

In the solid state, GaC(TMS)$_3$ is present as the tetrameric cluster [Ga$_4$(C(TMS)$_3$)$_4$] with a tetrahedral [Ga$_4$] core.[60] This cluster however dissolves into its monomeric form readily when diluted in benzene at ambient temperature.[61]

InC(TMS)$_3$ is also a tetrameric cluster with a tetrahedral [In$_4$] in the solid state.[62] Notably however it remains intact when dissolved in benzene at ambient temperature.[61] Trapping experiments, carried out with 1,2-diphenylethane-1,2-dione and derivatives thereof found that at the elevated temperature of boiling *n*-hexane broke the tetramer down into reactive monomers.[63]

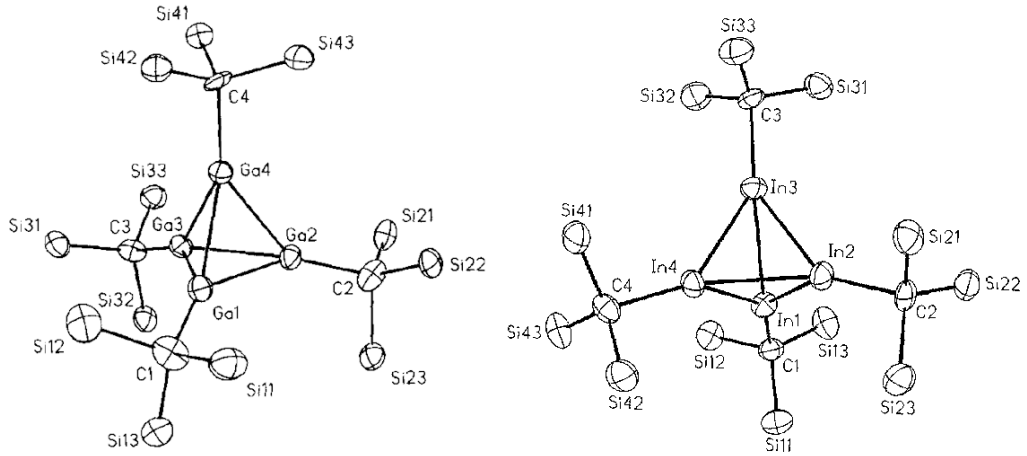

Figure 27: Crystal structures of $[Ga_4(C(TMS)_3)_4]$ (left) and $[In_4(C(TMS)_3)_4]$ (right). Methyl C and H atoms were omitted for clarity. Ellipsoids were drawn at the 40% probability level. Reprinted (adapted) with permission from W. Uhl, W. Hiller, M. Layh, W. Schwarz, Angewandte Chemie International Edition in English 1992, 31, 1364-1366. under license 6046510108384. Copyright 1992 by VCH Verlagsgesellschaft mbH, Germany, and W. Uhl, R. Graupner, M. Layh, U. Schütz, Journal of Organometallic Chemistry 1995, 493, C1-C5 under license 6046510560904. Copyright 1995 Published by Elsevier B.V.[60, 62a]

As both previous compounds, AlCp* forms the tetrameric and tetrahedral $[Al_4(Cp^*)_4]$.[20b] In order to produce the homoleptic $[Ni(AlCp^*)_4]$ or $[Pd(AlCp^*)_4]$, it must be once again refluxed in *n*-hexane in the presence of a respective metal source.[31c]

In contrast, GaCp* forms octahedral hexamers of $[Ga_6(Cp^*)_6]$ in the solid state.[64] So does InCp*, though no homoleptic, mononuclear compounds of InCp* are yet reported.[20a] From experimental data, it can be gleamed, that GaCp* is present in a reactive form in solution already well below room temperature.[17b, 31a, 31b]

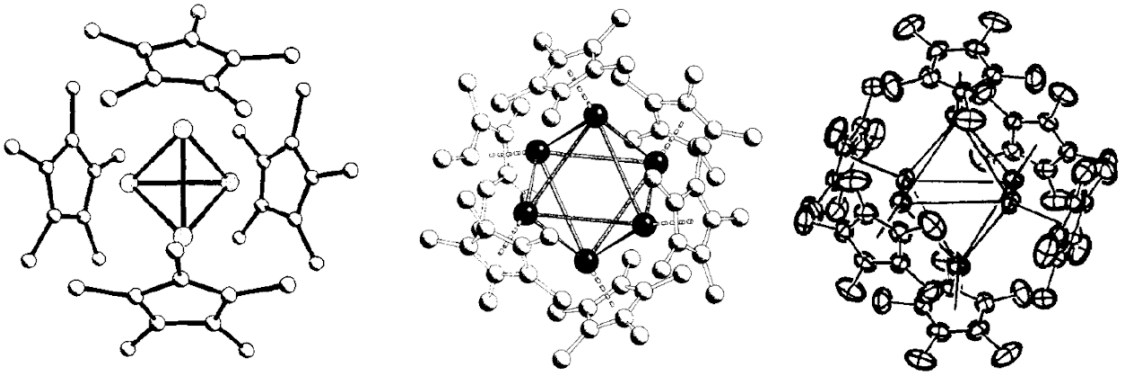

Figure 28: Crystal structures of $[Al_4(Cp^*)_4]$ (left), $[Ga_6(Cp^*)_6]$ (middle), $[In_6(Cp^*)_6]$ (right). Hydrogen atoms omitted for clarity. Ellipsoids drawn on the right are at 30% probability. Reprinted (adapted) with permission from C. Dohmeier, C. Robl, M. Tacke, H. Schnöckel, Angewandte Chemie International Edition in English 1991, 30, 564-565 under license 6046511273764. Copyright 1991 by VCH Verlagsgesellschaft mbH, Germany, and reprinted (adapted) with permission from D. Loos, E. Baum, A. Ecker, H. Schnöckel, A. J. Downs, Angewandte Chemie International Edition in English 1997, 36, 860-862 under license 6046520772606. Copyright 1997 by VCH Verlagsgesellschaft mbH, Germany and reprinted (adapted) with permission from O. T. Beachley, M. R. Churchill, J. C. Fettinger, J. C. Pazik, L. Victoriano, Journal of the American Chemical Society 1986, 108, 4666-4668. Copyright 1986 American Chemical Society.[20a, 20b, 64]

GaTMP then again forms a tetrahedral tetramer in the solid state.[44] Whilst the compounds presented in this writing, both required heating to 100 °C, 110 °C respectively in an aromatic solvent, this only represents the first result of currently ongoing research with this ligand, thus future publications of *R. A. Fischer et. al.* by

authors *I. Antsiburov*, *R. Bühler*, *F. Napoli*, *J. Stephan* and citing works should be consulted for additional synthetic advice. Previous works by *Linti et. al.* where heteroleptic and/or polynuclear compounds of GaTMP were prepared show however that GaTMP is already reactive at temperatures below ambient in mixtures of aromatic and aliphatic or purely aliphatic solvents.[46] It should be noted here, that GaTMP is remarkably soluble in *n*-hexane according to own observations.

When it comes to the starting material choice for the transition metal source, labile, olefinic, zero-valent compounds are clearly favored in literature. Here compounds with a coordination number of or exceeding four are also the focus of the discussion. All previously mentioned compounds of Ni, are synthesized from [Ni(η^4-COD)$_2$].[14-15, 23, 31c] Take note though that complex polynuclear products can also be obtained by the reaction of [Ni(η^4-COD)$_2$] with GaCp* and GaTMP respectively.[27, 46] Analogously the mononuclear, homoleptic compounds of Pt were all prepared from [Pt(η^4-COD)$_2$].[31b, 52] Pd is a remarkable exception to this trend within the group 10 metals and the preference for zero-valent precursor compounds in general. Pd(0) compounds are highly reactive and “simple” olefinic Pd(0) compounds do not exhibit properties conducive to their stoichiometric use in synthesis.[65] [Pd$_2$(DVDS)$_3$] (DVDS = 1,3-divinyl-1,1,3,3-tetramethyldisiloxane) provides a decent balance between accessibility, reactivity and stability in combination with the leaving ligand DVDS being inert enough to not cause large numbers of side reactions.[66] It has been successfully employed in reactions with ligands E^{I}R, though it produces polynuclear compounds.[12] Experience has shown that the stability and reactivity of [Pd$_2$(DVDS)$_3$] is highly sensitive to substance purity, especially amount of free DVDS in the substance and presence of Pd nanoparticles. Instead compounds [(TMEDA)Pd(X)$_2$] (TMEDA = N,N,N′,N′-Tetramethylethane-1,2-diamine) where X = Cl, CH$_3$, were used as *in situ* sources of Pd(0) to prepare homoleptic, mononuclear compounds of Pd.[31b, 31c] A similar *in situ* approach is used to prepare the homoleptic, mononuclear compound of Zn from Me$_2$Zn.[17b] The Fe compound is produced from [Fe(η^6-toluene)(η^4-C$_4$H$_6$)], which is accessible via metal vapor synthesis.[50a, 67] The syntheses of the already literature known Ru and Mo compounds with their precursor compounds [Ru(η^4-COD)(η^6-COT)] and [Mo(η^4-C$_4$H$_6$)$_3$] served as foundations for the syntheses of [Ru(GaTMP)$_5$] and [Mo(GaTMP)$_6$].[29b, 50a] Another exception is found among group 11 metals, where instead of olefinic compounds, cationic acetonitrile complexes of Cu and Ag were synthetically employed.[31a]

2.4 Steric Properties of [M(GaTMP)$_n$] vs. [M(E^{I}R)$_n$]

Buried volumes were calculated for all previously mentioned compounds [M(E^{I}R)$_n$] from literature, as well as the newly presented compounds [M(GaTMP)$_n$]. Where ligands were distinguishable in the crystal strucute, i.e. not symmetry generated, buried volumes were calculated for each distinguishable unit M(E^{I}R) using both, the standard

recommended coordination sphere size of 3.5 Å as well as an extended 4.5 Å coordination sphere size.[40] An exception here is [Pd(InC(TMS)$_3$)$_4$], since whilst it is reported, and analytical details have been published, its crystal structure has not been published.[31b]

Buried Volumes and steric maps of [M(E^{I}C(TMS)$_3$)$_4$]

Exemplary calculations for the E^{I}C(TMS)$_3$ ligands were based on the respective Ni compounds.[14-15] A value of 21.6% V_{Bur} was found for both, the Ni(GaC(TMS)$_3$) and the Ni(InC(TMS)$_3$) fragment.

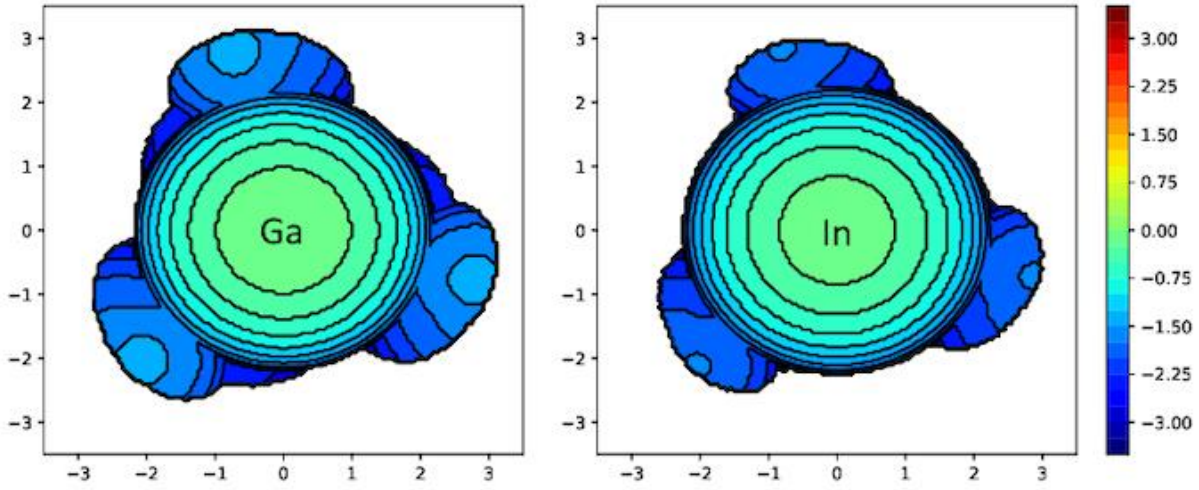

Figure 29: Steric maps of Ni(GaC(TMS)$_3$) (left) and Ni(InC(TMS)$_3$) (right) as calculated from their respective homoleptic, mononuclear Ni compounds. [14-15] The maps show the E^I atom (marked central at (0|0)) to be the deepest point of penetration into the constructed 3.5 Å coordination sphere around the central Ni atom. The three equally spaced appendages arise from the three TMS groups interacting with the outer layers of the coordination sphere as can be seen from the scale (Å) on the right. Due to the C atom binding the TMS groups to E^I being on the same axis as the Ni-E^I-bond it is "hidden" behind the Van der Waals radius of E^I.

M-E^{I}C(TMS)$_3$ compounds show the deepest penetration into the coordination sphere with their respective E^I-atom, with the TMS groups giving equally spaced impressions into the coordination sphere around E^I. The TMS groups of GaC(TMS)$_3$ are shown to have a deeper impression than those of InC(TMS)$_3$. This observation corresponds to the bond lengths found in [Ni(GaC(TMS)$_3$)$_4$] and [Ni(InC(TMS)$_3$)$_4$]. The Ni-Ga-bond length in this compound is 2.170(0) Å and the Ga-C-bond length is 2.014(2) Å compared to a Ni-In-bond length of 2.304(2) and a In-C-bond length of 2.211(5) Å.[14-15] This gives a difference of 0.331 Å. The TMS groups bound to the quaternary C atoms of the ligands are slightly flattened to a Si-C$_q$-Si angle of 114.3(3)° in the Ni-In-compound compared to 112.9(1)° found in the Ni-Ga compound. The Van der Waals radius of In is also slightly bigger than that of Ga in this calculation. The combination of the factors listed above leads to both, GaC(TMS)$_3$ and InC(TMS)$_3$ having the same value of 21.6% V_{Bur}, being thus numerically indistinguishable, were it not for the steric maps showing a greater proportion of the relevant volume of the coordination sphere attributed to the TMS groups in GaC(TMS)$_3$.

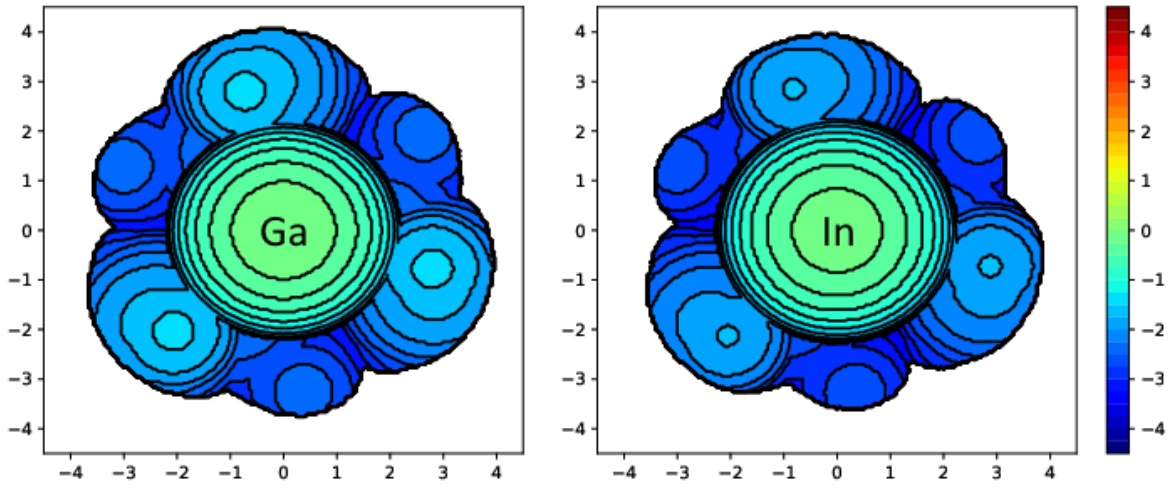

Figure 30: Steric maps of Ni(GaC(TMS)$_3$) (left) and Ni(InC(TMS)$_3$) (right) as calculated from their respective homoleptic, mononuclear Ni compounds. [14-15] The maps show the E^I atom (marked central at (0|0)) to be the deepest point of penetration into the constructed 4.5 Å coordination sphere around the central Ni atom. The two sets of three equally spaced appendages each arise from the methyl groups of the TMS groups interacting with the outer layers of the coordination sphere at different penetration depths, as can be seen from the scale (Å) on the right due to the tetrahedral nature of the TMS group. Due to the C atom binding the TMS groups to E^I being on the same axis as the Ni-E^I-bond it is "hidden" behind the Van der Waals radius of E^I.

At a coordination sphere size of 4.5 Å, the two ligands become distinguishable by virtue of their %V_{Bur} values. Here Ni(GaC(TMS)$_3$) has %V_{Bur} value of 22.2 and Ni(InC(TMS)$_3$) has a value of 20.4 %V_{Bur}. At this larger coordination sphere size, the difference in geometry of the C(TMS)$_3$ group comes more into effect. The flattened nature of the group at the In compound leads to a higher degree of overlap of the Van der Waals radii, thus taking up less space in the coordination sphere, whilst the extension of the sphere leads to more of the ligands bulk being inside the sphere. This however is counteracted by the expanding sphere having a higher absolute volume, thus percentage of the sphere occupied by the ligands bulk. The last entry in this category, with published crystallographic data is [Pt(InC(TMS)$_3$)$_4$], with values for %V_{Bur} of 20.2 at a coordination sphere size of 3.5 Å and 19.7 %V_{Bur} at a coordination sphere size of 4.5 Å.[52]

Buried Volumes and steric maps of [M(E^{I}Cp)$_n$]*

Of the E^{I}Cp* compounds of Ni there are [Ni(GaCp*)$_4$] and [Ni(AlCp*)$_4$].[23, 31c] %V_{Bur} values are found to be 21.0%V_{Bur} for [Ni(GaCp*)$_4$] and 20.5%V_{Bur} for [Ni(AlCp*)$_4$] at a coordination sphere size of 3.5 Å.

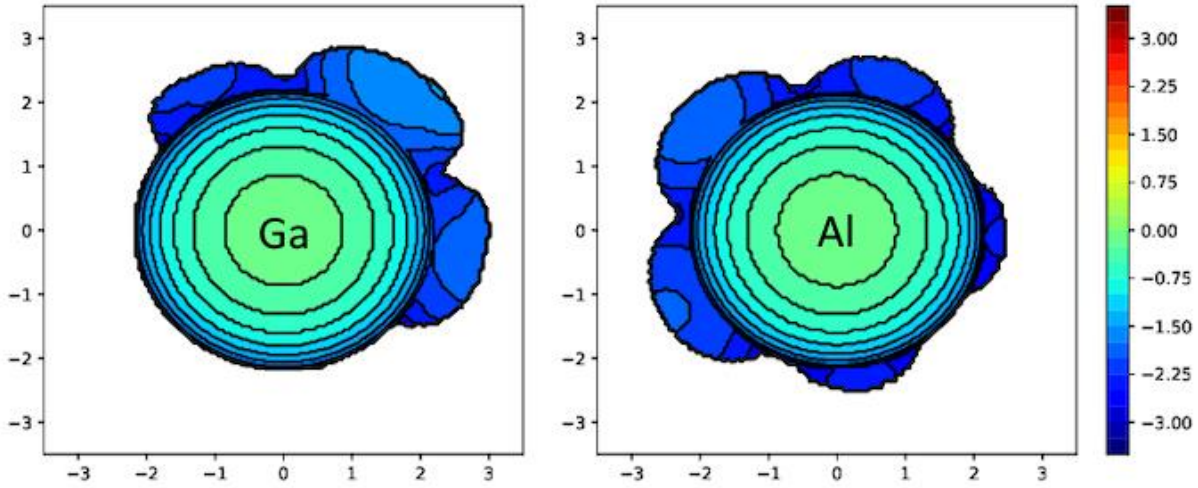

Figure 31: Steric maps of Ni(GaCp*) (left) and Ni(AlCp*) (right) as calculated from their respective homoleptic, mononuclear Ni compounds.[23, 31c] The maps show the E^{I} atom (marked central at (0|0)) to be the deepest point of penetration into the constructed 3.5 Å coordination sphere around the central Ni atom (scale on the right, values in Å). The map for Ni(GaCp*) shows only three of the five CH_3 groups of Cp* to penetrate the coordination sphere, whilst the map for Ni(AlCp*) shows all five CH_3 groups interacting with the coordination sphere, however the three represented in the upper left of the map are shown to penetrate deeper, whilst the two in the lower right are only shown as small appendages at the edge of 3.00-3.50 Å.

The maps reveal the influence of the angle found between Cp*$_{cent}$, E^{I} and M. For [Ni(GaCp*)$_4$] this angle is 164.7(1)° and 173.4(8)° for [Ni(AlCp*)$_4$].[23, 31c] The angle deviating more from the ideal 180° leads to a deeper penetration into the coordination sphere on one side of the ring and less on the other, corresponding to the observation within the maps. The lengths between Cp*$_{cent}$ and E^{I} as well as E^{I} and M were measured from the crystal structure. Al-Cp*$_{cent}$ was measured at 1.93(2) Å and Al-Ni at 2.17(3) Å. Ga-Cp*$_{cent}$ was measured at 2.00(4) Å and Ga-Ni at 2.21(8) Å.[23, 31c] The small difference in %V_{Bur} cannot be easily attributed to a single factor but is rather the result of a combination of bond angles and lengths.

From the crystal structure of [Ni(GaCp*)$_4$] an idealized geometry model was calculated, with the Cp*$_{cent}$ – Ga – Ni – angle equal to 180°. This structure gives a value for its buried volume of 20.3%V_{Bur}.

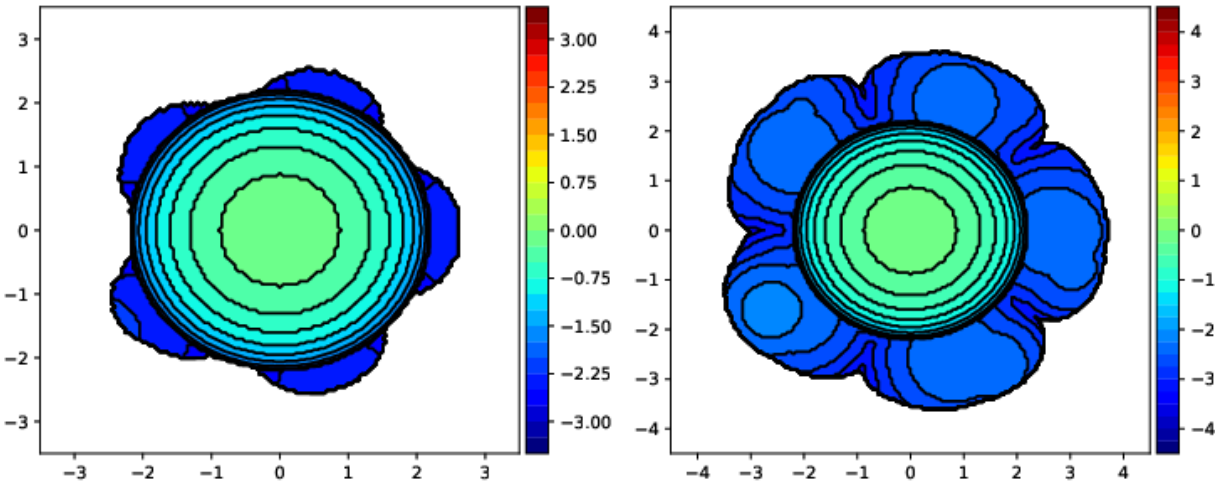

Figure 32: Steric map of a simulated Ni(GaCp*) with idealized Cp*$_{cent}$ – Ga – Ni – angle at 180°. At a coordination sphere of 3.5 Å (left) and 4.5 Å (right). Behind the bonding Ga atom, five appendages in C_5 symmetry penetrating equally into the coordination sphere originate from the five CH_3 groups of Cp*. Take note of the individual scaling depicted on the right of each map.

From the published crystallographic characterization of compounds [M(E^{I}Cp*)$_n$] %V_{Bur} values were calculated for all compounds and central geometric parameters extracted.

Table 3: List of compounds [M(E^{I}Cp*)$_n$] sorted by element E^I with respective geometric data and %V_{Bur} value. Values for compounds marked with ‡ stem from multiple distinguishable ligands within the same compound. Values for compounds marked with † were only taken the compounds η^5-coordinated E^{I}Cp* groups which are not bound additionally via C-H activation. Values for compounds marked with # were only taken from η^5-coordinated E^{I}Cp* groups which are not bound additionally via C-H activation and its isomers.

Compound	Cp*$_{cent}$-E^I-M Bond angle [°]	Cp*$_{cent}$-E^I Distance [Å]	E^I-M Bond length [Å]	%V_{Bur} 3.5 Å	%V_{Bur} 4.5 Å
Ni(GaCp*) (idealized)	180	2.00(4)	2.21(8)	20.3	19.0
[Ni(GaCp*)$_4$][23]	164.7(1)	2.00(4)	2.21(8)	21.0	19.7
[Pd(GaCp*)$_4$][31b]	155.5(5)	2.01(9)	2.366(8)	20.3	19.0
[Pt(GaCp*)$_4$][31b]	160.6(8)	1.99(5)	2.333(2)	20.2	18.9
[Ag(GaCp*)$_4$][BPh$_4$]‡[31a]	148.3(9)	1.95(1)	2.515(4)	19.6	18.8
	159.6(3)	1.95(6)	2.528(0)	18.1	17.0
	158.2(9)	1.95(3)	2.523(3)	18.4	17.4
	155.3(1)	1.94(2)	2.511(5)	18.9	18.1
[Zn(GaCp*)$_4$][BAr$^F{}_4$]$_2$‡[17b]	170.2(1)	1.85(0)	2.403(6)	18.9	18.1

	165.2(0)	1.86(1)	2.411(2)	19.2	18.4
$[Cu(GaCp^*)_4][BAr^F]$‡[31a]	158.1(0)	1.93(2)	2.351(7)	20.4	19.3
	153.1(6)	1.94(6)	2.349(6)	21.0	19.8
$[Ni(AlCp^*)_4]$[31c]	173.4(8)	1.93(2)	2.17(3)	20.5	19.9
$[Pd(AlCp^*)_4]$[31c]	169.2(1)	1.92(9)	2.29(5)	19.4	18.8
$[Ru(AlCp^*)_5]$†[50a]	164.5(6)	1.89(8)	2.313(2)	19.4	18.8
$[Fe(AlCp^*)_5]$#[50a]	161.0(0)	1.91(5)	2.212(2)	21.3	20.3
	172.2(2)	1.90(9)	2.242(2)	19.9	19.2
	162.1(1)	1.88(9)	2.210(2)	20.6	20.5
	160.7(9)	1.98(8)	2.213(2)	21.4	19.8

The Cp^*_{cent}-E^I distance is quite constant over all compounds, with an average value of 1.94(5) Å, the values showing a standard deviation of 0.04(8) Å. The E^I-M bond distance exhibits an average length of 2.319(6) Å with a standard deviation of 0.096(7) Å. Going from the idealized Ni(GaCp*) as a base, the influence of geometric parameters on %V_{Bur} can be derived. With bond lengths being otherwise equal the original structure of $[Ni(GaCp^*)_4]$ has a decreased Cp^*_{cent}-E^I-M-angle and an increased value %V_{Bur} from 20.3 to 21. The compounds $[Pd(GaCp^*)_4]$, $[Ag(GaCp^*)_4][BPh_4]$, and $[Cu(GaCp^*)_4][BAr^F]$ all exhibit nearly the same Cp^*_{cent}-E^I-M-angle of 155.5°, making them valuable for comparison especially since the Cp^*_{cent}-E^I distances of $[Ag(GaCp^*)_4][BPh_4]$ and $[Cu(GaCp^*)_4][BAr^F]$ are similar and the same is true for the E^I-M bond lengths of $[Pd(GaCp^*)_4]$ and $[Cu(GaCp^*)_4][BAr^F]$. Decreasing the Cp^*_{cent}-E^I-M-angle from 180° towards the lowest observed values around 155.5° increases %V_{Bur} moderately. Increasing the Cp^*_{cent}-E^I distance leads to a minor decrease in %V_{Bur}, whilst an increase in the E^I-M bond length leads to a more significant decrease in %V_{Bur} as this provides the most significant amount of distance, to lift the tilted Cp* ring out of the 3.5 Å coordination sphere, due to it being perpendicular to the surface of the sphere whilst the Cp^*_{cent}-E^I distance is always off perpendicular by an angle equal to 180° − Cp^*_{cent}-E^I-M-angle.

Shifting from η^5 to the lower hapticity binding modes of E-Cp* has only one true example for the $[M(E^ICp^*)_n]$ class, which is $[Mo(GaCp^*)_6]$ or to be precise $[Mo(\eta^1\text{-}GaCp^*)(\eta^5\text{-}GaCp^*)_5]$.[29b, 55] This highly coordinated molecule thus warrants a more in-depth description.

Table 4: List of individual GaCp* ligands of [Mo(GaCp*)$_6$] numbered according to the crystal structure with their associated binding modes, geometric parameters and values for %V_{Bur} at coordination sphere sizes of 3.5 Å and 4.5 Å.[29b, 55] Average values and standard deviations were calculated excluding Ga4 due to its η^1 binding mode.

Ga Number	Binding mode of Cp* to Ga	Mo-Ga-Cp*$_{cent}$ Bond Angle [°]	Cp*$_{cent}$-Ga Distance [Å]	Mo-Ga Bond length [Å]	%V_{Bur} 3.5 Å	%V_{Bur} 4.5 Å
1	η^5	175.2(1)	2.12(7)	2.458(0)	18.2	16.1
2	η^5	167.4(2)	2.09(1)	2.493(0)	18.1	16.5
3	η^5	170.3(0)	2.04(0)	2.475(8)	18.5	16.4
4	η^1	164.6(7)	2.64(6)	2.384(5)	18.1	14.9
5	η^5	167.3(6)	2.05(7)	2.474(1)	18.2	16.6
6	η^5	166.0(4)	2.02(4)	2.484(6)	18.2	16.8
Average		169.2(7)	2.06(8)	2.477(1)	18.2	16.5
Standard Dev		3.2(8)	0.03(7)	0.011(7)	0.1	0.2

It is apparent that the values generally follow the trend outlined previously. Whilst the decreased angle Mo-Ga-Cp*$_{cent}$ would lead to an increased value %V_{Bur} the longer bond distances compensate for this, leading over all to the lowest values %V_{Bur} of all presented compounds. In the associated publications, the authors argue that the η^1-binding mode of the Cp* attached to Ga4 is a result of steric crowding around the hexa-coordinated molybdenum center.[29b, 55] This is contradicted by the slightly higher value for Ga4 at 18.5%V_{Bur} compared to the 18.1-18.2%V_{Bur} found for the others.

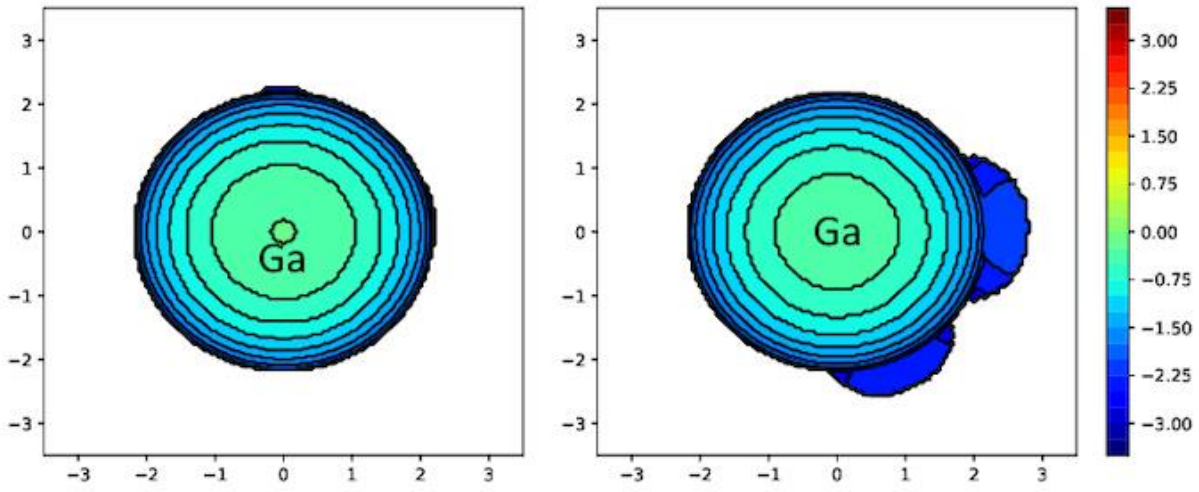

Figure 33: Steric maps of two GaCp* groups of [Mo(GaCp*)$_6$] calculated for a 3.5 Å coordination sphere. Left is the steric map calculated for Mo(η^1-GaCp*) (Ga4) and right is the steric map calculated for Mo(η^5-GaCp*) (Ga1). Ga1

was chosen exemplary as the maps for Ga2, Ga3, Ga5 and Ga6 are very similar as well as its similar Cp^*_{cent}-E^I-M angle to $[Ni(AlCp^*)_4]$.

The steric maps show that for Mo(η^1-GaCp*) (Ga4, left) only the Ga atom penetrates into the 3.5 Å coordination sphere whilst for Mo(η^5-GaCp*) (Ga1, right) the CH_3 groups barely penetrate the outer edge of the sphere. This however is counteracted by the slightly shorter Mo-Ga bond length for Mo(η^1-GaCp*) of 2.384(5) Å compared to 2.458(0) Å for Mo(η^5-GaCp*). The difference in bond length is visible in the steric maps as the light green circle visible within the van der Waals sphere of the map of Mo(η^1-GaCp*) on the left. Clearly the 3.5 Å coordination sphere is not large enough to capture the influence of the Cp* ligands sufficiently for this compound, which is attributed to its overall longer bond lengths, compared to previously examined compounds. When comparing the map of Mo(η^5-GaCp*) to the map of Ni(AlCp*) presented previously, which has nearly the same Cp^*_{cent}-E^I-M bond angle, it becomes clear that all five CH_3 groups of Mo(η^5-GaCp*) should be visible as impressions in the coordination sphere. Since the combined bond lengths of Mo(η^5-GaCp*) presented in the previous table exceed the equivalent bond lengths of Ni(AlCp*), presented in the table before that, by a sum of 0.48(0) Å the calculations were repeated for a larger coordination sphere. 4.5 Å was chosen instead of only 4.0 Å to better capture and visualize the impact of the tilted Cp* ring in the η^1-binding mode in $\%V_{Bur}$ value and steric map. At a sphere radius of 4.5 Å the values obtained were 16.1%V_{Bur} for Mo(η^5-GaCp*) and 14.9%V_{Bur} for Mo(η^1-GaCp*), which now supports the argument that a change from η^5 to η^1 coordination in E^ICp* compounds reduces crowding in the coordination sphere.

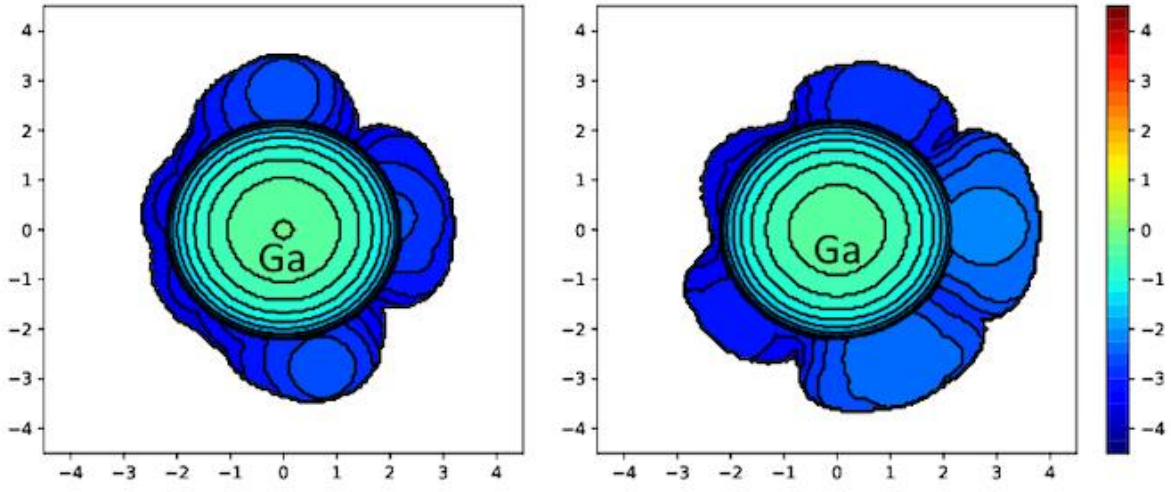

Figure 34: Steric maps of two GaCp* groups of $[Mo(GaCp^*)_6]$ calculated for a 4.5 Å coordination sphere. Left is the steric map calculated for Mo(η^1-GaCp*) (Ga4) and right is the steric map calculated for Mo(η^5-GaCp*) (Ga1). Note also the difference in color scaling indicated by the depth scale on the right.

As in the previous maps, the shorter Mo-Ga bond length is visible for Mo(η^1-GaCp*) (Ga4, left). Aside from the central Ga atom, the deepest penetrations into the sphere arise from three of the five CH_3 groups of its Cp* ligand. These are visible at the coordinates [Å] (0|3), (2|0), and (1|-3). The impression of the CH_3 group at (2|0)

appears comparatively small despite being technically the closest one, but it must be remembered that in its η^1-binding mode the binding C atom has more of an sp^3-character than the typical sp^2-character of Cp*, thus the CH_3 group attached to the binding carbon atom in Mo(η^1-GaCp*) is found to be 31.6(1)° out of plane from its associated C_5-ring resulting in it being roughly the same distance away from the central Mo-atom as its adjacent CH_3 groups according to the crystal structure (5.000(5), 5.437(5), 5.360(5) Å).[29, 55] The two impressions at (-2|0.5) and (-2|-1.5) originate from the two C atoms of the C_5-ring most distant from the central Mo atom. Their associated CH_3 groups are outside the 4.5 Å sphere and are thus not visible anymore. The steric map of Mo(η^5-GaCp*) (Ga1, right), now shows equally spaced impressions in the coordination sphere assignable to the five CH_3 groups of Cp*. The uneven depth of penetration into the sphere can be attributed to the angle Mo-Ga1-Cp*$_{cent}$ of 175.2(1)°.[29b] The Cp* ring of Mo(η^1-GaCp*) (Ga4) is slipped in this binding mode compared to the η^5-binding mode. No value has yet been defined in literature to mathematically express the ring slippage in Cp* compounds. This is made difficult by the wide range of geometric factors involved. For this simple case of η^1-E^{I}Cp* a slip angle can be defined.

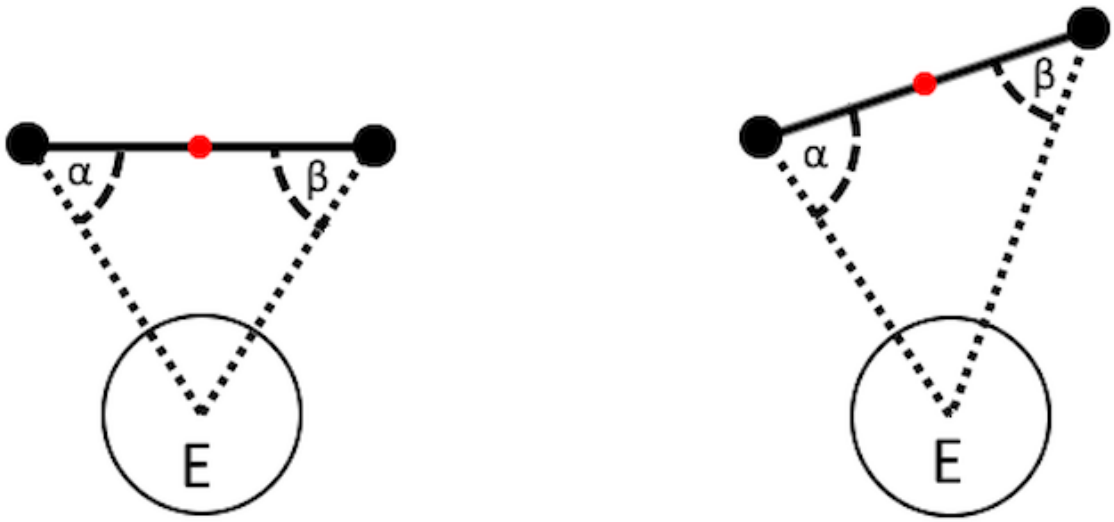

Figure 35: Definition of a slip angle for η^1-E^{I}Cp. Black circles indicate two of five C-atoms of a Cp ring coordinated to an atom E depicted as hollow circle. A centroid (red circle) is constructed from all five C atoms of a Cp ring. The angles (α, β, etc.) are measured between the centroid, one of the C atoms and E. The largest angle α is obtained around the binding C atom. Left depicts the relatively similar angles found in η^5-E^{I}Cp*, whilst on the right a ring slippage is depicted as is found in η^1-E^{I}Cp*, where the angle α is significantly larger than the other angles β, etc.

When constructing the centroid of the C_5-ring of a compound ECp, five angles Cp$_{cent}$-C$_{ring}$-E can be defined. For compounds M(η^5-E^{I}Cp) these angles are all roughly equivalent. For [Ni(AlCp*)$_4$] these angles are found to be between 57.7(1)° and 58.4(3)°.[31c] And between 58.4(4)° and 59.3(7)° for [Ni(GaCp*)$_4$].[23] When a ligand is present as M(η^1-E^{I}Cp), the angles now differ significantly, with the largest found at the now solely binding C atom. For Mo(η^1-GaCp*) this angle is found to be 102.4(3)°.[29b]

Buried Volumes and steric maps of [M(Ga(L)DDP)$_2$]

An examination on the buried volumes of the compounds [M(Ga(L)DDP)$_2$] must consider the ligands L coordinated to Ga on most of these compounds. One compound of this class [Cu(GaDDP)$_2$][OTf] has no additional ligands, which makes it serve as a baseline compound in this examination.[17c]

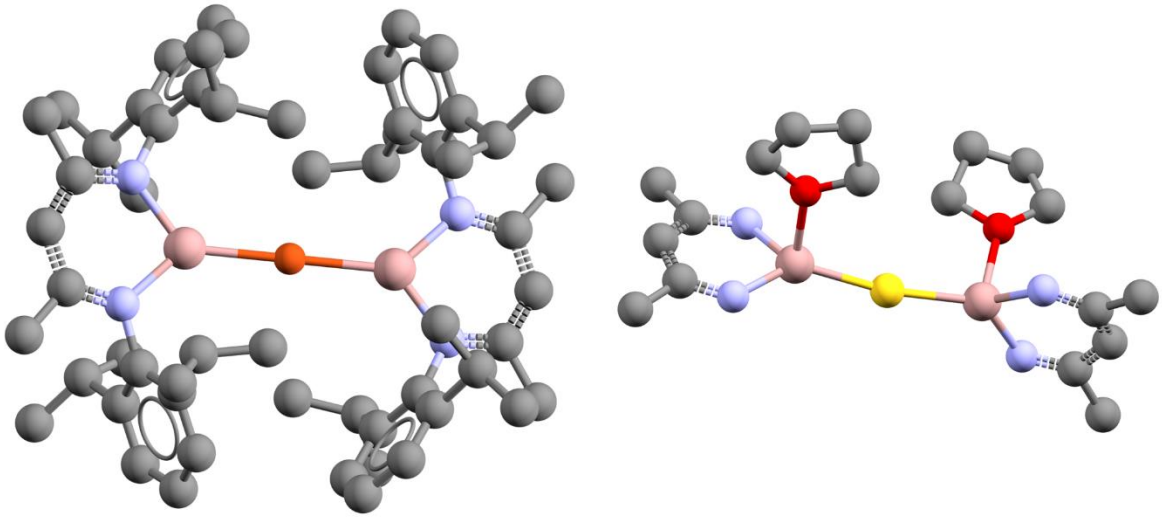

Figure 36: Crystal structures of [Cu(GaDDP)$_2$][OTf] (left, uncoordinated triflate anion and hydrogens omitted for clarity) and [Au(Ga·(THF)(DDP))$_2$][BAr$^F{}_4$] (right, uncoordinated BAr$^F{}_4$ anion, aromatic 2,6-diisopropylphenyl groups and hydrogens omitted for clarity).[17a, 17c] C: grey, N: blue, Ga: Pink, Cu: orange, Au: yellow, O: red. Two units of THF are coordinated to the gold compound on the right whilst nothing is coordinated to the Copper compound on the left.

For [Cu(GaDDP)$_2$][OTf] a value of 38.7% V_{Bur} was obtained. Both 2,6-diisopropylphenyl groups on both DDP have a torsion angle found between [Ga-N] and [C_{Ar1}-$C_{Ar2/6}$] of 77.8(7)°, respective -98.7(9)°, facing the same direction on the same DDP group with the other one inverted around the central Cu atom as an inversion center.[17c]

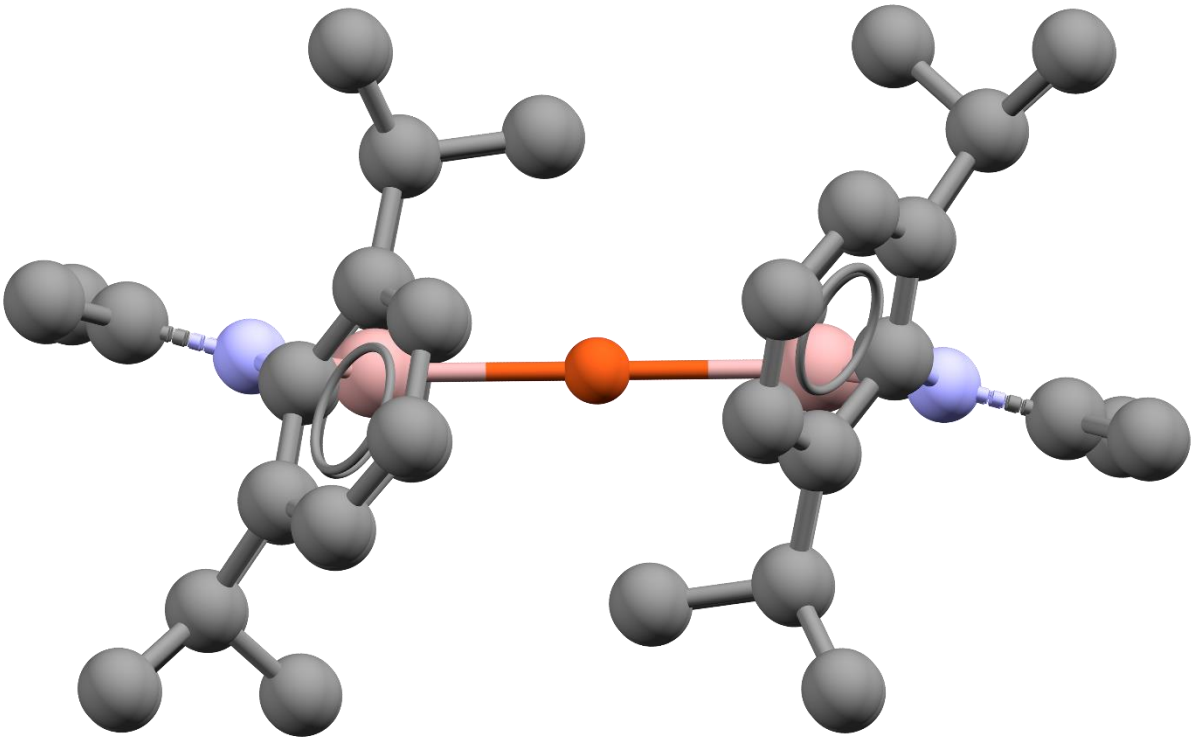

Figure 37: Crystal structure of [Cu(GaDDP)$_2$][OTf] viewed from the side. (uncoordinated triflate anion and hydrogens omitted for clarity). C: grey, N: blue, Ga: Pink, Cu: orange. The twist of the 2,6-diisopropylphenyl groups is visible with the Cu atom being the inversion center.[17c] The angle found between the rearmost C atom of the C_3N_2Ga ring the Ga atom and the Cu atom is 166.65°. Note that counterintuitively that angle bends Ga-Cu-Ga bond axis towards the inward facing isopropyl groups.

The steric map of Cu(GaDDP) shows the central Ga atom at (0|0). The twisted geometry of the DDP ligand is visible through the asymmetric depth of penetration of the terminal methyl groups of the 2,6-diisopropylphenyl groups. One set is visible as raised impressions of about 1.5 Å at (2|2) and (2|-2), and the other in the background at -1.5 Å at coordinates (-2.5|1) and (-2.5|-1).

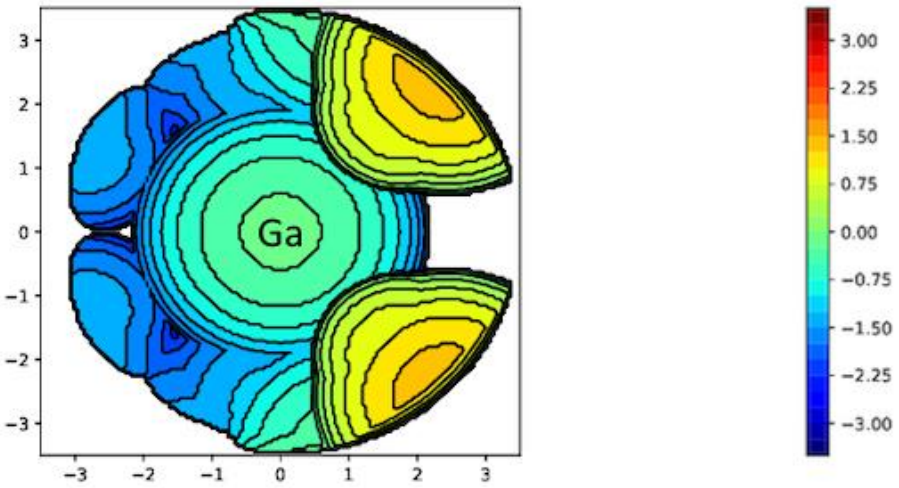

Figure 38: Steric map of the GaDDP group of [Cu(GaDDP)$_2$][OTf] constructed with a sphere of 3.5 Å The two inward facing methyl groups cause the raised impressions on the right, whilst the other two are visible as smaller impressions on the left. The Ga-Cu-Ga bond axis is pointing out of the plane towards the reader, slightly tilted towards the raised CH_3 groups.

Due to [M(Ga(L)DDP)$_2$] having a high degree of geometric freedom, influenced by the nature and size of L, there are no geometric properties from which trends in %V_{Bur} could easily be deduced. The orderly structure of the 2,6-diisopropylphenyl groups found in [Cu(GaDDP)$_2$][OTf] is not found amongst the structures of the other members of this compound class, as the torsion angles of the 2,6-diisopropylphenyl groups as well as the torsion angle of the DDP ligand itself is significantly altered by the presence of the additional ligands L bound to Ga, as this shifts the geometry of Ga away from a more planar sp^2 like binding geometry to a more tetrahedral sp^3 like geometry.

Table 5: List of homoleptic compounds [M(Ga(L)DDP)$_2$] with their associated M-Ga bond lengths and %V_{Bur} values for the total respective fragment Ga(L)DDP (total %V_{Bur}) and the fragment GaDDP where the ligand L was removed from the calculation, leaving only steric contributions of the GaDDP group to quantify the influence of L on the buried volume. Values were calculated for a sphere radius of 3.5 Å. ‡ denotes values that have been calculated as averages of all geometrically distinct groups within the respective crystal structure.

Compound	M-Ga bond length [Å]	%V_{Bur} - L	Total %V_{Bur}
[Cu(GaDDP)$_2$][OTf][17c]	2.315(8)	n/a	38.7
[Au(Ga·(THF)(DDP))$_2$][BAr$^F{}_4$]‡[17a]	2.397(6)	33.8	38.7
[Hg(Ga(SC$_6$F$_5$)(DDP))$_2$][56]	2.533(9)	37.4	40.4
[Zn(GaH(DDP))$_2$]‡[18]	2.434(0)	38.7	38.7
[Zn(Ga(Me)(DDP))$_2$]‡[17b]	2.462(0)	41.9	44.1

The M-Ga bond lengths found in this compound class are similar to those found in previously examined compound classes. %V_{Bur} values are significantly higher than previous, due to the extended steric bulk of the GaDDP ligand. On the note of expanding the sphere to 4.5 Å in to accommodate the larger depth of the ligand along the z-axis, no significant qualitative changes are found aside from the values for fragments with L removed approaching a common value as is expected. [Zn(GaH(DDP))$_2$] gains a difference of 0.3 between its values as the sphere expands and captures the additional H atom, this increase however is almost immediately offset by the increased volume of the sphere, relegating the absolute difference to a following percentile digit, which is lost in the single following digit precision of the calculations as the sphere is expanded further. All GaDDP groups without L approach a value for %V_{Bur} of very close to or at 13.0. The difference in buried volume observed between total %V_{Bur} of [Cu(GaDDP)$_2$][OTf] (38.7) and %V_{Bur} - L of [Au(Ga·(THF)(DDP))$_2$][BAr$^F{}_4$] is attributed to THF, respective L, causing the DDP group to spread out further outside the constructed sphere, thus reducing the value found for %V_{Bur}. The opposite however can also be found in the data when looking at [Zn(Ga(Me)(DDP))$_2$]. Here the compound shows a value %V_{Bur} - L of 41.9, significantly higher than for total %V_{Bur} of [Cu(GaDDP)$_2$][OTf] (38.7). The comparatively small CH$_3$ group causes the Ga atom to

assume a very much tetrahedral bonding geometry, as is visible in the crystal structure which in turn acts as a lever, pulling the entire DDP ligand closer to the center of the compound, causing it to take up more of the 3.5 Å coordination sphere. At the same time the CH_3 group itself is not sterically demanding enough to cause the aromatic groups of the DDP ligand to significantly spread out.

[Pt(Ga[N(Ar)]$_2$CNCy$_2$)$_3$]

Unique amongst the homoleptic, mononuclear $[M(E^IR)_n]$ compounds is $[Pt(Ga[N(Ar)]_2CNCy_2)_3]$, published by *C. Jones et. al.*, as it is the only one with a coordination number of three.[16] The central Pt(0) atom is in a close to perfect trigonal planar coordination geometry with Ga-Pt-Ga angles of 122.3(0)°, 119.4(7)° and 118.2(4)°. The three $Pt(Ga[N(Ar)]_2CNCy_2)$ units average a value of 26.3% V_{Bur} with an average Pt-Ga-bond length of 2.309(4) Å. The structure is closely related to $[Pt(PPh_3)_3]$ with central bond angles of 117.2(2)°, 120.9(8)°, and 121.8(3)°, and an average Pt-P-bond length of 2.266(1) Å.[68] % V_{Bur} values for $[Pt(PPh_3)_3]$ average to 29.4.

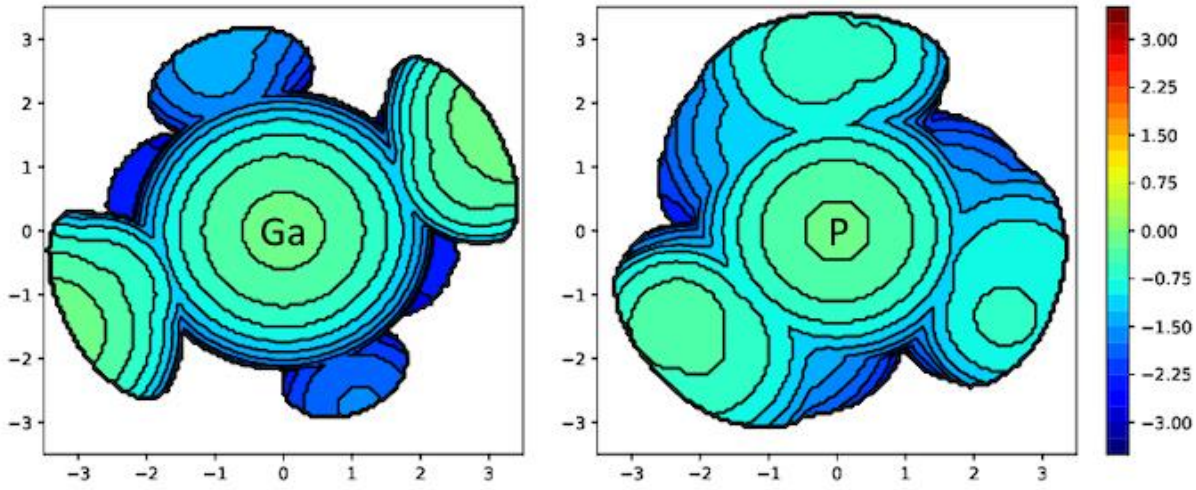

Figure 39: Steric maps of $Pt(Ga[N(Ar)]_2CNCy_2$[16] (left, calculated from Ga3) and $Pt(PPh_3)$[68b] (right, calculated from P2). Steric maps were calculated for a 3.5 Å sphere. The right map shows the phenyl groups tilted clockwise as indicated by the darkening blue topographic in the anti-clockwise direction.

The steric map of $Pt(Ga[N(Ar)]_2CNCy_2)$ (left) shows two impressions in the coordination sphere left (-2.5|-1.5) and right (2.5|1.5) of the central Ga atom of equal depth to the Ga atom, which originate from the CH_3 groups of the 2,6-diisopropylphenyl groups tilted towards the central Pt atom. The dark, blue impression just above the left (-2|1) and below the right (2|-0.5) impressions just mentioned on the map are attributed to the C1 atom of the 2,6-diisopropylphenyl groups. The remaining impressions on the left (-1|2.5) and right (1|-2.5) can be attributed to the CH_3 group of the backwards pointing isopropyl groups of the 2,6-diisopropylphenyl groups. The comparison with its analogue PPh_3 compound reveals that despite its perceived bulk, in the first coordination sphere of around 3.5 Å, the $Ga[N(Ar)]_2CNCy_2$ is not as densely packed

as PPh_3. At 4.5 Å, PPh_3 still has a higher %V_{Bur} value by 1%V_{Bur}, only at a sphere of 5.5 Å does the %V_{Bur} value of Pt(Ga[N(Ar)]$_2$CNCy$_2$) exceed the value of Pt(PPh_3).

[M(GaTMP)$_n$]

Homoleptic, mononuclear compounds of GaTMP have not been previously reported in literature, thus their absence in the list before.[47] As before, values %V_{Bur} and central geometric parameters have been compiled from the crystal structure.

For [Ru(GaTMP)$_5$] values were averaged from all six distinguishable GaTMP ligands, as half the molecule is symmetry generated, and the groups disordered, giving an average value of 20.1%V_{Bur}. Averaged over all twelve GaTMP ligands surrounding the two [Mo(GaTMP)$_6$] units in the crystal structure a value of 19.0%V_{Bur} is found. For this molecule, only one of every disordered group was taken into account.

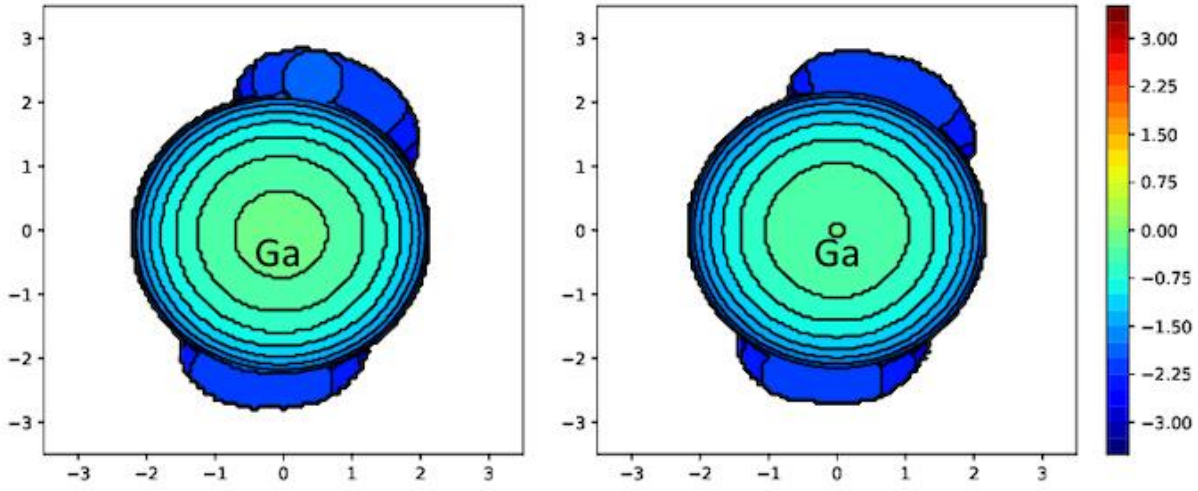

Figure 40: Steric maps of Ru(Ga1TMP) (left) and Mo1(Ga1TMP) (right). Numbers following atomic symbols match the numbering scheme in the published crystal structure. The two lobes surrounding the impression formed by the Ga atom arise from the equatorial methyl groups of TMP.

M(GaTMP) shows two distinct lobes on either side of the impression formed by the central Ga atom. These lobes originate from the equatorial methyl groups of TMP. The two axial methyl groups are pointing away from the central metal atom and are only visible on the steric maps when scaling the coordination sphere to 4.5 Å and beyond.

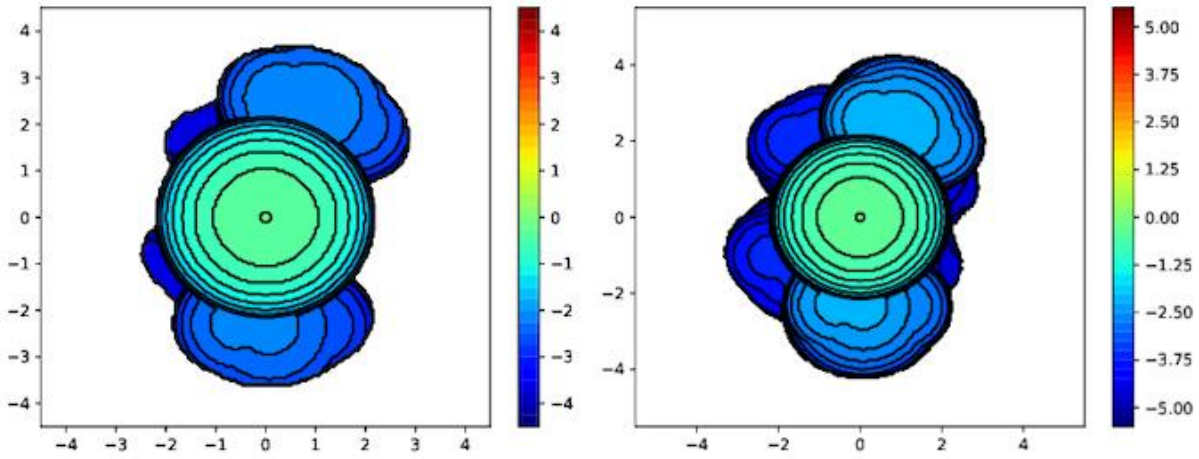

Figure 41: Steric maps of Mo1(Ga1TMP) calculated for coordination spheres of 4.5 Å (left) and 5.5 Å (right). Notice the axial methyl groups of TMP coming into view.

The structure of [Ru(GaTMP)$_5$] is symmetry generated around an axis running through Ru and Ga3, which is the axial Ga atom of the basally distorted square pyramid. The TMP group attached to Ga3 is thus not disordered in the classical sense but more a result of this symmetry and thus generates two crystallographic ligand units of identical geometric parameters and buried volumes. The two crystallographic ligand units associated with Ga1 have distinct N atoms, thus giving two distinguishable ligand units with differing geometric values. In the case of Ga2, the ligand units share a common positioned N atom but the hydrocarbon part of the TMP group is otherwise disordered, thus giving the same geometric parameters presented in the table below but a slightly different value for %V_{Bur}.

Table 6: Selected geometric parameters and values %V_{Bur} of [Ru(GaTMP)$_5$] calculated from the crystal structure together with average values and standard deviations. Note that the structure is symmetry generated and has a disorder in the TMP groups. Values marked with * originate from the disordered TMP groups attached to the respective Ga Atom, thus the Ru-Ga bond lengths and Ga-N bond lengths for n and n* are equivalent.

Ga Number	Ru-Ga Bond Length [Å]	Ga-N Bond Length [Å]	Ru-Ga-N Angle [°]	%V_{Bur} 3.5 Å	%V_{Bur} 4.5 Å
1	2.291(1)	1.872(0)	171.6	20.0	16.3
1*	2.291(1)	1.872(0)	175.8	20.1	16.9
2	2.280(7)	1.849(5)	175.8	20.0	17.0
2*	2.280(7)	1.849(5)	175.8	20.1	17.0
3	2.274(0)	1.852(0)	172.6	20.1	17.0
3*	2.274(0)	1.852(0)	172.6	20.1	17.0

Average	2.281(9)	1.858(5)	174.0	20.1	16.9
Standard Dev	0.007(0)	0.008(6)	1.8	0.1	0.3

For [Ru(GaTMP)$_5$] an average value %V_{Bur} of 20.1 is calculated with a standard deviation of 0.1%V_{Bur}. The average Ru-Ga bond length is 2.281(9) Å with a standard deviation of 0.007(0) Å. The average Ga-N bond length is 1.858(5) Å. With a standard deviation of 0.008(6) Å. Notably the axial ligand, attached to Ga3 does not show a significant difference in geometric parameters compared to the basal ligands attached to Ga1 and Ga2.

In the crystal structure of [Mo(GaTMP)$_6$], two distinct crystallographic units are contained. The one surrounding Mo1 encompasses the ligands associated with Ga1-6, and the one surrounding Mo2 encompasses the ligands associated with Ga7-12. Over both units, the average buried volume is 19.0 %V_{Bur} with a standard deviation of 0.1. The average Mo-Ga bond length is 2.385(4) Å with a standard deviation of 0.006(1) Å, and the average Ga-N bond length is 1.853(2) Å with a standard deviation of 0.010(8) Å. The Mo-Ga-N bond angle averages 177.1(1)° with a standard deviation of 1.4(5)°.

Table 7: Selected geometric parameters and values %V_{Bur} of [Mo(GaTMP)$_6$] calculated from the crystal structure together with average values and standard deviations. Not that due to two distinct crystallographic units being present, a set of twelve values was collected instead of just six.

Ga Number	Mo-Ga Bond Length [Å]	Ga-N Bond Length [Å]	Mo-Ga-N Angle [°]	%V_{Bur} 3.5 Å	%V_{Bur} 4.5 Å
1	2.388(1)	1.856(2)	174.4(2)	19.1	15.8
2	2.389(0)	1.857(2)	178.8(7)	18.9	15.5
3	2.396(0)	1.864(2)	176.1(1)	18.9	15.7
4	2.377(1)	1.846(2)	176.9(5)	19.2	15.9
5	2.392(2)	1.867(2)	175.9(5)	18.9	15.9
6	2.374(0)	1.851(1)	175.6(1)	19.2	16.0
7	2.391(7)	1.858(2)	178.4(0)	18.9	15.8
8	2.381(6)	1.856(1)	176.1(9)	19	15.9

9	2.384(5)	1.855(2)	178.4(3)	19.1	15.8
10	2.382(4)	1.852(1)	177.3(9)	19.1	15.9
11	2.384(0)	1.822(0)	177.56(0)	19.1	15.8
12	2.384(0)	1.853(2)	179.5(1)	19.1	15.8
Average	2.385(4)	1.853(2)	177.1(1)	19.0	15.8
Standard Dev	0.006(1)	0.010(8)	1.4(5)	0.1	0.1

Looking at the units Mo1 and Mo2 individually, the bond lengths and and buried volumes are within 1 × standard deviation of each other, only the Mo-Ga-N bond angles show slightly higher deviation within 2 × standard deviation.

In the crystal structure, in both units it is also notable that the GaTMP ligands are rotated in such a way that opposing ligands are close to being on the same plane and rotated approximately 90 degrees relative to their neighbors so that no two equatorial Methyl groups of two neighboring ligands directly face each other.

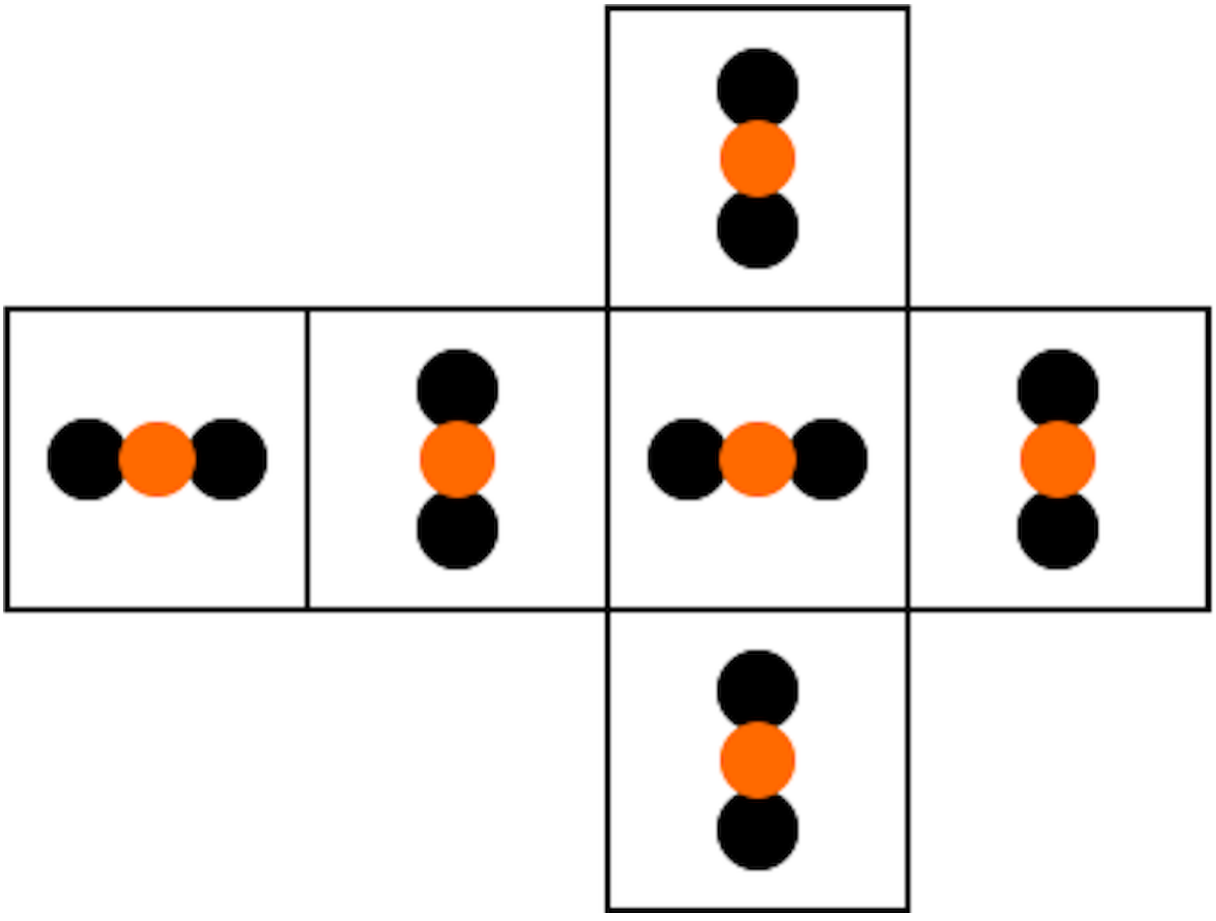

Figure 42: Simplified representation of the rotational arrangement of the six GaTMP groups of [Mo(GaTMP)$_6$]. Refer to the steric map of GaTMP pictured before for additional referencing. Picture the six connected squares as the net

of a cube surrounding Mo with the octahedrally distributed Ga atoms of the GaTMP ligands drawn as orange circles. Just as with the steric map of GaTMP presented before, the two axial methyl groups of each GaTMP ligand are indicated as black, spherical appendages. If the reader were to cut the figure out of this dissertation, and assemble it back into a cube with the figure facing inwards, and view it from within the cube, from its center, where the Mo atom would be, it would be a crude equivalent of a 360° spherical steric map of [Mo(GaTMP)$_6$] at a distance of 3.5 Å.

A discussion of buried volumes to characterize [M(E^{I}R)$_n$]

Buried volumes were calculated for almost all available fragments M(E^{I}R). The data obtained was found to be consistent with geometric parameters obtained from the crystal structure, such as angles and bond lengths. Changes in the value of %V_{Bur} can be assigned to specific geometric parameters and the amount of influence can be ascertained, based on the available dataset. The ease with which a common dataset, for comparative analysis of compounds reaching back 25 years, was created is remarkable. All obtained values were compiled into an initial graphic, displaying %V_{Bur} in relation to the coordination number of the respective compound.

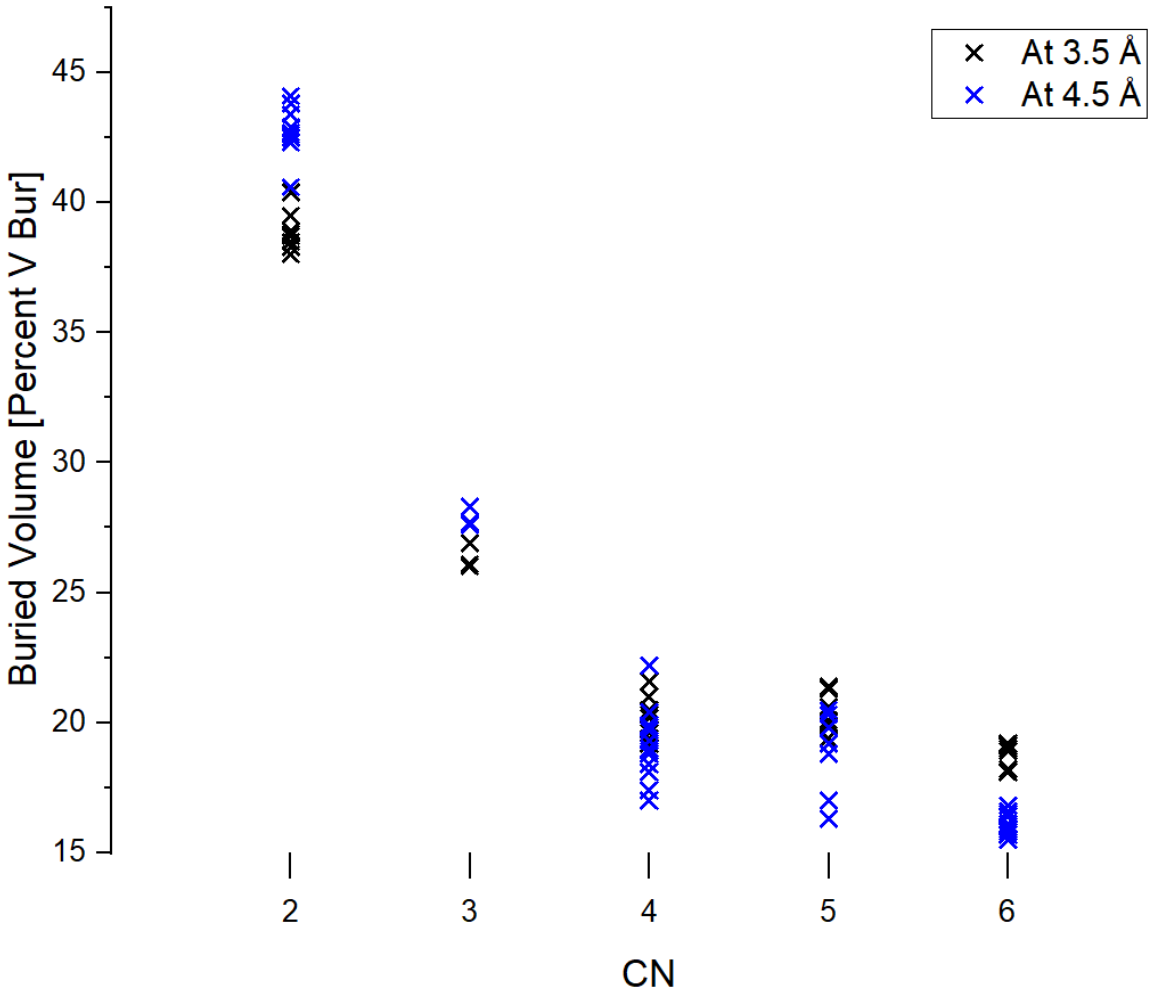

Figure 43: Plots of values for %V_{Bur}, calculated for coordination spheres of 3.5 Å (black) and 4.5 Å (blue) against the compounds respective coordination number (CN). Multiple entries for a single compound come from distinguishable ligand units in the crystal structure. For compounds [M(ECp*)$_n$], only values were used where ECp* was in a η^5 configuration and not bound in any other way (e.g. C-H activation in [Fe(AlCp*)$_5$]).

This also allows to compare values obtained from differently sized coordination spheres. As the coordination sphere is expanded, atoms of the ligand molecule which are further from the center of the sphere will be encompassed by the sphere, thereby increasing %V_{Bur}. However, at the same time, an expanding coordination sphere will increase the overall volume of the sphere, since the volume of the ligand already inside a smaller sphere is constant, the %V_{Bur} value originating from this part of the ligand will reduce. In practice this means that an increase in %V_{Bur} will only follow an increase in coordination sphere radius if a proportionally larger part of the ligand is encompassed within the larger sphere.

Thus, the difference in values obtained for CN = 2 can be understood as the comparatively large ligands within this category not being fully encompassed in a 3.5 Å coordination sphere. A 4.5 Å coordination sphere better encompasses this class of ligands but leads to less separation of values. At a sphere radius of 3.5 Å the values are spread across 4.7 %V_{Bur} from 38.0 to 42.7 %V_{Bur}, and from 40.6 to 44.1 %V_{Bur} across 3.5 %V_{Bur} at a sphere radius of 4.5 Å. It must be noted that not only does the spread of values change as the sphere size is changed, but also the order of the compounds if they were sorted by %V_{Bur}.

The values for CN = 3 must be observed with caution as they originate only from a single compound, with three distinguishable ligands. Here, whilst the values increase by between 1.4 – 1.7 %V_{Bur} when the sphere is expanded from 3.5 Å to 4.5 Å, they do not separate but rather start to contract slightly from a maximum separation of 0.9 %V_{Bur} at 3.5 Å to 0.7 %V_{Bur} at 4.5 Å. This can be interpreted as the maximum useful sphere radius for this compound.

The largest category by number of different compounds, is made up of compounds where CN = 4. At a sphere radius of 3.5 Å, the values are spread across 3.5 %V_{Bur} from 18.1 to 21.6 %V_{Bur} and from 17.0 to 22.2 %V_{Bur} across a range of 5.2 %V_{Bur} at a sphere radius of 4.5 Å.

More significant differences are once again observed at higher coordination numbers which now include [M(GaTMP)$_n$]. For CN = 5, at a sphere radius of 3.5 Å the values for %V_{Bur} lie between 19.4 and 21.4 giving a spread of 2.0 %V_{Bur}. Respective for a sphere of 4.5 Å values %V_{Bur} between 17.0 and 20.5, an increased spread of 3.5 %V_{Bur}. With the smallest values at 4.5 Å coming from [Ru(GaTMP)$_5$].

Made up of only two compounds, the CN = 6 compounds at a sphere radius of 3.5 Å range from 18.1 to 19.2 %V_{Bur}, giving a spread of 1.1%V_{Bur}. At a sphere radius of 4.5 Å this slightly increases to a spread of 1.3 %V_{Bur} ranging from values of 15.5 to 16.8 %V_{Bur}.

The same change in order as for CN = 2, observed when changing from a 3.5 Å sphere radius to a 4.5 Å sphere radius also observed throughout the data.

Due to the mathematically discrete nature of the values for CN, in contrast to the continuous values of %V_{Bur} it is not possible to plot a proper curve through the dataset. It is however visible from the graphic that the data for a sphere of 3.5 Å radius loses consistency at coordination numbers exceeding four, because the values rise at CN = 5 and stay the same as for CN = 4 at CN = 6. For a 4.5 Å sphere however the values %V_{Bur} continuously decrease as CN increases. For comparative purposes it is thus appropriate to utilize the %V_{Bur} values calculated for a 4.5 Å coordination sphere as these also provide a higher spread within the data points, allowing for better differentiation.

The class of [M(E^{I}Cp*)$_n$] compounds is very well established at this point and easily characterized by values for the M-E bond distance, the distance between E and the centroid of the C_5 ring in Cp* and the angle between M, E and the centroid of the C_5 ring. ^{13}C values for the C_5 ring atoms have also been published with every compound mentioned before, giving a broad base to explore relationships between these characteristic values and the buried volume %V_{Bur}.

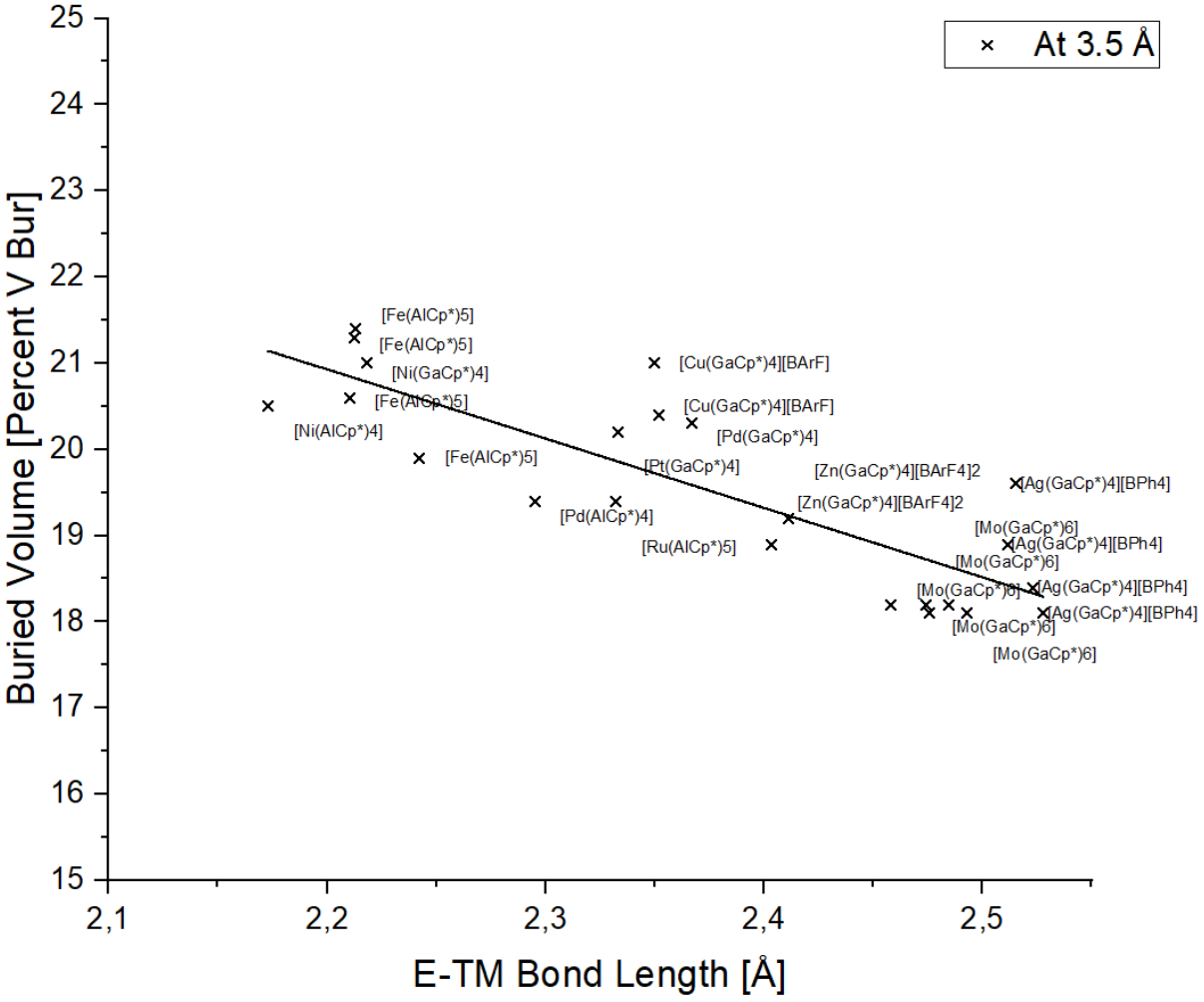

Figure 44: Values for %V_{Bur} obtained for compounds [M(E^{I}Cp*)$_n$] plotted against the E-transition metal bond length. Values were calculated for a coordination sphere radius of 3.5 Å. A linear fit has been calculated from the data, giving a slope of -8.03 with an associated R^2 value of 0.69.

Values on the x-axis approximately range from 2.15 Å to 2.55 Å. The data shows AlCp* compounds tending towards shorter TM-E bond lengths, the longest however are found not in [Mo(GaCp*)$_6$], but in [Ag(GaCp*)$_4$][BPh$_4$]. Though identified as a non-ideal coordination sphere size, at 3.5 Å the bond length between E^I and the transition metal shows good correlation with the buried volume. The slope of the linear fit in this graph is -8.03, with the fit equating to an R^2 value of 0.69. At a coordination sphere size of 4.5 Å, the slope of the linear fit increases in value to -9.44 with a similar value for R^2 at 0.68. A notable difference is that whilst between the data for 3.5 Å and 4.5 Å coordination sphere radii, the correlation between this bond length and %V_{Bur} is better at smaller bond lengths and less so at higher bond lengths as the values for [Mo(GaCp*)$_6$] and [Ag(GaCp*)$_4$][BPh$_4$] spread significantly, so much so that the R^2 value of the entire fit is roughly equal between 3.5 Å and 4.5 Å.

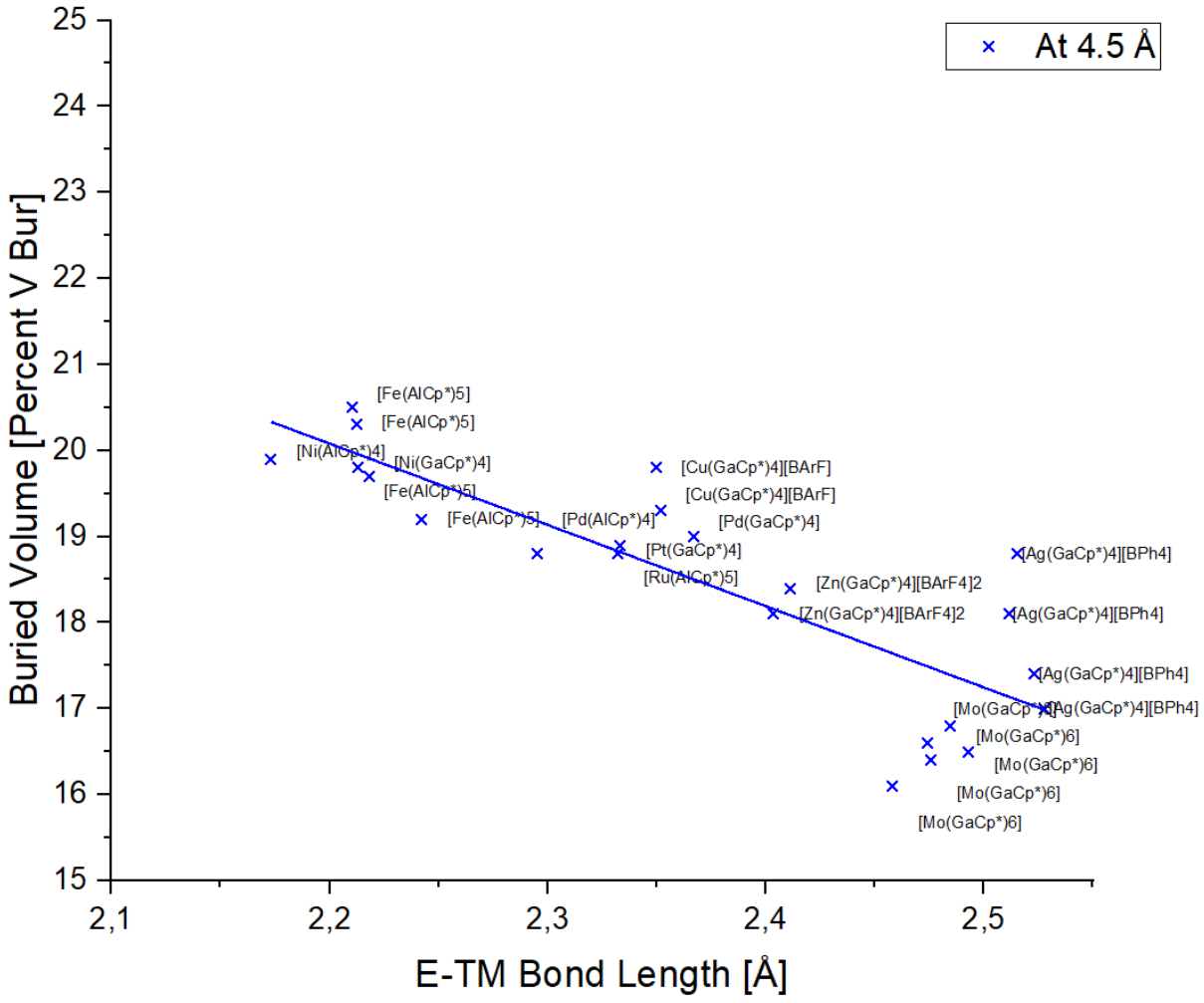

Figure 45: Values for %V_{Bur} obtained for compounds [M(E^{I}Cp*)$_n$] plotted against the E-transition metal bond length. Values were calculated for a coordination sphere radius of 4.5 Å. A linear fit has been calculated from the data, giving a slope of -9.44 with an associated R^2 value of 0.68.

Next, the relationship between %V_{Bur} and the distance between E and the centroid of the C$_5$ ring in Cp* was analyzed by the same method. The values on the x-axis range approximately from 1.825 Å, to 2.10 Å. Compared to the previous graphs, [Mo(GaCp*)$_6$] has the longest distances here, however [Ag(GaCp*)$_4$][BPh$_4$] now has

comparatively shorter distances. Plotting these distances against the associated values for %V_{Bur} of a 3.5 Å radius coordination sphere gives a very wide spread of data points. A linear fit for these data points gives a slope of -6.04, but notably only a R^2 value of 0.09, indicating only negligible correlation between the values.

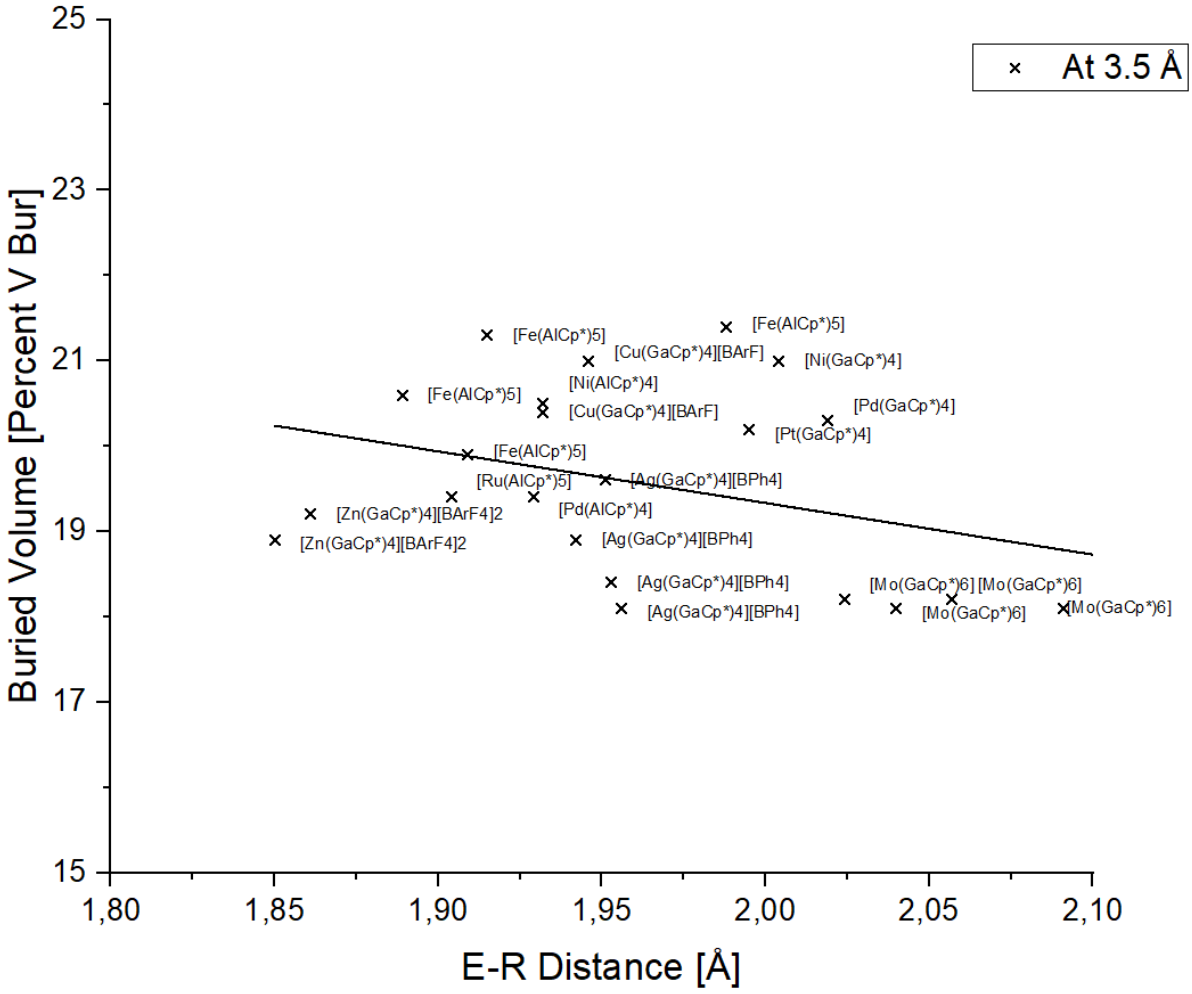

Figure 46: Values for %V_{Bur} obtained for compounds [M(E^{I}Cp*)$_n$] plotted against the distance between E and the centroid of the C_5 ring in Cp*. Values were calculated for a coordination sphere radius of 3.5 Å. A linear fit has been calculated from the data, giving a slope of -6.04 with an associated R^2 value of 0.09.

At 4.5 Å the slope of the associated linear fit increases to -11.65, with the value for R^2 increasing to 0.34, indicating an unreliable correlation.

This unreliable correlation is very likely due to the angle of the distance vector between the E atom and the centroid of the C_5 ring of Cp* which is not orthogonal to the central metal atom of the compound or parallel to the bond between the central metal atom and E, which has shown good correlation to the buried volumes.

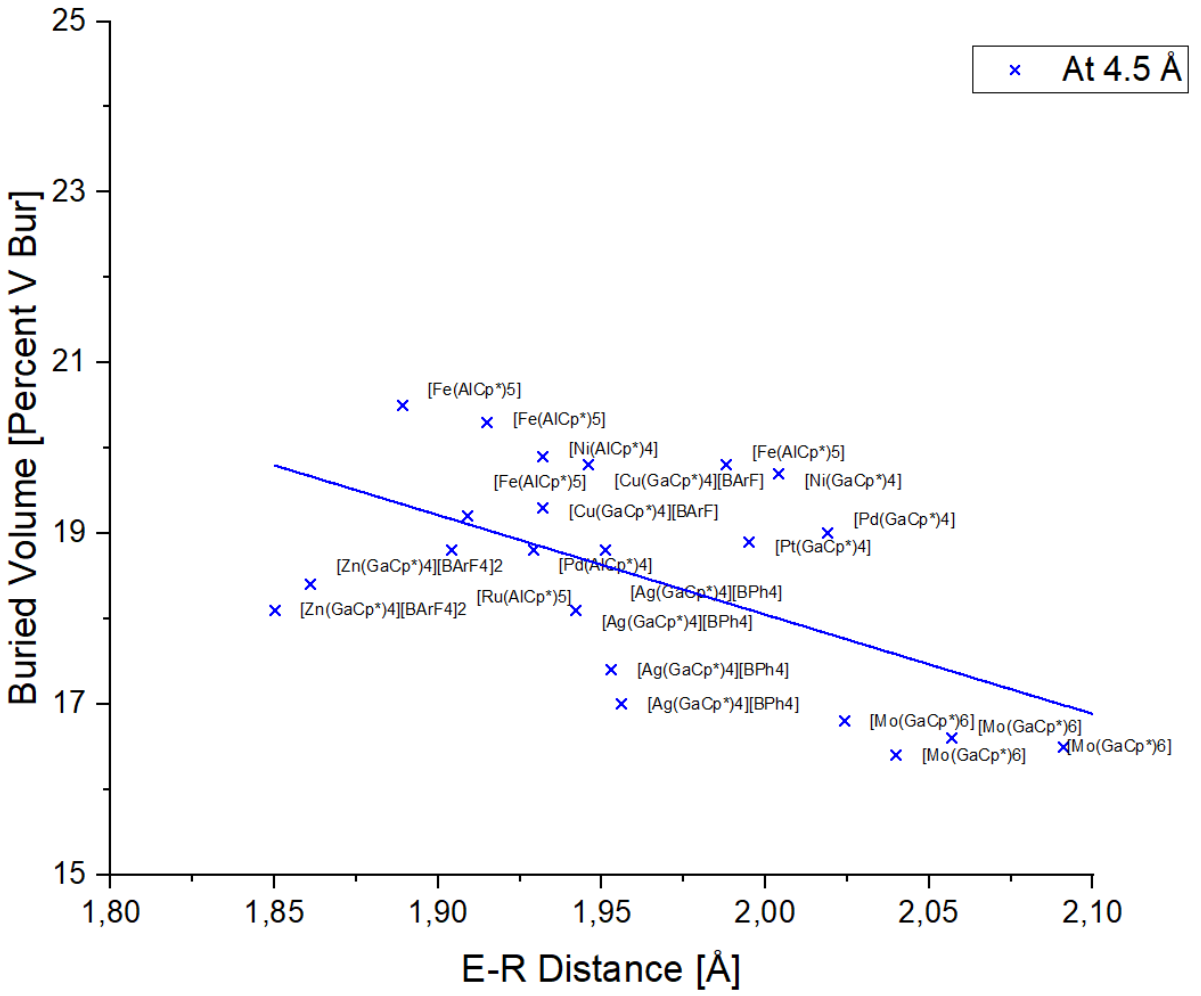

Figure 47: Values for $\%V_{Bur}$ obtained for compounds [M(E^{I}Cp*)$_n$] plotted against the distance between E and the centroid of the C_5 ring in Cp*. Values were calculated for a coordination sphere radius of 4.5 Å. A linear fit has been calculated from the data, giving a slope of -11.65 with an associated R^2 value of 0.34.

The argument for codependency between the distance of E to Cp* and the angle found between the central metal atom, E and the centroid of the C_5 ring of Cp* is strengthened when applying the same graphing method as before to the aforementioned angles. The values on the x-axis range approximately from 145° to 180°. Though for both datasets, 3.5 Å and 4.5 Å, there is a tendency towards higher buried volumes at lower angles, the correlation for both linear fits is calculated to be 0.05, indicating no reliable correlation.

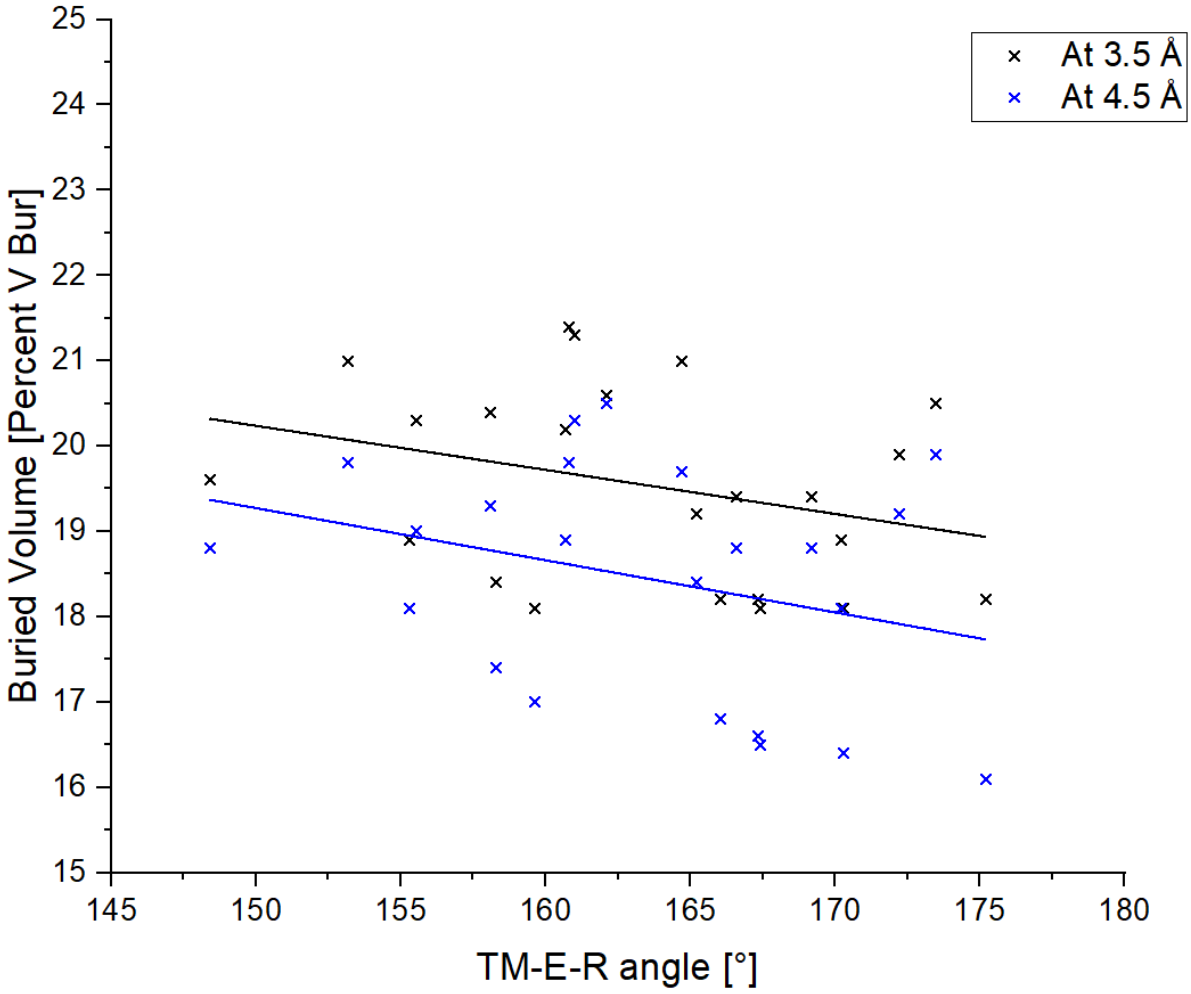

Figure 48: Values for %V_{Bur} obtained for compounds [M(E^{I}Cp*)$_n$] plotted against the angle found between the central metal atom, E and the centroid of the C_5 ring in Cp*. Values were calculated for a coordination sphere radius of 3.5 Å (black) and 4.5 Å (blue). A linear fit has been calculated from the data, for each set. Both fits have an associated R^2 value of 0.05.

A first takeaway from this is that, when it comes to the influence of geometric parameters on %V_{Bur}, the values which result in displacement of the ligand orthogonal to the central atom, have the highest influence on and best correlation to it.

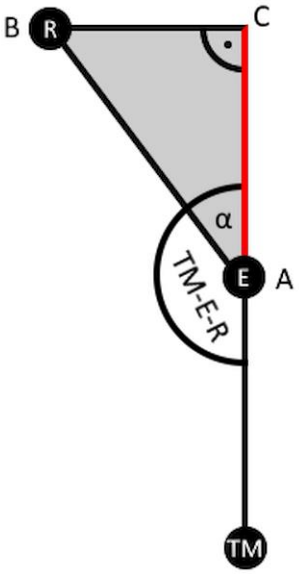

Figure 49: Schematic graphic to illustrate the calculation of the orthogonal component (red) of the E-R Bond. The Orthogonal component of the E-R bond must be in parallel to the E-TM bond, thus a line is extended from TM though E. As shown, the component of the E-R bond, which is parallel to the E-TM bond, can be calculated as the side of a right-angle triangle, as the distance between A and C.

As the distance E-R is angled away from the E-TM bond by the angle defined by TM-E-R, an orthogonal component of E-R can be calculated that is parallel to the E-TM bond by trigonometry as follows. The distance E-R is defined as the hypothenuse of a right-angle triangle, wherein E is defined as corner A, R is defined as corner B and the corner C encompassing the right angle is situated upon the elongation of the TM-E bond. The angle α, encompassed by corner A can be found by subtracting the angle TM-E-R from 180°. The orthogonal component of the distance E-R can thus be found by calculating the distance $\overline{AC}$ as follows:

$$\overline{AC} = \overline{AB} \times \cos(\alpha)$$

Plotting the resulting numbers against the corresponding value for $\%V_{Bur}$ of the compound gives a clearer picture.

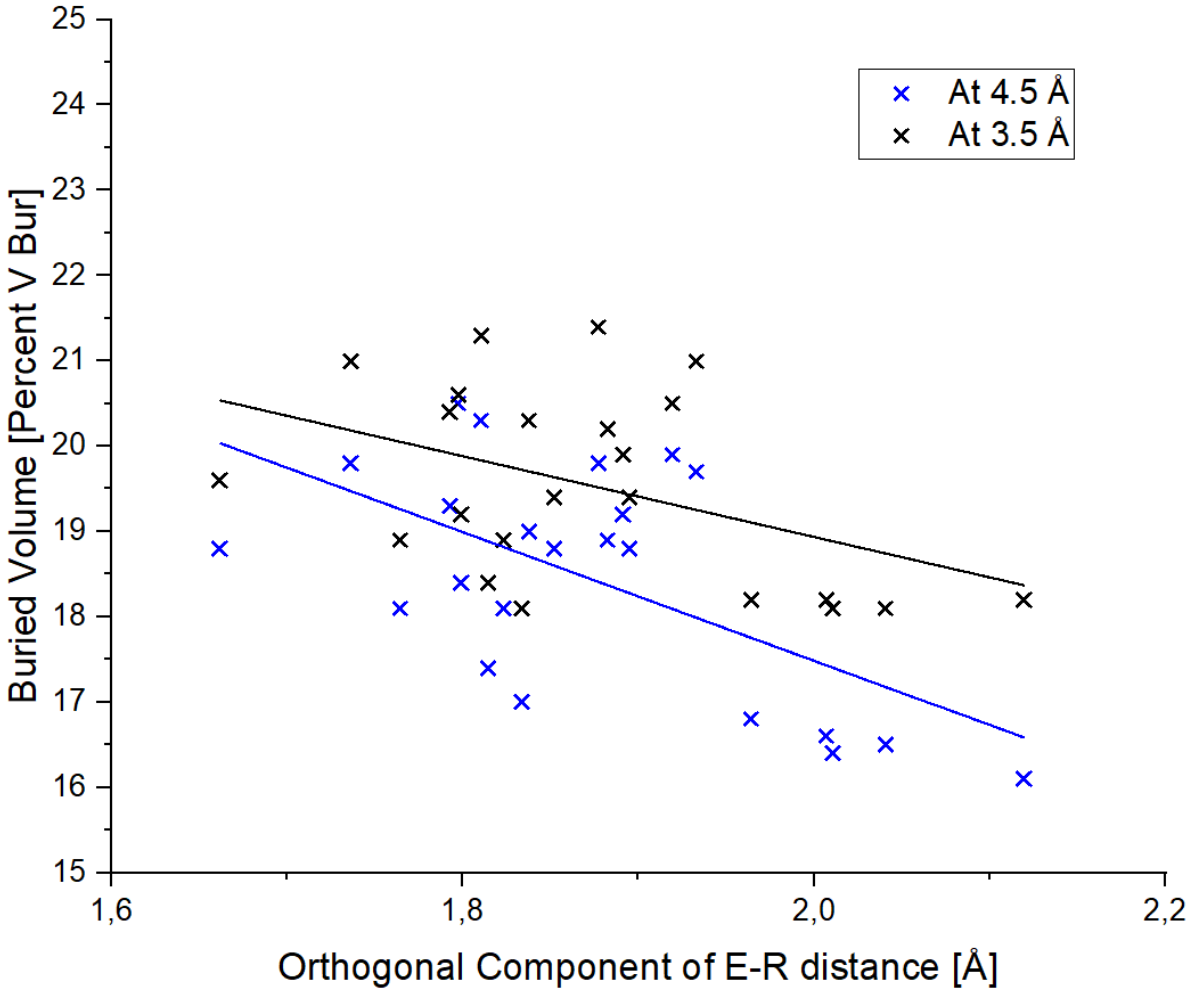

Figure 50: Values for $\%V_{Bur}$ obtained for compounds $[M(E^{I}Cp^{*})_{n}]$ plotted against the value calculated for the orthogonal component of the E-R distance. Values were calculated for a coordination sphere radius of 3.5 Å (black) and 4.5 Å (blue). A linear fit has been calculated from the data, for each set. The linear fit for a coordination sphere of 3.5 Å (black) has a slope of -4.73 and an associated R^2 value of 0.15. The linear fit for a coordination sphere of 4.5 Å (blue) has a slope of -7.54 and an associated R^2 value of 0.32.

The orthogonal component of the E-R distance gives broadly similar values R^2 when correlating to the components corresponding buried volume.

A more insightful picture is obtained when adding the orthogonal component of the E-R distance to its corresponding parallel value for TM-E bond length, forming a sum of orthogonal components for a system M-E^{I}-Cp* and correlating this to the components respective buried volumes.

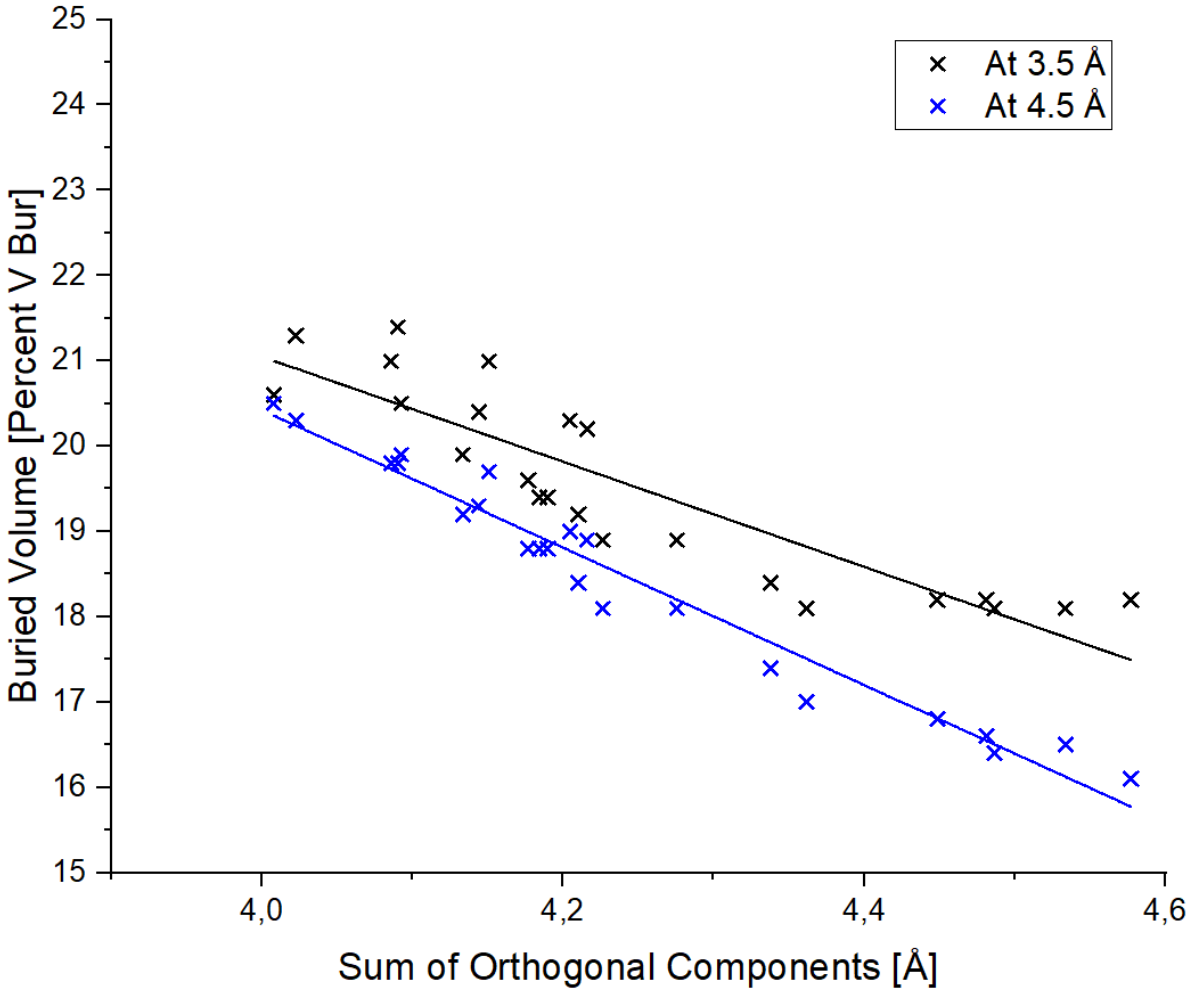

Figure 51: Values for %V_{Bur} obtained for compounds [M(E^{I}Cp*)$_n$] plotted against the value calculated for the sum of orthogonal components of the M-E^{I}-Cp* systems. Values were calculated for a coordination sphere radius of 3.5 Å (black) and 4.5 Å (blue). A linear fit has been calculated from the data, for each set. The linear fit for a coordination sphere of 3.5 Å (black) has a slope of -6.16 and an associated R^2 value of 0.78. The linear fit for a coordination sphere of 4.5 Å (blue) has a slope of -8.05 and an associated R^2 value of 0.96.

Comparing the corresponding values R^2 for correlating the sum of orthogonal components for a system M-E^{I}-Cp* to the respective values %V_{Bur} to just the correlation of the TM-E bond length to the respective values for %V_{Bur} shows that the sum of orthogonal components exceeds the previously obtained values for R^2. For a coordination sphere of 3.5 Å the value of R^2 increases from 0.69 to 0.78 and for a sphere of 4.5 Å the value of R^2 increases from 0.68 to 0.96.

To further support the merit of the correlation of the sum of orthogonal components to buried volumes, the results were compared to a value obtained by adding the TM-E bond length to the unmodified E-R distance giving a sum of unmodified distances and correlating this value to the respective components value for %V_{Bur}.

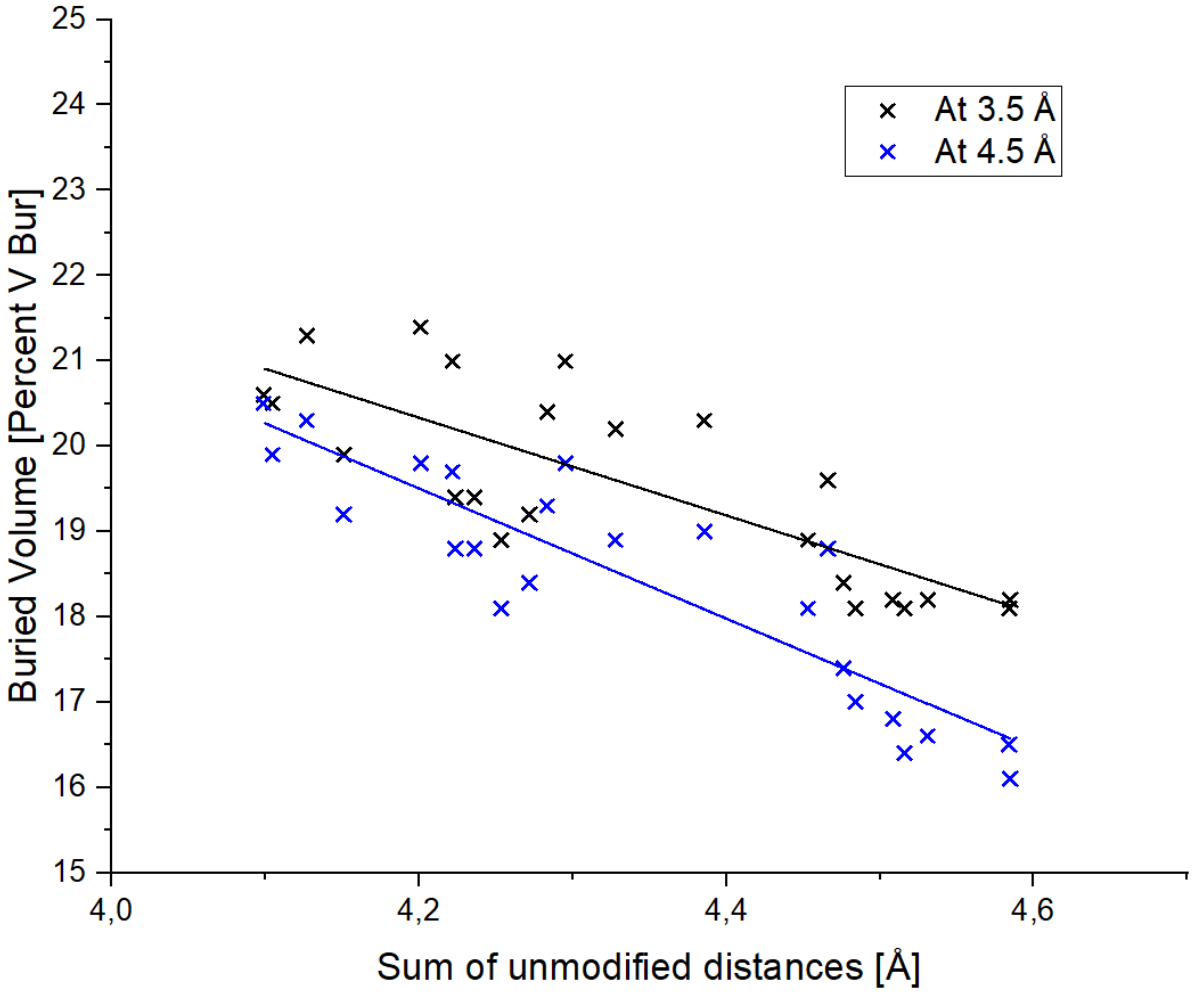

Figure 52: Values for $\%V_{Bur}$ obtained for compounds $[M(E^{I}Cp^{*})_{n}]$ plotted against the value calculated for the sum of unmodified distances of the M-E^{I}-Cp* systems. Values were calculated for a coordination sphere radius of 3.5 Å (black) and 4.5 Å (blue). A linear fit has been calculated from the data, for each set. The linear fit for a coordination sphere of 3.5 Å (black) has a slope of -5.72 and an associated R^2 value of 0.62. The linear fit for a coordination sphere of 4.5 Å (blue) has a slope of -7.62 and an associated R^2 value of 0.79.

A cursory visual comparison of the two datasets already shows that the sum of unmodified distances exhibits a noticeably larger scattering, compared to the sum of orthogonal components. The values for R^2 of the respective linear fits for the correlation of the sums of unmodified distances to the respective components buried volumes are also significantly lower than is the case for the previously mentioned correlation of the sum of orthogonal components at only 0.62 for a coordination sphere of 3.5 Å, which is also below the value obtained for just the correlation of the TM-E bond lengths to the buried volumes, and 0.79 for a coordination sphere of 4.5 Å.

Comparing the steric maps of $[Mo(GaTMP)_6]$ and $[Mo(GaCp^*)_6]$ allows to visualize a key difference in potential reactivities. Whilst the Methyl groups of Cp* shield the central metal atom, in a nearly circular manner, even at more significant TM-E-R angles, thus blocking potential substrate approach vectors, this is not the case for TMP. The equatorial Methyl groups shield a large part almost symmetrically on both sides, but the axial groups only shield one side of the approach vector to the center of the compound as they point in the same direction.

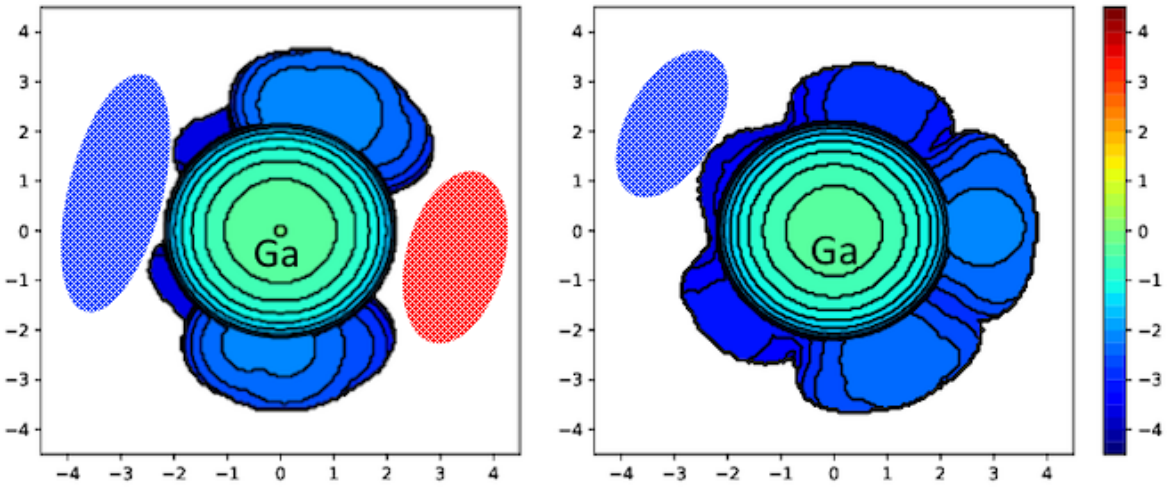

Figure 53: Steric maps of Mo(GaTMP) (left), and MoGa(η^5-Cp*) (right), drawn at a coordination sphere of 4.5 Å. Areas additionally shaded in blue indicate areas, where methyl groups will occupy space, if the coordination sphere is set beyond 4.5 Å. On the left side, an area shaded red indicates a space where no more of the TMP group will occupy space when the coordination sphere is expanded.

This potential opening can of course be blocked by neighboring ligands, thus it is necessary to take note of the steric surroundings of such a potential accessible site. The shape of the sterically blocked off region of space by GaTMP is very similar to that found for Ga(η^1-Cp*), which due to the ring slipping into an asymmetrical position above the Ga atom, creates a similar opening.

An initial understanding of the correlations between buried volumes and the geometric parameters of the [M(E^{I}Cp*)$_n$] class of compounds has thus been developed.

An increase of the standard coordination sphere of 3.5 Å[40] to 4.5 Å has been shown in several examples to yield superior results for the analysis of components [M(E^{I}R)$_n$].

In the case of [M(E^{I}Cp*)$_n$] a reliable correlation with an associated R^2 value of 0.96 between the sums of orthogonal components and respective components buried volumes has been found.

From what has been found, it is reasonable to assume that the findings for [M(E^{I}Cp*)$_n$] will likely also hold true for [M(GaTMP)$_n$], however as of now, only the two mononuclear, homoleptic compounds of GaTMP presented in this very thesis are reported. Thus, from only two compounds, despite each of them giving multiple data points due to distinguishable ligands in the crystal structure, no extrapolations for the entire compound class can be made in good conscience.

Finally, it is as of now, not possible in our case to correlate buried volumes to other properties, chemical or analytical. In the first case this is due to next to no follow-up chemistry having been reported for the examined compounds, and in the latter case due to buried volumes being calculated from the crystal structure and many analytical techniques such as NMR spectroscopy being done in solution, changing the geometry, or the analytical techniques such as FT-IR spectroscopy not being able to easily

resolve parameters associated with metal bonds and the data available in literature not being able to provide sufficient resolution to extract this data due to age.

2.5 Chemical Properties of GaTMP vs. GaCp* on the two examples

The Ruthenium Arc

Over the last two decades, the intermetallic complexes of Ruthenium and Gallium were explored in depth. The reactions of [(*p*-cymene)$RuCl_2$]$_2$ with GaCp* resulted in redox products such as the cube structured [(*p*-cymene)Ru_2(GaCp*)$_4Cl_2$], the reduced dimer [(*p*-cymene)Ru_2(μ-Cl)$_2$] and a series of piano chair type complexes formed as adducts of Ga^{III} side products to the Ru^0 center of (*p*-cymene)Ru(GaCp*)$_2$.[50b]

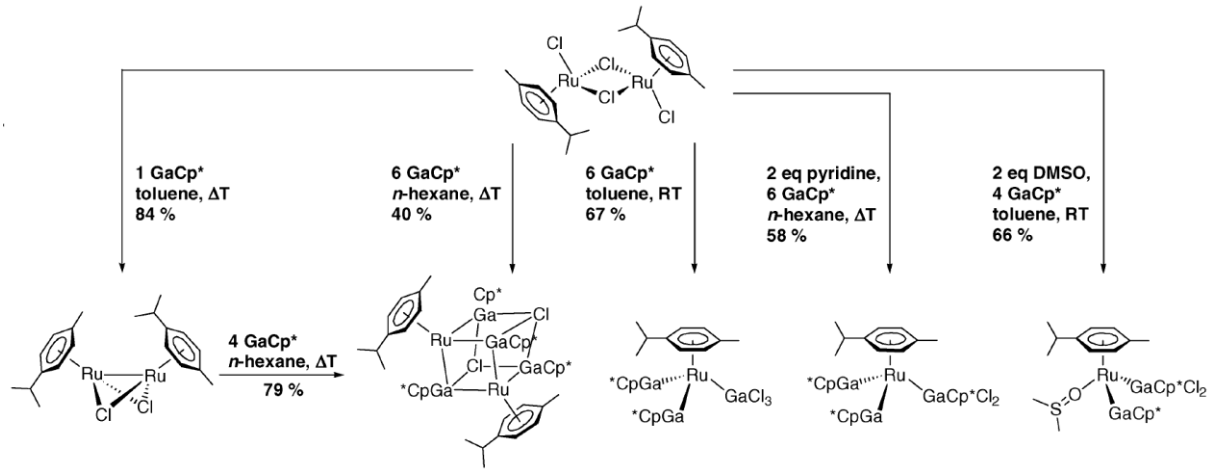

Figure 54: Reactions schemes of [(p-cymene)$RuCl_2$]$_2$ with GaCp* under different conditions. Reprinted (adapted) with permission from M. Cokoja, C. Gemel, T. Steinke, F. Schröder, R. A. Fischer, Dalton Transactions 2005, 44-54 under license 1619832-1. Copyright 2005 The Royal Society of Chemistry.[50b]

Similarly reactions of $Ru(PPh_3)_3Cl_2$ and $Ru(DMSO)_4Cl_2$ with GaCp* yielded oxidized, or in the case of $Ru(PPh_3)_3Cl_2$, orthometallated side products together with the octahedral complex [Ru(GaCp*)$_6Cl_2$]. This complex however exhibits a high degree of fluxionality in its exact bonding of conformation with just the crystal structure exhibiting two crystallographically distinct molecules where in one three of the six Cp* groups are bound via a η^5 bonding whilst the other three are η^1 bound, in the other, four are in η^1 and only two in η^5 binding mode.[50c] To reduce the complications added by the redox processes involved, olefinic Ru^0 complexes were chosen as starting materials, though initial results only managed to initiate a $\eta^6 \rightarrow \eta^4$ shift in [Ru(η^4-COD)(η^6-COT)] forming the [(η^4-COD)(η^4-COT)Ru(GaCp*)] complex.[50a] [Ru(GaCp*)$_3$(tmm)] (tmm = $(C(CH_3)_3)^-$) can be obtained by reacting [Ru(η^4-COD)(η^3-C_4H_7)$_2$] (C_4H_7 = 2-methylallyl) with GaCp*. This compound reacts with H[BAr^F_4] and [Ga_2Cp*][BAr^F_4] to give heteroleptic olefine/GaCp* compounds.[69]

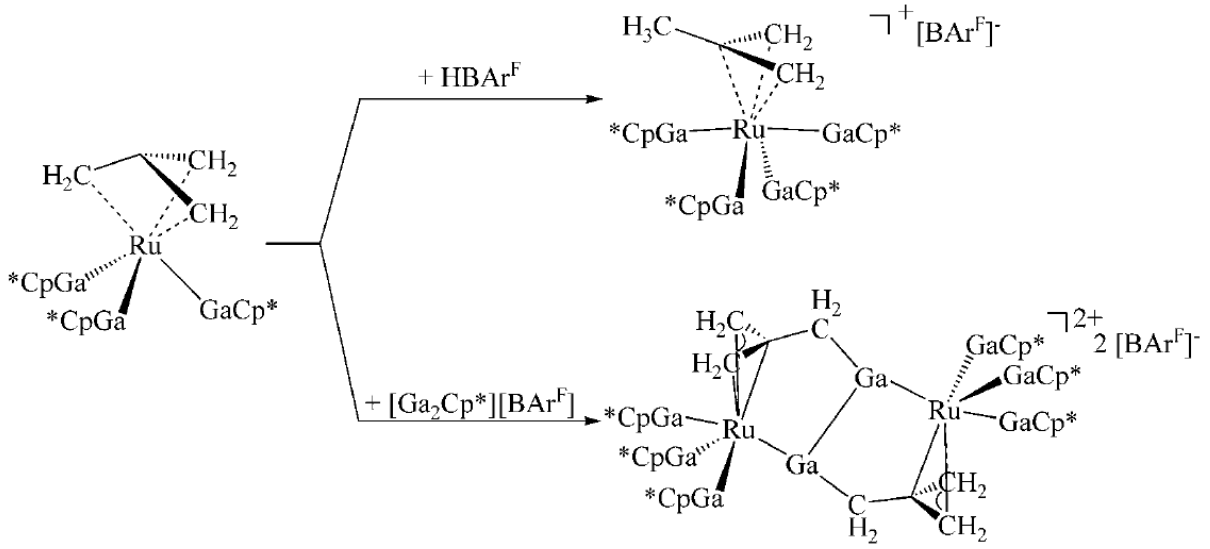

Figure 55: Reaction schemes of [Ru(GaCp*)$_3$(tmm)] with H[BAr$^F_4$] and [Ga$_2$Cp*][BAr$^F_4$]. Reprinted (adapted) with permission from T. Cadenbach, C. Gemel, T. Bollermann, I. Fernandez, G. Frenking, R. A. Fischer, Chemistry – A European Journal 2008, 14, 10789-10796 under license 6046531229533. Copyright 2008 WILEY-VCH Verlag GmbH & Co. KGaA, Weinheim.[69]

The reactivities of ruthenium hydrides, such as [Ru(PCy$_3$)$_2$(H$_2$)$_2$(H)$_2$], [(Cp*Ru)$_2$(μ-H)$_4$] and [(Cp*Ru)$_3$(μ-H)$_3$(μ^3-H)$_2$] towards GaCp* and [Ga$_2$Cp*][BAr$^F_4$], provided further important steps on a new reactivity pathway, though still affected by the $\eta^5 \rightarrow \eta^1$ shift between gallium and the Cp* ligand in their products.[50g, 69] Mild hydrogenolysis of [Ru(η^4-COD)(η^6-COT)] in the presence of GaCp* opened further reactivities, giving access to [Ru(η^4-COD)(GaCp*)$_3$].[50d] This compound is also accessible from the aforementioned [(η^4-COD)(η^4-COT)Ru(GaCp*)] via hydrogenolysis in the presence of GaCp*. When [Ru(η^4-COD)(GaCp*)$_3$] is further allowed to react with hydrogen and GaCp* it is possible to eliminate one Cp*H, forming the intermetallic cluster [(GaCp*)$_4$(H)Ru(μ-Ga)Ru(H)$_2$-(GaCp*)$_3$], which can also be synthesized in a single step from [Ru(η^4-COD)(η^6-COT)] and GaCp* when adjusting the conditions accordingly. An analogous preparation of [(GaCp*)$_4$(H)Ru(μ-Ga)Ru(H)$_2$-(GaCp*)$_3$] from the olefinic [Ru(η^4-COD)(η^3-C$_4$H$_7$)$_2$] is also reported. If this reaction is not carried out under hydrogenolytic conditions, an intermediate product of [Ru(GaCp*)$_3$(tmm)] is obtained, which can then further react in the presence of hydrogen and additional GaCp* to form [(GaCp*)$_4$(H)Ru(μ-Ga)Ru(H)$_2$-(GaCp*)$_3$].[50e] During all these works however, the comparatively simple compound [Ru(GaCp*)$_5$] has eluded all synthetic attempts to date. An analogous carbonyl compound [Ru(CO)$_5$] is reported in literature.[70]

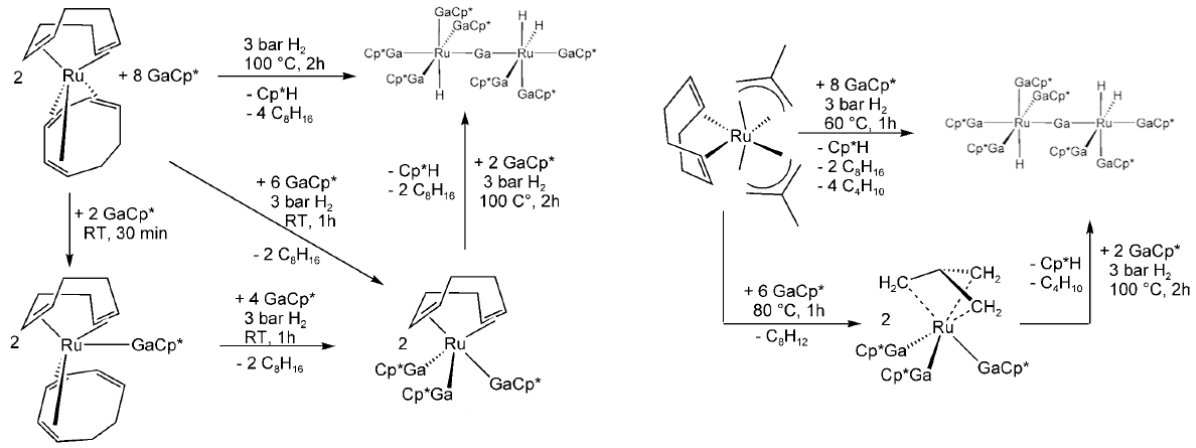

Figure 56: Reaction schemes of olefinic Ru^0 precursors with GaCp* under hydrogenolytic and non-hydrogenolytic conditions. Adapted graphic. Reprinted (adapted) with permission from T. Cadenbach, C. Gemel, R. Schmid, M. Halbherr, K. Yusenko, M. Cokoja, R. A. Fischer, Angewandte Chemie International Edition 2009, 48, 3872-3876 under license 6046540013928. Copyright 2009 WILEY-VCH Verlag GmbH & Co. KGaA, Weinheim.[50e]

The synthetic access to $[Ru(GaTMP)_5]$ starts from the same olefinic Ru^0 precursor $[Ru(\eta^4\text{-COD})(\eta^6\text{-COT})]$, though notably does not require hydrogenolytic conditions. Theoretical intermediates like $[(\eta^4\text{-COD})(\eta^4\text{-COT})Ru(GaTMP)]$ or $[Ru(\eta^4\text{-COD})(GaTMP)_3]$ were not observed, though no dedicated attempts at their synthesis were made.

The heteroleptic, monouclear compound $[(GaCp^*)_3Ru(H_3)(SiEt_3)]$ has been the subject of dedicated research in recent years. It was found as the result of Si-H activation attributed to the not-isolated reactive intermediate $[(GaCp^*)_3Ru(H_2)]$ when reacting $[Ru(\eta^4\text{-COD})(C_4H_7)_2]$ with GaCp* under hydrogenolytic conditions in the presence of $HSiEt_3$.[49, 50f]

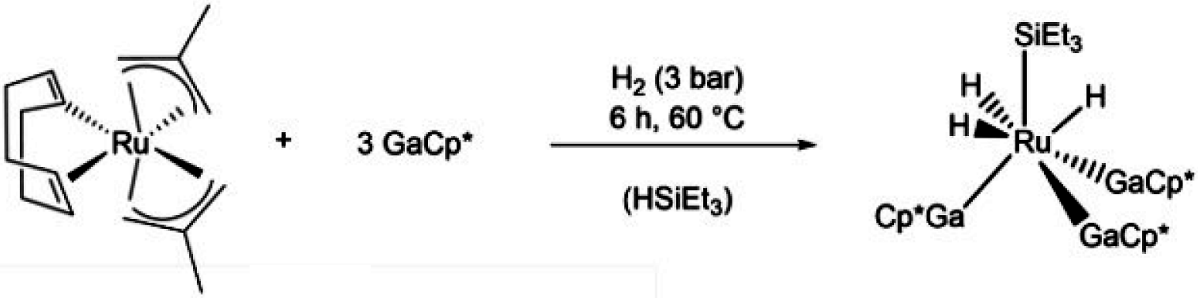

Figure 57: Reaction scheme of the formation of $[(GaCp^*)_3Ru(H_3)(SiEt_3)]$ from $[Ru(\eta^4\text{-COD})(C_4H_7)_2]$ and GaCp* under hydrogenolytic conditions in the presence of $HSiEt_3$. Reprinted (adapted) with permission from M. Muhr, R. Bühler, H. Liang, J. Gilch, C. Jandl, S. Kahlal, J.-Y. Saillard, C. Gemel, R. A. Fischer, Chemistry – A European Journal 2022, 28, e202200887 under license 6046540333704. Copyright 2022 The Authors. Chemistry - A European Journal published by Wiley-VCH GmbH.[49]

Replacing $HSiEt_3$ with toluene under the same conditions yields the C-H activated compound $[(GaCp^*)_3Ru(C_7H_7)(H_3)]$ though this has yet eluded isolation attemps.[49]

Further work then found that $[(GaCp^*)_3Ru(H_3)(SiEt_3)]$ could be converted back to a reactive form by irradiation with λv = 350 nm. This active species was then found to enable catalytic hydrogenation of 3-hexyne.[50f]

Transferring this work onto [Ru(GaTMP)$_5$] and its presumed related compounds would present unique opportunities. As pointed out previously, the formation of [Ru(GaTMP)$_5$] does not rely on the hydrogenolytic conditions necessary for the majority of the GaCp* compounds of Ru, however as of the time of writing, there have been no investigations into the effect hydrogenolytic conditions have on the synthesis of [Ru(GaTMP)$_5$]. Both, the increase in yield, as well as the formation of possibly new species worth exploring are within reason to assume, considering the results of the seminal work by *M. Muhr* on the subject of Ni-GaTMP compounds, indicating that GaTMP does not get altered in a permanent chemical manner when exposed to hydrogenolytic conditions in synthesis, though TMP-H is observed as the major product of the limited catalyst decomposition during prolonged catalytic semihydrogenation experiments.[27b]

The fact that GaTMP has not yet been observed to be susceptible to a similar reductive elimination process as GaCp* in the presence of hydrogen sources denies access to previously established synthetic pathways, yet this could also be a factor enhancing the stability of catalytically active species compared to species based on GaCp*. Similarly GaTMP does not undergo a transmetalation process like GaCp* that is the initial central formation mechanism of the Ni-GaCp* cluster chemistry.[27a, 32]

In case, the assumptions concerning the stable behavior of Ru-GaTMP compounds under hydrogenolytic conditions prove correct, an attempt to synthesize [(GaTMP)$_3$Ru(H$_3$)(SiEt$_3$)] would very likely be successful and deeper investigations into its photochemical behavior and catalytic properties using mass spectrometry and DFT calculations could add very valuable data to our understanding of the cooperative effects between TM and E when putting them into context with previous works.

The Molybdenum Arc

Exploration of the chemistry of E^{I}R in combination with molybdenum sources predate the analogous ruthenium chemistry slightly. GaCp* was found to substitute the olefinic ligand of [Mo(Nor)(CO)$_4$] (Nor = Norbornadiene) when heated in each other's presence within an aliphatic solvent, to form [*cis*-Mo(GaCp*)$_2$(CO)$_4$].[23] A higher degree of substitution can be achieved by heating [*fac*-Mo(MeCN)$_3$(CO)$_3$] in an aromatic solvent with GaCp* to form [*fac*-Mo(GaCp*)$_3$(CO)$_3$]. This product can be made to react with the former starting compound [*fac*-Mo(MeCN)$_3$(CO)$_3$] to form the dimer [(CO)$_3$Mo(μ^2-GaCp*)$_3$Mo(CO)$_3$].[71]

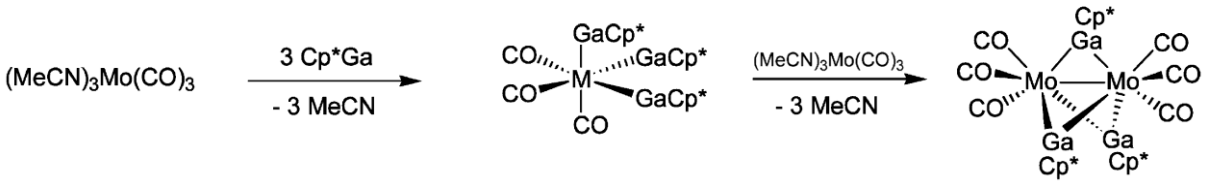

Figure 58: Reaction scheme of the substitution of MeCN from [*fac*-Mo(MeCN)$_3$(CO)$_3$] by GaCp* to from [*fac*-Mo(GaCp*)$_3$(CO)$_3$], followed by the dimerization reaction with more [*fac*-Mo(MeCN)$_3$(CO)$_3$] to form [(CO)$_3$Mo(μ^2-GaCp*)$_3$Mo(CO)$_3$]. Reprinted (adapted) with permission from M. Cokoja, T. Steinke, C. Gemel,

GaCp* was also shown to insert quickly into the lewis acidic metal centers of the dimeric $[Mo(Cp^*)(CO)_2]_2$ in an aliphatic solvent at ambient temperatures to yield the dimeric compound $[Mo(Cp^*)(CO)_2(\mu^2\text{-}(\eta^1\text{-}GaCp^*))]_2$.[71]

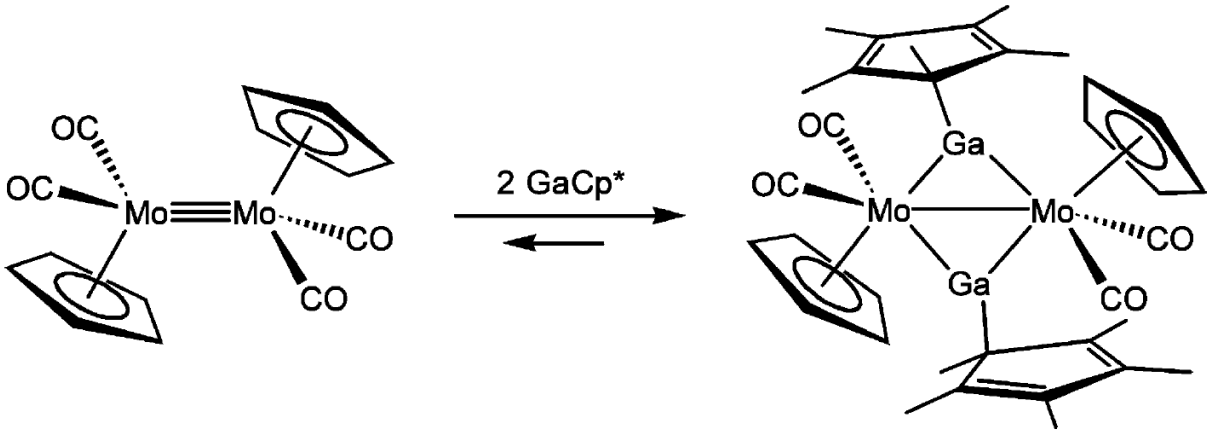

Figure 59:Reaction scheme of the insertion of GaCp* into the unsaturated compound $[Mo(Cp^*)(CO)_2]_2$ to form $[Mo(Cp^*)(CO)_2(\mu^2\text{-}(\eta^1\text{-}GaCp^*))]_2$. Reprinted (adapted) with permission from M. Cokoja, T. Steinke, C. Gemel, T. Welzel, M. Winter, K. Merz, R. A. Fischer, Journal of Organometallic Chemistry 2003, 684, 277-286 under license 6046540794376. Copyright 2003 Published by Elsevier B.V.[71]

Attempts to react [*fac*-$Mo(MeCN)_3(CO)_3$] with InCp* provided no indication of any reaction occurring, whilst a reaction with AlCp* was observed, presumably forming the analogous [*fac*-$Mo(AlCp^*)_3(CO)_3$] and $[(CO)_3Mo(\mu^2\text{-}AlCp^*)_3Mo(CO)_3]$. However no further information on the topic has been published since 2003 at the time of writing. Because an absolute exclusion can never genuinely be claimed, a molecular unit with a $MoAl_3$ unit in its structure is absent from literature. Alloys of the composition $(U/Mo)Al_3$ however are reported.[72]

A compound similar to [*cis*-$Mo(GaCp^*)_2(CO)_4$] can be obtained by reacting $[Mo(N)_2(PMe_3)_5]$ with GaCp* in an aromatic solvent at elevated temperatures to form [*cis*-$Mo(GaCp^*)_2(PMe_3)_4$]. In this case, the starting material $[Mo(N)_2(PMe_3)_5]$ shows no reactivity towards AlCp*, even at elevated temperatures and prolonged reaction times.[73]

The aforementioned $[Mo(Cp^*)(CO)_2]_2$ was also found by *C. Jones et. al.* to react with $Ga[N(C_6H_3{}^iPr_2)]_2CN(Cy)_2$ in the presence of water to give a hydroxy bridged monomeric addition product.[74]

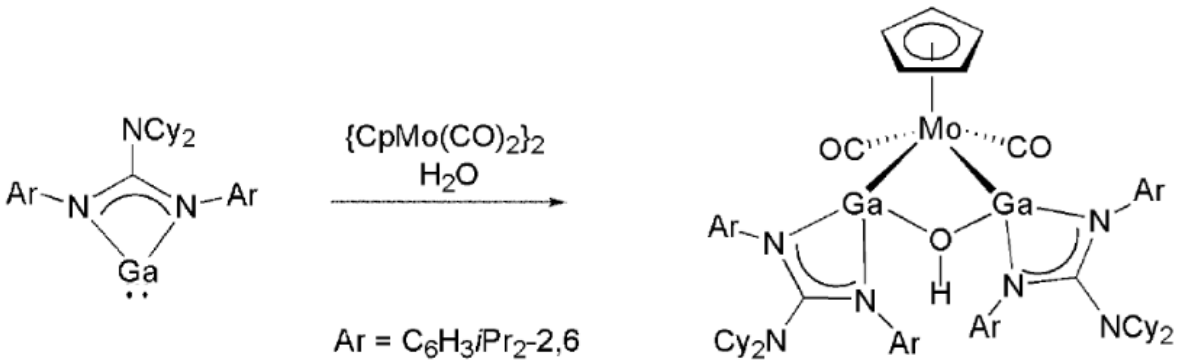

Figure 60: Reaction scheme for the insertion of $Ga[N(C_6H_3{}^iPr_2)]_2CN(Cy)_2$ into $[Mo(Cp^*)(CO)_2]_2$ in the presence of water. Reprinted (adapted) with permission from C. Jones, A. Stasch, G. J. Moxey, P. C. Junk, G. B. Deacon, European Journal of Inorganic Chemistry 2009, 2009, 3593-3599 under license 6046541158665. Copyright 2009 WILEY-VCH Verlag GmbH & Co. KGaA, Weinheim.[74]

The dihydogallane H_2GaDDP reacts with the heteroleptic olefin-carbonyl precursor $[(CO)_4Mo(\eta^4\text{-COD})]$ over the course of several days at elevated temperatures in an aliphatic solvent to give the compound $[(CO)_5Mo(GaDDP)]$. The appearance of a fifth carbonyl ligand is attributed to an exchange reaction with unreacted starting material.[75]

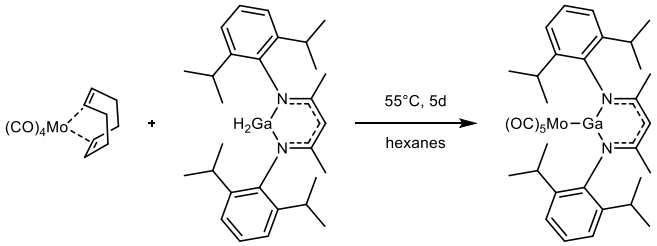

Figure 61: Reaction scheme of $[(CO)_4Mo(\eta^4\text{-COD})]$ reacting with dihydro-GaDDP to form $[(CO)_5Mo(GaDDP)]$. Graphic created according to cited literature.[75]

A photochemical approach was presented by *P. P. Power et. al.* when they found that a precursor terphenyl digallene reacted with $[Mo(CO)_6]$ at close to ambient temperature, when subjected to UV radiation in an aliphatic solvent, forming a disubstituted, heteroleptic tetracarbonyl molybdenum compound. The terphenyl digallene was also found to react without UV radiation when treating with $[Mo(CO)_5(NMe_3)]$ in THF at -78°C to give the mono terphenyl gallanediyl substituted pentacarbonyl.[76]

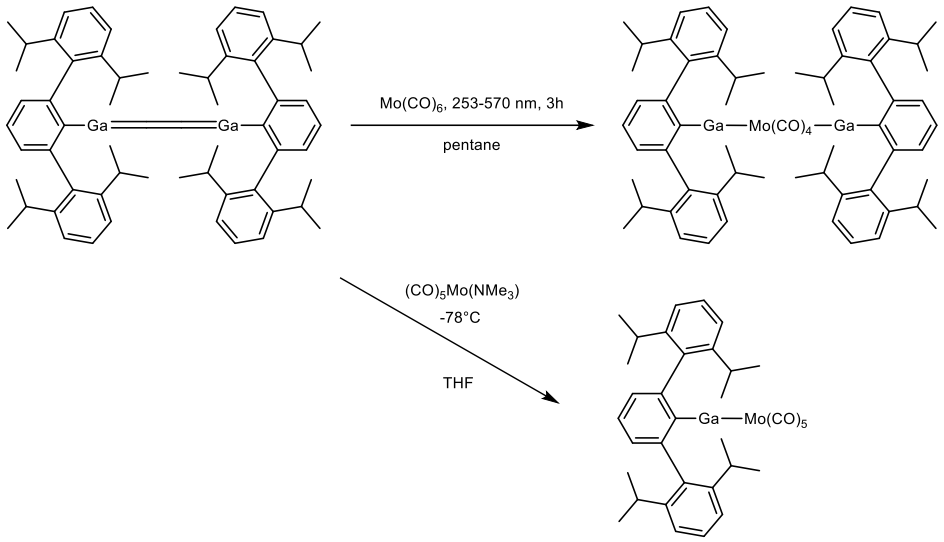

Figure 62: Reaction scheme of the terphenyl digallene reacting with molybdenum carbonyl compounds under different conditions. Graphic created according to cited literature.[76]

Another group showed even more possible substitution reactions on $[Mo(CO)_6]$ and insertions into the unsaturated $[CpMo(CO)_3]$ by a digallane derived from 1,2-bis[(2,6-diisopropylphenyl)imino]acenaphtene ($[(dpp\text{-}bian)Ga]_2$).[77]

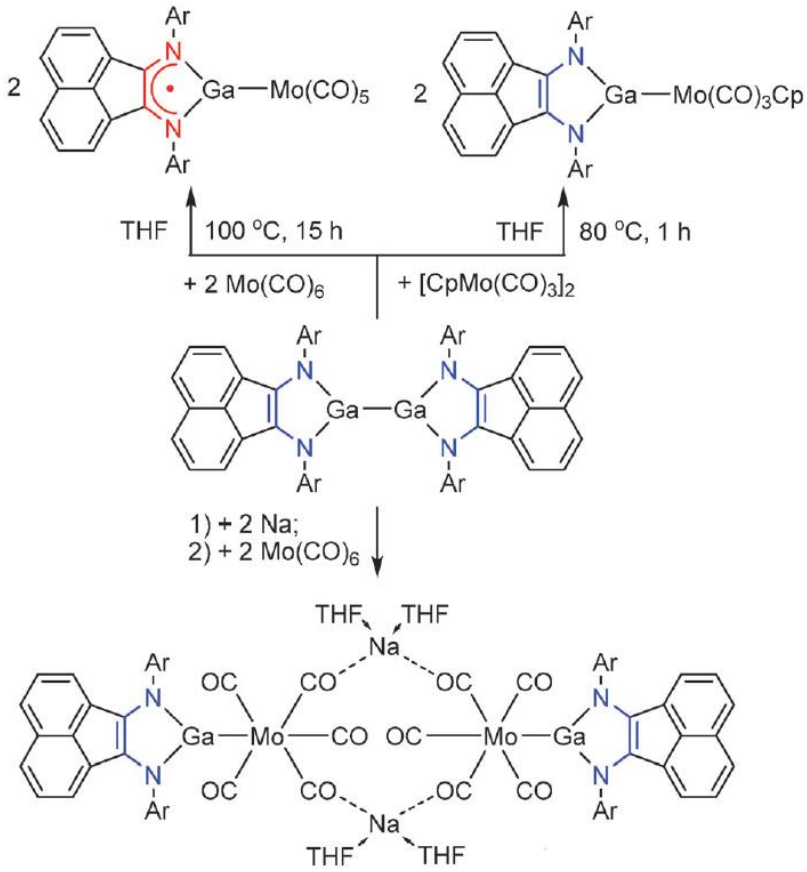

Figure 63: Reaction scheme outlining the observed reactions between Mo-carbonyl compounds and $[(dpp\text{-}bian)Ga]_2$ depicted in the middle. The red and blue highlighting points out an observed emergence of a heterocyclic radical. Reprinted (adapted) with permission from I. L. Fedushkin, V. G. Sokolov, A. V. Piskunov, V. M. Makarov, E. V. Baranov, G. A. Abakumov, Chemical Communications 2014, 50, 10108-10111 under license 1619850-1. Copyright 2014 The Royal Society of Chemistry.[77]

$[(dpp\text{-}bian)Ga]_2$ reacts with $[Mo(CO)_6]$ in a coordinating solvent beyond boiling temperatures in a sealed reaction vessel to form the monosubstituted, radical product $[((dpp\text{-}bian)Ga)Mo(CO)_5]$ within half a day. In the same fashion, the digallane reacts with $[CpMo(CO)_3]_2$ within just one hour to form the monomeric compound $[((dpp\text{-}bian)Ga)Mo(CO)_3Cp]$. Under ambient pressure and temperature, the digallane can be reduced in situ with sodium metal, and then further reacted with $[Mo(CO)_6]$ under the same conditions within one hour to give a product similar to $[((dpp\text{-}bian)Ga)Mo(CO)_5]$, but in a non-radical form and dimerized via two sodium cations to which four units of coordinating solvent are attached.[77]

A purely olefinic molybdenum precursor was only used once before to obtain a $[Mo(E^IR)_n]$ compound when $[Mo(\eta^4\text{-}C_4H_6)_3]$ was reacted with excess GaCp* under hydrogenolytic conditions to yield $[Mo(\eta^1\text{-}GaCp^*)(\eta^5\text{-}GaCp^*)_5]$, forming butane as side product over the course of 16 hours.[29b]

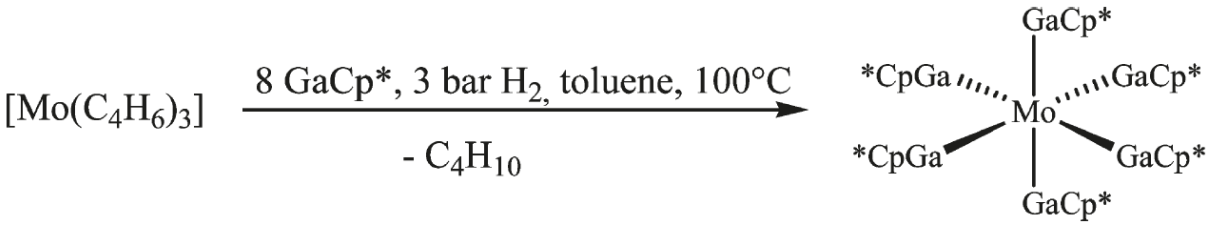

Figure 64: Reaction scheme of the reaction of $[Mo(\eta^4\text{-}C_4H_6)_3]$ under hydrogenolytic conditions with an excess GaCp* in toluene to form $[Mo(\eta^1\text{-}GaCp^*)(\eta^5\text{-}GaCp^*)_5]$, releasing butane. Reprinted (adapted) with permission from T. Bollermann, T. Cadenbach, C. Gemel, K. Freitag, M. Molon, V. Gwildies, R. A. Fischer, Inorganic Chemistry 2011, 50, 5808-5814. Copyright 2011 American Chemical Society.[29b]

The reaction yielding $[Mo(GaTMP)_6]$ is remarkably similar to the reaction yielding $[Mo(GaCp^*)_6]$. Using the same starting material $[Mo(\eta^4\text{-}C_4H_6)_3]$, in the same solvent toluene, at a slightly higher temperature 110 °C, but notably without the need for hydrogen, GaTMP is able to displace the olefinic ligands from $[Mo(\eta^4\text{-}C_4H_6)_3]$.

Notable about $[Mo(GaCp^*)_6]$ is its reactivity towards $ZnMe_2$, which involves a reduction from Zn^{II} to Zn^I and the formation of Ga^{III} byproducs like Me_2GaCp^* and Me_3Ga, fulvalene species and the transfer of Cp* from Ga to Zn to form $[Mo(ZnMe)_9(ZnCp^*)_3]$.[55]

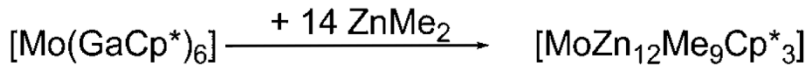

Figure 65: Scheme of the reaction between $[Mo(GaCp^*)_6]$ and $ZnMe_2$ to form $[Mo(ZnMe)_9(ZnCp^*)_3]$. Reprinted (adapted) with permission from T. Cadenbach, T. Bollermann, C. Gemel, I. Fernandez, M. von Hopffgarten, G. Frenking, R. A. Fischer, Angewandte Chemie International Edition 2008, 47, 9150-9154 under license 6046550954491. Copyright 2008 WILEY-VCH Verlag GmbH & Co. KGaA, Weinheim.[55]

Whether reactivity like this can also be expected from $[Mo(GaTMP)_6]$ to form a compounds akin to $[Mo(ZnMe)_9(ZnTMP)_3]$ depends mainly on two factors. The redox step and the transfer of TMP from Ga to Zn. The theoretical major byproduct of a reaction between $ZnMe_2$ and $[Mo(GaTMP)_6]$ aside from Me_3Ga would be Me_2GaTMP, which has already been isolated and reported in the past by *G. Linti et. al.*.[78]

Indications that the transfer step of TMP from Ga to Zn is possible are found within literature, where *C. Jones et. al.* report on the formation of multiple bulky amido Zn compounds L-Zn-Zn-L similar to $Zn_2Cp^*_2$ by means of transmetalation from Mg.[79]

It is, however, very likely, that GaTMP and GaCp* exhibit different kinetics, therefore it is very likely that from the reaction of $[Mo(GaTMP)_6]$ with Me_2Zn a product with a different ZnR shell composition will emerge. This can be assumed because a displacement of Cp* can occur in multiple steps as the bond transitions from Ga(η^5-Cp*) to Ga(η^1-Cp*) via intermediary steps, whilst such steps are naturally not possible with the GaTMP bond.

In light of the above mentioned preceding research history on Mo compounds as well as the work of *G. Linti et.al.* on the subject matter of the reactivity of GaTMP and its heteroleptic transition metal carbonyl compounds, it would be logical to follow this up with studies on the reactivity of $[Mo(GaTMP)_6]$ towards $[Mo(CO)_6]$. *G. Linti et.al.* have demonstrated in their work the substitution of CO ligands by GaTMP as well the reaction of heteroleptic $[TM(CO)_x(GaTMP)_y]$ type compounds with their respective homoleptic carbonyl compounds to form dimers bridged by GaTMP. Given the possibility of bridging on both sides by the homoleptic $[Mo(GaTMP)_6]$ this could reasonably open up a new pathway to intermetalloid cluster compounds.

2.6 Deducing Electronic Properties of GaTMP vs. GaCp*

Both, GaCp* and GaTMP are formally isolobal to CO but are predominantly only σ-donor ligands with notably weaker π-backbonding.[12, 21a, 44, 46] Between the bonds of GaCp* and GaTMP to ruthenium and molybdenum however, the shorter TM-GaTMP bond can be an indication of better π-backbonding, compared to GaCp*, leading to a more stable bond which is especially notable when comparing $[Mo(GaTMP)_6]$ to its direct homologue $[Mo(GaCp^*)_6]$.[29b, 44, 46-47]

Table 8: Comparison of the average Mo-Ga bond lengths in [Å] between $[Mo(GaCp^*)_6]$ and $[Mo(GaTMP)_6]$ with their associated standard deviations in [Å]. Bond lengths were extracted from published crystal structures. For $[Mo(GaTMP)_6]$ twelve bond lengths were extracted from the two crystallographically distinct units, whilst for $[Mo(GaCp^*)_6]$ only the five η^5-bound GaCp* ligands were used.[29b, 47]

Compound	$[Mo(GaCp^*)_6]$	$[Mo(GaTMP)_6]$
Average Mo-Ga bond length [Å]	2.477(1)	2.385(4)
Standard Deviation of Mo-Ga bond length [Å]	0.011(7)	0.006(1)

Though no such direct comparison is available for $[Ru(GaTMP)_5]$ an indirect comparison to previously reported heteroleptic Ru-GaCp* supports this.[47, 49, 50b-g, 69]

The average Ru-Ga bond length found in [Ru(GaTMP)$_6$] is 2.281(9) Å with a standard deviation of 0.007(0) Å.[47]

Table 9: Table of all crystallographically published compounds containing one or more "Ru(μ^1-Ga)(η^5-Cp*)" units with their associated average Ru-Ga bond lengths, as well as the respective compounds minimum and maximum value for said bond length. Global average minimum and average maximum as overall global maxima and minima provided at the end of the table.

Compound	Ru-GaCp* bond length average [Å]	Ru-GaCp* bond length minimum [Å]	Ru-GaCp* bond length maximum [Å]
[Ru(GaCp*)$_6$Cl$_2$][50c]	2.393(9)	2.375(1)	2.408(1)
[(*p*-cymene)Ru(GaCl$_3$)(GaCp*)$_2$][50b]	2.369(9)	2.367(8)	2.372(1)
[(Cp*)Ru(Cp*GaCl)(GaCp*)$_2$][50b]	2.363(3)	2.358(9)	2.367(8)
[(Cp*)Ru(GaCp*)$_3$][Cp*GaCl$_3$][50b]	2.389(8)	2.380(1)	2.396(1)
[(Cp*)Ru(GaCp*)$_3$][BPh$_4$][50b]	2.387(3)	2.376(8)	2.393(8)
[(COD)Ru(H)(GaCp*)$_3$][50g]	2.412(8)	2.404(1)	2.422(1)
[(butadiene)Ru(PPh$_3$)$_2$(GaCp*)][50d]	2.401(5)	2.401(5)	2.401(5)
[(COD)Ru(GaCp*)$_3$][50d]	2.375(1)	2.364(1)	2.394(1)
[Ru$_2$(Ga)(GaCp*)$_7$(H$_3$)][50e]	2.365(8)	2.313(0)	2.440(0)
[(SiEt$_3$)Ru(GaCp*)$_3$][49]	2.379(4)	2.376(3)	2.385(6)
[(dppe)Ru(GaCp*)$_3$][50f]	2.372(6)	2.353(3)	2.393(2)
[(PEt$_3$)$_2$Ru(GaCp*)$_3$][50f]	2.346(3)	2.324(8)	2.386(4)
[(tmm)Ru(GaCp*)$_3$][69]	2.350(2)	2.342(5)	2.357(9)
[(PCy$_3$)Ru(H)$_2$(GaCp*)$_2$][69]	2.407(5)	2.401(5)	2.422(2)
[((GaCp*)$_3$Ru(η^3-(CH$_2$))$_2$C(CH$_2$(μ-Ga))$_2$][BAr$^F_4$]$_2$[69]	2.391(9)	2.371(4)	2.427(0)
[((GaCp*)$_3$Ru(η^3-CH$_2$)(CH(μ-Ga)(CH$_3$))$_2$][BAr$^F_4$]$_2$[69]	2.391(2)	2.361(2)	2.427(0)
[(tmm)Ru(GaCp*)$_4$][69]	2.411(8)	2.385(0)	2.443(4)
[(PCy$_3$)$_2$(Ga)Ru(GaCp*)$_2$][69]	2.422(9)	2.420(6)	2.425(2)

Global average Ru-GaCp* bond length Minimum [Å]	2.346(3)[50f]
Global average Ru-GaCp* bond length Maximum [Å]	2.412(8)[50g]
Global Ru-GaCp* bond length Minimum [Å]	2.313(0)[50e]
Global Ru-GaCp* bond length Maximum [Å]	2.443(4)[69]

It is apparent that there is no crystallographically characterized compound reported in literature which has one or more Ru-μ^1(Ga)(η^5-Cp*)) bonds shorter than the average or longest Ru-GaTMP bond found in [Ru(GaTMP)$_6$]. Whilst this is far from conclusive proof of stronger π-back bonding of GaTMP compared to GaCp*, this is an indication that the Ru-Ga bond is stronger for compounds of GaTMP than it is for compounds of GaCp*.

The same trend towards shortened TM-Ga bonds when comparing GaTMP to GaCp* can be found across all currently published TM-GaTMP compounds. The heteroleptic carbonyl-TM-GaTMP compounds afford additional insight into the comparison between GaCp* and GaTMP since they allow for the direct comparison of opposing CO-TM-Ga bond lengths. For (CO)$_5$CrGaCp* and (CO)$_5$CrGaTMP the Cr-Ga bond lengths are reported as 2.4046(7) Å for GaCp* and 2.374(1) Å for GaTMP. Conversely their respective opposing axial Cr-CO bond lengths are reported as 1.858(4) Å for GaCp* and 1.897(5) Å for GaTMP, indicating a weakening of the Cr-CO bond where the Cr-Ga bond lengths indicate a stronger bond.[21a, 46] The two μ^2-Ga ligated derivatives of (CO)$_3$Co(μ^2-CO)$_2$Co(CO$_3$) are reported as (CO)$_3$Co(μ^2-GaCp*)$_2$Co(CO$_3$) and (CO)$_3$Co(μ^2-GaTMP)$_2$Co(CO$_3$) and exhibit the same tendency, where the Ga-Co bonds are shorter for the TMP compound compared to the Cp* compound, whilst the Co-CO bonds are inversely longer for the TMP compound. Indicating that π-backbonding is also stronger for GaTMP in μ^2-binding mode.[21a, 46] Though no such direct comparison is yet possible for the μ^3-binding mode of GaCp* and GaTMP, comparing the Ga-Ni bond lengths in Ni$_4$(CO)$_6$(μ^2-GaCp*)$_2$(μ^3-GaCp*)$_2$ and [Ni$_3$(GaTMP)$_3$(μ^2-GaTMP)$_3$(μ^3-GaTMP)] equivalently shows shorter Ni-Ga Bonds for Ni-GaTMP compared to GaCp*.[27b, 46]

2.7 Synthetic accessibility and usage of GaTMP

As research into the chemistry of GaTMP as a ligand in organometallic chemistry is ramping up at the time of writing it is important to take note of several certain aspects.

The initial synthesis of GaTMP as presented by *G. Linti et. al.* follows the same principle as the modern synthesis of GaCp*, namely the usage of “GaI” produced from ultrasonic synthesis from elemental Ga metal and Iodine in aromatic solvent, followed by reaction with KCp* or LiTMP respectively.[21b, 44]

For GaCp* this has been established as the *de-facto* routine synthesis with satisfactory yields, with the notable drawback of the very labor intensive preceding four step synthesis of KCp*, starting from 3-pentanone and acetaldehyde.[21b, 80]

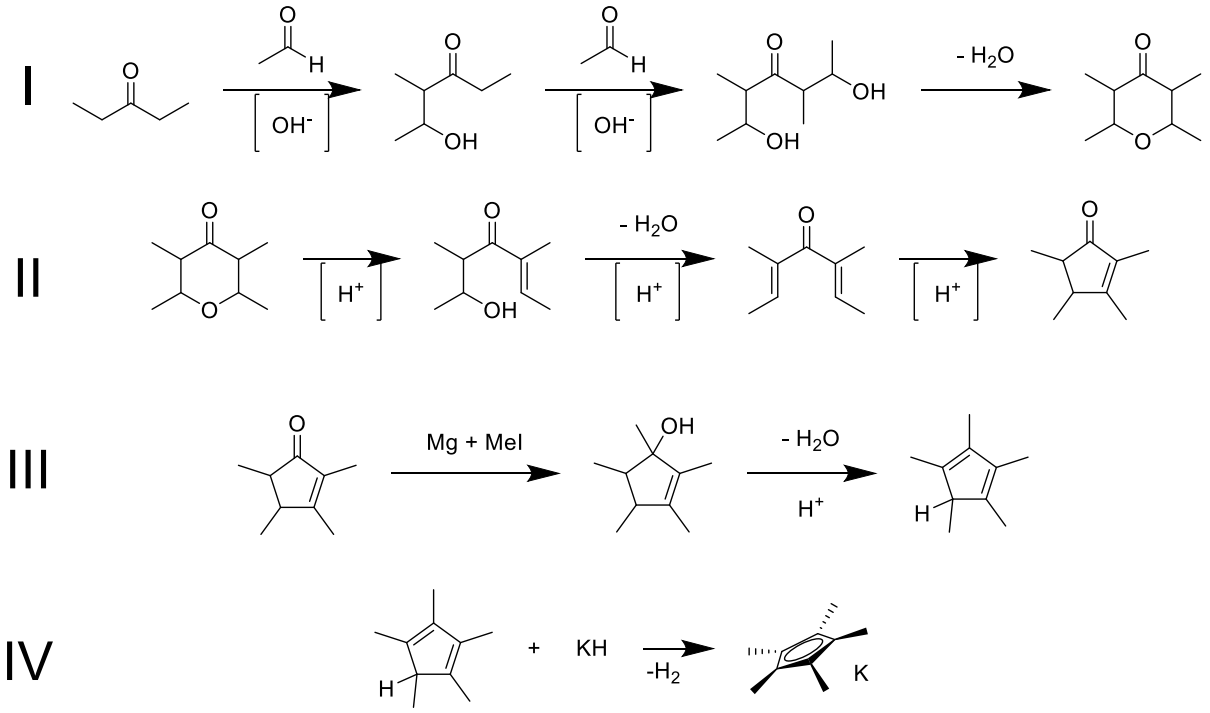

Figure 66: Reaction schemes for the four step synthesis of KCp*. **I**: 2,3,5,6-Tetrahydro-2,3,5,6-tetramethyl-γ-pyrone, is produced by reacting 3-pentanone with acetaldehyde under strongly basic conditions. **II**: Under acidic conditions, the product of **I** forms a divinyl ketone, which then undergoes a *Nazarov* cyclization reaction to yield 2,3,4,5-Tetramethyl-2-cyclopentenone. **III**: The fifth methyl group is introduced via *Grignard* reaction, forming the second double bond in an elimination reaction due to acidic, aqueous workup. **IV**: Pentamethylcyclopentadiene is reacted with KH to give KCp* by means of hydrogen elimination. This four step synthesis takes approximately two weeks to complete.

In contrast to Cp*H, TMPH is widely commercially available in quantity at reasonable cost and the synthesis of LiTMP can be considered trivial, making GaTMP in theory significantly more accessible than GaCp*.[81]

In practice, however, the route to produce GaTMP presented by *G. Linti et. al.* has eluded successful reproduction thus far for reasons unknown. Currently, GaTMP must be obtained from a reaction of GaCp* with LiTMP in yields regularly not exceeding 60%, significantly bottlenecking all further research, revolving around GaTMP even at small scale.[27b]

Considerable amounts of time were spent attempting to find a more accessible synthesis of GaTMP in the past, to no avail. A promising avenue, yet unpursued, is found in the synthesis of GaDDP by *P. P. Power*. Herein GaDDP is produced from “GaI” and LiDDP, though with relevant changes to the temperature of the reaction and a second reaction step involving elemental potassium to convert side products into the desired product.[82]

The chemistry of $[M(E^IR)_n]$ has been limited to late or middle transition metals up until now mostly due to the formation of thermodynamically very stable and inert early

transition metal-arene-sandwich compounds via Cp* transfer from E to the transition metal. [12, 31a, 32] GaTMP possesses no such tendency, as it is not an arene opening up the possibilities to expand the scope of our research beyond pre established metals.

3. Conclusion

In this work, a new class of highly coordinated, mononuclear, homoleptic compounds was introduced to the family of compounds $[M(E^IR)_n]$ in the form of $[M(GaTMP)_n]$. The first two compounds of this class, $[Mo(GaTMP)_6]$, and $[Ru(GaTMP)_5]$ were characterized canonically and by means of “buried volume” calculations.

The titular compounds were prepared from previously reported, neutral, olefinic precursor compounds. The synthetic methodology behind the family of $[M(E^IR)_n]$, was analyzed through the entirety of its 25 years of past research history and the synthesis of the titular compounds was found to align with previously successful methods, giving rise to an expectation that previously successful methods will translate well in significant parts to the future exploration of $[M(GaTMP)_n]$.

By employing buried volume calculations, for the first time, a unified and homogeneous dataset for the entirety of $[M(E^IR)_n]$ has been produced. The unique geometric properties of individual ligands were analyzed in detail and parameters established by which new additions to the family of $[M(E^IR)_n]$ can be added to the dataset.

Along this dataset, commonalities and trends have been found, relating to coordination number, and ligand geometry. Though conclusive in itself, no predictive properties could be established within the dataset, which is mostly due to a lack common follow up chemistry and solvated geometries differing from solid phase geometries.

The titular compounds, $[Mo(GaTMP)_6]$ and $[Ru(GaTMP)_5]$ were contextualized among related compounds. The geometric data of $[Ru(GaTMP)_5]$ was especially compared to all available related compounds GaCp* to establish a credible first qualitative estimation of the bonding properties of GaTMP compared to the well established properties of GaCp*, showing that a slight increase in bond strength between the ligand and a transition metal is credible and likely explained in part by an increase in π-back bonding. It must be noted at this point however that GaTMP is conventionally still a “rather weak” π-back bonding ligand, and that this is a comparison of weak back bonding ligands among themselves.

GaTMP is a promising ligand and despite its introduction more than 15 years ago its chemistry as a ligand is still in its infancy. It is reasonable to expect GaTMP to produce a similar variety of compounds in the near future as GaCp* has done 20 years ago. Should the indications of its bonding properties gained by this work hold true, it is expected that elements, which haven’t yet produced $[M(E^IR)_n]$ type compounds, become accessible given the right precursor compounds, most probable olefinic ones.

Following the footsteps of the previous generation of homoleptic, mononuclear compounds, which gave rise to a rich chemistry of polynuclear “living cluster libraries”, it is very probable that a “second generation” of these compounds will be found. Given the experience gained over the last years within the field and todays available methods, the mononuclear, homoleptic compounds of GaTMP provide a clear path forward to build upon past research and expand our knowledge around intermetalloid clusters.

4. Experimental

4.1 Materials and Methods

Spectroscopy

NMR spectra were recorded on a Bruker Avance III 400US (^{1}H, 400 MHz; ^{13}C 101 MHz). The deuterated solvents were degassed and stored under argon, over molecular sieves (3 Å). Chemical shifts are given relative to TMS and were referenced to the residual solvent peak as internal standards. Chemical shifts are reported in parts per million, downfield shifted from TMS, and are consecutively reported as position (δH or δC), relative integral, multiplicity (s = singlet, t = triplet, and m = multiplet) and assignment. FT-IR spectra were measured on an ATR setup with a Bruker Alpha FTIR spectrometer under an inert gas atmosphere in a glovebox.

Elemental Analysis

Elemental Analysis was performed by the in house microanalytical laboratory.

Mass Spectrometry

The mass spectra of filtered solutions were taken using a Linden CMS LIFDI as ionization source and a ThermoFisher Scientific Exactive Plus Orbitrap as detector. The sample application was performed via a fumed silica capillary from a glovebox under an argon atmosphere to enable the measurement of highly air-sensitive compounds. The recorded mass spectra were integrated using the FreeStyle 1.3 program from ThermoFisher Scientific.

Computational Details

Bruied Volumes (%V_{Bur})[83] and steric maps[41a] for ligands were calculated by using the *SambVca* 2.1 browser application package.[40, 41b, 84] .xyz input files for comparative studies were generated from crystal structures of representative compounds pulled

from the *Cambridge Crystallographic Data Collection*, processed in the *Mercury* software package locally and the respective sources cited. Calculations selected the central metal atom of a representative compound as center of the coordination sphere. The z axis was defined as z-positive from the atom E of the ligand to the central metal atom. The xz plane was chosen arbitrarily. Atomic radii were selected as Bondi radii scaled by 1.17 and the sphere radius was set according to notations with a mesh spacing of 0.05. H atoms were included into the calculation. An input file for a GaCp* coordinated in a manner such as the C_5 ring plane is perpendicular to the Ga-TM-bond-axis was calculated manually as follows. The centroid of the C_5 ring was determined as the geometric mean of the coordinate's vectors of the five individual carbons. The vector from the centroid to the attached Ga-atom was determined and elongated through the Ga-atom, by the value of the length of the Ni-Ga-bond found in $[Ni(GaCp^*)_4]$.[23] At this point a Ni-atom was placed in the input file.

General procedure (work-flow) for computerized peak identification in LIFDI-MS

The general procedure for computerized peak identification in LIFDI-MS involves utilizing a Java computer program (Java 11, openjdk-1.11.0). The program's fundamental principles and workflow are outlined below.

To begin spectrum analysis, the program employs automated pattern recognition, identifying local maxima above a specified threshold value (which users can adjust, defaulting to 1% of the highest peak in the spectrum) as peaks. These peaks are then grouped automatically into peak groups and subsequently into isotopic patterns through a recursive process. The algorithm initiates at the highest remaining peak in the peak list and searches both left and right for peaks with an exact *m/z* shift of 1/z from each other, within a user-defined error range (ε). Users input the charge z of the ions (defaulting to 1) and the recursive process terminates when no peaks remain in the peak list. The resulting list comprises peak groups, which are considered isotopic patterns if they contain a minimum number of peaks (defaulting to 5, user-adjustable).

For pattern analysis, users provide a list of potential fragments by loading a file containing all conceivable fragments the observed ions may consist of (such as metal atoms, ligands, solvents, etc.). The program generates weight matches for each pattern by recursively combining these fragments into ions. All possible fragment combinations up to the *m/z* value of the respective pattern are calculated, using the pattern centroid (intensity-weighted average, (*m/z*)centroid) as the experimental average weight. Acceptable fragment combinations have a molar weight (Mw) falling within the range: (*m/z*)centroid – 2.1 < Mw < (*m/z*)centroid + 4.1. The subtraction of 2.1 accounts for a possible loss of 2 hydrogen atoms and the addition of 4.1 accounts for the possibility of up to four additional hydrogens, which are not part of the input

fragments (accounting for dehydrogenation or hydrogenation/protonation during ionization).

As the list of fragment formulas is often extensive, a "sieving" step is conducted. Isotopic patterns for each fragment are calculated, and an "offset" value is determined by comparing exact m/z values of calculated and experimental patterns. Only patterns with an average offset value below a specified threshold (defaulting to 0.2, user-adjustable) are further considered. The program then computes the goodness of fit (GoF) value between experimental and calculated patterns, and vice versa, using least squares fitting resulting in a total GoF, ranging between 0 (no common peaks) and 1 (identical patterns).

In the output file, each pattern is listed with possible pattern matches and their corresponding final GoF values. Additionally, users can visually compare patterns to their calculated counterparts.

Continuous Shape Measure

The method of continuous shape measure uses the N vertices of an experimentally determined coordination polyhedron normalized and centered in the origin of a three-dimensional cartesian coordinate system as their position vectors Q_i (i = 1,2,3 …, N). These are compared to the position vectors P_i (i = 1,2,3, …, N) of the N vertices of an ideal reference polyhedron that is equally centered and normalized. This is expressed as:

$$S_Q(P) = \frac{1}{N} min \sum_{i=1}^{N} \left|\overrightarrow{Q_i} - \overrightarrow{P_i}\right|^2 \times 100$$

A value of $S_Q(P)$ = 0 thus represents the exact ideal shape, with increasing values indicating increasing distortions. This value was calculated from most ideal superimposition, determined by minimizing the distance between the superimposed polyhedral vertices by a numerical rotation algorithm. $S_Q(P)$ thus is the global minimum of these permutations.

In order to identify the cartesian coordinates of two polyhedra with minimized average distances of their vertices, a Java program has been used (Java 15, openjdk-15). The program takes as input the cartesian coordinates of two polyhedra, both centered at the origin. The program then freely rotates (and also stretches/shrinks on demand) one of the two polyhedra, finally locating the coordinates with minimized distances between the vertices of the two polyhedra in a recursive process.

4.2 Synthesis

General

All experiments were conducted using standard Schlenk and glovebox techniques under an atmosphere of purified argon. All solvents and chemicals, respectively, were carefully dried (water content < 5 ppm) and saturated with argon prior to their use. Basic starting materials were purchased from standard suppliers. The organometallic starting compounds were prepared according to the following literature procedures:

[GaCp]$_4$*[21b]	*[LiTMP]$_4$*[81]
Ru(η^4-COD)(η^6-COT)[85]	*[GaTMP]$_4$*[27b]
MoCl$_4$(MeCN)$_2$[86]	*MoCl$_4$(THF)$_2$*[86]

The synthesis of Mo(η^4-C$_4$H$_6$)$_3$ is described hereafter separately despite being literature known due to significant changes to the synthetic protocol.[87]

Synthesis of [Mo(η^4-C$_4$H$_6$)$_3$]

A 500 mL Schlenk-flask with liquid thermostat mantle was loaded with 2.43 g Mg (100 mmol, 2.5 eq.) a large stir bar and a small kernel of iodine. This was then heated with a heat gun for 10 minutes in static vacuum. After cooling down to RT, THF (100 mL) was added and under vigorous stirring the flask is cooled to -20 °C. 200 mL of a solution of butadiene in THF (2 M, 400 mmol, 10 eq.) was added via cannula. After a few minutes of stirring, 15.2 g MoCl$_4$(THF)$_2$ (40.0 mmol, 1.00 eq.) was added, and the mixture was continuously stirred at -20 °C for 72 h. The then dense brown reaction mixture was reduced to $1/10^{\text{th}}$ volume at -10 °C *in vacuo*, before removing the rest of the liquid completely *in vacuo* at RT. The dark, solid residue is extracted with 400 mL toluene, by stirring for 2 h at RT, followed by cannula filtration after the remaining solids had settled. The dark liquid obtained is again reduced to a dark, sticky solid at RT *in vacuo*. In the same manner as before this solid was extracted with 700 mL pentane and the resulting solution reduced to $1/5^{\text{th}}$ volume *in vacuo* at RT before setting it to crystallize at -80 °C for 12 days. A brown, crystalline solid was obtained by filtration of the supernatant at -80 °C. This solid was recrystallized from THF (20 mL, 50 °C) by cooling down to -32 °C for 24 h, before diluting with cold Et$_2$O (20 mL). At -32 °C the crystalline solid was recovered by filtration, washed with Et$_2$O (3 x 10 mL) and dried *in vacuo* at RT. [Mo(η^4-C$_4$H$_6$)$_3$] was obtained as a crystalline, flaky solid of grey metallic appearance in a yield of 1.74 g (17%).

^{1}H-NMR (THF-*d*$_8$): *δ* (ppm) = 0.53 [m, 6 H,], 1.62 [m, 6 H,], 4.28 [m, 6 H].

Synthesis of [Ru(GaTMP)$_5$]

A 50 mL *Schlenk*-tube was loaded with a sample of 49.0 mg [Ru(η^4-COD)(η^6-COT)] (0.16 mmol, 1.00 eq.) and a sample of 164 mg (GaTMP)$_4$ (0.78 mmol, 1.22 eq.) and the two solids were then dissolved in 5 mL of toluene. The orange-coloured solution was then stirred at 100 °C for 19 h, during this time a change in colour to dark red occurred. Removing the liquid *in vacuo* yielded a brown solid, which was extracted with 10 mL n-hexane. The resulting solution was reduced *in vacuo* to $1/3^{\text{rd}}$ volume and cooled to -80 °C overnight. A brown, crystalline product suitable for SC-XRD was isolated from the reddish-brown supernatant solution via filtration at -78 °C and dried *in vacuo*. This yielded 35.0 mg (30 µmol, 20%) of [Ru(GaTMP)$_5$] as brown crystals.

^{1}H-NMR (C_6D_6): *δ* (ppm) = 1.34 [t, $^3J_{HH}$ = 6.05 Hz, 20 H, $(CH_3)_2CCH_2$], 1.57 [m, 10 H, $CH_2CH_2CH_2$], 1.71 [s, 60 H, CH_3].

^{13}C-NMR (C_6D_6): *δ* (ppm) = 18.9 [$CH_2CH_2CH_2$], 36.3 [CH_3], 41.0 [$CH_2CH_2CH_2$], 55.2 [$C(CH_3)_2$].

$C_{45}H_{90}Ga_5N_5Ru$ (1150.94): calcd. C 46.96, H 7.88, Ga 30.29, N 6.09, Ru 8.78; found C 47.31, H 8.12, N 6.14.

LIFDI-MS: *m/z* 1151.25 $[M]^+$ (calcd. *m/z* 1151.25).

Synthesis of [Mo(GaTMP)$_5$]

A 100 mL Schlenk-tube was loaded with a sample of 100 mg [Mo(η^4-C_4H_6)$_3$] (385.8 µmol, 1.00 eq.) and a sample of 485 mg (GaTMP)$_4$ (2.31 mmol, 6.00 eq.) and both solids were dissolved in 30 mL toluene. The solution was stirred at 110 °C for 22 hours. The liquid was removed *in vacuo* and the remaining solid extracted with 5 ml boiling hexane. The resulting solution was set to 0 °C overnight after which a beige, crystalline product was isolated via filtration and was then dried *in vacuo* affording 218 mg of [Mo(GaTMP)$_6$] (160.8 µmol, 42%).

^{1}H-NMR (Tol-d_8): *δ* (ppm) = 1.35 [t, $^3J_{HH}$ = 6.11 Hz, 24 H, $(CH_3)_2CCH_2$], 1.60 [m, 12 H, $CH_2CH_2CH_2$], 1.73 [s, 72 H, CH_3].

^{13}C-NMR (Tol-d_8): *δ* (ppm) = 18.9 [$CH_2CH_2CH_2$], 36.6 [CH_3], 41.2 [$CH_2CH_2CH_2$], 55.1 [$C(CH3)_2$].

$C_{54}H_{108}Ga_6MoN_6$ (1355.79) Calc: C 47.84; H 8.03; N 6.20; Mo 7.08; Ga 40.86. Found: C 47.40; H 8.07; N 5.98.

LIFDI-MS: *m/z* 1356.32 $[M]^+$ (calcd. m/z 1356.32).

5. References

[1] C. Janiak, H.-J. Meyer, D. Gudat, C. Schulzke, *Riedel Moderne Anorganische Chemie*, De Gruyter, **2023**.

[2] N. Wiberg, *Lehrbuch der Anorganischen Chemie*, De Gruyter, **2008**.

[3] aS. C. Avanzino, A. A. Bakke, H.-W. Chen, C. J. Donahue, W. L. Jolly, T. H. Lee, A. J. Ricco, *Inorganic Chemistry* **1980**, *19*, 1931-1936; bA. M. Ricks, Z. E. Reed, M. A. Duncan, *Journal of Molecular Spectroscopy* **2011**, *266*, 63-74.

[4] A. S. Goldman, K. Krogh-Jespersen, *Journal of the American Chemical Society* **1996**, *118*, 12159-12166.

[5] R. Colton, M. J. McCormick, *Coordination Chemistry Reviews* **1980**, *31*, 1-52.

[6] G. Frenking, N. Fröhlich, *Chemical Reviews* **2000**, *100*, 717-774.

[7] aF. H. Köhler, in *eMagRes*, **2011**; bK. E. Schwarzhans, *Angewandte Chemie International Edition in English* **1970**, *9*, 946-953.

[8] aE. O. Fischer, W. Pfab, **1952**, *7*, 377-379; bW. Erb, N. Richy, J.-P. Hurvois, P. J. Low, F. Mongin, *Dalton Transactions* **2021**, *50*, 16933-16938.

[9] aG. Wilkinson, P. L. Pauson, F. A. Cotton, *Journal of the American Chemical Society* **1954**, *76*, 1970-1974; bN. Hebendanz, F. H. Köhler, F. Scherbaum, B. Schlesinger, *Magnetic Resonance in Chemistry* **1989**, *27*, 798-802.

[10] aB. M. Still, P. G. A. Kumar, J. R. Aldrich-Wright, W. S. Price, *Chemical Society Reviews* **2007**, *36*, 665-686; bD. Rehder, *Coordination Chemistry Reviews* **2008**, *252*, 2209-2223.

[11] J. Uddin, C. Boehme, G. Frenking, *Organometallics* **2000**, *19*, 571-582.

[12] C. Gemel, T. Steinke, M. Cokoja, A. Kempter, Roland A. Fischer, *European Journal of Inorganic Chemistry* **2004**, *2004*, 4161-4176.

[13] A. Purath, H. Schnöckel, *Journal of Organometallic Chemistry* **1999**, *579*, 373-375.

[14] W. Uhl, M. Pohlmann, R. Wartchow, *Angewandte Chemie International Edition* **1998**, *37*, 961-963.

[15] W. Uhl, M. Benter, S. Melle, W. Saak, G. Frenking, J. Uddin, *Organometallics* **1999**, *18*, 3778-3780.

[16] S. P. Green, C. Jones, A. Stasch, *Inorganic Chemistry* **2007**, *46*, 11-13.

[17] aA. Kempter, C. Gemel, N. J. Hardman, R. A. Fischer, *Inorganic Chemistry* **2006**, *45*, 3133-3138; bA. Kempter, C. Gemel, T. Cadenbach, R. A. Fischer, *Inorganic Chemistry* **2007**, *46*, 9481-9487; cG. Prabusankar, S. Gonzalez-Gallardo, A. Doddi, C. Gemel, M. Winter, R. A. Fischer, *European Journal of Inorganic Chemistry* **2010**, *2010*, 4415-4418.

[18] L. J. Morris, T. Rajeshkumar, L. Maron, J. Okuda, *Chemistry – A European Journal* **2022**, *28*, e202201480.

[19] E. O. Fischer, H. P. Hofmann, *Angewandte Chemie* **1957**, *69*, 639-640.

[20] aO. T. Beachley, M. R. Churchill, J. C. Fettinger, J. C. Pazik, L. Victoriano, *Journal of the American Chemical Society* **1986**, *108*, 4666-4668; bC. Dohmeier, C. Robl, M. Tacke, H. Schnöckel, *Angewandte Chemie International*

Edition in English **1991**, *30*, 564-565; cD. Loos, H. Schnöckel, *Journal of Organometallic Chemistry* **1993**, *463*, 37-40.

[21] aP. Jutzi, B. Neumann, G. Reumann, H.-G. Stammler, *Organometallics* **1998**, *17*, 1305-1314; bP. Jutzi, L. O. Schebaum, *Journal of Organometallic Chemistry* **2002**, *654*, 176-179; cC. Ganesamoorthy, S. Loerke, C. Gemel, P. Jerabek, M. Winter, G. Frenking, R. A. Fischer, *Chemical Communications* **2013**, *49*, 2858-2860.

[22] C. Dohmeier, H. Krautscheid, H. Schnöckel, *Angewandte Chemie International Edition in English* **1995**, *33*, 2482-2483.

[23] P. Jutzi, B. Neumann, L. O. Schebaum, A. Stammler, H.-G. Stammler, *Organometallics* **1999**, *18*, 4462-4464.

[24] C. Ganesamoorthy, J. Weßing, C. Kroll, R. W. Seidel, C. Gemel, R. A. Fischer, *Angewandte Chemie International Edition* **2014**, *53*, 7943-7947.

[25] J. Weßing, C. Ganesamoorthy, S. Kahlal, R. Marchal, C. Gemel, O. Cador, A. C. H. Da Silva, J. L. F. Da Silva, J.-Y. Saillard, R. A. Fischer, *Angewandte Chemie International Edition* **2018**, *57*, 14630-14634.

[26] M. Schütz, C. Gemel, M. Muhr, C. Jandl, S. Kahlal, J.-Y. Saillard, R. A. Fischer, *Chemical Science* **2021**, *12*, 6588-6599.

[27] aM. Muhr, J. Stephan, L. Staiger, K. Hemmer, M. Schütz, P. Heiß, C. Jandl, M. Cokoja, T. Kratky, S. Günther, D. Huber, S. Kahlal, J.-Y. Saillard, O. Cador, A. C. H. Da Silva, J. L. F. Da Silva, J. Mink, C. Gemel, R. A. Fischer, *Communications Chemistry* **2024**, *7*, 29; bM. Muhr, H. Liang, L. Allmendinger, R. Bühler, F. E. Napoli, D. Ukaj, M. Cokoja, C. Jandl, S. Kahlal, J.-Y. Saillard, C. Gemel, R. A. Fischer, *Angewandte Chemie International Edition* **2023**, *62*, e202308790.

[28] I. Antsiburov, M. Schütz, R. Bühler, M. Muhr, J. Stephan, C. Gemel, W. Klein, S. Kahlal, J.-Y. Saillard, R. A. Fischer, *Inorganic Chemistry* **2024**.

[29] aL. F. Veiros, *Organometallics* **2000**, *19*, 5549-5558; bT. Bollermann, T. Cadenbach, C. Gemel, K. Freitag, M. Molon, V. Gwildies, R. A. Fischer, *Inorganic Chemistry* **2011**, *50*, 5808-5814.

[30] aC. C. Romão, L. F. Veiros, *Organometallics* **2007**, *26*, 1777-1781; bM. J. Calhorda, L. F. Veiros, *Comments on Inorganic Chemistry* **2001**, *22*, 375-391; cL. F. Veiros, *Journal of Organometallic Chemistry* **1999**, *587*, 221-232.

[31] aT. Bollermann, A. Puls, C. Gemel, T. Cadenbach, R. A. Fischer, *Dalton Transactions* **2009**, 1372-1377; bC. Gemel, T. Steinke, D. Weiss, M. Cokoja, M. Winter, R. A. Fischer, *Organometallics* **2003**, *22*, 2705-2710; cB. Buchin, T. Steinke, C. Gemel, T. Cadenbach, R. A. Fischer, *Zeitschrift für anorganische und allgemeine Chemie* **2005**, *631*, 2756-2762.

[32] M. Muhr, J. Hornung, J. Weßing, C. Jandl, C. Gemel, R. A. Fischer, *Inorganic Chemistry* **2020**, *59*, 5086-5092.

[33] C. A. Tolman, *Journal of the American Chemical Society* **1970**, *92*, 2956-2965.

[34] C. A. Tolman, W. C. Seidel, L. W. Gosser, *Journal of the American Chemical Society* **1974**, *96*, 53-60.

[35] C. A. Tolman, *Chemical Reviews* **1977**, *77*, 313-348.

[36] A. Immirzi, A. Musco, *Inorganica Chimica Acta* **1977**, *25*, L41-L42.

[37] T. L. Brown, K. J. Lee, *Coordination Chemistry Reviews* **1993**, *128*, 89-116.

[38] T. Niksch, H. Görls, W. Weigand, *European Journal of Inorganic Chemistry* **2010**, *2010*, 95-105.

[39] L. Cavallo, A. Correa, C. Costabile, H. Jacobsen, *Journal of Organometallic Chemistry* **2005**, *690*, 5407-5413.

[40] A. Poater, B. Cosenza, A. Correa, S. Giudice, F. Ragone, V. Scarano, L. Cavallo, *European Journal of Inorganic Chemistry* **2009**, *2009*, 1759-1766.

[41] aA. Poater, F. Ragone, R. Mariz, R. Dorta, L. Cavallo, *Chemistry – A European Journal* **2010**, *16*, 14348-14353; bL. Falivene, R. Credendino, A. Poater, A. Petta, L. Serra, R. Oliva, V. Scarano, L. Cavallo, *Organometallics* **2016**, *35*, 2286-2293.

[42] M. Molon, C. Gemel, M. von Hopffgarten, G. Frenking, R. A. Fischer, *Inorganic Chemistry* **2011**, *50*, 12296-12302.

[43] A. G. Blackman, E. B. Schenk, R. E. Jelley, E. H. Krenske, L. R. Gahan, *Dalton Transactions* **2020**, *49*, 14798-14806.

[44] A. Seifert, G. Linti, *European Journal of Inorganic Chemistry* **2007**, *2007*, 5080-5086.

[45] M. L. H. Green, P. Mountford, G. J. Smout, S. R. Speel, *Polyhedron* **1990**, *9*, 2763-2765.

[46] A. Seifert, G. Linti, *Inorganic Chemistry* **2008**, *47*, 11398-11404.

[47] R. Bühler, R. J. J. Weininger, J. Stephan, M. Muhr, B. M. T. Bock, C. Gemel, R. A. Fischer, *Dalton Transactions* **2024**, *53*, 17162-17168.

[48] W. Zou, Y. Tao, E. Kraka, *Journal of Chemical Theory and Computation* **2020**, *16*, 3162-3193.

[49] M. Muhr, R. Bühler, H. Liang, J. Gilch, C. Jandl, S. Kahlal, J.-Y. Saillard, C. Gemel, R. A. Fischer, *Chemistry – A European Journal* **2022**, *28*, e202200887.

[50] aT. Steinke, M. Cokoja, C. Gemel, A. Kempter, A. Krapp, G. Frenking, U. Zenneck, R. A. Fischer, *Angewandte Chemie International Edition* **2005**, *44*, 2943-2946; bM. Cokoja, C. Gemel, T. Steinke, F. Schröder, R. A. Fischer, *Dalton Transactions* **2005**, 44-54; cB. Buchin, C. Gemel, A. Kempter, T. Cadenbach, R. A. Fischer, *Inorganica Chimica Acta* **2006**, *359*, 4833-4839; dT. Cadenbach, C. Gemel, T. Bollermann, R. A. Fischer, *Inorganic Chemistry* **2009**, *48*, 5021-5026; eT. Cadenbach, C. Gemel, R. Schmid, M. Halbherr, K. Yusenko, M. Cokoja, R. A. Fischer, *Angewandte Chemie International Edition* **2009**, *48*, 3872-3876; fR. Bühler, M. Muhr, J. Stephan, R. A. Wolf, M. Schütz, C. Gemel, R. A. Fischer, *Dalton Transactions* **2023**, *52*, 10905-10910; gT. Cadenbach, T. Bollermann, C. Gemel, R. A. Fischer, *Dalton Transactions* **2009**, 322-329.

[51] aX. Wang, L. Andrews, *The Journal of Physical Chemistry A* **2005**, *109*, 9021-9027; bH.-G. Cho, L. Andrews, *Journal of the American Chemical Society* **2005**, *127*, 8226-8231.

[52] W. Uhl, S. Melle, *Zeitschrift für anorganische und allgemeine Chemie* **2000**, *626*, 2043-2045.

[53] T. Steinke, C. Gemel, M. Cokoja, M. Winter, R. A. Fischer, *Angewandte Chemie International Edition* **2004**, *43*, 2299-2302.

[54] T. Cadenbach, C. Gemel, D. Zacher, R. A. Fischer, *Angewandte Chemie International Edition* **2008**, *47*, 3438-3441.

[55] T. Cadenbach, T. Bollermann, C. Gemel, I. Fernandez, M. von Hopffgarten, G. Frenking, R. A. Fischer, *Angewandte Chemie International Edition* **2008**, *47*, 9150-9154.

[56] G. Prabusankar, C. Gemel, M. Winter, R. W. Seidel, R. A. Fischer, *Chemistry – A European Journal* **2010**, *16*, 6041-6047.

[57] C. Schnitter, H. W. Roesky, C. Röpken, R. Herbst-Irmer, H.-G. Schmidt, M. Noltemeyer, *Angewandte Chemie International Edition* **1998**, *37*, 1952-1955.

[58] aG. Linti, *Journal of Organometallic Chemistry* **1996**, *520*, 107-113; bA. Purath, C. Dohmeier, A. Ecker, H. Schnöckel, K. Amelunxen, T. Passler, N. Wiberg, *Organometallics* **1998**, *17*, 1894-1896; cN. Wiberg, K. Amelunxen, H. W. Lerner, H. Nöth, W. Ponikwar, H. Schwenk, *Journal of Organometallic Chemistry* **1999**, *574*, 246-251.

[59] G. Linti, W. Köstler, *Chemistry – A European Journal* **1998**, *4*, 942-949.

[60] W. Uhl, W. Hiller, M. Layh, W. Schwarz, *Angewandte Chemie International Edition in English* **1992**, *31*, 1364-1366.

[61] A. Haaland, K.-G. Martinsen, H. V. Volden, W. Kaim, E. Waldhör, W. Uhl, U. Schütz, *Organometallics* **1996**, *15*, 1146-1150.

[62] aW. Uhl, R. Graupner, M. Layh, U. Schütz, *Journal of Organometallic Chemistry* **1995**, *493*, C1-C5; bR. D. Schluter, A. H. Cowley, D. A. Atwood, R. A. Jones, J. L. Atwood, *Journal of Coordination Chemistry* **1993**, *30*, 25-28.

[63] W. Uhl, S. U. Keimling, S. Phol, W. Saak, R. Wartchow, *Chemische Berichte* **1997**, *130*, 1269-1272.

[64] D. Loos, E. Baum, A. Ecker, H. Schnöckel, A. J. Downs, *Angewandte Chemie International Edition in English* **1997**, *36*, 860-862.

[65] L. Canovese, F. Visentin, *Inorganica Chimica Acta* **2010**, *363*, 2375-2386.

[66] J. Krause, G. Cestaric, K.-J. Haack, K. Seevogel, W. Storm, K.-R. Pörschke, *Journal of the American Chemical Society* **1999**, *121*, 9807-9823.

[67] aU. Zenneck, *Angewandte Chemie International Edition in English* **1990**, *29*, 126-137; bS. D. Ittel, C. A. Tolman, *Organometallics* **1982**, *1*, 1432-1436; cD. L. Williams-Smith, L. R. Wolf, P. S. Skell, *Journal of the American Chemical Society* **1972**, *94*, 4042-4043.

[68] aV. Albano, P. L. Bellon, V. Scatturin, *Chemical Communications (London)* **1966**, 507-507; bP. A. Chaloner, P. B. Hitchcock, G. T. L. Broadwood-Strong, *Acta Crystallographica Section C* **1989**, *45*, 1309-1311.

[69] T. Cadenbach, C. Gemel, T. Bollermann, I. Fernandez, G. Frenking, R. A. Fischer, *Chemistry – A European Journal* **2008**, *14*, 10789-10796.

[70] W. Manchot, W. J. Manchot, *Zeitschrift für anorganische und allgemeine Chemie* **1936**, *226*, 385-415.

[71] M. Cokoja, T. Steinke, C. Gemel, T. Welzel, M. Winter, K. Merz, R. A. Fischer, *Journal of Organometallic Chemistry* **2003**, *684*, 277-286.

[72] aH. J. Ryu, Y. S. Kim, G. L. Hofman, J. M. Park, C. K. Kim, *Journal of Nuclear Materials* **2006**, *358*, 52-56; bH. Palancher, P. Martin, V. Nassif, R. Tucoulou, O.

Proux, J.-L. Hazemann, O. Tougait, E. Lahéra, F. Mazaudier, C. Valot, S. Dubois, *Journal of Applied Crystallography* **2007**, *40*, 1064-1075.

[73] M. Molon, T. Bollermann, C. Gemel, J. Schaumann, R. A. Fischer, *Dalton Transactions* **2011**, *40*, 10769-10774.

[74] C. Jones, A. Stasch, G. J. Moxey, P. C. Junk, G. B. Deacon, *European Journal of Inorganic Chemistry* **2009**, *2009*, 3593-3599.

[75] J. Turner, J. A. B. Abdalla, J. I. Bates, R. Tirfoin, M. J. Kelly, N. Phillips, S. Aldridge, *Chemical Science* **2013**, *4*, 4245-4250.

[76] M. L. McCrea-Hendrick, C. A. Caputo, C. J. Roberts, J. C. Fettinger, H. M. Tuononen, P. P. Power, *Organometallics* **2016**, *35*, 579-586.

[77] I. L. Fedushkin, V. G. Sokolov, A. V. Piskunov, V. M. Makarov, E. V. Baranov, G. A. Abakumov, *Chemical Communications* **2014**, *50*, 10108-10111.

[78] G. Linti, R. Frey, K. Polborn, *Chemische Berichte* **1994**, *127*, 1387-1393.

[79] aJ. Hicks, E. J. Underhill, C. E. Kefalidis, L. Maron, C. Jones, *Angewandte Chemie International Edition* **2015**, *54*, 10000-10004; bM. Juckel, D. Dange, C. de Bruin-Dickason, C. Jones, *Zeitschrift für anorganische und allgemeine Chemie* **2020**, *646*, 603-608; cI. Resa, E. Carmona, E. Gutierrez-Puebla, A. Monge, *Science* **2004**, *305*, 1136-1138.

[80] F. X. Kohl, P. Jutzi, *Journal of Organometallic Chemistry* **1983**, *243*, 119-121.

[81] M. F. Lappert, M. J. Slade, A. Singh, J. L. Atwood, R. D. Rogers, R. Shakir, *Journal of the American Chemical Society* **1983**, *105*, 302-304.

[82] N. J. Hardman, B. E. Eichler, P. P. Power, *Chemical Communications* **2000**, 1991-1992.

[83] A. Poater, F. Ragone, S. Giudice, C. Costabile, R. Dorta, S. P. Nolan, L. Cavallo, *Organometallics* **2008**, *27*, 2679-2681.

[84] L. Falivene, Z. Cao, A. Petta, L. Serra, A. Poater, R. Oliva, V. Scarano, L. Cavallo, *Nature Chemistry* **2019**, *11*, 872-879.

[85] P. Pertici, G. Vitulli, M. Paci, L. Porri, *Journal of the Chemical Society, Dalton Transactions* **1980**, 1961-1964.

[86] J. R. Dilworth, R. L. Richards, G. J. J. Chen, J. W. McDonald, in *Inorganic Syntheses*, **1990**, pp. 33-43.

[87] W. Gausing, G. Wilke, *Angewandte Chemie International Edition in English* **1981**, *20*, 186-187.

6. Appendix

6.1 Characterization of [Ru(GaTMP)$_5$]

^{1}H-NMR spectrum of [Ru(GaTMP)$_5$]

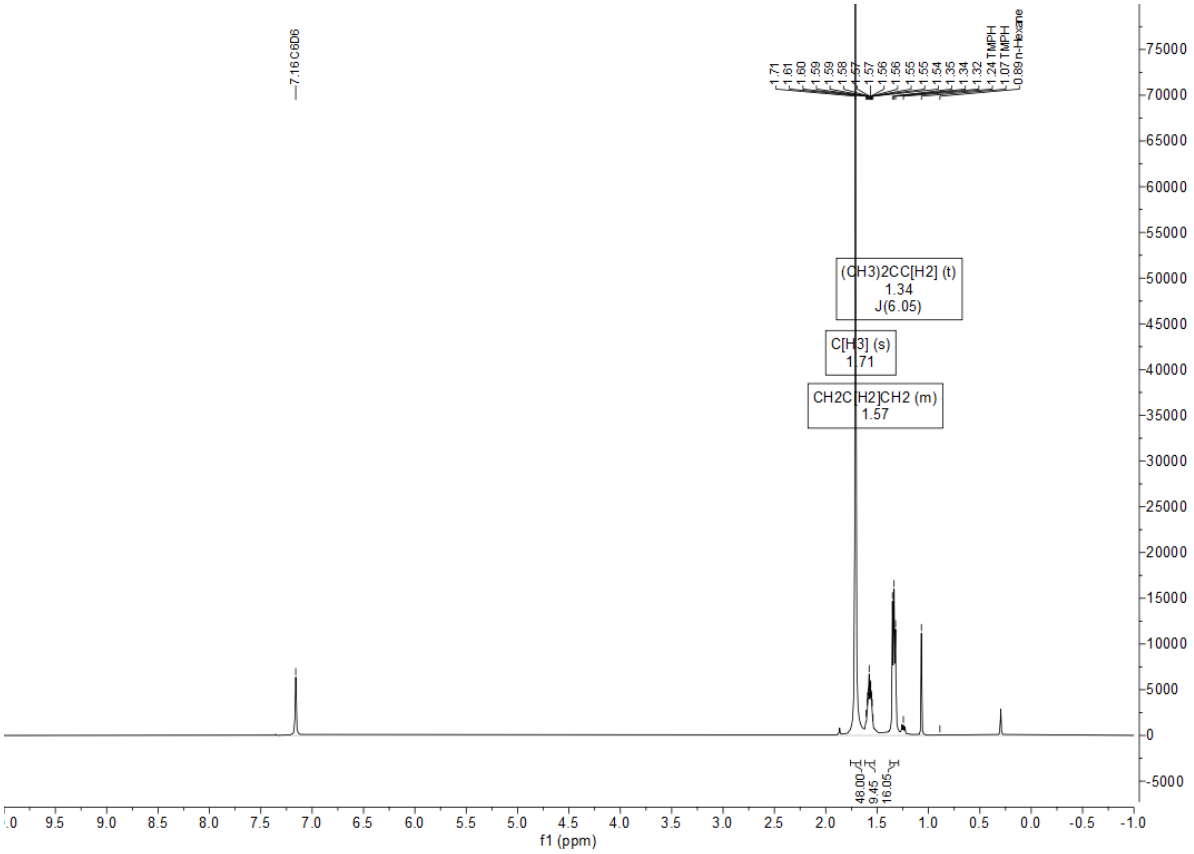

Figure S 1: ^{1}H-NMR spectrum of [Ru(GaTMP)$_5$] in C_6D_6, recorded at 298 K. Signals at 1.24 and 1.07 ppm are attributed to TMPH. The signal at 0.89 pp is attributed to *n*-hexane. The signal around 0.25 ppm is attributed to silicone grease. Reprinted (adapted) with permission from R. Bühler, R. J. J. Weininger, J. Stephan, M. Muhr, B. M. T. Bock, C. Gemel, R. A. Fischer, Dalton Transactions 2024, under CC BY 3.0 license. Copyright 2024 The Royal Society of Chemistry.

^{13}C-NMR spectrum of [Ru(GaTMP)$_5$]

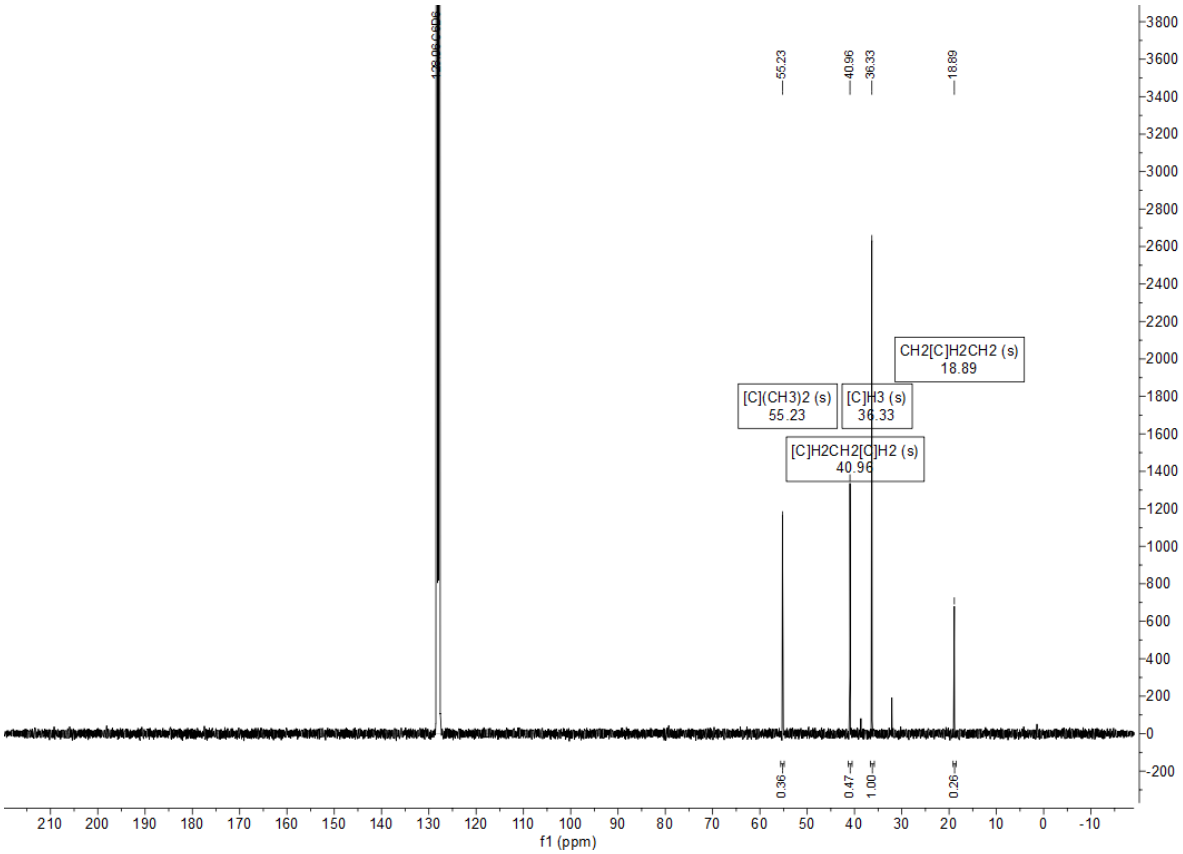

Figure S 2: ^{13}C-NMR spectrum of [Ru(GaTMP)$_5$] in C_6D_6, recorded at 298 K. Reprinted (adapted) with permission from R. Bühler, R. J. J. Weininger, J. Stephan, M. Muhr, B. M. T. Bock, C. Gemel, R. A. Fischer, Dalton Transactions 2024, under CC BY 3.0 license. Copyright 2024 The Royal Society of Chemistry.

FT-IR spectrum of [Ru(GaTMP)$_5$]

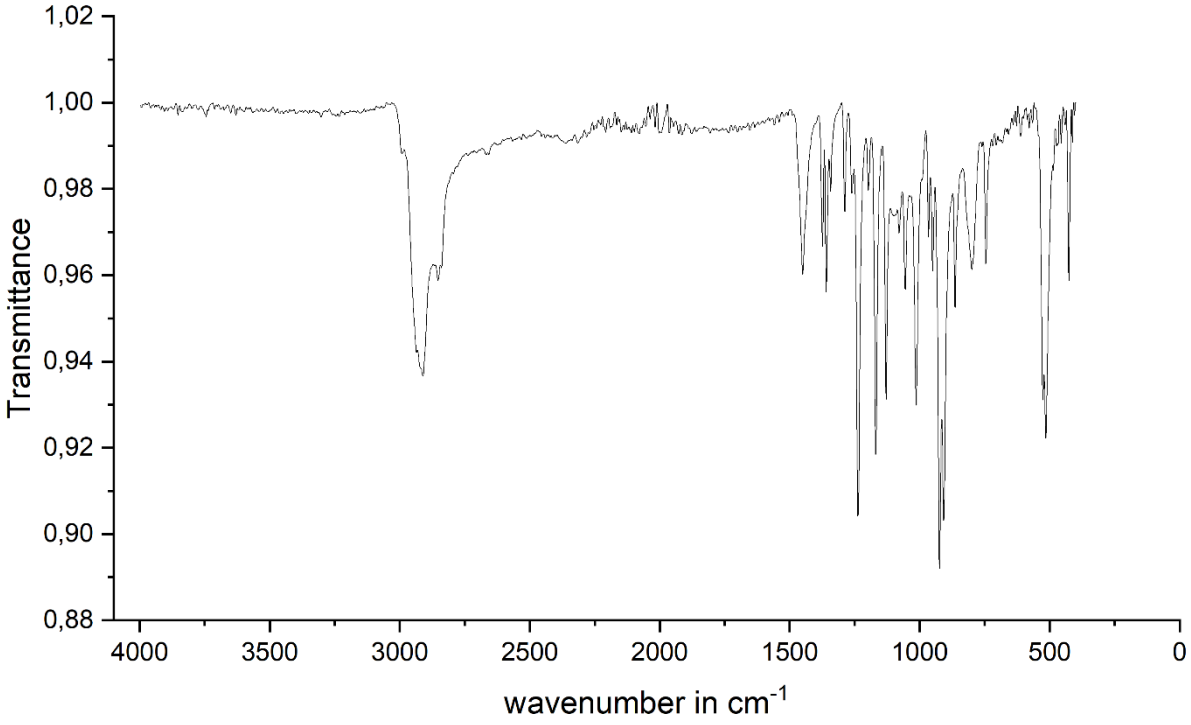

Figure S 3: FT-IR spectrum of [Ru(GaTMP)$_5$]. Reprinted (adapted) with permission from R. Bühler, R. J. J. Weininger, J. Stephan, M. Muhr, B. M. T. Bock, C. Gemel, R. A. Fischer, Dalton Transactions 2024, under CC BY 3.0 license. Copyright 2024 The Royal Society of Chemistry.

LIFDI-MS spectrum of [Ru(GaTMP)$_5$]

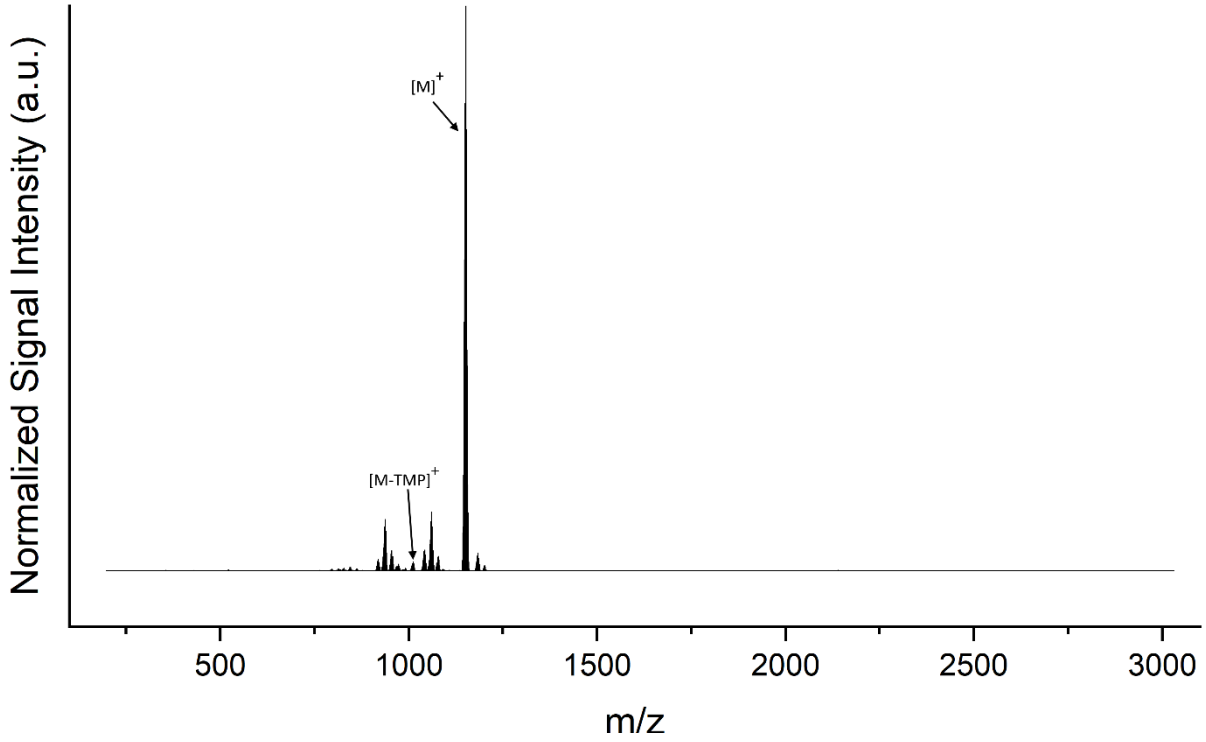

Figure S 4: LIFDI-MS spectrum of [Ru(GaTMP)$_5$]. A molecular ion $[M]^+$ with *m/z* = 1151.25 can be observed at 100% relative intensity. A fragment ion $[M\text{-}TMP]^+$ with *m/z* = 1011.11 is also observed at 1.6% relative intensity. No sensible compounds directly related to the parent ion can be suggested for the remaining signals. Reprinted (adapted) with permission from R. Bühler, R. J. J. Weininger, J. Stephan, M. Muhr, B. M. T. Bock, C. Gemel, R. A. Fischer, Dalton Transactions 2024, under CC BY 3.0 license. Copyright 2024 The Royal Society of Chemistry.

SC-XRD structure report for [Ru(GaTMP)$_5$]

Measurements, structure solutions and refinement by Johannes Stephan (AMC Group @ TUM)

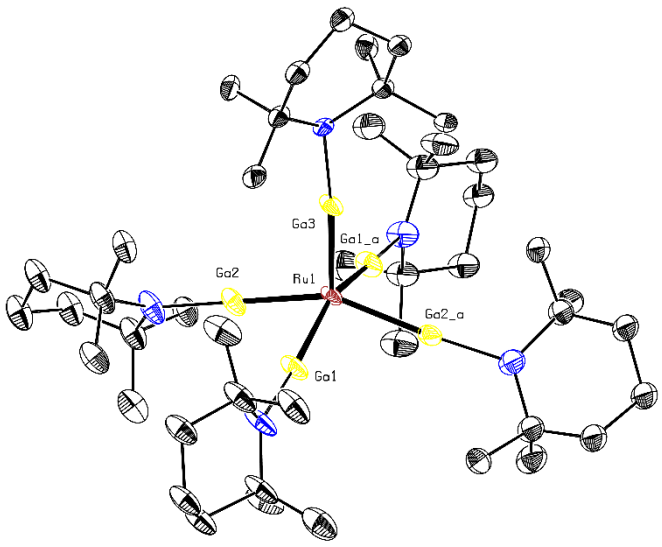

Figure S 5: Molecular structure of [Ru(GaTMP)$_5$] in the solid state determined by single crystal X-ray diffraction. Ru: orange, Ga: yellow, N: blue and C: black. Hydrogen atoms and disordered molecule fragments are omitted. Thermal ellipsoids are shown at the 50% probability level. Reprinted (adapted) with permission from R. Bühler, R. J. J. Weininger, J. Stephan, M. Muhr, B. M. T. Bock, C. Gemel, R. A. Fischer, Dalton Transactions 2024, under CC BY 3.0 license. Copyright 2024 The Royal Society of Chemistry.

A yellow, block-shaped crystal of $C_{45}H_{90}Ga_5N_5Ru$ coated with perfluorinated ether and fixed on top of a Kapton micro sampler was used for X-ray crystallographic analysis. The X-ray intensity data were collected at 100(2) K on a Bruker D8 VENTURE Duo three-angle diffractometer with an IMS microsource with MoK_α radiation (λ=0.71073 Å) using APEX4.[1C1] The diffractometer was equipped with a Helios optic monochromator, a Bruker PHOTON II detector, and a low temperature device.

A matrix scan was used to determine the initial lattice parameters. All data were integrated with the Bruker SAINT V8.40B software package using a narrow-frame algorithm and the reflections were corrected for Lorentz and polarisation effects, scan speed, and background.[2C1] The integration of the data using a monoclinic unit cell yielded a total of 5479 reflections within a 2θ range [°] of 3.82 to 52.83 (0.80 Å), of which 5479 were independent. Data were corrected for absorption effects including odd and even ordered spherical harmonics by the multi-scan method (TWINABS 2012/1).[3C1] Space group assignment was based upon systematic absences, E statistics, and successful refinement of the structure.

Appendix

The structure was solved by direct methods using SHELXT and refined by full-matrix least-squares methods against F^2 by minimizing $\Sigma w(F_o^2 - F_c^2)^2$ using SHELXL in conjunction with SHELXLE.[4C1-6C1] All non-hydrogen atoms were refined with anisotropic displacement parameters. Hydrogen atoms were refined isotropically on calculated positions using a riding model with their U_{iso} values constrained to 1.5 times the U_{eq} of their pivot atoms for terminal sp^3 carbon atoms and a C–H distance of 0.98 Å. Non-methyl hydrogen atoms were refined using a riding model with methylene, aromatic, and other C–H distances of 0.99 Å, 0.95 Å, and 1.00 Å, respectively, and U_{iso} values constrained to 1.2 times the U_{eq} of their pivot atoms.

Neutral atom scattering factors for all atoms and anomalous dispersion corrections for the non-hydrogen atoms were taken from International Tables for Crystallography.[7C1] Crystallographic data for the structures reported in this paper have been deposited with the Cambridge Crystallographic Data Centre.[8C1] Supplementary crystallographic data reported in this paper have been deposited with the Cambridge Crystallographic Data Centre (CCDC 2341048) and can be obtained free of charge from The Cambridge Crystallographic Data Centre via www.ccdc.cam.ac.uk/structures.[8C1] This report and the CIF file were generated using FinalCif.[9C1] Figures showing the coordination polyhedra around the ruthenium centre were created using VESTA 3.[10C1]

Refinement details for compound $[Ru(GaTMP)_5]$.

[Ru(GaTMP)] was refined as a two-component twin.

Table S 1: Crystal data and structure refinement for $[Ru(GaTMP)_5]$. Reprinted (adapted) with permission from R. Bühler, R. J. J. Weininger, J. Stephan, M. Muhr, B. M. T. Bock, C. Gemel, R. A. Fischer, Dalton Transactions 2024, under CC BY 3.0 license. Copyright 2024 The Royal Society of Chemistry.

CCDC number	2341048
Empirical formula	$C_{45}H_{90}Ga_5N_5Ru$
Formula weight	1150.88
Temperature [K]	100(2)
Crystal system	monoclinic
Space group (number)	$\frac{C2}{c}$ (15)
a [Å]	23.4724(19)
b [Å]	11.9908(9)
c [Å]	18.9429(14)
α [°]	90
β [°]	93.343(3)
γ [°]	90
Volume [Å^3]	5322.5(7)
Z	4
ρ_{calc} [gcm^{-3}]	1.436

μ [mm^{-1}]	2.804
F(000)	2376
Crystal size [mm^3]	0.113×0.120×0.312
Crystal colour	yellow
Crystal shape	fragment
Radiation	MoK_α (λ=0.71073 Å)
2θ range [°]	3.82 to 52.83 (0.80 Å)
Index ranges	−29 ≤ h ≤ 29 0 ≤ k ≤ 14 0 ≤ l ≤ 23
Reflections collected	5479
Independent reflections	5479 R_{int} = 0.0617 R_{sigma} = 0.0456
Completeness to θ = 25.242°	96.5 %
Data / Restraints / Parameters	5479 / 1051 / 493
Goodness-of-fit on F^2	1.154
Final R indexes [I≥2σ(I)]	R_1 = 0.0562 wR_2 = 0.0928
Final R indexes [all data]	R_1 = 0.0745 wR_2 = 0.0989
Largest peak/hole [eÅ^{-3}]	0.56/−0.85

Table S 2: Atomic coordinates and Ueq [Å^2] for [Ru(GaTMP)$_5$]. Reprinted (adapted) with permission from R. Bühler, R. J. J. Weininger, J. Stephan, M. Muhr, B. M. T. Bock, C. Gemel, R. A. Fischer, Dalton Transactions 2024, under CC BY 3.0 license. Copyright 2024 The Royal Society of Chemistry.

Atom	***x***	***y***	***z***	U_{eq}
Ru1	0.500000	0.62210(5)	0.250000	0.02208(15)
Ga1	0.54972(3)	0.66491(5)	0.35415(4)	0.03276(17)
Ga2	0.58257(3)	0.67017(5)	0.19995(4)	0.02960(16)
Ga3	0.500000	0.43247(7)	0.250000	0.0291(2)
N1	0.5932(9)	0.6901(17)	0.4384(8)	0.041(2)
C1	0.5972(7)	0.8026(13)	0.4684(9)	0.041(2)
C2	0.6580(9)	0.8257(16)	0.5006(10)	0.040(2)
H2A	0.658150	0.897449	0.526483	0.048
H2B	0.684447	0.832707	0.462032	0.048
C3	0.6794(8)	0.7323(13)	0.5517(10)	0.038(2)
H3A	0.719147	0.748050	0.569220	0.045
H3B	0.655297	0.729391	0.592794	0.045
C4	0.6769(10)	0.6216(15)	0.5133(12)	0.039(2)
H4A	0.688781	0.561740	0.546980	0.047
H4B	0.704345	0.622822	0.475570	0.047
C5	0.6179(9)	0.5942(15)	0.4804(13)	0.042(2)
C6	0.5850(8)	0.8876(12)	0.4073(9)	0.047(3)
H6A	0.587460	0.963650	0.426192	0.070
H6B	0.546673	0.874656	0.385587	0.070

H6C	0.613242	0.878024	0.371643	0.070
C7	0.5519(6)	0.8297(14)	0.5222(9)	0.051(3)
H7A	0.556279	0.907314	0.537795	0.077
H7B	0.557187	0.779979	0.563142	0.077
H7C	0.513654	0.818878	0.499738	0.077
C8	0.6266(10)	0.5004(19)	0.4318(11)	0.048(4)
H8A	0.643388	0.437233	0.458478	0.071
H8B	0.652374	0.523534	0.395649	0.071
H8C	0.589818	0.478035	0.409011	0.071
C9	0.5779(7)	0.5612(15)	0.5421(9)	0.047(3)
H9A	0.592847	0.493955	0.566039	0.071
H9B	0.539162	0.546769	0.522041	0.071
H9C	0.576997	0.622536	0.576220	0.071
N1A	0.5983(12)	0.706(2)	0.4301(11)	0.040(2)
C1A	0.6047(9)	0.8248(18)	0.4473(11)	0.041(2)
C2A	0.6620(12)	0.847(2)	0.4865(13)	0.040(3)
H2AA	0.692444	0.840795	0.452648	0.048
H2AB	0.662358	0.923890	0.504984	0.048
C3A	0.6753(10)	0.7674(17)	0.5471(13)	0.038(3)
H3AA	0.647526	0.777662	0.583928	0.046
H3AB	0.714029	0.782508	0.568585	0.046
C4A	0.6720(13)	0.648(2)	0.5188(16)	0.039(3)
H4AA	0.681585	0.595472	0.558038	0.047
H4AB	0.700717	0.638341	0.482984	0.047
C5A	0.6110(12)	0.619(2)	0.4844(17)	0.042(2)
C6A	0.6022(9)	0.8935(17)	0.3796(11)	0.041(4)
H6AA	0.614037	0.970279	0.390516	0.062
H6AB	0.563118	0.893498	0.358416	0.062
H6AC	0.627930	0.860971	0.346195	0.062
C7A	0.5581(9)	0.8675(19)	0.4945(12)	0.053(4)
H7AA	0.559700	0.949103	0.497036	0.079
H7AB	0.564387	0.836327	0.542181	0.079
H7AC	0.520534	0.844317	0.474445	0.079
C8A	0.6113(12)	0.502(2)	0.4464(15)	0.044(4)
H8AA	0.628414	0.445931	0.478954	0.066
H8AB	0.633723	0.506809	0.404444	0.066
H8AC	0.572102	0.479980	0.432218	0.066
C9A	0.5672(10)	0.605(2)	0.5387(13)	0.051(4)
H9AA	0.579426	0.545748	0.571978	0.077
H9AB	0.530420	0.584703	0.515012	0.077
H9AC	0.563269	0.675034	0.564466	0.077
N2	0.6524(2)	0.7043(4)	0.1650(3)	0.0368(11)
C10	0.6515(9)	0.819(2)	0.1320(12)	0.039(2)
C11	0.7010(8)	0.822(2)	0.0799(11)	0.041(2)
H11A	0.690824	0.772220	0.039188	0.049
H11B	0.705054	0.898292	0.061478	0.049
C12	0.7575(8)	0.7846(19)	0.1140(11)	0.041(3)
H12A	0.769394	0.835346	0.153365	0.049
H12B	0.787205	0.785707	0.079012	0.049
C13	0.7497(9)	0.6647(19)	0.1422(12)	0.038(2)
H13A	0.738295	0.614730	0.102204	0.046
H13B	0.786530	0.637535	0.163816	0.046
C14	0.7055(14)	0.660(2)	0.1958(17)	0.035(2)

C15	0.5967(9)	0.840(2)	0.0897(12)	0.039(4)
H15A	0.566325	0.854872	0.121778	0.059
H15B	0.586802	0.773750	0.061138	0.059
H15C	0.601091	0.904138	0.058599	0.059
C16	0.6573(11)	0.917(2)	0.1829(14)	0.043(4)
H16A	0.652021	0.986753	0.156741	0.065
H16B	0.695416	0.915590	0.207063	0.065
H16C	0.628359	0.910564	0.217918	0.065
C17	0.6923(14)	0.537(3)	0.211(2)	0.033(4)
H17A	0.724477	0.504077	0.238777	0.049
H17B	0.686007	0.496921	0.166340	0.049
H17C	0.657858	0.532817	0.237848	0.049
C18	0.7298(13)	0.715(2)	0.2626(13)	0.035(4)
H18A	0.759930	0.667459	0.284472	0.053
H18B	0.699438	0.724452	0.295472	0.053
H18C	0.745692	0.787679	0.251256	0.053
N2A	0.6524(2)	0.7043(4)	0.1650(3)	0.0368(11)
C10A	0.6627(8)	0.8017(16)	0.1190(10)	0.037(2)
C11A	0.7135(7)	0.7851(17)	0.0738(9)	0.040(2)
H11C	0.703185	0.730181	0.036226	0.048
H11D	0.722167	0.856634	0.050614	0.048
C12A	0.7663(7)	0.7451(18)	0.1155(10)	0.042(2)
H12C	0.778136	0.801217	0.151791	0.050
H12D	0.797864	0.735985	0.083473	0.050
C13A	0.7546(8)	0.6351(17)	0.1508(10)	0.038(2)
H13C	0.789297	0.611213	0.178975	0.046
H13D	0.746098	0.577999	0.113925	0.046
C14A	0.7029(12)	0.642(2)	0.2008(15)	0.035(2)
C15A	0.6075(7)	0.8121(16)	0.0697(10)	0.034(3)
H15D	0.611861	0.873574	0.036323	0.050
H15E	0.574862	0.826961	0.098240	0.050
H15F	0.601131	0.742361	0.043450	0.050
C16A	0.6699(10)	0.9092(19)	0.1643(11)	0.044(4)
H16D	0.668057	0.974615	0.133188	0.066
H16E	0.706996	0.907597	0.190933	0.066
H16F	0.639368	0.913355	0.197251	0.066
C17A	0.6845(13)	0.523(2)	0.2160(18)	0.036(4)
H17D	0.718084	0.478067	0.230889	0.054
H17E	0.665952	0.490178	0.173086	0.054
H17F	0.657678	0.523166	0.253707	0.054
C18A	0.7211(11)	0.694(2)	0.2740(11)	0.038(4)
H18D	0.753080	0.651506	0.296018	0.056
H18E	0.688822	0.691660	0.304519	0.056
H18F	0.732788	0.771492	0.267376	0.056
N3	0.4948(6)	0.2783(6)	0.2606(6)	0.0199(17)
C19	0.552(3)	0.222(4)	0.277(3)	0.0236(18)
C20	0.5625(5)	0.1045(9)	0.2457(6)	0.0275(18)
H20A	0.577562	0.112768	0.198186	0.033
H20B	0.591748	0.065380	0.276252	0.033
C21	0.5094(6)	0.0360(8)	0.2399(7)	0.0296(19)
H21A	0.496829	0.019344	0.287794	0.036
H21B	0.517101	−0.035641	0.216300	0.036
C22	0.4620(5)	0.0988(9)	0.1974(6)	0.0271(18)

Appendix

H22A	0.472904	0.105249	0.147835	0.033
H22B	0.426635	0.053724	0.197066	0.033
C23	0.449(3)	0.215(4)	0.225(3)	0.0233(18)
C24	0.6073(5)	0.2904(9)	0.2642(7)	0.030(2)
H24A	0.640895	0.246930	0.280671	0.045
H24B	0.606635	0.360761	0.290410	0.045
H24C	0.609144	0.306023	0.213605	0.045
C25	0.5491(5)	0.2139(9)	0.3582(6)	0.028(2)
H25A	0.587368	0.199039	0.379577	0.042
H25B	0.523386	0.153058	0.369864	0.042
H25C	0.534832	0.284307	0.376554	0.042
C26	0.4176(5)	0.2794(9)	0.1664(6)	0.027(2)
H26A	0.382069	0.240506	0.151958	0.041
H26B	0.441553	0.285107	0.125830	0.041
H26C	0.408741	0.354294	0.183223	0.041
C27	0.4136(5)	0.2104(9)	0.2887(6)	0.026(2)
H27A	0.377318	0.172859	0.276234	0.039
H27B	0.406147	0.286245	0.305040	0.039
H27C	0.434520	0.168760	0.326450	0.039

U_{eq} is defined as 1/3 of the trace of the orthogonalized U_{ij} tensor

References

[1C1] *APEX4 Suite of Crystallographic Software, Version 2021-10.0,* Bruker AXS Inc., Madison, Wisconsin, USA, **2021**.

[2C1] Bruker, *SAINT*, *V8.40B*, Bruker AXS Inc., Madison, Wisconsin, USA.

[3C1] L. Krause, R. Herbst-Irmer, G. M. Sheldrick, D. Stalke, *J. Appl. Cryst.* **2015**, *48*, 3–10, doi:10.1107/S1600576714022985.

[4C1] G. M. Sheldrick, *Acta Cryst.* **2015**, *A71*, 3–8, doi:10.1107/S2053273314026370.

[5C1] G. M. Sheldrick, *Acta Cryst.* **2015**, *C71*, 3–8, doi:10.1107/S2053229614024218.

[6C1] C. B. Huebschle, G. M. Sheldrick, B. Dittrich, *J. Appl. Cryst.* **2011**, *44*, 1281–1284, doi:10.1107/S0021889811043202.

[7C1] Ed. E. Prince, *International Tables for Crystallography Volume C, Mathematical, Physical and Chemical Tables*, International Union of Crystallography, Chester, England, **2006**, 500–502; 219–222; 193–199.

[8C1] C. R. Groom, I. J. Bruno, M. P. Lightfoot, S. C. Ward, *Acta Cryst.* **2016**, *B72*, 171–179, doi:10.1107/S2052520616003954.

[9C1] D. Kratzert, *FinalCif*, *V106*, https://dkratzert.de/finalcif.html.

[10C2] K. Momma, F. Izumi, *J. Appl. Crystallogr.* **2011**, *44*, 1272-1276.

6.2 Characterization of [Mo(GaTMP)$_6$]

^{1}H-NMR spectrum of [Mo(GaTMP)$_6$]

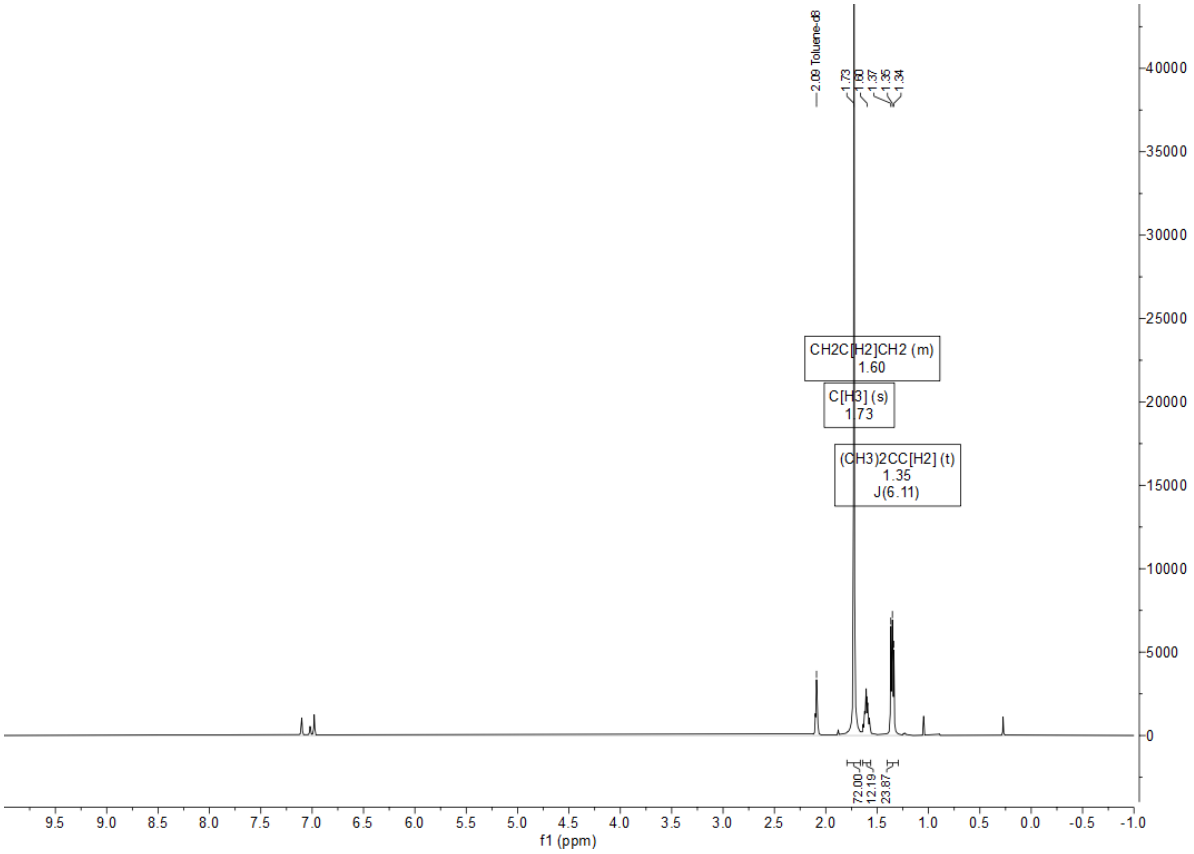

Figure S 6: 1H-NMR spectrum of [Mo(GaTMP)$_6$] in toluene-d_8, recorded at 298 K. Signals at 1.24 and 1.07 ppm are attributed to TMPH. The signal around 0.25 ppm is attributed to silicone grease. Reprinted (adapted) with permission from R. Bühler, R. J. J. Weininger, J. Stephan, M. Muhr, B. M. T. Bock, C. Gemel, R. A. Fischer, Dalton Transactions 2024, under CC BY 3.0 license. Copyright 2024 The Royal Society of Chemistry.

^{13}C-NMR spectrum of [Mo(GaTMP)$_6$]

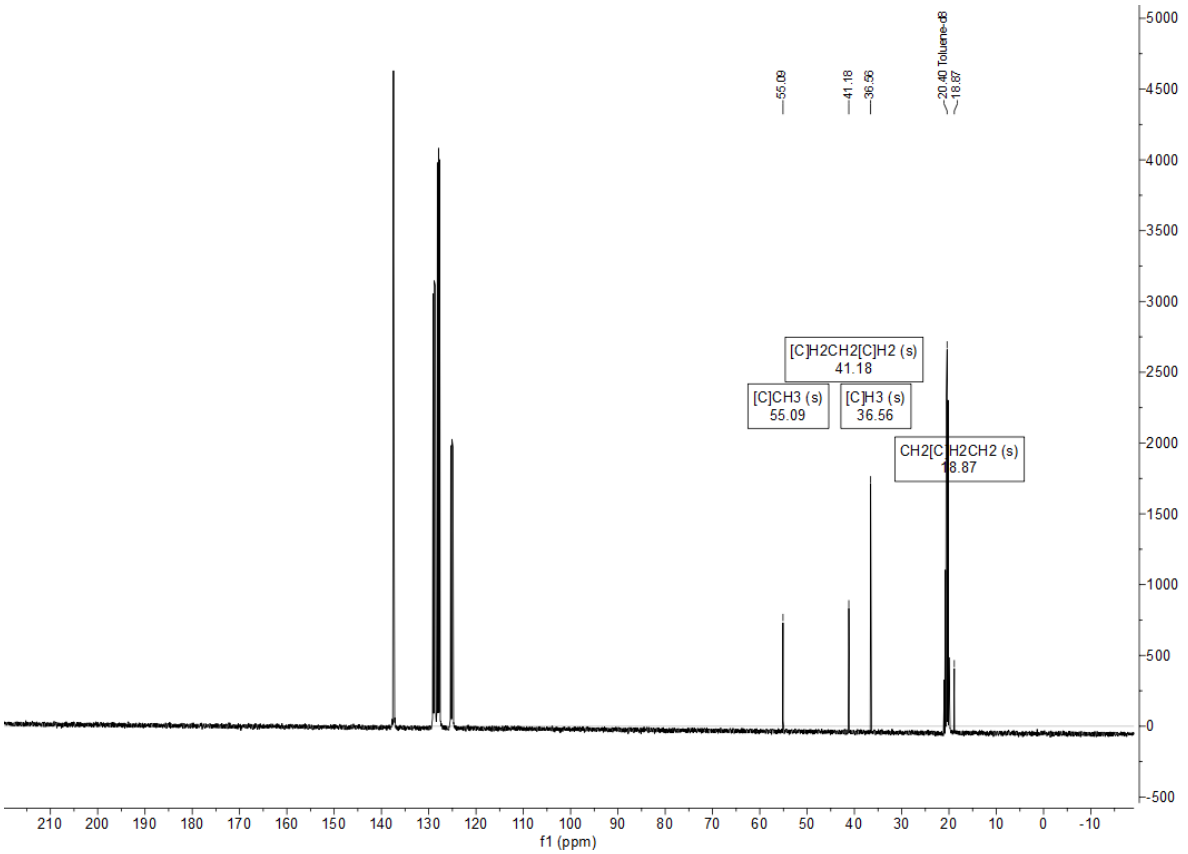

Figure S 7: ^{13}C-NMR spectrum of [Mo(GaTMP)$_6$] in toluene-d_8, recorded at 298 K. Reprinted (adapted) with permission from R. Bühler, R. J. J. Weininger, J. Stephan, M. Muhr, B. M. T. Bock, C. Gemel, R. A. Fischer, Dalton Transactions 2024, under CC BY 3.0 license. Copyright 2024 The Royal Society of Chemistry.

FT-IR spectrum of [Mo(GaTMP)$_6$]

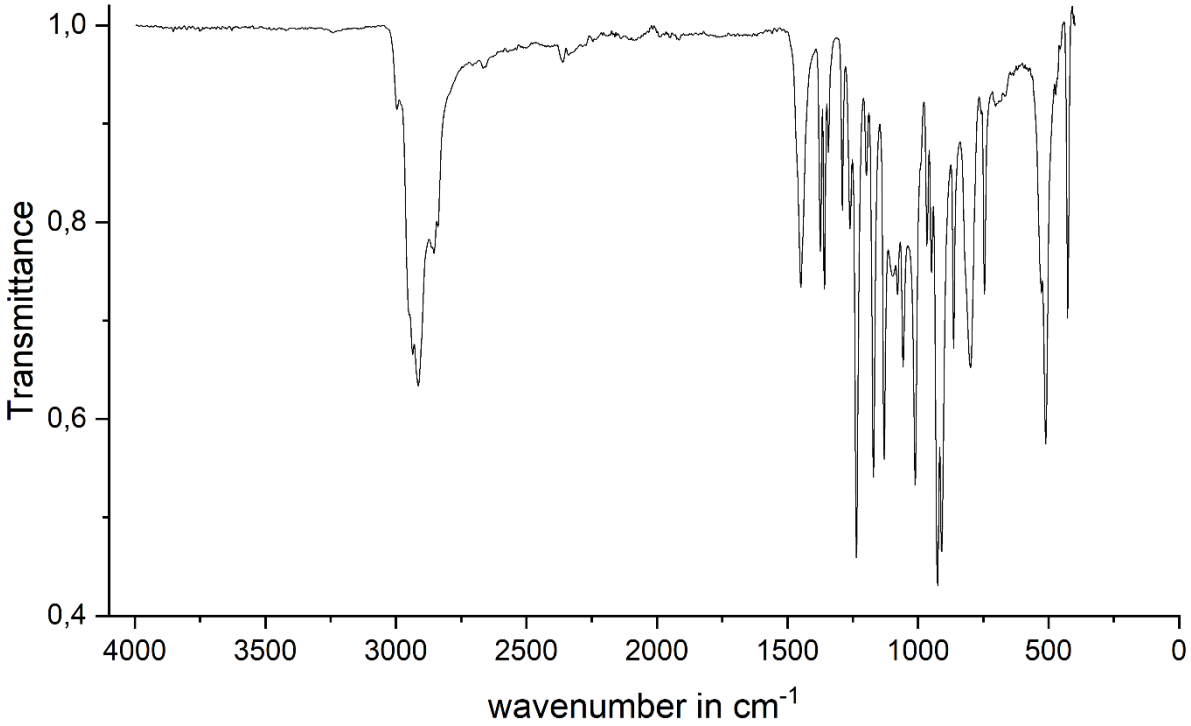

Figure S 8: FT-IR spectrum of [Mo(GaTMP)$_6$]. Reprinted (adapted) with permission from R. Bühler, R. J. J. Weininger, J. Stephan, M. Muhr, B. M. T. Bock, C. Gemel, R. A. Fischer, Dalton Transactions 2024, under CC BY 3.0 license. Copyright 2024 The Royal Society of Chemistry.

LIFDI-MS spectrum of [Mo(GaTMP)$_6$]

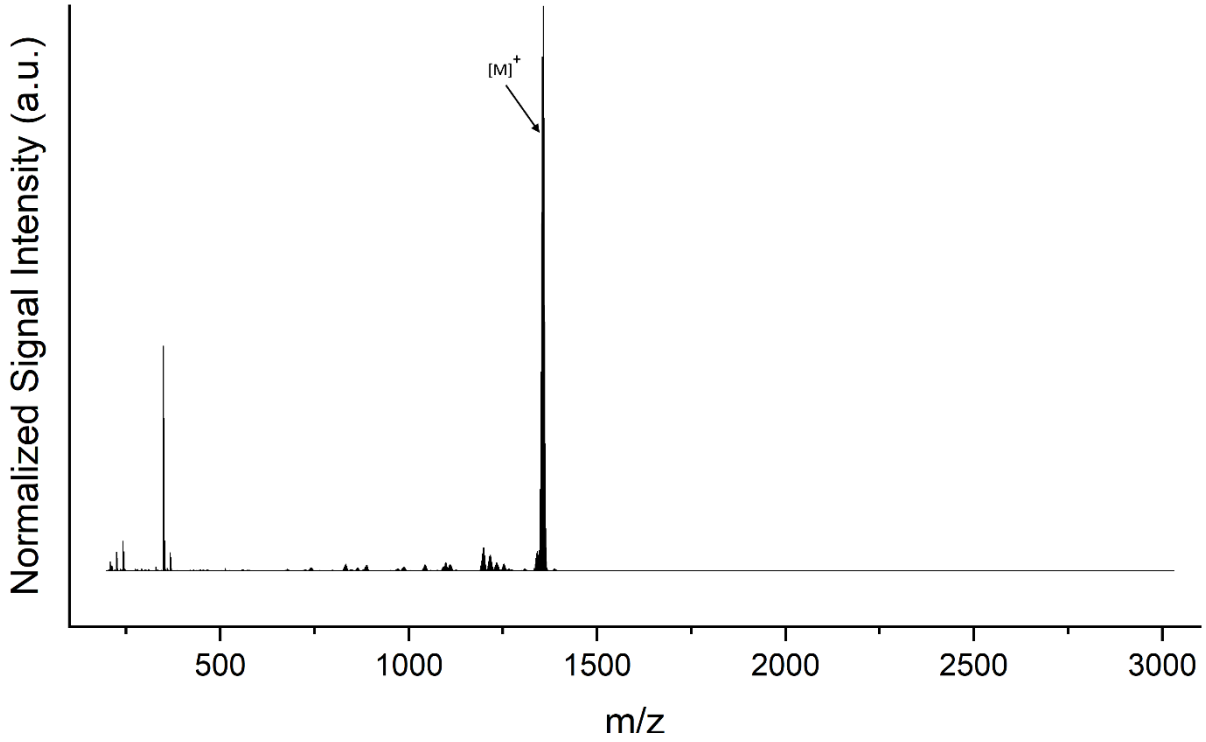

Figure S 9: LIFDI-MS spectrum of [Mo(GaTMP)$_6$]. A molecular ion $[M]^+$ with *m/z* = 1356.32 can be observed at 100% relative intensity. No sensible compounds directly related to the parent ion can be suggested for the remaining signals. Reprinted (adapted) with permission from R. Bühler, R. J. J. Weininger, J. Stephan, M. Muhr, B. M. T. Bock, C. Gemel, R. A. Fischer, Dalton Transactions 2024, under CC BY 3.0 license. Copyright 2024 The Royal Society of Chemistry.

SC-XRD structure report for [Mo(GaTMP)$_6$]

Measurements, structure solutions and refinement by Johannes Stephan (AMC Group @ TUM)

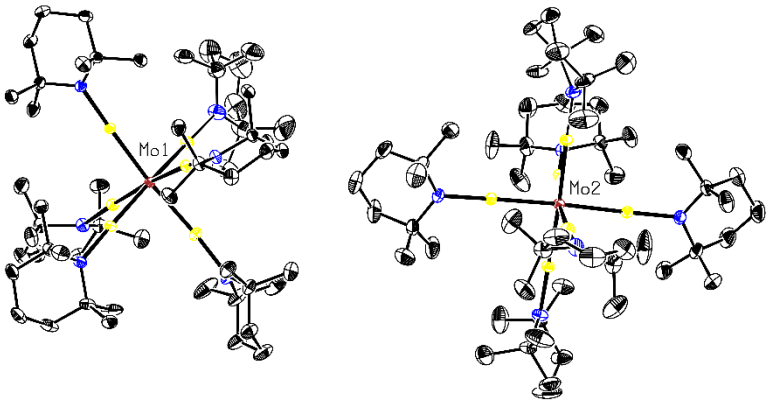

Figure S 10: Molecular structure of [Mo(GaTMP)$_6$] in the solid state determined by single crystal X-ray diffraction. Mo: red, Ga: yellow, N: blue and C: black. Hydrogen atoms and disordered molecule fragments are omitted. Thermal ellipsoids are shown at the 50% probability level. Reprinted (adapted) with permission from R. Bühler, R. J. J. Weininger, J. Stephan, M. Muhr, B. M. T. Bock, C. Gemel, R. A. Fischer, Dalton Transactions 2024, under CC BY 3.0 license. Copyright 2024 The Royal Society of Chemistry.

A colourless, block-shaped crystal of $C_{54}H_{108}Ga_6MoN_6$ coated with perfluorinated ether and fixed on top of a Kapton micro sampler was used for X-ray crystallographic analysis. The X-ray intensity data were collected at 100(2) K on a Bruker D8 VENTURE Duo three-angle diffractometer with an IMS microsource with MoK_α radiation (λ=0.71073 Å) using APEX4.[1C2] The diffractometer was equipped with a Helios optic monochromator, a Bruker PHOTON II detector, and a low temperature device.

A matrix scan was used to determine the initial lattice parameters. All data were integrated with the Bruker SAINT V8.40B software package using a narrow-frame algorithm and the reflections were corrected for Lorentz and polarisation effects, scan speed, and background.[2C2] The integration of the data using a monoclinic unit cell yielded a total of 776202 reflections within a 2θ range [°] of 4.08 to 52.83 (0.80 Å), of which 26306 were independent. Data were corrected for absorption effects including odd and even ordered spherical harmonics by the multi-scan method (SADABS 2016/2).[3C2] Space group assignment was based upon systematic absences, E statistics, and successful refinement of the structure.

The structure was solved by direct methods using SHELXT and refined by full-matrix least-squares methods against F^2 by minimizing $\Sigma w(F_o^2 - F_c^2)^2$ using SHELXL in conjunction with SHELXLE.[4C2-6C2] All non-hydrogen atoms were refined with anisotropic displacement parameters. Hydrogen atoms were refined isotropically on calculated positions using a riding model with their U_{iso} values constrained to 1.5 times the U_{eq} of their pivot atoms for terminal sp^3 carbon atoms and a C–H distance of 0.98 Å. Non-methyl hydrogen atoms were refined

using a riding model with methylene, aromatic, and other C–H distances of 0.99 Å, 0.95 Å, and 1.00 Å, respectively, and U_{iso} values constrained to 1.2 times the U_{eq} of their pivot atoms.

Neutral atom scattering factors for all atoms and anomalous dispersion corrections for the non-hydrogen atoms were taken from International Tables for Crystallography.[7C2] Crystallographic data for the structures reported in this paper have been deposited with the Cambridge Crystallographic Data Centre.[8C2] Supplementary crystallographic data reported in this paper have been deposited with the Cambridge Crystallographic Data Centre (CCDC 2341049) and can be obtained free of charge from The Cambridge Crystallographic Data Centre via www.ccdc.cam.ac.uk/structures.[8C2] This report and the CIF file were generated using FinalCif.[9C2] Figures showing the coordination polyhedra around the molybdenum centre were created using VESTA 3.[10C2]

Table S 3: Crystal data and structure refinement for $[Mo(GaTMP)_6]$. Reprinted (adapted) with permission from R. Bühler, R. J. J. Weininger, J. Stephan, M. Muhr, B. M. T. Bock, C. Gemel, R. A. Fischer, Dalton Transactions 2024, under CC BY 3.0 license. Copyright 2024 The Royal Society of Chemistry.

CCDC number	2341049
Empirical formula	$C_{54}H_{108}Ga_6MoN_6$
Formula weight	1355.72
Temperature [K]	100(2)
Crystal system	monoclinic
Space group (number)	$\frac{P2_1}{c}$ (14)
a [Å]	26.9295(18)
b [Å]	21.9030(15)
c [Å]	24.2260(15)
α [°]	90
β [°]	116.221(2)
γ [°]	90
Volume [Å^3]	12819.0(15)
Z	8
ρ_{calc} [gcm^{-3}]	1.405
μ [mm^{-1}]	2.709
F(000)	5616
Crystal size [mm^3]	0.278×0.339×0.428
Crystal colour	colourless
Crystal shape	block
Radiation	MoK_α (λ=0.71073 Å)
2θ range [°]	4.08 to 52.83 (0.80 Å)
Index ranges	−33 ≤ h ≤ 33 −27 ≤ k ≤ 27 −30 ≤ l ≤ 30
Reflections collected	776202
Independent reflections	26306 R_{int} = 0.0429 R_{sigma} = 0.0122

Completeness to θ = 25.242°	99.9 %
Data / Restraints / Parameters	26306 / 739 / 1436
Goodness-of-fit on F^2	1.028
Final R indexes [$I \geq 2\sigma(I)$]	R_1 = 0.0198 wR_2 = 0.0441
Final R indexes [all data]	R_1 = 0.0255 wR_2 = 0.0466
Largest peak/hole [eÅ^{-3}]	0.55/−0.46

Table S 4: Atomic coordinates and Ueq [Å²] for [Mo(GaTMP)₆]. Reprinted (adapted) with permission from R. Bühler, R. J. J. Weininger, J. Stephan, M. Muhr, B. M. T. Bock, C. Gemel, R. A. Fischer, Dalton Transactions 2024, under CC BY 3.0 license. Copyright 2024 The Royal Society of Chemistry.

Atom	***x***	***y***	***z***	U_{eq}
Mo1	0.38238(2)	0.74227(2)	0.23060(2)	0.01366(3)
Mo2	0.11461(2)	0.23662(2)	0.34993(2)	0.01461(3)
Ga1	0.32971(2)	0.72828(2)	0.28718(2)	0.01931(4)
Ga2	0.32465(2)	0.67490(2)	0.15029(2)	0.02012(4)
Ga3	0.45061(2)	0.74184(2)	0.19234(2)	0.01487(4)
Ga4	0.43058(2)	0.81839(2)	0.30507(2)	0.01559(4)
Ga5	0.32948(2)	0.82742(2)	0.17237(2)	0.01659(4)
Ga6	0.43626(2)	0.66305(2)	0.29688(2)	0.01627(4)
Ga7	0.17039(2)	0.31657(2)	0.33955(2)	0.01780(4)
Ga8	0.05019(2)	0.23283(2)	0.24396(2)	0.01641(4)
Ga9	0.06052(2)	0.15865(2)	0.36589(2)	0.01725(4)
Ga10	0.17637(2)	0.22566(2)	0.45628(2)	0.02001(4)
Ga11	0.16747(2)	0.16462(2)	0.32425(2)	0.01861(4)
Ga12	0.06146(2)	0.31313(2)	0.36953(2)	0.01758(4)
N1	0.29434(6)	0.72121(8)	0.33751(7)	0.0263(3)
N3	0.50659(6)	0.73802(6)	0.16701(7)	0.0174(3)
N4	0.46444(6)	0.87955(7)	0.36181(7)	0.0194(3)
N5	0.28979(6)	0.89690(7)	0.13216(7)	0.0201(3)
N6	0.47526(6)	0.60219(6)	0.35206(7)	0.0192(3)
N7	0.21475(6)	0.37883(7)	0.33388(7)	0.0249(3)
N8	0.00095(6)	0.22435(7)	0.16147(7)	0.0215(3)
N9	0.01804(6)	0.09709(7)	0.37621(7)	0.0237(3)
N10	0.22489(7)	0.21346(8)	0.53826(7)	0.0297(4)
N12	0.01959(6)	0.37220(7)	0.38440(7)	0.0237(3)
C1	0.23537(9)	0.73903(12)	0.31267(10)	0.0377(5)
C2	0.22532(10)	0.77367(12)	0.36204(11)	0.0444(6)
H2A	0.243627	0.814038	0.368915	0.053
H2B	0.185091	0.780681	0.346790	0.053
C3	0.24697(10)	0.73964(12)	0.42285(11)	0.0421(6)
H3A	0.226736	0.700635	0.417299	0.051
H3B	0.241021	0.764449	0.453562	0.051
C4	0.30852(9)	0.72711(10)	0.44553(9)	0.0339(5)
H4A	0.322256	0.703565	0.484364	0.041
H4B	0.328707	0.766428	0.454504	0.041
C5	0.32101(8)	0.69143(9)	0.39859(8)	0.0256(4)

C6	0.22264(10)	0.78276(14)	0.25888(11)	0.0521(7)
H6A	0.184035	0.796219	0.242405	0.078
H6B	0.228561	0.761795	0.226543	0.078
H6C	0.247180	0.818304	0.273221	0.078
C7	0.19534(9)	0.68477(14)	0.28765(12)	0.0545(7)
H7A	0.157326	0.699981	0.265770	0.082
H7B	0.198428	0.658743	0.321925	0.082
H7C	0.204756	0.661015	0.259309	0.082
C8	0.38354(8)	0.69198(10)	0.42046(9)	0.0307(4)
H8A	0.402001	0.675794	0.462440	0.046
H8B	0.395957	0.733939	0.419926	0.046
H8C	0.392833	0.666552	0.393050	0.046
C9	0.30443(10)	0.62397(10)	0.39771(11)	0.0401(5)
H9A	0.328994	0.604630	0.436808	0.060
H9B	0.307645	0.602779	0.363811	0.060
H9C	0.266099	0.621596	0.391963	0.060
N2	0.27960(7)	0.62157(8)	0.08901(8)	0.0349(4)
C10	0.3029(11)	0.5847(11)	0.0551(11)	0.0364(10)
C11	0.2653(2)	0.5913(3)	−0.0148(2)	0.0575(11)
H11A	0.266396	0.634142	−0.027383	0.069
H11B	0.279534	0.564952	−0.037783	0.069
C12	0.20507(18)	0.5736(3)	−0.0316(2)	0.0659(12)
H12A	0.181951	0.576998	−0.076578	0.079
H12B	0.203153	0.531120	−0.018832	0.079
C13	0.18584(19)	0.6161(2)	0.0011(3)	0.0626(12)
H13A	0.146786	0.606624	−0.009114	0.075
H13B	0.187099	0.658064	−0.013345	0.075
C14	0.2206(2)	0.6138(3)	0.0722(3)	0.0454(10)
C15	0.3611(2)	0.6059(3)	0.0684(3)	0.0413(12)
H15A	0.375016	0.581172	0.044519	0.062
H15B	0.385568	0.601152	0.112365	0.062
H15C	0.359954	0.648909	0.056808	0.062
C16	0.3103(3)	0.5173(3)	0.0706(3)	0.0547(13)
H16A	0.334648	0.499190	0.054657	0.082
H16B	0.274211	0.496940	0.051942	0.082
H16C	0.326916	0.512129	0.115415	0.082
C17	0.2010(2)	0.6722(3)	0.0926(3)	0.0661(16)
H17A	0.161698	0.668300	0.082728	0.099
H17B	0.206200	0.707611	0.070952	0.099
H17C	0.222638	0.677838	0.137081	0.099
C18	0.2073(2)	0.5550(3)	0.0960(3)	0.0683(14)
H18A	0.167733	0.554073	0.085610	0.102
H18B	0.229035	0.552911	0.140731	0.102
H18C	0.216390	0.520096	0.076862	0.102
N2A	0.27960(7)	0.62157(8)	0.08901(8)	0.0349(4)
C10A	0.302(2)	0.584(2)	0.055(2)	0.0370(18)
C11A	0.2620(5)	0.5657(5)	−0.0058(5)	0.064(2)
H11C	0.278599	0.534945	−0.022701	0.077
H11D	0.251095	0.601578	−0.033557	0.077
C12A	0.2077(4)	0.5369(6)	−0.0018(5)	0.073(2)
H12C	0.218161	0.501218	0.026113	0.088
H12D	0.179698	0.523969	−0.043000	0.088
C13A	0.1823(4)	0.5951(6)	0.0266(5)	0.062(2)

H13C	0.176649	0.632577	0.001704	0.074
H13D	0.146523	0.583148	0.025772	0.074
C14A	0.2248(5)	0.6056(6)	0.0911(4)	0.0411(16)
C15A	0.3473(5)	0.6245(6)	0.0523(5)	0.044(2)
H15D	0.363682	0.603996	0.028385	0.067
H15E	0.376072	0.632194	0.094145	0.067
H15F	0.331011	0.663437	0.032686	0.067
C16A	0.3266(5)	0.5244(5)	0.0967(5)	0.053(2)
H16D	0.343453	0.497756	0.077192	0.080
H16E	0.296690	0.502485	0.100818	0.080
H16F	0.354670	0.536638	0.137499	0.080
C17A	0.2094(4)	0.6519(5)	0.1238(5)	0.055(2)
H17D	0.169384	0.650146	0.110636	0.082
H17E	0.219370	0.692309	0.114551	0.082
H17F	0.229049	0.644285	0.168144	0.082
C18A	0.2292(4)	0.5579(6)	0.1343(6)	0.070(3)
H18D	0.193717	0.553577	0.136138	0.105
H18E	0.258137	0.568533	0.175132	0.105
H18F	0.238611	0.519306	0.120779	0.105
C19	0.51820(7)	0.79215(8)	0.13789(8)	0.0196(4)
C20	0.52709(8)	0.77282(9)	0.08185(9)	0.0272(4)
H20A	0.491310	0.759234	0.048595	0.033
H20B	0.539732	0.808635	0.066550	0.033
C21	0.56921(9)	0.72171(9)	0.09642(9)	0.0298(4)
H21A	0.606124	0.736057	0.126670	0.036
H21B	0.571854	0.709207	0.058538	0.036
C22	0.55100(8)	0.66763(9)	0.12271(9)	0.0251(4)
H22A	0.579100	0.634881	0.133592	0.030
H22B	0.515711	0.651432	0.090653	0.030
C23	0.54311(7)	0.68420(8)	0.17998(8)	0.0185(3)
C24	0.46758(8)	0.83436(9)	0.11477(9)	0.0269(4)
H24A	0.472927	0.868209	0.091493	0.040
H24B	0.463018	0.850562	0.149964	0.040
H24C	0.434433	0.811269	0.088080	0.040
C25	0.56786(8)	0.82959(8)	0.18306(9)	0.0255(4)
H25A	0.570468	0.867667	0.163256	0.038
H25B	0.601931	0.805910	0.194889	0.038
H25C	0.562843	0.839046	0.219814	0.038
C26	0.51522(8)	0.62998(8)	0.19461(9)	0.0241(4)
H26A	0.537459	0.593127	0.199685	0.036
H26B	0.478207	0.623952	0.160796	0.036
H26C	0.512097	0.638092	0.232742	0.036
C27	0.59985(8)	0.69257(9)	0.23643(9)	0.0273(4)
H27A	0.618156	0.652832	0.248911	0.041
H27B	0.594346	0.710234	0.270483	0.041
H27C	0.623001	0.719955	0.225650	0.041
C28	0.43591(8)	0.90769(9)	0.39572(8)	0.0245(4)
C29	0.44225(9)	0.97736(9)	0.39691(9)	0.0314(5)
H29A	0.419117	0.993657	0.355205	0.038
H29B	0.428324	0.994850	0.425096	0.038
C30	0.50149(9)	0.99782(9)	0.41740(9)	0.0325(5)
H30A	0.524339	0.985431	0.460640	0.039
H30B	0.502906	1.042868	0.415028	0.039

C31	0.52428(9)	0.96906(9)	0.37626(9)	0.0309(4)
H31A	0.563313	0.981763	0.390591	0.037
H31B	0.503015	0.984301	0.333717	0.037
C32	0.52130(7)	0.89904(8)	0.37603(8)	0.0220(4)
C33	0.37425(9)	0.89261(11)	0.36199(10)	0.0384(5)
H33A	0.354416	0.914032	0.381744	0.058
H33B	0.369018	0.848488	0.363617	0.058
H33C	0.359781	0.905646	0.318976	0.058
C34	0.45670(9)	0.88248(9)	0.46152(9)	0.0316(5)
H34A	0.431697	0.895581	0.478814	0.047
H34B	0.494022	0.898037	0.487153	0.047
H34C	0.457609	0.837781	0.460473	0.047
C35	0.53536(8)	0.87578(9)	0.32518(9)	0.0271(4)
H35A	0.571621	0.891587	0.331841	0.041
H35B	0.507131	0.889766	0.285160	0.041
H35C	0.536338	0.831047	0.325908	0.041
C36	0.56549(8)	0.87318(10)	0.43711(9)	0.0313(4)
H36A	0.602412	0.881481	0.440257	0.047
H36B	0.560344	0.828995	0.438363	0.047
H36C	0.561840	0.892599	0.471574	0.047
C37	0.32059(8)	0.95043(8)	0.12662(8)	0.0233(4)
C38	0.28620(9)	1.00868(9)	0.11634(10)	0.0340(5)
H38A	0.283365	1.018844	0.154670	0.041
H38B	0.305480	1.042827	0.107175	0.041
C39	0.22840(9)	1.00251(10)	0.06410(11)	0.0381(5)
H39A	0.207251	1.040562	0.060184	0.046
H39B	0.230616	0.995555	0.024873	0.046
C40	0.19938(8)	0.94928(10)	0.07730(10)	0.0324(5)
H40A	0.162238	0.944405	0.042362	0.039
H40B	0.194205	0.958731	0.114382	0.039
C41	0.23088(7)	0.88885(9)	0.08755(8)	0.0228(4)
C42	0.37251(8)	0.95758(9)	0.18803(10)	0.0330(5)
H42A	0.391383	0.995742	0.187732	0.050
H42B	0.397487	0.923066	0.193777	0.050
H42C	0.361818	0.958485	0.221790	0.050
C43	0.33947(9)	0.94339(10)	0.07555(10)	0.0332(5)
H43A	0.363154	0.977943	0.077061	0.050
H43B	0.306980	0.942492	0.035380	0.050
H43C	0.360280	0.905253	0.081688	0.050
C44	0.20537(8)	0.84438(10)	0.11618(10)	0.0325(5)
H44A	0.165907	0.839311	0.088610	0.049
H44B	0.209743	0.860448	0.155830	0.049
H44C	0.224042	0.804787	0.122505	0.049
C45	0.22342(9)	0.86214(11)	0.02565(9)	0.0344(5)
H45A	0.184506	0.851125	0.000928	0.052
H45B	0.246580	0.825678	0.033047	0.052
H45C	0.234412	0.892614	0.003530	0.052
C46	0.45656(8)	0.53804(8)	0.33662(8)	0.0211(4)
C47	0.46760(8)	0.50261(8)	0.39547(9)	0.0254(4)
H47A	0.442399	0.517678	0.412301	0.030
H47B	0.459346	0.458862	0.385256	0.030
C48	0.52708(8)	0.50908(9)	0.44423(9)	0.0290(4)
H48A	0.552644	0.492463	0.428601	0.035

H48B	0.532468	0.485894	0.481539	0.035
C49	0.53934(8)	0.57630(9)	0.45991(8)	0.0277(4)
H49A	0.578235	0.580732	0.491234	0.033
H49B	0.515223	0.591588	0.478071	0.033
C50	0.53019(7)	0.61551(8)	0.40361(8)	0.0209(4)
C51	0.39382(8)	0.53840(9)	0.29622(9)	0.0300(4)
H51A	0.380113	0.496303	0.288420	0.045
H51B	0.385646	0.558575	0.257027	0.045
H51C	0.375617	0.560536	0.317375	0.045
C52	0.48286(9)	0.50489(9)	0.30007(9)	0.0305(4)
H52A	0.464100	0.465740	0.285073	0.046
H52B	0.522192	0.497658	0.326839	0.046
H52C	0.479052	0.530154	0.265033	0.046
C53	0.53139(8)	0.68243(9)	0.42189(9)	0.0279(4)
H53A	0.566188	0.690969	0.458282	0.042
H53B	0.500169	0.690659	0.431280	0.042
H53C	0.528591	0.708597	0.387816	0.042
C54	0.57812(8)	0.60617(9)	0.38612(9)	0.0285(4)
H54A	0.613135	0.617490	0.420997	0.043
H54B	0.572168	0.631855	0.350616	0.043
H54C	0.579569	0.563204	0.375624	0.043
C55	0.20120(10)	0.44307(10)	0.33975(12)	0.0382(5)
C56	0.21250(10)	0.48399(11)	0.29543(13)	0.0478(6)
H56A	0.184122	0.475959	0.252920	0.057
H56B	0.208950	0.527216	0.305088	0.057
C57	0.26963(10)	0.47416(11)	0.29850(12)	0.0458(6)
H57A	0.274039	0.499946	0.267393	0.055
H57B	0.298541	0.485831	0.339675	0.055
C58	0.27583(10)	0.40737(11)	0.28625(11)	0.0412(6)
H58A	0.313236	0.400660	0.289085	0.049
H58B	0.248479	0.397122	0.243826	0.049
C59	0.26748(8)	0.36473(9)	0.33125(10)	0.0293(4)
C60	0.13849(11)	0.44646(11)	0.32025(16)	0.0621(9)
H60A	0.126919	0.489314	0.316121	0.093
H60B	0.130244	0.426619	0.351514	0.093
H60C	0.118425	0.425616	0.280717	0.093
C61	0.23238(16)	0.46717(13)	0.40545(14)	0.0703(10)
H61A	0.217585	0.507239	0.408504	0.105
H61B	0.271799	0.471018	0.415935	0.105
H61C	0.227738	0.438709	0.434042	0.105
C62	0.26371(11)	0.29959(11)	0.30717(15)	0.0532(7)
H62A	0.296285	0.290825	0.300398	0.080
H62B	0.230169	0.295339	0.268269	0.080
H62C	0.262256	0.270805	0.337394	0.080
C63	0.31807(10)	0.36727(13)	0.39407(12)	0.0523(7)
H63A	0.350446	0.351223	0.390397	0.078
H63B	0.311113	0.342551	0.423651	0.078
H63C	0.325028	0.409673	0.408386	0.078
C64	−0.04103(8)	0.17506(9)	0.14135(8)	0.0253(4)
C65	−0.05258(9)	0.15229(10)	0.07698(9)	0.0346(5)
H65A	−0.019939	0.129433	0.079452	0.042
H65B	−0.084390	0.123810	0.062184	0.042
C66	−0.06525(10)	0.20423(11)	0.03088(10)	0.0429(6)

H66A	−0.071277	0.187825	−0.009676	0.051
H66B	−0.099291	0.225811	0.025879	0.051
C67	−0.01646(11)	0.24819(12)	0.05473(10)	0.0457(6)
H67A	−0.024368	0.282160	0.025065	0.055
H67B	0.016837	0.226565	0.057488	0.055
C68	−0.00438(9)	0.27456(9)	0.11835(9)	0.0315(5)
C69	−0.01728(10)	0.12078(10)	0.18522(10)	0.0396(5)
H69A	−0.042134	0.085655	0.169339	0.059
H69B	−0.013769	0.131764	0.226000	0.059
H69C	0.019238	0.110243	0.188343	0.059
C70	−0.09531(9)	0.19318(12)	0.14289(12)	0.0460(6)
H70A	−0.119252	0.157237	0.134398	0.069
H70B	−0.114040	0.224473	0.111630	0.069
H70C	−0.087386	0.209414	0.183644	0.069
C71	0.05074(10)	0.30848(12)	0.14301(11)	0.0521(7)
H71A	0.049637	0.338697	0.112655	0.078
H71B	0.080688	0.279303	0.150738	0.078
H71C	0.057296	0.329221	0.181471	0.078
C72	−0.04880(11)	0.32117(11)	0.11205(12)	0.0518(7)
H72A	−0.047036	0.355901	0.087471	0.078
H72B	−0.042452	0.335460	0.152978	0.078
H72C	−0.085396	0.302057	0.091665	0.078
C73	0.03434(8)	0.03234(9)	0.37763(9)	0.0276(4)
C74	−0.01559(9)	−0.00660(10)	0.33765(11)	0.0377(5)
H74A	−0.027495	0.003895	0.293866	0.045
H74B	−0.004723	−0.050182	0.343247	0.045
C75	−0.06394(10)	0.00268(11)	0.35331(13)	0.0469(6)
H75A	−0.053215	−0.009888	0.396342	0.056
H75B	−0.095825	−0.022540	0.325862	0.056
C76	−0.07983(9)	0.06997(11)	0.34505(13)	0.0459(6)
H76A	−0.111037	0.076500	0.355534	0.055
H76B	−0.092557	0.081286	0.301324	0.055
C77	−0.03136(9)	0.11180(10)	0.38551(10)	0.0328(5)
C78	0.07655(9)	0.02801(10)	0.35152(11)	0.0369(5)
H78A	0.085477	−0.014962	0.348991	0.055
H78B	0.110292	0.050015	0.378507	0.055
H78C	0.060945	0.046195	0.310336	0.055
C79	0.06286(10)	0.00571(10)	0.44324(10)	0.0424(6)
H79A	0.079146	−0.034022	0.442160	0.064
H79B	0.035513	0.000618	0.459327	0.064
H79C	0.092058	0.033608	0.469933	0.064
C80	−0.04799(10)	0.17755(11)	0.36528(13)	0.0461(6)
H80A	−0.083448	0.186440	0.365806	0.069
H80B	−0.051683	0.183222	0.323511	0.069
H80C	−0.019551	0.205282	0.393507	0.069
C81	−0.02065(12)	0.10718(12)	0.45312(12)	0.0519(7)
H81A	−0.051952	0.124893	0.457878	0.078
H81B	0.013255	0.129510	0.479042	0.078
H81C	−0.016405	0.064190	0.465583	0.078
C82	0.27721(8)	0.24819(10)	0.56663(9)	0.0335(5)
C83	0.32433(9)	0.20704(13)	0.61050(10)	0.0481(6)
H83A	0.333748	0.177170	0.585932	0.058
H83B	0.357511	0.232469	0.633617	0.058

C84	0.31003(10)	0.17306(14)	0.65551(11)	0.0532(7)
H84A	0.303248	0.202327	0.682580	0.064
H84B	0.341140	0.146171	0.681570	0.064
C85	0.25867(12)	0.13531(12)	0.61999(11)	0.0521(7)
H85A	0.248817	0.113077	0.649348	0.063
H85B	0.266629	0.104681	0.594911	0.063
C86	0.20942(10)	0.17456(11)	0.57773(9)	0.0403(5)
C87	0.29190(10)	0.26886(14)	0.51538(11)	0.0549(7)
H87A	0.328594	0.287940	0.533534	0.082
H87B	0.264352	0.298445	0.488960	0.082
H87C	0.292180	0.233444	0.490799	0.082
C88	0.27367(11)	0.30556(12)	0.60092(13)	0.0533(7)
H88A	0.307613	0.329588	0.613296	0.080
H88B	0.269366	0.293649	0.637560	0.080
H88C	0.241759	0.330126	0.573820	0.080
C89	0.16355(14)	0.13091(15)	0.53620(12)	0.0787(12)
H89A	0.157577	0.099570	0.561520	0.118
H89B	0.174546	0.111389	0.506901	0.118
H89C	0.129211	0.153900	0.513666	0.118
C90	0.18668(11)	0.21071(16)	0.61543(13)	0.0627(8)
H90A	0.170047	0.182561	0.633979	0.094
H90B	0.158519	0.239503	0.588553	0.094
H90C	0.216869	0.233279	0.647974	0.094
N11	0.2084(8)	0.1077(9)	0.3077(6)	0.0258(17)
C91	0.2496(4)	0.0715(5)	0.3456(4)	0.0376(15)
C92	0.3036(2)	0.0753(3)	0.3378(2)	0.0501(12)
H92A	0.319553	0.116681	0.349433	0.060
H92B	0.330736	0.045705	0.365995	0.060
C93	0.29378(19)	0.0618(2)	0.2721(2)	0.0419(11)
H93A	0.278950	0.019941	0.260268	0.050
H93B	0.329048	0.064718	0.268763	0.050
C94	0.2521(2)	0.1087(3)	0.2293(3)	0.0348(11)
H94A	0.267735	0.150293	0.240560	0.042
H94B	0.245203	0.100797	0.186262	0.042
C95	0.1977(4)	0.1050(4)	0.2342(4)	0.0256(13)
C96	0.2629(5)	0.0979(5)	0.4108(5)	0.063(3)
H96A	0.294784	0.076186	0.442104	0.094
H96B	0.230766	0.092445	0.419155	0.094
H96C	0.271631	0.141428	0.411990	0.094
C97	0.2307(3)	0.0043(3)	0.3390(3)	0.0609(15)
H97A	0.257565	−0.019488	0.373519	0.091
H97B	0.228033	−0.012251	0.300247	0.091
H97C	0.194354	0.002047	0.339101	0.091
C98	0.16093(18)	0.1583(2)	0.19836(18)	0.0353(10)
H98A	0.155274	0.156765	0.155554	0.053
H98B	0.178847	0.196935	0.217052	0.053
H98C	0.125083	0.155392	0.199512	0.053
C99	0.1642(2)	0.0476(2)	0.2019(3)	0.0539(14)
H99A	0.152643	0.050489	0.157573	0.081
H99B	0.131350	0.044651	0.209445	0.081
H99C	0.187216	0.011200	0.218295	0.081
N11A	0.2087(8)	0.1106(9)	0.2992(7)	0.0246(16)
C91A	0.1959(5)	0.0934(5)	0.2440(5)	0.0337(16)

C92A	0.2018(2)	0.0249(2)	0.2357(3)	0.0462(12)
H92C	0.170366	0.003483	0.237987	0.055
H92D	0.198754	0.018029	0.193901	0.055
C93A	0.2535(3)	−0.0032(3)	0.2805(3)	0.0575(14)
H93C	0.284811	0.012128	0.273421	0.069
H93D	0.251395	−0.047978	0.274627	0.069
C94A	0.2640(3)	0.0120(3)	0.3478(3)	0.0558(15)
H94C	0.236587	−0.010114	0.357113	0.067
H94D	0.301295	−0.002853	0.376523	0.067
C95A	0.2602(4)	0.0804(5)	0.3585(4)	0.0351(16)
C96A	0.1358(3)	0.1090(4)	0.2040(2)	0.069(2)
H96D	0.123972	0.090708	0.163198	0.104
H96E	0.131562	0.153468	0.199892	0.104
H96F	0.113026	0.093004	0.222939	0.104
C97A	0.2322(4)	0.1274(4)	0.2202(4)	0.0614(19)
H97D	0.216525	0.122865	0.175442	0.092
H97E	0.269681	0.110281	0.239291	0.092
H97F	0.233674	0.170776	0.230714	0.092
C98A	0.2521(5)	0.0829(5)	0.4161(6)	0.0430(19)
H98D	0.281904	0.060239	0.449010	0.064
H98E	0.216353	0.064610	0.408146	0.064
H98F	0.252809	0.125543	0.428721	0.064
C99A	0.3135(2)	0.1112(4)	0.3676(3)	0.0657(17)
H99D	0.344635	0.092460	0.402499	0.099
H99E	0.311642	0.154746	0.375807	0.099
H99F	0.318819	0.106419	0.330307	0.099
C100	0.04312(8)	0.40672(9)	0.44309(9)	0.0289(4)
C101	−0.00032(10)	0.41389(13)	0.46661(11)	0.0489(6)
H10A	−0.006929	0.373665	0.480786	0.059
H10B	0.014111	0.441745	0.502484	0.059
C102	−0.05435(10)	0.43851(16)	0.41900(14)	0.0667(9)
H10C	−0.048952	0.480501	0.407513	0.080
H10D	−0.081571	0.440162	0.436140	0.080
C103	−0.07628(9)	0.39785(12)	0.36227(12)	0.0446(6)
H10E	−0.110975	0.415635	0.330596	0.054
H10F	−0.085153	0.357150	0.373325	0.054
C104	−0.03495(8)	0.39025(9)	0.33516(9)	0.0239(4)
C105	0.09140(12)	0.36994(13)	0.49063(11)	0.0603(8)
H10G	0.106259	0.391035	0.530376	0.090
H10H	0.120514	0.365952	0.476983	0.090
H10I	0.078354	0.329273	0.494961	0.090
C106	0.06694(11)	0.46889(12)	0.43887(12)	0.0500(6)
H10J	0.086543	0.486406	0.480176	0.075
H10K	0.036787	0.496224	0.413041	0.075
H10L	0.092768	0.463911	0.420690	0.075
C107	−0.05646(9)	0.33879(11)	0.28784(10)	0.0370(5)
H10M	−0.093896	0.348740	0.256731	0.055
H10N	−0.057352	0.300617	0.308484	0.055
H10O	−0.031938	0.334007	0.267956	0.055
C108	−0.03275(12)	0.44783(12)	0.30095(13)	0.0570(7)
H10P	−0.068921	0.454604	0.265935	0.085
H10Q	−0.004543	0.442992	0.286059	0.085
H10R	−0.023362	0.482902	0.328871	0.085

Appendix

U_{eq} is defined as 1/3 of the trace of the orthogonalized U_{ij} tensor.

References

[1C2] *APEX4 Suite of Crystallographic Software, Version 2021-10.0,* Bruker AXS Inc., Madison, Wisconsin, USA, **2021**.

[2C2] Bruker, *SAINT*, *V8.40B*, Bruker AXS Inc., Madison, Wisconsin, USA.

[3C2] L. Krause, R. Herbst-Irmer, G. M. Sheldrick, D. Stalke, *J. Appl. Cryst.* **2015**, *48*, 3–10, doi:10.1107/S1600576714022985.

[4C2] G. M. Sheldrick, *Acta Cryst.* **2015**, *A71*, 3–8, doi:10.1107/S2053273314026370.

[5C2] G. M. Sheldrick, *Acta Cryst.* **2015**, *C71*, 3–8, doi:10.1107/S2053229614024218.

[6C2] C. B. Huebschle, G. M. Sheldrick, B. Dittrich, *J. Appl. Cryst.* **2011**, *44*, 1281–1284, doi:10.1107/S0021889811043202.

[7C2] Ed. E. Prince, *International Tables for Crystallography Volume C, Mathematical, Physical and Chemical Tables*, International Union of Crystallography, Chester, England, **2006**, 500–502; 219–222; 193–199.

[8C2] C. R. Groom, I. J. Bruno, M. P. Lightfoot, S. C. Ward, *Acta Cryst.* **2016**, *B72*, 171–179, doi:10.1107/S2052520616003954.

[9C2] D. Kratzert, *FinalCif*, *V106*, https://dkratzert.de/finalcif.html.

[10C2] K. Momma, F. Izumi, *J. Appl. Crystallogr.* **2011**, *44*, 1272-1276.

6.3 Supplementary data of starting materials

FT-IR spectrum of GaTMP

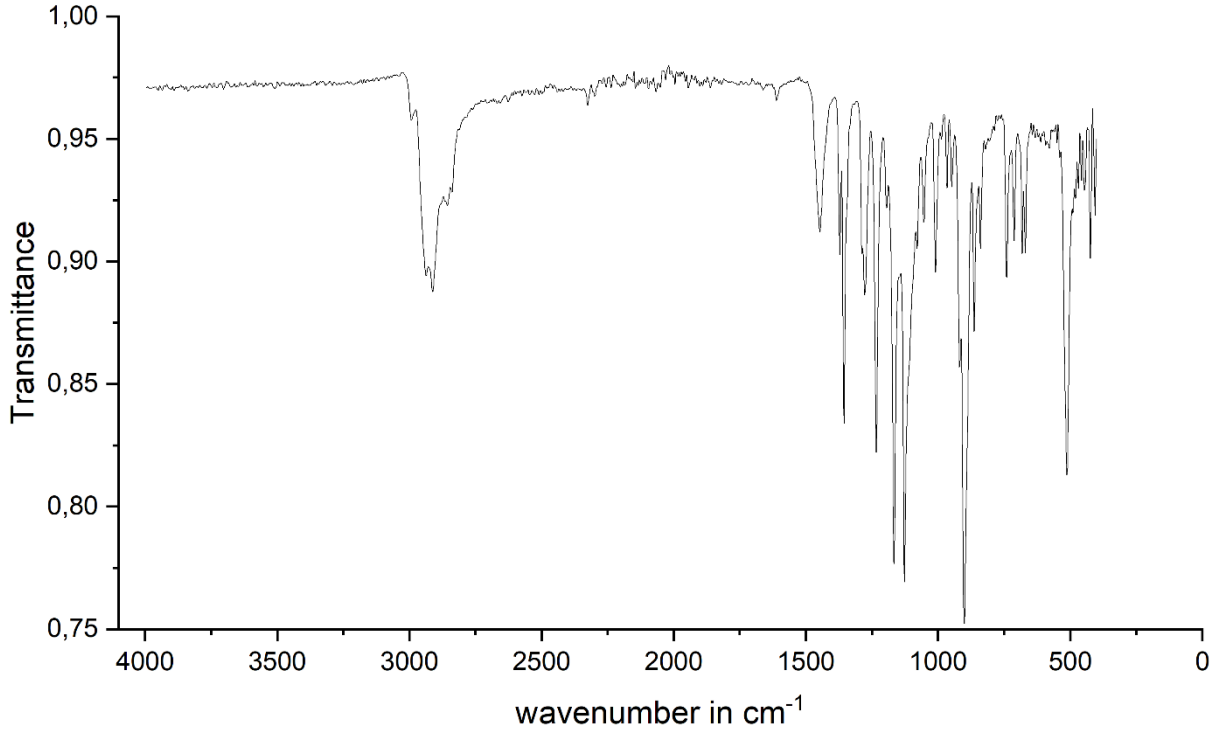

Figure S 11: FT-IR spectrum of GaTMP. The data was graciously provided by Fabrizio E. Napoli (AMC Group @ TUM). Reprinted (adapted) with permission from R. Bühler, R. J. J. Weininger, J. Stephan, M. Muhr, B. M. T. Bock, C. Gemel, R. A. Fischer, Dalton Transactions 2024, under CC BY 3.0 license. Copyright 2024 The Royal Society of Chemistry.

^{1}H-NMR spectrum of [Mo(η^4-C$_4$H$_6$)$_3$]

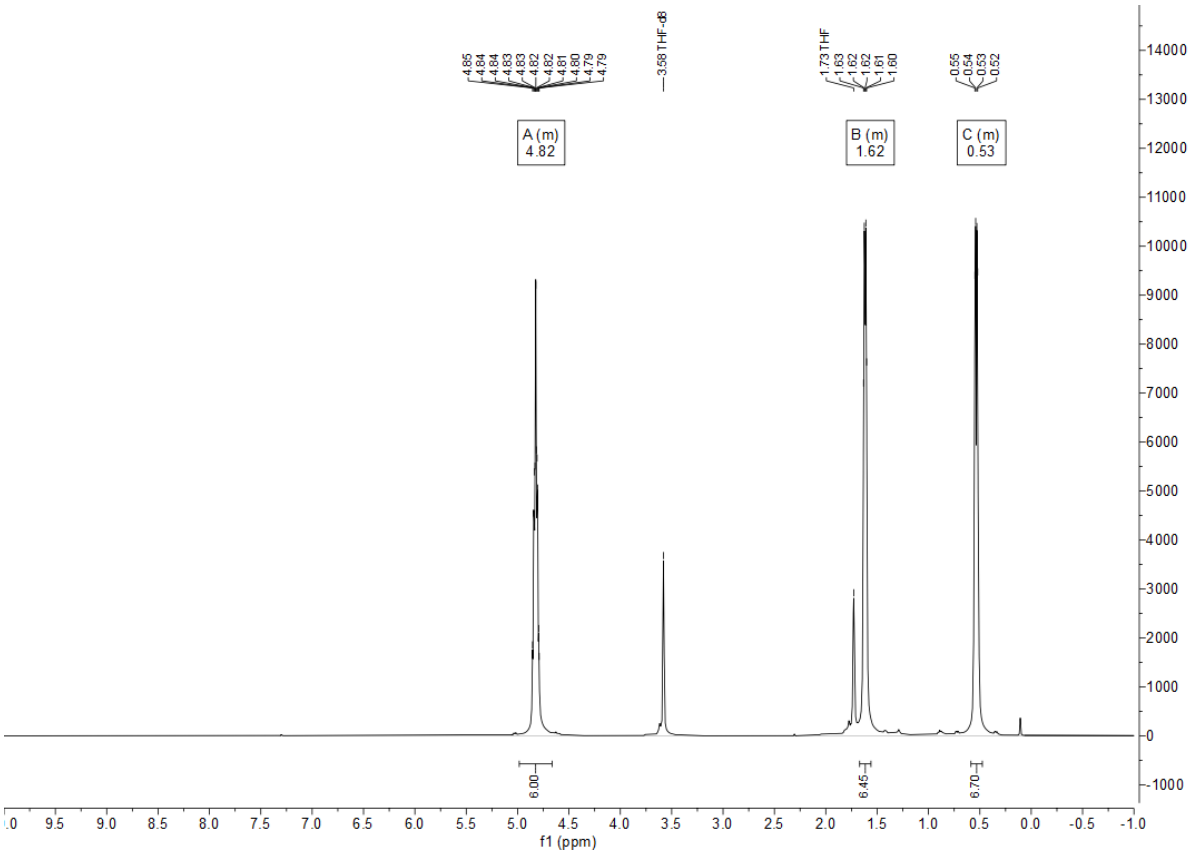

Figure S 12: ^{1}H-NMR spectrum of [Mo(η^4-C$_4$H$_6$)$_3$] in THF-d_8 at 298 K. The signal around 0.25 ppm is attributed to silicone grease. Reprinted (adapted) with permission from R. Bühler, R. J. J. Weininger, J. Stephan, M. Muhr, B. M. T. Bock, C. Gemel, R. A. Fischer, Dalton Transactions 2024, under CC BY 3.0 license. Copyright 2024 The Royal Society of Chemistry.

6.4 Buried Volume Datapoints

Table S 5: Table of structural data, classification and buried volumes. Compounds were indexed individually with the subsequent number behind a comma indicating a crystallographically distinguishable ligand. CN = Coordination Number. Additional structural data was only gathered for compounds of Cp* and TMP.

Index	Compound	Ligand Type	CN	%V_{Bur} @ 3.5 Å	%V_{Bur} @ 3.5 Å	E-TM-Bond Length [Å]	E-R Distance [Å]	TM-E-R Angle [°]
1,1	[Au(Ga(THF)(DDP))2][BArF]	GaDDP	2	39,5	43,8			
1,2	[Au(Ga(THF)(DDP))2][BArF]	GaDDP	2	38	42,9			
1,3	[Au(Ga(THF)(DDP))2][BArF]	GaDDP	2	38,9	43,4			
1,4	[Au(Ga(THF)(DDP))2][BArF]	GaDDP	2	38,3	42,7			
2	[Hg(Ga(SC6F5)(DDP))2]	GaDDP	2	40,4	44,1			
3,1	[Zn(GaH(DDP))2]	GaDDP	2	38,5	42,6			
3,2	[Zn(GaH(DDP))2]	GaDDP	2	38,5	42,6			
3,3	[Zn(GaH(DDP))2]	GaDDP	2	38,9	42,3			
3,4	[Zn(GaH(DDP))2]	GaDDP	2	38,8	42,5			
4	[Cu(Ga(DDP))2][OTf]	GaDDP	2	38,7	40,6			
5,1	[Zn(Ga(Me)(DDP))2]	GaDDP	2	42,5	42,7			
5,2	[Zn(Ga(Me)(DDP))2]	GaDDP	2	42,7	42,6			
6,1	[Pt(Ga[N(Ar)]2CNCy2)3]	Ga[N(Ar)]2CNCy2	3	26	27,7			
6,2	[Pt(Ga[N(Ar)]2CNCy2)3]	Ga[N(Ar)]2CNCy2	3	26,9	28,3			
6,3	[Pt(Ga[N(Ar)]2CNCy2)3]	Ga[N(Ar)]2CNCy2	3	26,1	27,6			
7	[Pt(GaCp*)4]	GaCp*	4	20,2	18,9	2,3332	1,995	160,68
8	[Pd(GaCp*)4]	GaCp*	4	20,3	19	2,3668	2,019	155,55
9	[Ni(GaCp*)4]	GaCp*	4	21	19,7	2,218	2,004	164,71
10,1	[Ag(GaCp*)4][BPh4]	GaCp*	4	19,6	18,8	2,51535	1,951	148,39
10,2	[Ag(GaCp*)4][BPh4]	GaCp*	4	18,1	17	2,52795	1,956	159,63
10,3	[Ag(GaCp*)4][BPh4]	GaCp*	4	18,4	17,4	2,52325	1,953	158,29
10,4	[Ag(GaCp*)4][BPh4]	GaCp*	4	18,9	18,1	2,51145	1,942	155,31
11,1	[Zn(GaCp*)4][BArF4]2	GaCp*	4	18,9	18,1	2,4036	1,85	170,21
11,2	[Zn(GaCp*)4][BArF4]2	GaCp*	4	19,2	18,4	2,4112	1,861	165,2
12,1	[Cu(GaCp*)4][BArF]	GaCp*	4	20,4	19,3	2,3517	1,932	158,1
12,2	[Cu(GaCp*)4][BArF]	GaCp*	4	21	19,8	2,3496	1,946	153,16
13	[Pd(AlCp*)4]	AlCp*	4	19,4	18,8	2,295	1,929	169,21
14	[Ni(AlCp*)4]	AlCp*	4	20,5	19,9	2,173	1,932	173,48
15	[Ni(GaC(TMS)3)4]	GaC(TMS)3	4	21,6	22,2			
16	[Ni(InC(TMS)3)4]	InC(TMS)3	4	21,6	20,4			
17	[Pt(InC(TMS)3)4]	InC(TMS)3	4	20,2	19,7			
18	[Pd(InC(TMS)3)4]	InC(TMS)3	4					
19a1	[Fe(AlCp*)5]	AlCp*	5	21,3	20,3	2,2122	1,915	161
19a2	[Fe(AlCp*)5]	AlCp*	5	19,9	19,2	2,2422	1,909	172,22
19b1	[Fe(AlCp*)5]	AlCp*	5	20,6	20,5	2,2102	1,889	162,11
19b5B	[Fe(AlCp*)5]	AlCp*	5	21,4	19,8	2,2132	1,988	160,79
20,2	[Ru(AlCp*)5]	AlCp*	5	19,4	18,8	2,3322	1,904	166,58
21,1	[Mo(GaCp*)6]	GaCp*	6	18,2	16,1	2,45797	2,127	175,21
21,2	[Mo(GaCp*)6]	GaCp*	6	18,1	16,5	2,49297	2,091	167,42
21,3	[Mo(GaCp*)6]	GaCp*	6	18,1	16,4	2,47577	2,04	170,3
21,5	[Mo(GaCp*)6]	GaCp*	6	18,2	16,6	2,47407	2,057	167,36
21,6	[Mo(GaCp*)6]	GaCp*	6	18,2	16,8	2,48457	2,024	166,04
22,1	[Mo(GaTMP)6]	GaTMP	6	19,1	15,8	2,38809	1,8562	174,416
22,2	[Mo(GaTMP)6]	GaTMP	6	18,9	15,5	2,38896	1,8572	178,866

22,3	[Mo(GaTMP)6]	GaTMP	6	18,9	15,7	2,39599	1,8642	176,106
22,4	[Mo(GaTMP)6]	GaTMP	6	19,2	15,9	2,37706	1,8462	176,946
22,5	[Mo(GaTMP)6]	GaTMP	6	18,9	15,9	2,39216	1,8672	175,946
22,6	[Mo(GaTMP)6]	GaTMP	6	19,2	16	2,37396	1,8511	175,606
22,7	[Mo(GaTMP)6]	GaTMP	6	18,9	15,8	2,39167	1,8582	178,396
22,8	[Mo(GaTMP)6]	GaTMP	6	19	15,9	2,38156	1,8561	176,186
22,9	[Mo(GaTMP)6]	GaTMP	6	19,1	15,8	2,38448	1,8552	178,426
22,1	[Mo(GaTMP)6]	GaTMP	6	19,1	15,9	2,38236	1,8521	177,386
22,11	[Mo(GaTMP)6]	GaTMP	6	19,1	15,8	2,38398	1,822	177,56
22,12	[Mo(GaTMP)6]	GaTMP	6	19,1	15,8	2,38398	1,8532	179,506
23,1	[Ru(GaTMP)5]	GaTMP	5	20	16,3	2,2911	1,872	171,6
23,2	[Ru(GaTMP)5]	GaTMP	5	20	17	2,2807	1,8495	175,8
23,3	[Ru(GaTMP)5]	GaTMP	5	20,1	17	2,274	1,864	172,6

Table S 6: Table of compounds and structural parameters calculated from the data found in table S 5. Compounds were indexed individually with the subsequent number behind a comma indicating a crystallographically distinguishable ligand.

Index	Compound	Orthogonal Component of E-R Distance [Å]	Sum of Orthogonal Components [Å]	Sum of Unmodified Distanceds [Å]
1,1	[Au(Ga(THF)(DDP))2][BArF]			
1,2	[Au(Ga(THF)(DDP))2][BArF]			
1,3	[Au(Ga(THF)(DDP))2][BArF]			
1,4	[Au(Ga(THF)(DDP))2][BArF]			
2	[Hg(Ga(SC6F5)(DDP))2]			
3,1	[Zn(GaH(DDP))2]			
3,2	[Zn(GaH(DDP))2]			
3,3	[Zn(GaH(DDP))2]			
3,4	[Zn(GaH(DDP))2]			
4	[Cu(Ga(DDP))2][OTf]			
5,1	[Zn(Ga(Me)(DDP))2]			
5,2	[Zn(Ga(Me)(DDP))2]			
6,1	[Pt(Ga[N(Ar)]2CNCy2)3]			
6,2	[Pt(Ga[N(Ar)]2CNCy2)3]			
6,3	[Pt(Ga[N(Ar)]2CNCy2)3]			
7	[Pt(GaCp*)4]	1,88265	4,21585	4,3282
8	[Pd(GaCp*)4]	1,83794	4,20474	4,3858
9	[Ni(GaCp*)4]	1,93307	4,15107	4,222
10,1	[Ag(GaCp*)4][BPh4]	1,66154	4,17689	4,46635
10,2	[Ag(GaCp*)4][BPh4]	1,83368	4,36163	4,48395
10,3	[Ag(GaCp*)4][BPh4]	1,81447	4,33772	4,47625
10,4	[Ag(GaCp*)4][BPh4]	1,76446	4,27591	4,45345
11,1	[Zn(GaCp*)4][BArF4]2	1,82306	4,22666	4,2536
11,2	[Zn(GaCp*)4][BArF4]2	1,79926	4,21046	4,2722
12,1	[Cu(GaCp*)4][BArF]	1,79258	4,14428	4,2837
12,2	[Cu(GaCp*)4][BArF]	1,73636	4,08596	4,2956
13	[Pd(AlCp*)4]	1,8949	4,1899	4,224
14	[Ni(AlCp*)4]	1,9195	4,0925	4,105
15	[Ni(GaC(TMS)3)4]			
16	[Ni(InC(TMS)3)4]			

17	[Pt(InC(TMS)3)4]			
18	[Pd(InC(TMS)3)4]			
19a1	[Fe(AlCp*)5]	1,81067	4,02287	4,1272
19a2	[Fe(AlCp*)5]	1,89143	4,13363	4,1512
19b1	[Fe(AlCp*)5]	1,79766	4,00786	4,0992
19b5B	[Fe(AlCp*)5]	1,87731	4,09051	4,2012
20,2	[Ru(AlCp*)5]	1,85201	4,18421	4,2362
21,1	[Mo(GaCp*)6]	2,11957	4,57754	4,58497
21,2	[Mo(GaCp*)6]	2,0408	4,53377	4,58397
21,3	[Mo(GaCp*)6]	2,01084	4,48661	4,51577
21,5	[Mo(GaCp*)6]	2,00715	4,48122	4,53107
21,6	[Mo(GaCp*)6]	1,96422	4,44879	4,50857
22,1	[Mo(GaTMP)6]	1,84739	4,23548	4,24429
22,2	[Mo(GaTMP)6]	1,85684	4,2458	4,24616
22,3	[Mo(GaTMP)6]	1,8599	4,25589	4,26019
22,4	[Mo(GaTMP)6]	1,84358	4,22064	4,22326
22,5	[Mo(GaTMP)6]	1,86253	4,25469	4,25936
22,6	[Mo(GaTMP)6]	1,84566	4,21962	4,22506
22,7	[Mo(GaTMP)6]	1,85747	4,24914	4,24987
22,8	[Mo(GaTMP)6]	1,85199	4,23355	4,23766
22,9	[Mo(GaTMP)6]	1,8545	4,23898	4,23968
22,1	[Mo(GaTMP)6]	1,85017	4,23253	4,23446
22,11	[Mo(GaTMP)6]	1,82035	4,20433	4,20598
22,12	[Mo(GaTMP)6]	1,85313	4,23711	4,23718
23,1	[Ru(GaTMP)5]	1,85192	4,14302	4,1631
23,2	[Ru(GaTMP)5]	1,84453	4,12523	4,1302
23,3	[Ru(GaTMP)5]	1,84848	4,12248	4,138

6.5 Reprint Permissions

11.06.2025 – 16:10

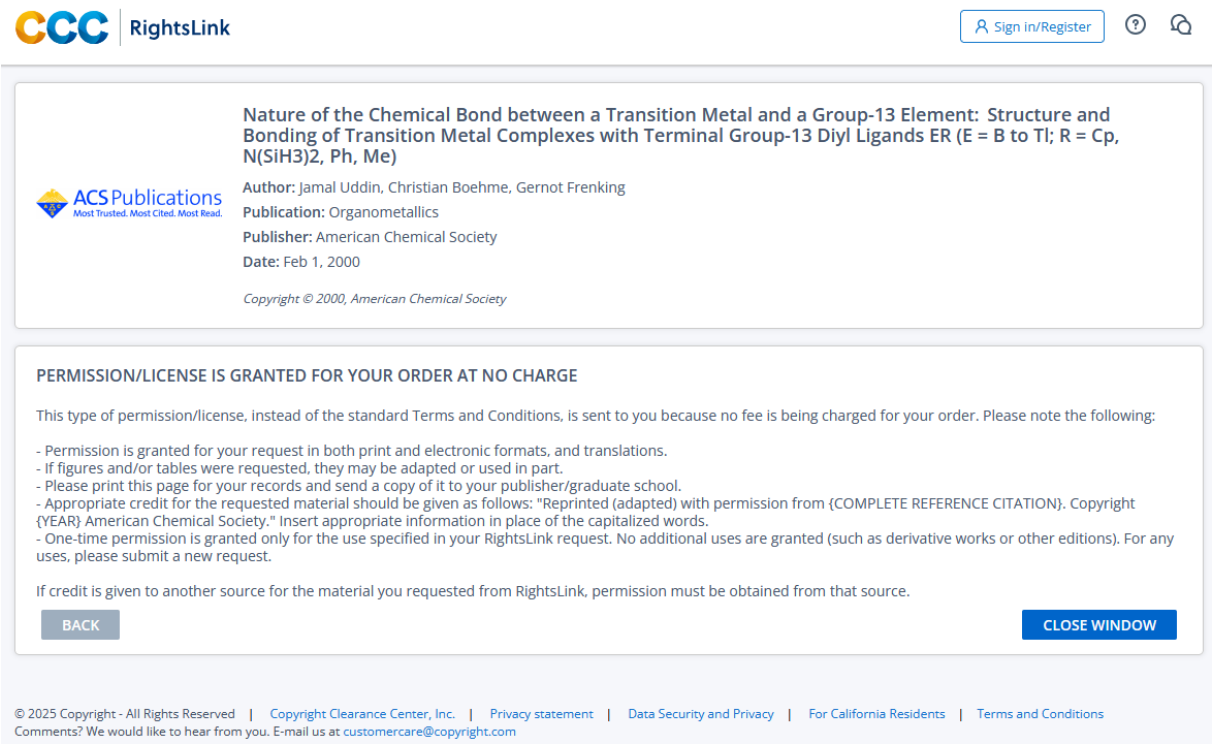

RightsLink

Sign in/Register

ACS Publications
Most Trusted. Most Cited. Most Read.

Nature of the Chemical Bond between a Transition Metal and a Group-13 Element: Structure and Bonding of Transition Metal Complexes with Terminal Group-13 Diyl Ligands ER (E = B to Tl; R = Cp, N(SiH3)2, Ph, Me)

Author: Jamal Uddin, Christian Boehme, Gernot Frenking
Publication: Organometallics
Publisher: American Chemical Society
Date: Feb 1, 2000

Copyright © 2000, American Chemical Society

PERMISSION/LICENSE IS GRANTED FOR YOUR ORDER AT NO CHARGE

This type of permission/license, instead of the standard Terms and Conditions, is sent to you because no fee is being charged for your order. Please note the following:

- Permission is granted for your request in both print and electronic formats, and translations.
- If figures and/or tables were requested, they may be adapted or used in part.
- Please print this page for your records and send a copy of it to your publisher/graduate school.
- Appropriate credit for the requested material should be given as follows: "Reprinted (adapted) with permission from {COMPLETE REFERENCE CITATION}. Copyright {YEAR} American Chemical Society." Insert appropriate information in place of the capitalized words.
- One-time permission is granted only for the use specified in your RightsLink request. No additional uses are granted (such as derivative works or other editions). For any uses, please submit a new request.

If credit is given to another source for the material you requested from RightsLink, permission must be obtained from that source.

BACK CLOSE WINDOW

© 2025 Copyright - All Rights Reserved | Copyright Clearance Center, Inc. | Privacy statement | Data Security and Privacy | For California Residents | Terms and Conditions
Comments? We would like to hear from you. E-mail us at customercare@copyright.com

11.06.2025 – 16:17

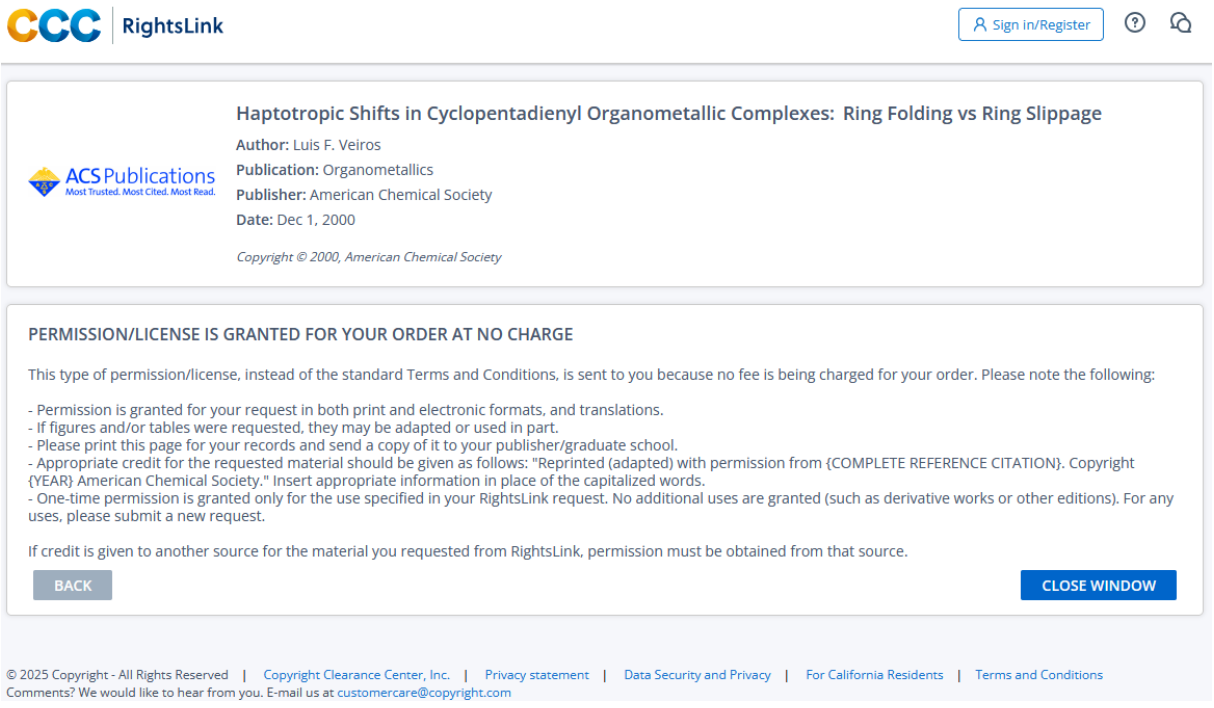

RightsLink

Sign in/Register

ACS Publications
Most Trusted. Most Cited. Most Read.

Haptotropic Shifts in Cyclopentadienyl Organometallic Complexes: Ring Folding vs Ring Slippage

Author: Luis F. Veiros
Publication: Organometallics
Publisher: American Chemical Society
Date: Dec 1, 2000

Copyright © 2000, American Chemical Society

PERMISSION/LICENSE IS GRANTED FOR YOUR ORDER AT NO CHARGE

This type of permission/license, instead of the standard Terms and Conditions, is sent to you because no fee is being charged for your order. Please note the following:

- Permission is granted for your request in both print and electronic formats, and translations.
- If figures and/or tables were requested, they may be adapted or used in part.
- Please print this page for your records and send a copy of it to your publisher/graduate school.
- Appropriate credit for the requested material should be given as follows: "Reprinted (adapted) with permission from {COMPLETE REFERENCE CITATION}. Copyright {YEAR} American Chemical Society." Insert appropriate information in place of the capitalized words.
- One-time permission is granted only for the use specified in your RightsLink request. No additional uses are granted (such as derivative works or other editions). For any uses, please submit a new request.

If credit is given to another source for the material you requested from RightsLink, permission must be obtained from that source.

BACK CLOSE WINDOW

© 2025 Copyright - All Rights Reserved | Copyright Clearance Center, Inc. | Privacy statement | Data Security and Privacy | For California Residents | Terms and Conditions
Comments? We would like to hear from you. E-mail us at customercare@copyright.com

Appendix

11.06.2025 – 16:22

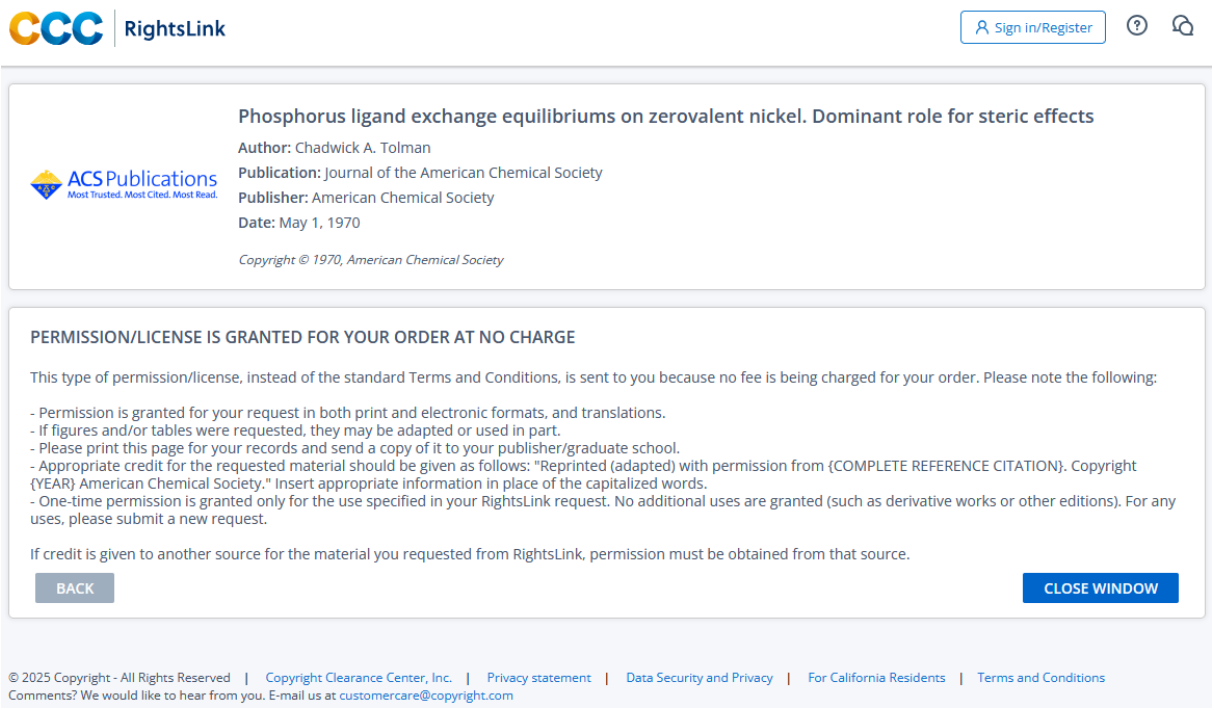

RightsLink

Sign in/Register

ACS Publications
Most Trusted. Most Cited. Most Read.

Phosphorus ligand exchange equilibriums on zerovalent nickel. Dominant role for steric effects

Author: Chadwick A. Tolman
Publication: Journal of the American Chemical Society
Publisher: American Chemical Society
Date: May 1, 1970

Copyright © 1970, American Chemical Society

PERMISSION/LICENSE IS GRANTED FOR YOUR ORDER AT NO CHARGE

This type of permission/license, instead of the standard Terms and Conditions, is sent to you because no fee is being charged for your order. Please note the following:

- Permission is granted for your request in both print and electronic formats, and translations.
- If figures and/or tables were requested, they may be adapted or used in part.
- Please print this page for your records and send a copy of it to your publisher/graduate school.
- Appropriate credit for the requested material should be given as follows: "Reprinted (adapted) with permission from {COMPLETE REFERENCE CITATION}. Copyright {YEAR} American Chemical Society." Insert appropriate information in place of the capitalized words.
- One-time permission is granted only for the use specified in your RightsLink request. No additional uses are granted (such as derivative works or other editions). For any uses, please submit a new request.

If credit is given to another source for the material you requested from RightsLink, permission must be obtained from that source.

BACK CLOSE WINDOW

© 2025 Copyright - All Rights Reserved | Copyright Clearance Center, Inc. | Privacy statement | Data Security and Privacy | For California Residents | Terms and Conditions
Comments? We would like to hear from you. E-mail us at customercare@copyright.com

11.06.2025 - 16:28

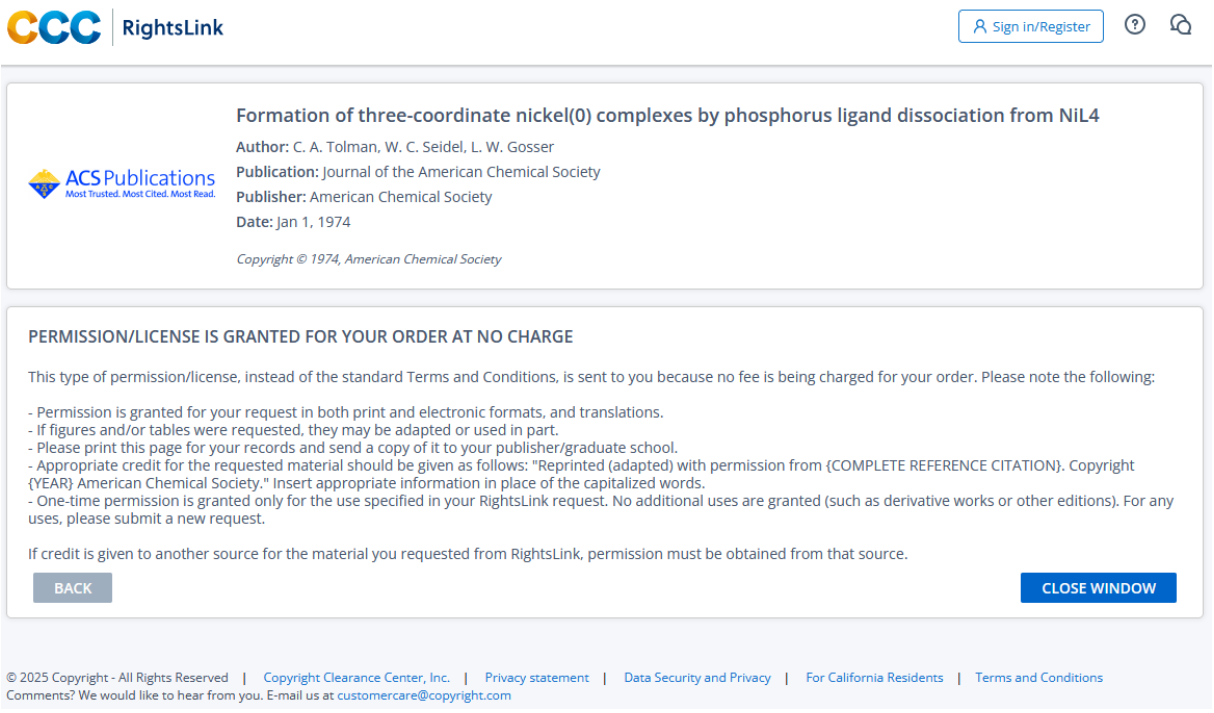

RightsLink

Sign in/Register

ACS Publications
Most Trusted. Most Cited. Most Read.

Formation of three-coordinate nickel(0) complexes by phosphorus ligand dissociation from NiL4

Author: C. A. Tolman, W. C. Seidel, L. W. Gosser
Publication: Journal of the American Chemical Society
Publisher: American Chemical Society
Date: Jan 1, 1974

Copyright © 1974, American Chemical Society

PERMISSION/LICENSE IS GRANTED FOR YOUR ORDER AT NO CHARGE

This type of permission/license, instead of the standard Terms and Conditions, is sent to you because no fee is being charged for your order. Please note the following:

- Permission is granted for your request in both print and electronic formats, and translations.
- If figures and/or tables were requested, they may be adapted or used in part.
- Please print this page for your records and send a copy of it to your publisher/graduate school.
- Appropriate credit for the requested material should be given as follows: "Reprinted (adapted) with permission from {COMPLETE REFERENCE CITATION}. Copyright {YEAR} American Chemical Society." Insert appropriate information in place of the capitalized words.
- One-time permission is granted only for the use specified in your RightsLink request. No additional uses are granted (such as derivative works or other editions). For any uses, please submit a new request.

If credit is given to another source for the material you requested from RightsLink, permission must be obtained from that source.

BACK CLOSE WINDOW

© 2025 Copyright - All Rights Reserved | Copyright Clearance Center, Inc. | Privacy statement | Data Security and Privacy | For California Residents | Terms and Conditions
Comments? We would like to hear from you. E-mail us at customercare@copyright.com

Appendix

11.06.2025 – 16:32

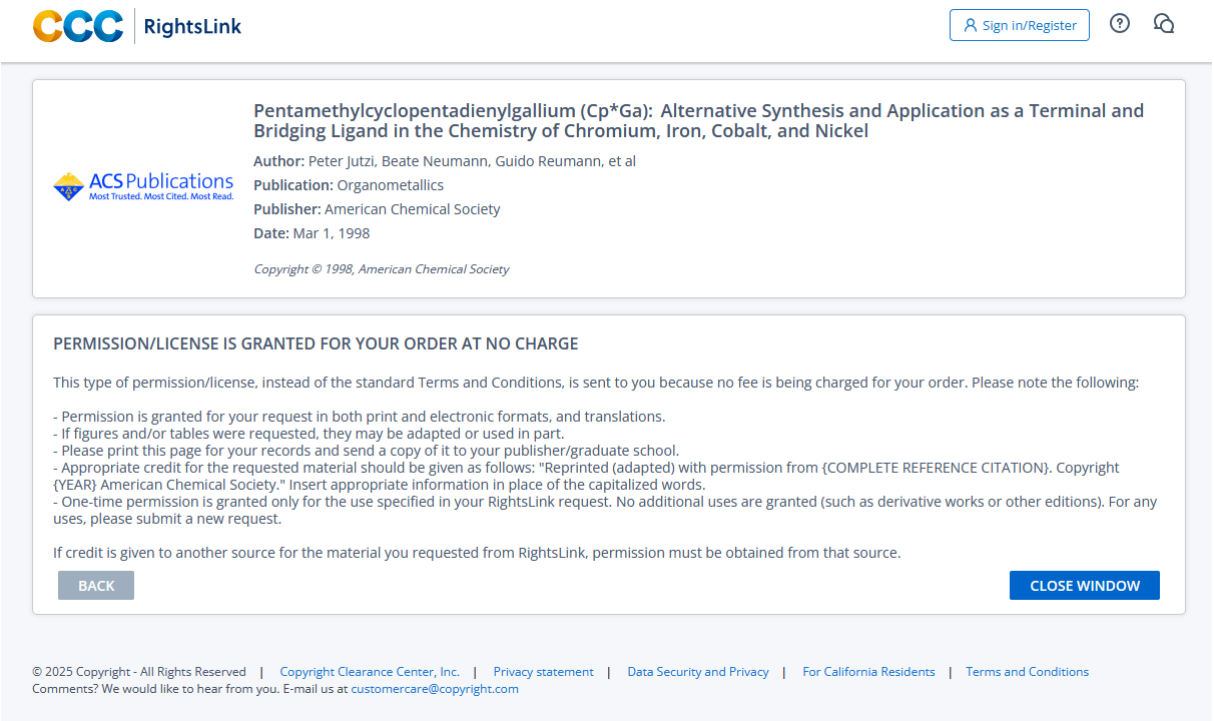

12.06.2025 – 15:06

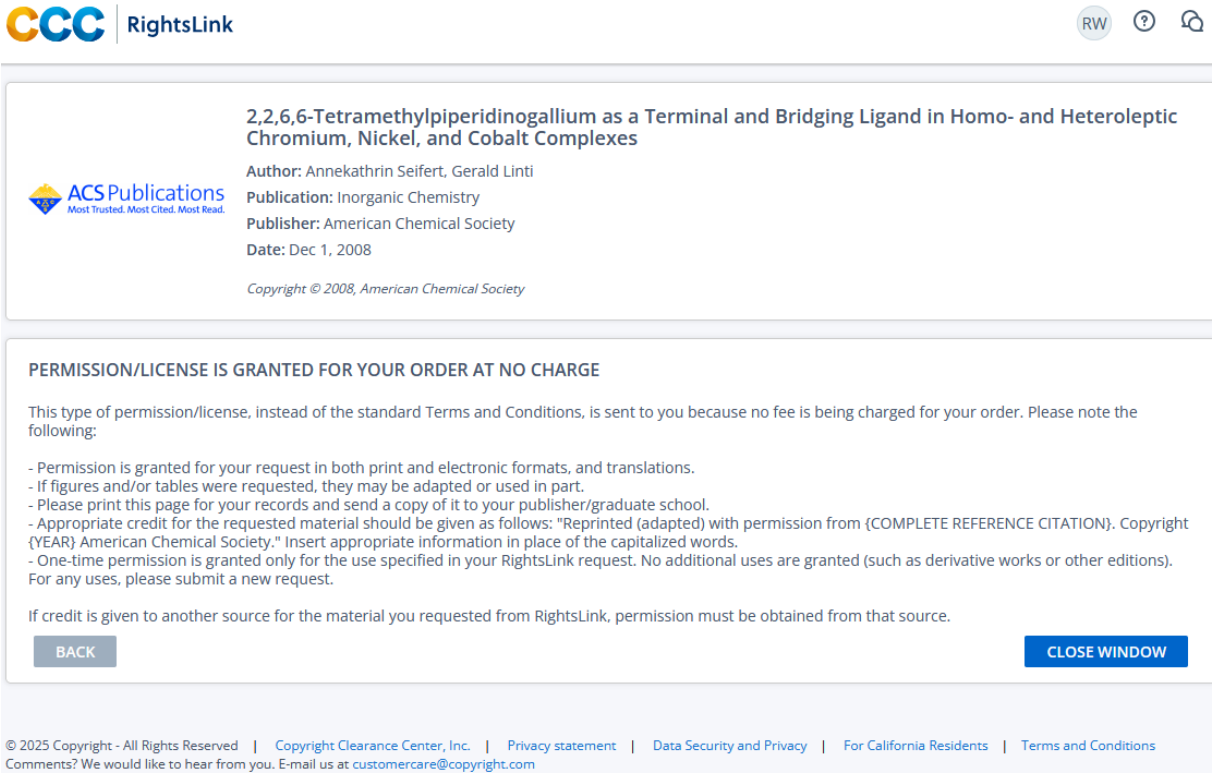

ORGANOMETALLICS

Article

pubs.acs.org/Organometallics

SambVca 2. A Web Tool for Analyzing Catalytic Pockets with Topographic Steric Maps

Laura Falivene,[†] Raffaele Credendino,[†] Albert Poater,[†,‡] Andrea Petta,[§] Luigi Serra,[§] Romina Oliva,[∥] Vittorio Scarano,[§] and Luigi Cavallo*[,†]

[†]Physical Sciences & Engineering Division (PSE), KAUST Catalysis Center (KCC), King Abdullah University of Science and Technology (KAUST), Thuwal, 23955-6900, Saudi Arabia

[‡]Institut de Química Computacional i Catàlisi and Departament de Química, Universitat de Girona, Girona 17003, Spain

[§]Dipartimento di Informatica ed Applicazioni, University of Salerno, Fisciano (SA), Italy

[∥]Department of Sciences and Technologies, University "Parthenope" of Naples, Centro Direzionale Isola C4, Naples 80143, Italy

Supporting Information

ABSTRACT: Developing more efficient catalysts remains one of the primary targets of organometallic chemists. To accelerate reaching this goal, effective molecular descriptors and visualization tools can represent a remarkable aid. Here, we present a Web application for analyzing the catalytic pocket of metal complexes using topographic steric maps as a general and unbiased descriptor that is suitable for every class of catalysts. To show the broad applicability of our approach, we first compared the steric map of a series of transition metal complexes presenting popular mono-, di-, and tetracoordinated ligands and three classic zirconocenes. This comparative analysis highlighted similarities and differences between totally unrelated ligands. Then, we focused on a recently developed Fe(II) catalyst that is active in the asymmetric transfer hydrogenation of ketones and imines. Finally, we expand the scope of these tools to rationalize the inversion of enantioselectivity in enzymatic catalysis, achieved by point mutation of three amino acids of mononuclear *p*-hydroxymandelate synthase.

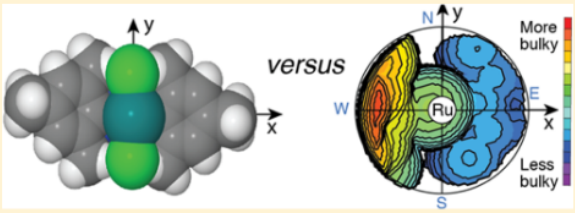

INTRODUCTION

Selecting the best catalyst in a disorganized catalyst space, composed of transition metal complexes, is a challenging task often driven by trial and error, or intuition, rather than a rational science. A classic solution to the problem is to use molecular descriptors capable of reorganizing the catalysts space as shown in Figure 1, paving the route to in silico design

Figure 1. Representation of the potential of molecular descriptors in rationalizing catalyst behavior.

of new catalysts.[1−5] The scope of these descriptors is to quantitatively correlate properties of the catalytic pocket (defined by analogy to enzymatic catalysis as the space around the active metal center) to how it behaves experimentally.

In a transition metal complex, the metal and the way the ligand wraps around the metal are fundamental to determining stability, activity, and selectivities (e.g., chemo, regio, and stereo) of the resulting catalyst. Therefore, developing a good catalyst means properly shaping the catalytic pocket with the caveat that good selectivity (i.e., greater than 95%) typically means favoring one reaction pathway over the others by roughly 2 kcal/mol.[6] As a consequence, the challenge is to develop descriptors capable of capturing small structural differences in the catalytic pocket, which result in energy pathways differing by roughly 2 kcal/mol.

Molecular descriptors are usually split into two categories depending on whether they influence catalytic behavior by altering the electronic status at the metal (i.e., electronic effects) or by constraining the space available to reactants (i.e., steric effects).[7] Here, we focus on steric descriptors, of which one of the most successful is the Tolman cone angle, shown in Figure 2a.[7] This popular descriptor appears in organometallic

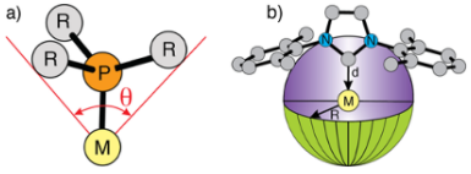

Figure 2. Representation of the Tolman cone angle (a) and the buried volume (b) steric descriptors.

Received: May 9, 2016
Published: June 27, 2016

DOI: 10.1021/acs.organomet.6b00371
Organometallics 2016, 35, 2286−2293

Appendix

12.06.2025 – 14:28

CCC RightsLink RW

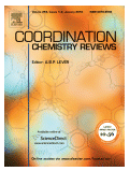

Ligand steric properties

Author: Theodore L. Brown,Kevin J. Lee
Publication: Coordination Chemistry Reviews
Publisher: Elsevier
Date: October 1993

Order Completed

Thank you for your order.

This Agreement between Richard J. J. Weininger ("You") and Elsevier ("Elsevier") consists of your license details and the terms and conditions provided by Elsevier and Copyright Clearance Center.

Your confirmation email will contain your order number for future reference.

License Number	6046480938290
License date	Jun 12, 2025

Printable Details

Licensed Content

Licensed Content Publisher	Elsevier
Licensed Content Publication	Coordination Chemistry Reviews
Licensed Content Title	Ligand steric properties
Licensed Content Author	Theodore L. Brown,Kevin J. Lee
Licensed Content Date	Oct 1, 1993
Licensed Content Volume	128
Licensed Content Issue	1-2
Licensed Content Pages	28

Order Details

Type of Use	reuse in a thesis/dissertation
Portion	figures/tables/illustrations
Number of figures/tables/ illustrations	1
Format	both print and electronic
Are you the author of this Elsevier article?	No
Will you be translating?	No

About Your Work

Title of new work	Mononuclear-Homoleptic Transition Metal Compounds of GaTMP
Institution name	Technical University of Munich
Expected presentation date	Sep 2025

Additional Data

Portions	Figure 6 on page 98
The Requesting Person / Organization to Appear on the License	Richard J. J. Weininger

Requestor Location

Requestor Location	Technical University of Munich Chair of Inorganic and Metal-Organic Chemistry Lichtenbergstraße 4 Garching bei München, Bavaria 85748 Germany

Tax Details

Publisher Tax ID	GB 494 6272 12

Total: 0.00 EUR

CLOSE WINDOW ORDER MORE

Appendix

12.06.2025 – 14:37

CCC | RightsLink

SambVca: A Web Application for the Calculation of the Buried Volume of N-Heterocyclic Carbene Ligands

Author: Luigi Cavallo, Vittorio Scarano, Francesco Ragone, et al
Publication: European Journal of Inorganic Chemistry
Publisher: John Wiley and Sons
Date: Apr 15, 2009

Order Completed

Thank you for your order.

This Agreement between Richard J. J. Weininger ("You") and John Wiley and Sons ("John Wiley and Sons") consists of your license details and the terms and conditions provided by John Wiley and Sons and Copyright Clearance Center.

Your confirmation email will contain your order number for future reference.

Printable Details

License Number	6046490077581
License date	Jun 12, 2025

Licensed Content

Licensed Content Publisher	John Wiley and Sons
Licensed Content Publication	European Journal of Inorganic Chemistry
Licensed Content Title	SambVca: A Web Application for the Calculation of the Buried Volume of N-Heterocyclic Carbene Ligands
Licensed Content Author	Luigi Cavallo, Vittorio Scarano, Francesco Ragone, et al
Licensed Content Date	Apr 15, 2009
Licensed Content Volume	2009
Licensed Content Issue	13
Licensed Content Pages	8

Order Details

Type of use	Dissertation/Thesis
Requestor type	University/Academic
Format	Print and electronic
Portion	Figure/table
Number of figures/tables	1
Will you be translating?	No

About Your Work

Title of new work	Mononuclear-Homoleptic Transition Metal Compounds of GaTMP
Institution name	Technical University of Munich
Expected presentation date	Sep 2025

Additional Data

Portions	Figure 1, p 1760
The Requesting Person / Organization to Appear on the License	Richard J. J. Weininger

Requestor Location

Requestor Location	Mr. Richard Weininger Technical University of Munich Chair of Inorganic and Metal-Organic Chemistry Lichtenbergstraße 4 Garching Bei München, Bavaria 85748 Germany

Tax Details

Publisher Tax ID	EU826007151

Would you like to purchase the full text of this article? If so, please continue on to the content ordering system located here: Purchase PDF
If you click on the buttons below or close this window, you will not be able to return to the content ordering system.

Total: 0.00 EUR

CLOSE WINDOW ORDER MORE

Appendix

12.06.2025 – 14:49

CCC Marketplace

This is a License Agreement between Richard J. J. Weininger ("User") and Copyright Clearance Center, Inc. ("CCC") on behalf of the Rightsholder identified in the order details below. The license consists of the order details, the Marketplace Permissions General Terms and Conditions below, and any Rightsholder Terms and Conditions which are included below.

All payments must be made in full to CCC in accordance with the Marketplace Permissions General Terms and Conditions below.

Order Date	12-Jun-2025	**Type of Use**	Republish in a thesis/dissertation
Order License ID	1619769-1	**Publisher**	ROYAL SOCIETY OF CHEMISTRY
ISSN	1477-9234	**Portion**	Image/photo/illustration

LICENSED CONTENT

Publication Title	Dalton transactions	**Rightsholder**	Royal Society of Chemistry
Article Title	Five-Coordinate Transition Metal Complexes and the Value of τ5: Observations and Caveats	**Publication Type**	e-Journal
		Start Page	14798
Author / Editor	Royal Society of Chemistry (Great Britain)	**End Page**	14806
Date	01/01/2003	**Issue**	42
Language	English	**Volume**	49
Country	United Kingdom of Great Britain and Northern Ireland		

REQUEST DETAILS

Portion Type	Image/photo/illustration	**Distribution**	Worldwide
Number of Images / Photos / Illustrations	2	**Translation**	Original language of publication
Format (select all that apply)	Print, Electronic	**Copies for the Disabled?**	No
Who Will Republish the Content?	Academic institution	**Minor Editing Privileges?**	Yes
Duration of Use	Life of current edition	**Incidental Promotional Use?**	No
Lifetime Unit Quantity	Up to 499	**Currency**	EUR
Rights Requested	Main product		

NEW WORK DETAILS

Title	Mononuclear-Homoleptic Transition Metal Compounds of GaTMP	**Institution Name**	Technical University of Munich
		Expected Presentation Date	2025-09-01
Instructor Name	Prof. Dr. Roland A. Fischer		

ADDITIONAL DETAILS

Order Reference Number	N/A	**The Requesting Person / Organization to Appear on the License**	Richard J. J. Weininger

REQUESTED CONTENT DETAILS

Title, Description or Numeric Reference of the Portion(s)	Figures 1, and 10	**Title of the Article / Chapter the Portion Is From**	Five-Coordinate Transition Metal Complexes and the Value of τ5: Observations and Caveats
Editor of Portion(s)	Blackman, Allan G; Schenk, Elaine; Jelley, Rebecca; Krenske, Elizabeth; Gahan, Lawrence	**Author of Portion(s)**	Blackman, Allan G; Schenk, Elaine; Jelley, Rebecca; Krenske, Elizabeth; Gahan, Lawrence
Volume / Edition	49		
Page or Page Range of Portion	14798-14806	**Issue, if Republishing an Article From a Serial**	42
		Publication Date of Portion	2020-11-03

Appendix

12.06.2025 – 15:02

CCC RightsLink RW

Synthesis and Structure of Tetrameric Gallium(I) Amides

Author: Gerald Linti, Annekathrin Seifert
Publication: European Journal of Inorganic Chemistry
Publisher: John Wiley and Sons
Date: Oct 26, 2007

Order Completed

Thank you for your order.

This Agreement between Richard J. J. Weininger ("You") and John Wiley and Sons ("John Wiley and Sons") consists of your license details and the terms and conditions provided by John Wiley and Sons and Copyright Clearance Center.

Your confirmation email will contain your order number for future reference.

License Number	6046500000776
License date	Jun 12, 2025

Printable Details

Licensed Content

Licensed Content Publisher	John Wiley and Sons
Licensed Content Publication	European Journal of Inorganic Chemistry
Licensed Content Title	Synthesis and Structure of Tetrameric Gallium(I) Amides
Licensed Content Author	Gerald Linti, Annekathrin Seifert
Licensed Content Date	Oct 26, 2007
Licensed Content Volume	2007
Licensed Content Issue	32
Licensed Content Pages	7

Order Details

Type of use	Dissertation/Thesis
Requestor type	University/Academic
Format	Print and electronic
Portion	Figure/table
Number of figures/tables	1
Will you be translating?	No

About Your Work

Title of new work	Mononuclear-Homoleptic Transition Metal Compounds of GaTMP
Institution name	Technical University of Munich
Expected presentation date	Sep 2025

Additional Data

Portions	Figure 2, p 5082
The Requesting Person / Organization to Appear on the License	Richard J. J. Weininger

Requestor Location

Requestor Location	Mr. Richard Weininger Technical University of Munich Chair of Inorganic and Metal-Organic Chemistry Lichtenbergstraße 4 Garching Bei München, Bavaria 85748 Germany

Tax Details

Publisher Tax ID	EU826007151

Would you like to purchase the full text of this article? If so, please continue on to the content ordering system located here: Purchase PDF
If you click on the buttons below or close this window, you will not be able to return to the content ordering system.

Total: 0.00 EUR

CLOSE WINDOW ORDER MORE

Dalton Transactions

ROYAL SOCIETY OF CHEMISTRY

PAPER

View Article Online
View Journal | View Issue

Check for updates

Cite this: *Dalton Trans.*, 2024, **53**, 17162

Homoleptic hexa- and penta-coordinated gallium(I) amide complexes of ruthenium and molybdenum†

Raphael Bühler, ‡ Richard J. J. Weininger, ‡ Johannes Stephan, Maximilian Muhr, Balasai M.-T. Bock, Christian Gemel and Roland A. Fischer *

Received 19th March 2024,
Accepted 17th April 2024

DOI: 10.1039/d4dt00823e

rsc.li/dalton

Reaction of neutral olefin complexes of ruthenium and molybdenum with GaTMP (TMP = 2,2,6,6-tetramethylpiperidinyl) by substitution leads to the formation of respective five- and six-coordinated homoleptic products. [Ru(GaTMP)$_5$] (**1**) and [Mo(GaTMP)$_6$] (**2**) were isolated and characterized. Core structure geometries were analyzed using continuous shape measure, and the complexes were subjected to DFT calculations unveiling competing π-interactions between the transition metal center and the amido substituent with the unoccupied p$_\pi$ orbitals of the gallium.

Introduction

Exploring the chemistry of low valent group-13 metallo-ligands ER* (E = Al, Ga, In; R* = sterically demanding protection group) coordinated to d- and f-block metal centers (transition metals, M) has significantly been motivated by the isolobal relationship between ER* and CO. The choice or design of R* has been crucial to allow for preparative access to ER* compounds and utilize them in organometallic coordination chemistry. The first example of a mononuclear homoleptic complex of the general formula [M(ER*)$_n$], namely [Ni(InC(SiMe$_3$)$_3$)$_4$] (R* = C(SiMe$_3$)$_3$), was reported by W. Uhl in 1998,[1] followed by P. Jutzi's [Ni(GaCp*)$_4$] in 1999 and our [Ni(AlCp*)$_4$] in 2005 (Cp* = C$_5$(CH$_3$)$_5$).[2,3] All these complexes can be viewed as analogues of [Ni(CO)$_4$]. However, there are cases such as the trinuclear, linear [(Cp*In)$_2$Pd(μ-(InCp*))$_2$Pd(μ-(InCp*)$_2$)Pd(InCp*)$_2$],[4] which has no analogous metal carbonyl [M$_n$(CO)$_m$] structure. Other protecting groups, R*, including amides (*e.g.* N(SiMe$_3$)(2,6-bis-mesityl phenyl)),[5] ketoiminates (*e.g.* DDP = 2-{(2,6-diisopropylphenyl)amino}-4-{(2,6-diisopropylphenyl)-imino}-2-pentene) and amidinates (*e.g.* [N(Ar)]$_2$CNCy$_2$; Ar = C$_6$H$_3$^{i}Pr$_2$-2,6; Cy = cyclohexyl), have been introduced with great success, for example, to yield [Pt(Ga[N(Ar)]$_2$CNCy$_2$)$_3$], as reported by Jones and co-workers.[6] Due to the high steric bulk of these types of metallo-ligands ER*, the transition metal coordination number of any of their homoleptic complexes has not exceeded three. We and others have reviewed the development of this chemistry in the past.[7–10] Specifically, an updated comprehensive listing of all structurally elucidated homoleptic complexes [M$_a$(ER*)$_b$], including [Mo(GaCp*)$_6$] as the only example of that series with coordination number cn (M) greater than five, is provided in the ESI.†[11]

The history of heterometallic group-13 metal/transition metal complexes of the more general formula [(L$_n$M)$_a$(ER$_{3-a}$)] (L = CO, phosphines, *etc.*; R = any inorganic or organic substituent, *i.e.* including hydrides or halides) featuring unsupported covalent (donor/acceptor) bonds M–E dates back to the early work of Hieber on [((CO)$_4$Co)$_3$In] in 1942.[12,13] The related work since the mid-1990s focused on synthesis, structure and the elucidation of details of the M–E bonding by theoretical approaches applying various computational frameworks.[14,15] Herein, we are particularly interested in exploring the transition from discrete heterometallic complexes to the related clusters in which an intermetalloid M$_a$E$_b$ core is protected by an all-hydrocarbon shell of R*, *i.e.* matching with the general formula [M$_a$E$_b$](R*)$_c$, with $(a + b) > c$.[16–18] A recent example of that work is the assignment of individual structures from a preparative inseparable ensemble of Ni/Ga clusters [Ni$_{6+x}$Ga$_{6+y}$](Cp*)$_6$ = [Ni$_x$Ga$_{6+y}$](NiCp*)$_6$ ($x + y \leq 2$). Notably, in this particular case, protection group transfer (R* = Cp*) occurs from the Ga to the Ni during the synthesis of the clusters from Ni(0) olefin complexes with GaCp* in toluene or mesitylene at elevated temperatures.[19,20]

A relationship exists between the molecular coordination and cluster chemistry of the solid-state and the materials chemistry of the respective intermetallic M/E (nano) phases

Chair of Inorganic and Metalorganic Chemistry, Technical University of Munich, School of Natural Sciences, Department of Chemistry, Lichtenbergstraße 4, 85748 Garching, Germany and Catalysis Research Center, Erst-Otto-Fischer-Straße 1, 85748 Garching, Germany. E-mail: roland.fischer@tum.de

†Electronic supplementary information (ESI) available. CCDC 2341048 and 2341049. For ESI and crystallographic data in CIF or other electronic format see DOI: https://doi.org/10.1039/d4dt00823e

‡These authors contributed equally to this work.

Appendix

12.06.2025 – 15:27

CCC RightsLink RW

[Ga4{C(SiMe3)3}4] with a Tetrahedral Ga4 Skeleton

Author: Wolfgang Schwarz, Marcus Layh, Wolfgang Hiller, et al
Publication: Angewandte Chemie International Edition
Publisher: John Wiley and Sons
Date: Dec 22, 2003

Order Completed

Thank you for your order.

This Agreement between Richard J. J. Weininger ("You") and John Wiley and Sons ("John Wiley and Sons") consists of your license details and the terms and conditions provided by John Wiley and Sons and Copyright Clearance Center.

Your confirmation email will contain your order number for future reference.

Printable Details

License Number	6046510108384
License date	Jun 12, 2025

Licensed Content

Licensed Content Publisher	John Wiley and Sons
Licensed Content Publication	Angewandte Chemie International Edition
Licensed Content Title	[Ga4{C(SiMe3)3}4] with a Tetrahedral Ga4 Skeleton
Licensed Content Author	Wolfgang Schwarz, Marcus Layh, Wolfgang Hiller, et al
Licensed Content Date	Dec 22, 2003
Licensed Content Volume	31
Licensed Content Issue	10
Licensed Content Pages	3

Order Details

Type of use	Dissertation/Thesis
Requestor type	University/Academic
Format	Print and electronic
Portion	Figure/table
Number of figures/tables	1
Will you be translating?	No

About Your Work

Title of new work	Mononuclear-Homoleptic Transition Metal Compounds of GaTMP
Institution name	Technical University of Munich
Expected presentation date	Sep 2025

Additional Data

Portions	Figure 1, p 1365
The Requesting Person / Organization to Appear on the License	Richard J. J. Weininger

Requestor Location

Requestor Location	Mr. Richard Weininger Technical University of Munich Chair of Inorganic and Metal-Organic Chemistry Lichtenbergstraße 4 Garching Bei München, Bavaria 85748 Germany

Tax Details

Publisher Tax ID	EU826007151

Would you like to purchase the full text of this article? If so, please continue on to the content ordering system located here: Purchase PDF
If you click on the buttons below or close this window, you will not be able to return to the content ordering system.

Total: 0.00 USD

CLOSE WINDOW ORDER MORE

12.06.2025 - 15:36

CCC RightsLink RW

In4{C(SiMe3)3}4 mit In4-tetraeder und In4Se4{C(SiMe3)3}4 mit In4Se4-heterocubanstruktur

Author: Werner Uhl,Rene Graupner,Marcus Layh,Uwe Schütz
Publication: Journal of Organometallic Chemistry
Publisher: Elsevier
Date: 17 May 1995

Order Completed

Thank you for your order.

This Agreement between Richard J. J. Weininger ("You") and Elsevier ("Elsevier") consists of your license details and the terms and conditions provided by Elsevier and Copyright Clearance Center.

Your confirmation email will contain your order number for future reference.

License Number	6046510560904
License date	Jun 12, 2025

Printable Details

Licensed Content

Licensed Content Publisher	Elsevier
Licensed Content Publication	Journal of Organometallic Chemistry
Licensed Content Title	In4{C(SiMe3)3}4 mit In4-tetraeder und In4Se4{C(SiMe3)3}4 mit In4Se4-heterocubanstruktur
Licensed Content Author	Werner Uhl,Rene Graupner,Marcus Layh,Uwe Schütz
Licensed Content Date	May 17, 1995
Licensed Content Volume	493
Licensed Content Issue	1-2
Licensed Content Pages	5

Order Details

Type of Use	reuse in a thesis/dissertation
Portion	figures/tables/illustrations
Number of figures/tables/illustrations	1
Format	both print and electronic
Are you the author of this Elsevier article?	No
Will you be translating?	No

About Your Work

Title of new work	Mononuclear-Homoleptic Transition Metal Compounds of GaTMP
Institution name	Technical University of Munich
Expected presentation date	Sep 2025

Additional Data

Portions	Abb 1, p. C2
The Requesting Person / Organization to Appear on the License	Richard J. J. Weininger

Requestor Location

Requestor Location	Mr. Richard Weininger Technical University of Munich Chair of Inorganic and Metal-Organic Chemistry Lichtenbergstraße 4 Garching Bei München, Bavaria 85748 Germany

Tax Details

Publisher Tax ID	GB 494 6272 12

Total: 0.00 EUR

CLOSE WINDOW ORDER MORE

Appendix

12.06.2025 - 15:41

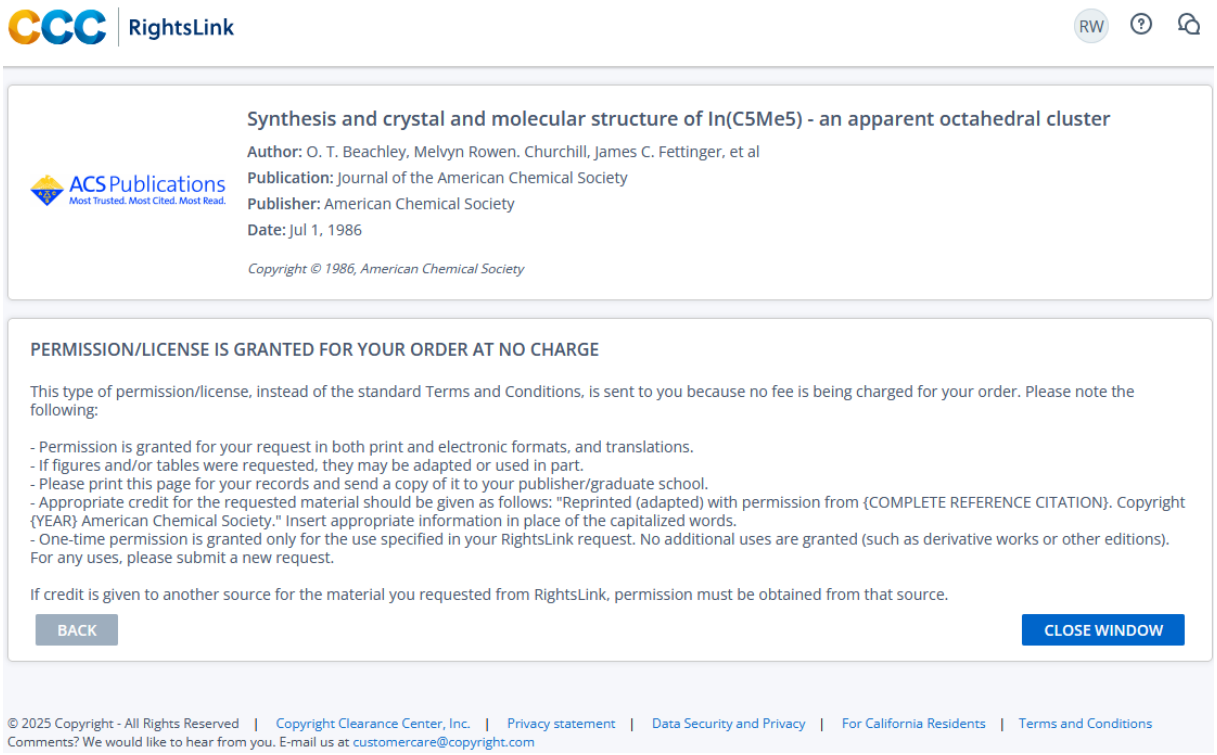

RightsLink

RW

ACS Publications
Most Trusted. Most Cited. Most Read.

Synthesis and crystal and molecular structure of In(C5Me5) - an apparent octahedral cluster

Author: O. T. Beachley, Melvyn Rowen. Churchill, James C. Fettinger, et al
Publication: Journal of the American Chemical Society
Publisher: American Chemical Society
Date: Jul 1, 1986

Copyright © 1986, American Chemical Society

PERMISSION/LICENSE IS GRANTED FOR YOUR ORDER AT NO CHARGE

This type of permission/license, instead of the standard Terms and Conditions, is sent to you because no fee is being charged for your order. Please note the following:

- Permission is granted for your request in both print and electronic formats, and translations.
- If figures and/or tables were requested, they may be adapted or used in part.
- Please print this page for your records and send a copy of it to your publisher/graduate school.
- Appropriate credit for the requested material should be given as follows: "Reprinted (adapted) with permission from {COMPLETE REFERENCE CITATION}. Copyright {YEAR} American Chemical Society." Insert appropriate information in place of the capitalized words.
- One-time permission is granted only for the use specified in your RightsLink request. No additional uses are granted (such as derivative works or other editions). For any uses, please submit a new request.

If credit is given to another source for the material you requested from RightsLink, permission must be obtained from that source.

BACK CLOSE WINDOW

12.06.2025 – 17:18

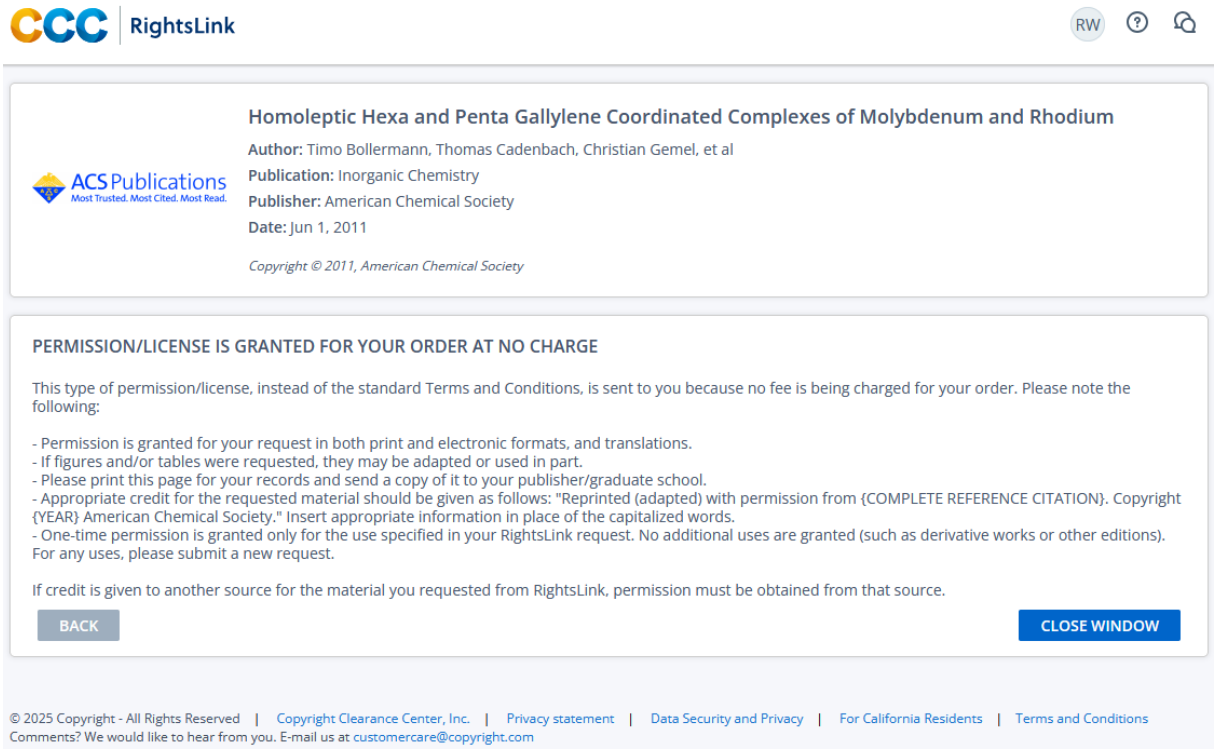

RightsLink

RW

ACS Publications
Most Trusted. Most Cited. Most Read.

Homoleptic Hexa and Penta Gallylene Coordinated Complexes of Molybdenum and Rhodium

Author: Timo Bollermann, Thomas Cadenbach, Christian Gemel, et al
Publication: Inorganic Chemistry
Publisher: American Chemical Society
Date: Jun 1, 2011

Copyright © 2011, American Chemical Society

PERMISSION/LICENSE IS GRANTED FOR YOUR ORDER AT NO CHARGE

This type of permission/license, instead of the standard Terms and Conditions, is sent to you because no fee is being charged for your order. Please note the following:

- Permission is granted for your request in both print and electronic formats, and translations.
- If figures and/or tables were requested, they may be adapted or used in part.
- Please print this page for your records and send a copy of it to your publisher/graduate school.
- Appropriate credit for the requested material should be given as follows: "Reprinted (adapted) with permission from {COMPLETE REFERENCE CITATION}. Copyright {YEAR} American Chemical Society." Insert appropriate information in place of the capitalized words.
- One-time permission is granted only for the use specified in your RightsLink request. No additional uses are granted (such as derivative works or other editions). For any uses, please submit a new request.

If credit is given to another source for the material you requested from RightsLink, permission must be obtained from that source.

BACK CLOSE WINDOW

12.06.2025 – 15:45

CCC RightsLink RW

The Tetrameric Aluminum(I) Compound [{Al(η5-C5Me5)}4]

Author: Hansgeorg Schnöckel, Matthias Tacke, Christian Robl, et al
Publication: Angewandte Chemie International Edition
Publisher: John Wiley and Sons
Date: Dec 22, 2003

Order Completed

Thank you for your order.

This Agreement between Richard J. J. Weininger ("You") and John Wiley and Sons ("John Wiley and Sons") consists of your license details and the terms and conditions provided by John Wiley and Sons and Copyright Clearance Center.

Your confirmation email will contain your order number for future reference.

Printable Details

License Number	6046511273764
License date	Jun 12, 2025

Licensed Content

Licensed Content Publisher	John Wiley and Sons
Licensed Content Publication	Angewandte Chemie International Edition
Licensed Content Title	The Tetrameric Aluminum(I) Compound [{Al(η5-C5Me5)}4]
Licensed Content Author	Hansgeorg Schnöckel, Matthias Tacke, Christian Robl, et al
Licensed Content Date	Dec 22, 2003
Licensed Content Volume	30
Licensed Content Issue	5
Licensed Content Pages	2

Order Details

Type of use	Dissertation/Thesis
Requestor type	University/Academic
Format	Print and electronic
Portion	Figure/table
Number of figures/tables	1
Will you be translating?	No

About Your Work

Title of new work	Mononuclear-Homoleptic Transition Metal Compounds of GaTMP
Institution name	Technical University of Munich
Expected presentation date	Sep 2025

Additional Data

Portions	Figure 1, p. 565
The Requesting Person / Organization to Appear on the License	Richard J. J. Weininger

Requestor Location

Requestor Location	Mr. Richard Weininger Technical University of Munich Chair of Inorganic and Metal-Organic Chemistry Lichtenbergstraße 4 Garching Bei München, Bavaria 85748 Germany

Tax Details

Publisher Tax ID	EU826007151

Would you like to purchase the full text of this article? If so, please continue on to the content ordering system located here: Purchase PDF
If you click on the buttons below or close this window, you will not be able to return to the content ordering system.

Total: 0.00 EUR

CLOSE WINDOW ORDER MORE

Appendix

12.06.2025 – 16:05

RightsLink

Hexameric Aggregates in Crystalline (Pentamethylcyclopentadienyl)gallium(I) at 200 K

Author: Anthony J. Downs, Hansgeorg Schnöckel, Achim Ecker, et al
Publication: Angewandte Chemie International Edition
Publisher: John Wiley and Sons
Date: Dec 22, 2003

Order Completed

Thank you for your order.

This Agreement between Richard J. J. Weininger ("You") and John Wiley and Sons ("John Wiley and Sons") consists of your license details and the terms and conditions provided by John Wiley and Sons and Copyright Clearance Center.

Your confirmation email will contain your order number for future reference.

Printable Details

License Number	6046520772606
License date	Jun 12, 2025

Licensed Content

Licensed Content Publisher	John Wiley and Sons
Licensed Content Publication	Angewandte Chemie International Edition
Licensed Content Title	Hexameric Aggregates in Crystalline (Pentamethylcyclopentadienyl)gallium(I) at 200 K
Licensed Content Author	Anthony J. Downs, Hansgeorg Schnöckel, Achim Ecker, et al
Licensed Content Date	Dec 22, 2003
Licensed Content Volume	36
Licensed Content Issue	8
Licensed Content Pages	3

Order Details

Type of use	Dissertation/Thesis
Requestor type	University/Academic
Format	Print and electronic
Portion	Figure/table
Number of figures/tables	1
Will you be translating?	No

About Your Work

Title of new work	Mononuclear-Homoleptic Transition Metal Compounds of GaTMP
Institution name	Technical University of Munich
Expected presentation date	Sep 2025

Additional Data

Portions	Figure 1, p 861
The Requesting Person / Organization to Appear on the License	Richard J. J. Weininger

Requestor Location

Requestor Location	Mr. Richard Weininger Technical University of Munich Chair of Inorganic and Metal-Organic Chemistry Lichtenbergstraße 4 Garching Bei München, Bavaria 85748 Germany

Tax Details

Publisher Tax ID	EU826007151

Would you like to purchase the full text of this article? If so, please continue on to the content ordering system located here: Purchase PDF
If you click on the buttons below or close this window, you will not be able to return to the content ordering system.

Appendix

12.06.2025 – 16:30

CCC Marketplace

RW

Payment Details | Review Details | Confirmation Details

Thank you for your order. You will receive a confirmation email with details about your order.

CUSTOMER INFORMATION

Payment by invoice: You can cancel your order until the invoice is generated by contacting customer service.

Billing Address

Mr. Richard Weininger
Technical University of Munich
Technical University of Munich
Chair of Inorganic and Metal-Organic Chemistry
Lichtenbergstraße 4
Garching Bei München, Bavaria 85748
Germany

+49 1708954554
richard.weininger@tum.de

Customer Location

Mr. Richard Weininger
Technical University of Munich
Technical University of Munich
Chair of Inorganic and Metal-Organic Chemistry
Lichtenbergstraße 4
Garching Bei München, Bavaria 85748
Germany

PO Number (optional)

N/A

Payment options

Invoice

ORDER CONFIRMATION

Confirmation Number: 1619832
Order Date: 12-Jun-2025

Print Friendly Format
Includes Publisher Terms and Conditions

1. Dalton transactions

0,00 EUR

Article: Insertion reactions of GaCp*, InCp* and In[C(SiMe3)3] into the Ru-Cl bonds of [(p-cymene)RuIICl2]2 and [Cp*RuIICl]4.

Order License ID	1619832-1	**Publisher**	ROYAL SOCIETY OF CHEMISTRY
ISSN	1477-9234		
Type of Use	Republish in a thesis/ dissertation	**Portion**	Chart/graph/table/figure

Hide Details

LICENSED CONTENT

Publication Title	Dalton transactions	**Rightsholder**	Royal Society of Chemistry
Article Title	Insertion reactions of GaCp*, InCp* and In[C(SiMe3)3] into the Ru-Cl bonds of [(p-cymene)RuIICl2]2 and [Cp*RuIICl]4.	**Publication Type**	e-Journal
		Start Page	44
		End Page	54
Author / Editor	Royal Society of Chemistry (Great Britain)	**Issue**	1
		Volume	0
Date	01/01/2003		
Language	English		
Country	United Kingdom of Great Britain and Northern Ireland		

REQUEST DETAILS

Portion Type	Chart/graph/table/figure	**Distribution**	Worldwide
Number of Charts / Graphs / Tables / Figures Requested	1	**Translation**	Original language of publication
		Copies for the Disabled?	No
Format (select all that apply)	Print, Electronic	**Minor Editing Privileges?**	Yes
Who Will Republish the Content?	Academic institution	**Incidental Promotional Use?**	No
Duration of Use	Life of current edition	**Currency**	EUR
Lifetime Unit Quantity	Up to 499		
Rights Requested	Main product		

NEW WORK DETAILS

Title	Mononuclear-Homoleptic Transition Metal Compounds of GaTMP	**Institution Name**	Technical University of Munich
		Expected Presentation Date	2025-09-01
Instructor Name	Prof. Dr. Roland A. Fischer		

ADDITIONAL DETAILS

Order Reference Number	N/A	**The Requesting Person / Organization to Appear on the License**	Richard J. J. Weininger

REQUESTED CONTENT DETAILS

Title, Description or Numeric Reference of the Portion(s)	Scheme 1	**Title of the Article / Chapter the Portion Is From**	Insertion reactions of GaCp*, InCp* and In[C(SiMe3)3] into the Ru-Cl bonds of [(p-cymene)RuIICl2]2 and [Cp*RuIICl]4.
Editor of Portion(s)	Cokoja, Mirza; Gemel, Christian; Steinke, Tobias; Schroder, Felicitas; Fischer, Roland A	**Author of Portion(s)**	Cokoja, Mirza; Gemel, Christian; Steinke, Tobias; Schroder, Felicitas; Fischer, Roland A
Volume / Edition	0		
Page or Page Range of Portion	44-54	**Issue, if Republishing an Article From a Serial**	1
		Publication Date of Portion	2005-01-07

Print License

Total Items: 1

Total Due: 0,00 EUR

Accepted: Marketplace Permissions General Terms and Conditions and any applicable Publisher Terms and Conditions

Continue Shopping

Appendix

12.06.2025 – 16:36

CCC RightsLink RW

Organometallic Chemistry of Ga : Formation of an Unusual Gallium Dimer in the Coordination Sphere of Ruthenium

Author: Roland A. Fischer, Gernot Frenking, Israel Fernandez, et al
Publication: Chemistry - A European Journal
Publisher: John Wiley and Sons
Date: Nov 21, 2008

Order Completed

Thank you for your order.

This Agreement between Richard J. J. Weininger ("You") and John Wiley and Sons ("John Wiley and Sons") consists of your license details and the terms and conditions provided by John Wiley and Sons and Copyright Clearance Center.

Your confirmation email will contain your order number for future reference.

Printable Details

License Number	6046531229533
License date	Jun 12, 2025

Licensed Content

Licensed Content Publisher	John Wiley and Sons
Licensed Content Publication	Chemistry - A European Journal
Licensed Content Title	Organometallic Chemistry of Ga : Formation of an Unusual Gallium Dimer in the Coordination Sphere of Ruthenium
Licensed Content Author	Roland A. Fischer, Gernot Frenking, Israel Fernandez, et al
Licensed Content Date	Nov 21, 2008
Licensed Content Volume	14
Licensed Content Issue	34
Licensed Content Pages	8

Order Details

Type of use	Dissertation/Thesis
Requestor type	University/Academic
Format	Print and electronic
Portion	Figure/table
Number of figures/tables	1
Will you be translating?	No

About Your Work

Title of new work	Mononuclear-Homoleptic Transition Metal Compounds of GaTMP
Institution name	Technical University of Munich
Expected presentation date	Sep 2025

Additional Data

Portions	Scheme 1
The Requesting Person / Organization to Appear on the License	Richard J. J. Weininger

Requestor Location

Requestor Location	Mr. Richard Weininger Technical University of Munich Chair of Inorganic and Metal-Organic Chemistry Lichtenbergstraße 4 Garching Bei München, Bavaria 85748 Germany

Tax Details

Publisher Tax ID	EU826007151

Would you like to purchase the full text of this article? If so, please continue on to the content ordering system located here: Purchase PDF
If you click on the buttons below or close this window, you will not be able to return to the content ordering system.

Total: 0.00 EUR

CLOSE WINDOW ORDER MORE

12.06.2025 - 16:40

CCC RightsLink RW

Substituent-Free Gallium by Hydrogenolysis of Coordinated GaCp*: Synthesis and Structure of Highly Fluxional [Ru2(Ga)(GaCp*)7(H)3]

Author: Roland A. Fischer, Mirza Cokoja, Kirill Yusenko, et al
Publication: Angewandte Chemie International Edition
Publisher: John Wiley and Sons
Date: May 4, 2009

Order Completed

Thank you for your order.

This Agreement between Richard J. J. Weininger ("You") and John Wiley and Sons ("John Wiley and Sons") consists of your license details and the terms and conditions provided by John Wiley and Sons and Copyright Clearance Center.

Your confirmation email will contain your order number for future reference.

License Number	6046540013928
License date	Jun 12, 2025

Printable Details

Licensed Content

Licensed Content Publisher	John Wiley and Sons
Licensed Content Publication	Angewandte Chemie International Edition
Licensed Content Title	Substituent-Free Gallium by Hydrogenolysis of Coordinated GaCp*: Synthesis and Structure of Highly Fluxional [Ru2(Ga)(GaCp*)7(H)3]
Licensed Content Author	Roland A. Fischer, Mirza Cokoja, Kirill Yusenko, et al
Licensed Content Date	May 4, 2009
Licensed Content Volume	48
Licensed Content Issue	21
Licensed Content Pages	5

Order Details

Type of use	Dissertation/Thesis
Requestor type	University/Academic
Format	Print and electronic
Portion	Figure/table
Number of figures/tables	1
Will you be translating?	No

About Your Work

Title of new work	Mononuclear-Homoleptic Transition Metal Compounds of GaTMP
Institution name	Technical University of Munich
Expected presentation date	Sep 2025

Additional Data

Portions	Scheme 1
The Requesting Person / Organization to Appear on the License	Richard J. J. Weininger

Requestor Location

Requestor Location	Mr. Richard Weininger Technical University of Munich Chair of Inorganic and Metal-Organic Chemistry Lichtenbergstraße 4 Garching Bei München, Bavaria 85748 Germany

Tax Details

Publisher Tax ID	EU826007151

Would you like to purchase the full text of this article? If so, please continue on to the content ordering system located here: Purchase PDF
If you click on the buttons below or close this window, you will not be able to return to the content ordering system.

Total: 0.00 EUR

CLOSE WINDOW ORDER MORE

Appendix

12.06.2025 – 16:47

RightsLink

C–H and Si–H Activation Reactions at Ru/Ga Complexes: A Combined Experimental and Theoretical Case Study on the Ru–Ga Bond

Author: Roland A. Fischer, Christian Gemel, Jean-Yves Saillard, et al
Publication: Chemistry - A European Journal
Publisher: John Wiley and Sons
Date: Aug 3, 2022

Order Completed

Thank you for your order.

This Agreement between Richard J. J. Weininger ("You") and John Wiley and Sons ("John Wiley and Sons") consists of your license details and the terms and conditions provided by John Wiley and Sons and Copyright Clearance Center.

Your confirmation email will contain your order number for future reference.

Printable Details

License Number	6046540333704
License date	Jun 12, 2025

Licensed Content

Licensed Content Publisher	John Wiley and Sons
Licensed Content Publication	Chemistry - A European Journal
Licensed Content Title	C–H and Si–H Activation Reactions at Ru/Ga Complexes: A Combined Experimental and Theoretical Case Study on the Ru–Ga Bond
Licensed Content Author	Roland A. Fischer, Christian Gemel, Jean-Yves Saillard, et al
Licensed Content Date	Aug 3, 2022
Licensed Content Volume	28
Licensed Content Issue	54
Licensed Content Pages	6

Order Details

Type of use	Dissertation/Thesis
Requestor type	University/Academic
Format	Print and electronic
Portion	Figure/table
Number of figures/tables	1
Will you be translating?	No

About Your Work

Title of new work	Mononuclear-Homoleptic Transition Metal Compounds of GaTMP
Institution name	Technical University of Munich
Expected presentation date	Sep 2025

Additional Data

Portions	Figure 1
The Requesting Person / Organization to Appear on the License	Richard J. J. Weininger

Requestor Location

Requestor Location	Mr. Richard Weininger Technical University of Munich Chair of Inorganic and Metal-Organic Chemistry Lichtenbergstraße 4 Garching Bei München, Bavaria 85748 Germany

Tax Details

Publisher Tax ID	EU826007151

Would you like to purchase the full text of this article? If so, please continue on to the content ordering system located here: Purchase PDF
If you click on the buttons below or close this window, you will not be able to return to the content ordering system.

Total: 0.00 USD

CLOSE WINDOW | ORDER MORE

Appendix

12.06.2025 – 16:54

CCC RightsLink RW

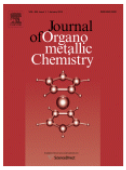

Ligand properties of Cp*Ga: new examples of Mo–Ga and W–Ga complexes

Author: Mirza Cokoja,Tobias Steinke,Christian Gemel,Thea Welzel,Manuela Winter,Klaus Merz,Roland A Fischer
Publication: Journal of Organometallic Chemistry
Publisher: Elsevier
Date: 1 November 2003

Order Completed

Thank you for your order.

This Agreement between Richard J. J. Weininger ("You") and Elsevier ("Elsevier") consists of your license details and the terms and conditions provided by Elsevier and Copyright Clearance Center.

Your confirmation email will contain your order number for future reference.

License Number	6046540794376
License date	Jun 12, 2025

Printable Details

Licensed Content

Licensed Content Publisher	Elsevier
Licensed Content Publication	Journal of Organometallic Chemistry
Licensed Content Title	Ligand properties of Cp*Ga: new examples of Mo–Ga and W–Ga complexes
Licensed Content Author	Mirza Cokoja,Tobias Steinke,Christian Gemel,Thea Welzel,Manuela Winter,Klaus Merz,Roland A Fischer
Licensed Content Date	Nov 1, 2003
Licensed Content Volume	684
Licensed Content Issue	1-2
Licensed Content Pages	10

Order Details

Type of Use	reuse in a thesis/dissertation
Portion	figures/tables/illustrations
Number of figures/tables/ illustrations	2
Format	both print and electronic
Are you the author of this Elsevier article?	No
Will you be translating?	No

About Your Work

Title of new work	Mononuclear-Homoleptic Transition Metal Compounds of GaTMP
Institution name	Technical University of Munich
Expected presentation date	Sep 2025

Additional Data

Portions	Scheme 1 + Scheme 2 p.279
The Requesting Person / Organization to Appear on the License	Richard J. J. Weininger

Requestor Location

Requestor Location	Mr. Richard Weininger Technical University of Munich Chair of Inorganic and Metal-Organic Chemistry Lichtenbergstraße 4 Garching Bei München, Bavaria 85748 Germany

Tax Details

Publisher Tax ID	GB 494 6272 12

Total: 0.00 EUR

CLOSE WINDOW ORDER MORE

Appendix

12.06.2025 – 17:00

RightsLink

Complexes of Four-Membered Group 13 Metal(I) N-Heterocyclic Carbene Analogues with Metal Carbonyl Fragments

Author: Glen B. Deacon, Peter C. Junk, Graeme J. Moxey, et al
Publication: European Journal of Inorganic Chemistry
Publisher: John Wiley and Sons
Date: Aug 6, 2009

Order Completed

Thank you for your order.

This Agreement between Richard J. J. Weininger ("You") and John Wiley and Sons ("John Wiley and Sons") consists of your license details and the terms and conditions provided by John Wiley and Sons and Copyright Clearance Center.

Your confirmation email will contain your order number for future reference.

Printable Details

License Number	6046541158665
License date	Jun 12, 2025

Licensed Content

Licensed Content Publisher	John Wiley and Sons
Licensed Content Publication	European Journal of Inorganic Chemistry
Licensed Content Title	Complexes of Four-Membered Group 13 Metal(I) N-Heterocyclic Carbene Analogues with Metal Carbonyl Fragments
Licensed Content Author	Glen B. Deacon, Peter C. Junk, Graeme J. Moxey, et al
Licensed Content Date	Aug 6, 2009
Licensed Content Volume	2009
Licensed Content Issue	24
Licensed Content Pages	7

Order Details

Type of use	Dissertation/Thesis
Requestor type	University/Academic
Format	Print and electronic
Portion	Figure/table
Number of figures/tables	1
Will you be translating?	No

About Your Work

Title of new work	Mononuclear-Homoleptic Transition Metal Compounds of GaTMP
Institution name	Technical University of Munich
Expected presentation date	Sep 2025

Additional Data

Portions	Scheme 1, p 3594
The Requesting Person / Organization to Appear on the License	Richard J. J. Weininger

Requestor Location

Requestor Location	Mr. Richard Weininger Technical University of Munich Chair of Inorganic and Metal-Organic Chemistry Lichtenbergstraße 4 Garching Bei München, Bavaria 85748 Germany

Tax Details

Publisher Tax ID	EU826007151

Would you like to purchase the full text of this article? If so, please continue on to the content ordering system located here: Purchase PDF
If you click on the buttons below or close this window, you will not be able to return to the content ordering system.

Total: 0.00 EUR

CLOSE WINDOW ORDER MORE

Appendix

12.06.2025 – 17:10

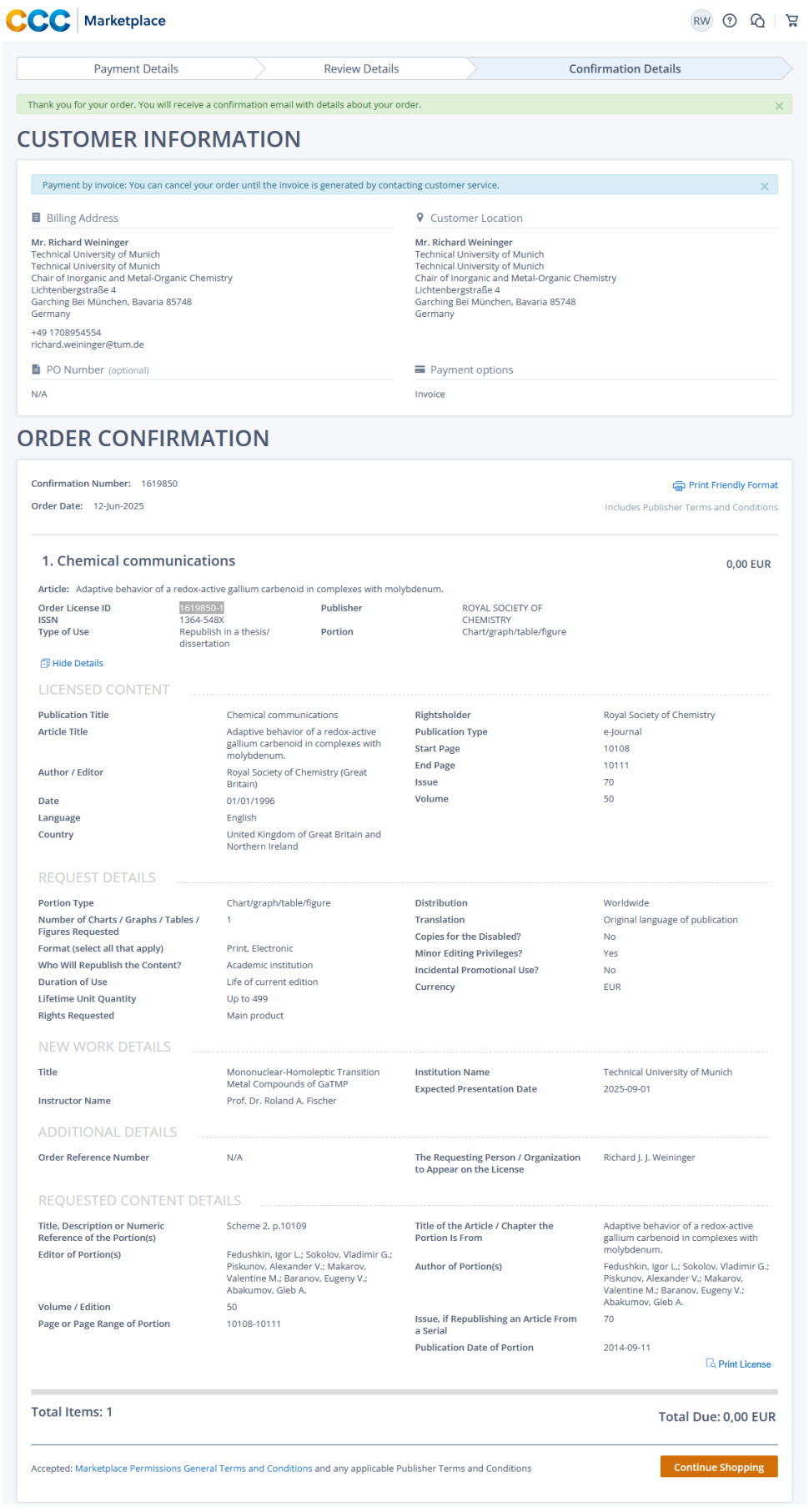

CCC Marketplace

RW

Payment Details | Review Details | Confirmation Details

Thank you for your order. You will receive a confirmation email with details about your order.

CUSTOMER INFORMATION

Payment by invoice: You can cancel your order until the invoice is generated by contacting customer service.

Billing Address

Mr. Richard Weininger
Technical University of Munich
Technical University of Munich
Chair of Inorganic and Metal-Organic Chemistry
Lichtenbergstraße 4
Garching Bei München, Bavaria 85748
Germany

+49 1708954554
richard.weininger@tum.de

Customer Location

Mr. Richard Weininger
Technical University of Munich
Technical University of Munich
Chair of Inorganic and Metal-Organic Chemistry
Lichtenbergstraße 4
Garching Bei München, Bavaria 85748
Germany

PO Number (optional)

N/A

Payment options

Invoice

ORDER CONFIRMATION

Confirmation Number: 1619850
Order Date: 12-Jun-2025

Print Friendly Format
Includes Publisher Terms and Conditions

1. Chemical communications

0,00 EUR

Article: Adaptive behavior of a redox-active gallium carbenoid in complexes with molybdenum.

Order License ID	1619850-1	**Publisher**	ROYAL SOCIETY OF CHEMISTRY
ISSN	1364-548X		
Type of Use	Republish in a thesis/ dissertation	**Portion**	Chart/graph/table/figure

Hide Details

LICENSED CONTENT

Publication Title	Chemical communications	**Rightsholder**	Royal Society of Chemistry
Article Title	Adaptive behavior of a redox-active gallium carbenoid in complexes with molybdenum.	**Publication Type**	e-Journal
		Start Page	10108
Author / Editor	Royal Society of Chemistry (Great Britain)	**End Page**	10111
		Issue	70
Date	01/01/1996	**Volume**	50
Language	English		
Country	United Kingdom of Great Britain and Northern Ireland		

REQUEST DETAILS

Portion Type	Chart/graph/table/figure	**Distribution**	Worldwide
Number of Charts / Graphs / Tables / Figures Requested	1	**Translation**	Original language of publication
		Copies for the Disabled?	No
Format (select all that apply)	Print, Electronic	**Minor Editing Privileges?**	Yes
Who Will Republish the Content?	Academic institution	**Incidental Promotional Use?**	No
Duration of Use	Life of current edition	**Currency**	EUR
Lifetime Unit Quantity	Up to 499		
Rights Requested	Main product		

NEW WORK DETAILS

Title	Mononuclear-Homoleptic Transition Metal Compounds of GaTMP	**Institution Name**	Technical University of Munich
		Expected Presentation Date	2025-09-01
Instructor Name	Prof. Dr. Roland A. Fischer		

ADDITIONAL DETAILS

Order Reference Number	N/A	**The Requesting Person / Organization to Appear on the License**	Richard J. J. Weininger

REQUESTED CONTENT DETAILS

Title, Description or Numeric Reference of the Portion(s)	Scheme 2, p.10109	**Title of the Article / Chapter the Portion Is From**	Adaptive behavior of a redox-active gallium carbenoid in complexes with molybdenum.
Editor of Portion(s)	Fedushkin, Igor L.; Sokolov, Vladimir G.; Piskunov, Alexander V.; Makarov, Valentine M.; Baranov, Eugeny V.; Abakumov, Gleb A.	**Author of Portion(s)**	Fedushkin, Igor L.; Sokolov, Vladimir G.; Piskunov, Alexander V.; Makarov, Valentine M.; Baranov, Eugeny V.; Abakumov, Gleb A.
Volume / Edition	50		
Page or Page Range of Portion	10108-10111	**Issue, if Republishing an Article From a Serial**	70
		Publication Date of Portion	2014-09-11

Print License

Total Items: 1

Total Due: 0,00 EUR

Accepted: Marketplace Permissions General Terms and Conditions and any applicable Publisher Terms and Conditions

Continue Shopping

Appendix

12.06.2025 – 17:22

CCC RightsLink

Twelve One-Electron Ligands Coordinating One Metal Center: Structure and Bonding of [Mo(ZnCH3)9(ZnCp*)3]

Author: Roland A. Fischer, Gernot Frenking, Moritz von Hopffgarten, et al
Publication: Angewandte Chemie International Edition
Publisher: John Wiley and Sons
Date: Nov 5, 2008

Order Completed

Thank you for your order.

This Agreement between Richard J. J. Weininger ("You") and John Wiley and Sons ("John Wiley and Sons") consists of your license details and the terms and conditions provided by John Wiley and Sons and Copyright Clearance Center.

Your confirmation email will contain your order number for future reference.

Printable Details

License Number	6046550954491
License date	Jun 12, 2025

Licensed Content

Licensed Content Publisher	John Wiley and Sons
Licensed Content Publication	Angewandte Chemie International Edition
Licensed Content Title	Twelve One-Electron Ligands Coordinating One Metal Center: Structure and Bonding of [Mo(ZnCH3)9(ZnCp*)3]
Licensed Content Author	Roland A. Fischer, Gernot Frenking, Moritz von Hopffgarten, et al
Licensed Content Date	Nov 5, 2008
Licensed Content Volume	47
Licensed Content Issue	47
Licensed Content Pages	5

Order Details

Type of use	Dissertation/Thesis
Requestor type	University/Academic
Format	Print and electronic
Portion	Figure/table
Number of figures/tables	1
Will you be translating?	No

About Your Work

Title of new work	Mononuclear-Homoleptic Transition Metal Compounds of GaTMP
Institution name	Technical University of Munich
Expected presentation date	Sep 2025

Additional Data

Portions	Scheme 1, p.9150
The Requesting Person / Organization to Appear on the License	Richard J. J. Weininger

Requestor Location

Requestor Location	Mr. Richard Weininger Technical University of Munich Chair of Inorganic and Metal-Organic Chemistry Lichtenbergstraße 4 Garching Bei München, Bavaria 85748 Germany

Tax Details

Publisher Tax ID	EU826007151

Would you like to purchase the full text of this article? If so, please continue on to the content ordering system located here: Purchase PDF
If you click on the buttons below or close this window, you will not be able to return to the content ordering system.

Total: 0.00 EUR

CLOSE WINDOW | ORDER MORE